UNIVERSIDADE DE LISBOA

Faculdade de Medicina

U

LISBOA

UNIVERSIDADE
DE LISBOA

©Helena Pinheiro

The transcriptional landscape of

Alzheimer's and Parkinson's diseases

Marie Catherine Bordone

Orientadores:

Prof. Doutor Nuno Luís Barbosa Morais

Prof. Doutor Sérgio Alexandre Fernandes de Almeida

Tese especialmente elaborada para a obtenção do grau de

Doutor em Ciências Biomédicas

Especialidade em Biologia Computacional

2021

UNIVERSIDADE DE LISBOA

Faculdade de Medicina

U

LISBOA

UNIVERSIDADE
DE LISBOA

The transcriptional landscape of Alzheimer's and Parkinson's diseases

Marie Catherine Bordone

Orientadores:

Prof. Doutor Nuno Luís Barbosa Morais

Prof. Doutor Sérgio Alexandre Fernandes de Almeida

Tese especialmente elaborada para a obtenção do grau de

Doutor em Ciências Biomédicas

Especialidade em Biologia Computacional

Júri:

Presidente: Doutor João Eurico Cortez Cabral da Fonseca, Professor Catedrático e Vice-Presidente do Conselho Científico da Faculdade de Medicina da Universidade de Lisboa.

Vogais:

- Doutor José Miguel Tomás Brás, Associate Professor do Van Andel Institute (USA);
- Doutora Ana Rita Fialho Grosso, Investigadora Auxiliar da Faculdade de Ciências e Tecnologia da Universidade Nova de Lisboa;
- Doutor Joaquim José Coutinho Ferreira, Professor Associado da Faculdade de Medicina da Universidade de Lisboa;
- Doutora Luísa Maria Vaqueiro Lopes, Professora Associada Convidada da Faculdade de Medicina da Universidade de Lisboa;
- Doutor Nuno Luís Barbosa Morais, Professor Associado Convidado da Faculdade de Medicina da Universidade de Lisboa;
- Doutora Vanessa Alexandra dos Santos Morais Epifânio, Professora Associada Convidada da Faculdade de Medicina da Universidade de Lisboa;

2021

A impressão desta tese foi aprovada pelo Conselho Científico da Faculdade de Medicina de Lisboa em reunião de 20 de Outubro de 2020.

I may not have gone where I intended to go,
but I think I have ended up where I needed to be.

Douglas Adams

Table of Contents

Acknowledgments

First, I would like to thank my supervisor Nuno Morais for having me as his first PhD student. I owe him the awakening of the left side of my brain and always pushing further my logical reasoning. I also would like to thank him for all the scientific discussions, we had during the past years, even if we wouldn't agree every time, as well as increasing my scientific critical thinking to the next level. I also would like to thank Sérgio Almeida who, although he didn't probably realize it, knew always what to say, at the right moments, in this PhD journey.

A PhD journey can be a crazy roller coaster and we must be surrounded of good friends, otherwise we would not finish in one piece. I consider myself very lucky because I was always very well accompanied during the ride. Lina Gallego, my favourite Colombian, was one of the first persons to be present in it. Sharing a similar academic background, we were each other support during the first years of my PhD. With her I learned even more about biology and how to look at the world in a more "Japanese" way. Thank you for all the laughing and insane moments we shared together. To Mariana Ferreira and Nuno Agostinho, my older "*piu-pius*", you were present in the highest and lowest curves of my PhD, always with the support I needed. Mariana, my soul sister, thank you for laughing as hard as me and sharing my sorrows during this journey. Nuno, my special computer guy, thank you for all the help, no matter the hours of the day. To Sara Mendes, my youngest "*piu-piu*" that also became a very good friend, thank you for being the best student I could have asked for. Arthur, the other French in the lab, thank you for always getting on board in crazy and silly talks and of course, to your strawberry pies. To all the other members that passed (and still are) in Nmorais Lab during my stay (Marta Bica, Ana Carolina Leote, Sofia Borges, Teresa Maia, Rita Belo and Bernardo Almeida) thank you for keeping the best social and scientific environment, someone could ask for in a lab.

I started this journey with the LisbonBiomed batch 2015 with whom I shared very good moments, especially in those first 2 months of classes. However, I would like to thank especially Margarida Vaz, Pedro Barbacena and Pedro Papotto. Margarida, thank you for always speaking the truth even when it was not the easiest

thing to do. Pedro Barbacena, my favourite lab neighbour, thank you for always been there and ready for a coffee. Pedro Papotto, thank you for all the cheering, open heart conversations and best parties shared.

I was also very lucky to meet other important persons along this trip that were not directly linked to my PhD. To Catarina Fonseca, my cutest and also favourite lab neighbour, thank you for sharing the joy of all my achievements and being there when I needed to vent about the PhD as well as pushing me to the gym (or walking home) to maintain a minimal decent physical form. To Filipa Nunes, the Training Hub Director, we met when I started the Workshops Committee and from then on we became very good friends. Thank you for always being available for hearing the same PhD stories over and over again and for all the mentoring you gave to me during this PhD journey. To Eunice Paisana and Elvira Leites, I would like to thank you for all the fun moments and scientific discussions we shared along the way. iMM was the perfect place to do a PhD along amazing people that I had the privilege to know and be with. I cannot list everyone but thank you for being part of my journey in one way or another.

Finally, I would like to thank to the core people of my life. I would like to thank my mom Ana Campino, dad Richard Bordone and my sister Myriam Bordone for all their constant support and believing, despite not always understanding the crazy paths of this PhD journey. To Rui Talhadas dos Santos, my 10 years' partner, thank you for celebrating all my achievements, even the small ones, thank you for always being there in the lowest moments and, most of all, thank you for always keep cheering me up to finish this PhD adventure.

Funding

A

AD – Alzheimer's Disease

APOE – Apolipoprotein E

APP – Amyloid Precursor Protein

Aβ – Amyloid-beta

B

BBB – Blood-Brain-Barrier

C

cDNA – complementary DNA

CNS – Central Nervous System

CSF – Cerebrospinal Fluid

D

DALY – Disability-Adjusted Life Year

DBS – Deep Brain Stimulation

E

EMA – European Medicines Agency

EOAD – Early Onset AD

ER – Endoplasmic Reticulum

F

FACS – Fluorescence-Activated Cell Sorting

FAD – Familial Alzheimer's disease

FDA – US Food and Drug Administration

G_____

GBD – Global Burden of Diseases, Injuries, and Risk Factors Study

GFAP – Glial Fibrillary Acidic Protein

GNR – Glia-Neuron Ratio

GWAS – Genome-Wide Association Studies

H_____

HLA – Human Leucocyte Antigen

HLA-DRA – Human Leucocyte Antigen, DR Alpha Chain

I_____

IgG – Immunoglobulin G

iPSC – Induced-Pluripotent Stem Cell

IVT – *In Vitro* Transcription

J_____

K_____

L_____

LCM – Laser Capture Microdissection

LOAD – Late Onset AD

M_____

MAM – Mitochondria-Associated Endoplasmic Reticulum Membrane

MCI – Mild Cognitive Impairment

MPP$^+$ – 1-Methyl-4-Phenylpyridinium

MPTP – 1-methyl-4-phenyl-1,2,3,6-tetrahydropyridine

MRI – Magnetic Resonance Imaging

mRNA – Messenger RNA

MS – Multiple Sclerosis

N_____

NFT – Neurofibrillary Tangles

NMDA – N-Methyl-A-Aspartate

O_____

OPC – Oligodendrocyte Precursor Cell

P_____

PCA – Principal Component Analysis

PCR – Polymerase Reaction Chain

PD – Parkinson's Disease

PET – Positron-Emission Tomography

PNS – Peripheral Nervous System

PSEN 1 – Presenilin 1

PSEN 2 – Presenilin 2

Q_____

QSBB – Queen Square Brain Bank

R_____

RNA-seq – RNA-Sequencing

RT-qPCR – Reverse Transcriptase Quantitative Polymerase Chain Reaction

S_____

scRNA-seq – Single-Cell RNA-seq

snRNA-seq – Single-Nuclei RNA-seq

SPECT – Single-Photon Emission Computed Tomography

T_____

TLR – Tool-Like Receptor

U_____

UPS – Ubiquitin-Proteasome System

V_____

VEC – Vascular Endothelial Cell

W_____

X_____

Y_____

Z_____

#_____

6-OHDA – 6-hydroxydopamine

Figures

Resumo

A doença de Alzheimer (DA) e a doença de Parkinson (DP) são as duas doenças neurodegenerativas mais comuns no mundo. Embora a etiologia, a região cerebral afetada e as características clínicas sejam particulares a cada uma dessas doenças, ambas partilham mecanismos comuns, tais como disfunção mitocondrial, perda neuronal e acumulação de proteína tau. O principal fator de risco para estas doenças é o envelhecimento, sendo a idade de aparecimento da DA e da DP em torno dos 65 anos. Em conjunto, a DA e a DP são responsáveis por 50 milhões de casos no mundo, número que deve aumentar devido ao facto da esperança de vida da população mundial estar continuamente a subir. A maioria dos casos de DA e DP são idiopáticos e, apesar de toda a investigação feita durante os últimos séculos para compreender melhor a sua natureza molecular, os tratamentos atuais ainda só atuam ao nível dos sintomas. Portanto, o desenvolvimento de terapias eficazes requer uma melhor compreensão da etiologia das doenças e dos mecanismos subjacentes, bem como encontrar alvos específicos das doenças para o desenvolvimento de fármacos para a terapia respetiva.

Uma estratégia comum para identificar vias biológicas e processos celulares alterados nas doenças neurodegenerativas é a comparação dos perfis de expressão génica entre tecidos cerebrais *post-mortem* com e sem doença, de mesma idade. No entanto, os perfis de expressão derivados de mRNA de tecido cerebral refletem bastante as alterações da composição celular, nomeadamente a conhecida perda de neurónios associada à DA ou à DP, mas não necessariamente as alterações moleculares relacionadas com a doença em si nas células do cérebro. O avanço tecnológico recente na área da transcritómica de célula individual (*single-cell RNA-seq (scRNA-seq)*) permite agora enfrentar essa limitação, permitindo a determinação de perfis de expressão de genes de referência para cada um dos principais tipos de célula cerebral (i.e. neurónios, astrócitos, micróglia e oligodendrócitos) que podem então ser usados para estimar computacionalmente o conteúdo celular especifico de amostras de tecido cerebral em condições de doença e não doença, desacoplando o efeito de neurodegeneração (ou seja, a relativamente acentuada perda de neurónios) dos efeitos da doença sistémicos ou específicos do tipo celular.

Esta abordagem já foi aplicada na determinação dos efeitos da idade e dos distúrbios psiquiátricos na composição celular do cérebro humano, assim como da contribuição de cada tipo de célula no transcritoma patológico do autismo. O mesmo princípio foi também aplicado na DA modelando a expressão de seus genes de risco em função da composição celular estimada de amostras cerebrais. Por exemplo, os níveis de expressão dos genes *APP*, *PSEN1*, *APOE* e *TREM2* foram associados à abundância relativa de neurónios, oligodendrócitos, astrócitos e micróglia, respectivamente. Além disso, dois estudos recentes traçaram o perfil de expressão obtido de núcleos das principais células de amostras de cérebro *post-mortem* com e sem DA, revelando alterações transcricionais específicas do tipo de célula. Todos esses estudos destacam a importância de caracterizar fenótipos específicos do tipo de célula associados à doença, que podem não apenas desvendar as bases celulares e moleculares dos mecanismos patológicos, mas também ser terapeuticamente alvejados.

No entanto, alguns desses estudos ainda carecem de validação independente e não dissecaram totalmente a natureza das alterações transcritómicas em cérebros com DA. Além disso, não temos conhecimento de que abordagens semelhantes tenham sido aplicadas à DP, apesar da acumulação de evidências da importância da modelação da composição celular em doenças neurodegenerativas. Pelas razões supradescritas, nesta tese usámos dados de scRNA-seq para derivar as assinaturas de expressão génica dos principais tipos de células cerebrais humanas e estimar a composição celular dos transcritomas de amostras cerebrais *post-mortem* de DA e DP idiopáticas, avaliando se a perda neuronal poderia estar a confundir ou mascarar os efeitos intrínsecos das doenças na expressão génica. Validámos os resultados em conjuntos de dados independentes. Além disso, uma vez que as DA e DP podem partilhar os mesmos mecanismos de progressão de doença, também investigámos as semelhanças entre as alterações transcritómicas induzidas por DA e DP em tecidos cerebrais humanos.

Esta abordagem permitiu a identificação inédita de genes e vias biológicas cuja atividade no cérebro é intrinsecamente alterada pelas DA e DP, de formas sistémica e específica do tipo celular. Além disso, identificámos genes que são comumente

alterados por ambas as doenças neurodegenerativas, bem como aqueles que são especificamente alterados em cada uma.

Usámos também dados públicos de transcritómica de perturbações químicas de linhas celulares humanas com milhares de compostos diferentes. Comparámos computacionalmente esta miríade de alterações transcritómicas induzidas farmacologicamente com as que identificámos em tecidos cerebrais humanos como potencialmente causadas por DA e DP. Esta abordagem permitiu-nos assim identificar fármacos candidatos a reverter especificamente as alterações moleculares causadas pelas doenças.

Porém, o nosso estudo apresenta algumas limitações. Concentrámo-nos nos quatro principais tipos de células cerebrais mas a nossa abordagem não é sensível o suficiente para estimar a quantidade relativa de mRNA proveniente da microglia, perdendo assim o seu sinal transcritómico fisiológico. Além disso, apesar de termos validado os nossos resultados usando um conjunto de dados públicos independentes, a desejável validação experimental adicional, com amostras independentes do conjunto de dados analisados, não é viável, devido à extrema dificuldade em ter acesso a amostras de cérebro humanas *post-mortem*. Este estudo apresenta também uma dificuldade na interpretação dos seus resultados: os medicamentos usados atualmente para o tratamento de DA e DP não estão entre aqueles que a nossa análise considerou serem os mais prováveis de reverter as alterações de expressão génica específicas de DA e DP. Provavelmente este resultado deve-se às diferenças entre as alterações de expressão génica induzidas por fármacos em linhas celulares derivadas de cancros (aquelas a cujos dados de perturbações transcritómicas quimicamente induzidas tivemos acesso) e as alterações que os mesmos fármacos possam induzir nas células do cérebro, ilustrando assim a principal limitação da nossa abordagem quimio-transcritómica.

Esperamos que o desenvolvimento permanente das tecnologias de *single-cell* ajude a aumentar a resolução do nosso conhecimento sobre as particularidades de cada tipo celular do cérebro humano, bem como na identificação das perturbações moleculares em cada célula que são críticas para o desenvolvimento e progressão das doenças neurodegenerativas como DA e DP. Aliás, alguns estudos já usaram

scRNA-seq para caracterizar a composição celular em cérebros não doentes, em contextos de neurogénese e reprogramação somática para neurónios, e em cérebros com DA. No entanto, tendo em conta que continuam a acumular-se dados de *single-cell* e que já existem vários transcritomas de cérebros com doenças neurodegenerativas disponíveis, abordagens como a nossa poderão ajudar a desvendar um pouco da complexidade celular e molecular associada à neurodegeneração em humanos.

Em suma, os nossos resultados demonstram a relevância de considerar a composição celular do cérebro ao analisar alterações moleculares associadas a doenças neurodegenerativas, identificando assim um conjunto de novos candidatos moleculares relacionados com as próprias DA e DP, em vez de com a perda de neurónios associada. Além disso, os nossos resultados ilustram o potencial de análises *in silico* de perturbações químicas dos transcritomas de células humanas como estudos preliminares de reaproveitamento de fármacos para novas terapias que possam vir a ser mais eficazes a mitigar, ou mesmo reverter, alguns dos fenótipos associados a doenças neurodegenerativas.

Palavras-chave

Doença de Alzheimer, doença de Parkinson, neurodegeneração, deconvolução celular, citometria digital, *single-cell RNA-seq*, quimio-transcritómica.

Summary

Alzheimer's disease (AD) and Parkinson's disease (PD) are the two most common neurodegenerative disorders worldwide. Although the aetiology, affected brain region and clinical features are particular to each of these diseases, they nevertheless share common mechanisms such as mitochondria dysfunction, neuronal loss and tau protein accumulation. The major risk factor for those disorders is ageing, the age of onset of both AD or PD being around 65 years old. Together, they account for 50 million cases worldwide, a number expected to increase due to the fact that the world population is living longer than ever. Most of AD and PD cases are sporadic and, despite all the research during the last centuries to better understand their molecular nature, current treatments are still symptomatic. Therefore, the development of effective therapies requires a better comprehension of the diseases' aetiology and underlying mechanisms as well as finding disease-specific targets for drug discovery.

A common strategy to identify biological pathways and cellular processes altered in neurodegenerative disorders is to compare gene expression profiles between age-matched diseased and non-diseased *post-mortem* brain tissues. However, the expression profiles derived from whole brain tissue mRNA highly reflect alterations in cellular composition, namely the well-known AD- or PD-associated loss of neurons, but not necessarily the disease-related molecular changes in brain cells. The advent of single-cell transcriptomes has made it possible to tackle this limitation, enabling the determination of reference gene expression profiles for each major brain cell type (namely neurons, astrocytes, microglia and oligodendrocytes) that can then be used to computationally estimate the cell type-specific content of bulk brain sample's in healthy and diseased conditions, decoupling the neurodegeneration effect (i.e. the relative loss of neurons) from the intrinsic systemic or cell type-specific disease effects.

This approach has already been applied in determining the effects of age and psychiatric disorders on the cellular composition of human brain, or the contribution of each cell type in shaping the pathological autism transcriptome. The same principle was applied in AD by modelling the expression of its risk genes as a

function of estimated cellular composition of brain samples. For instance, *APP*, *PSEN1*, *APOE* and *TREM2* had their expression levels associated with the relative abundance of respectively neurons, oligodendrocytes, astrocytes and microglia. Additionally, two recent studies profiled single nuclei of major brain cell types in AD and non-AD *post-mortem* brain samples, unveiling cell type-specific transcriptional changes. All these studies highlight the importance of charactering disease-associated cell type-specific phenotypes that can not only unveil the cellular and molecular bases of pathological mechanisms but also be therapeutically targeted.

However, some of these studies still lack independent validation and have not fully dissected the nature of transcriptomic alterations in AD brains. Moreover, to our knowledge, similar approaches have not yet been applied to PD, despite increasing evidence regarding the importance of modelling cellular composition in neurodegenerative disorders. We therefore used scRNA-seq data to derive gene expression signatures for the major human brain cell types and estimate the cellular composition of idiopathic AD and PD *post-mortem* brain samples from their bulk transcriptomes, investigating whether neuronal loss could be confounding or masking the intrinsic disease effects on gene expression, and validating the results in independent datasets. Additionally, since AD and PD might share the same mechanisms of disease progression, we also investigated the similarities between the transcriptomic alterations induced by AD and PD in human brain tissues.

This approach allowed the novel identification of genes and pathways whose activity in the brain is intrinsically altered by AD and PD in systemic and cell type-specific ways. Additionally, we pinpoint the genes that are commonly altered by these major neurodegenerative disorders as well as those specifically perturbed in each illness. Moreover, using chemical perturbagen data, we computationally identified candidate small molecules for specifically targeting the profiled AD/PD-associated molecular alterations. Thus, we unveil a set of novel candidates that can potentially be targeted in AD and PD therapeutics. Moreover, we herein demonstrate the potential of modelling cellular composition in transcriptomics analyses in the discovery of therapeutic targets for other neurodegenerative diseases.

<u>Keywords</u>

I - Introduction

1. The human brain

The human brain is the most complex system in the animal kingdom [1]. It controls our thoughts, memory and speech, arm and leg movements, as well as the function of many organs within the body. Additionally, throughout the human lifespan, the whole brain's volume changes [2]. It grows until adolescence and then sets until around 35 years of age, when it starts a steady volume loss [2].

1.1   The meninges

The brain is located inside the skull, that protects it from external injuries. Between the skull and the brain, there are three layers of tissue called meninges, that cover and protect the brain and spinal cord [3]. From the outermost to the deepest layer, they are: the dura mater, arachnoid mater and pia mater (Figure 1) [3,4].
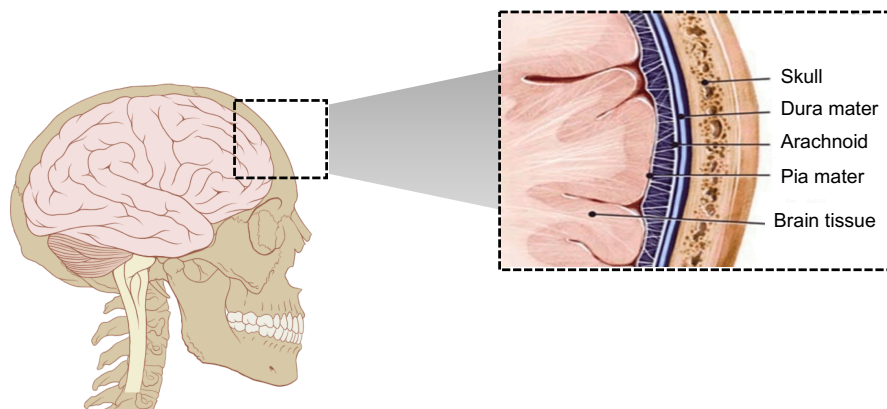
Figure 1 – The human brain meninges
The human brain is enveloped by three layers of tissue called meninges: dura mater, arachnoid and pia mater.
Figure inspired by [4] and https://en.wikipedia.org/wiki/Human_brain .

The dura mater is a thick, dense and fibrous membrane that is quite inelastic. It is composed of two fused layers: the periosteal layer that is close to the skull and is mainly composed of fibroblasts, osteoblasts and extracellular collagen conferring the dura's strength; and the meningeal layer that is closer to the brain tissue [5].

The arachnoid layer is a thin wispy avascular membrane that lies between the dura and the pia maters and is involved in cerebrospinal fluid (CSF) [3]. Its structure consists of three layers: a superficial mesothelial layer below the dura, a central layer composed of cells conjoined by many junction proteins, and a deep layer of less tightly packed cells with many collagen fibbers within their intercellular space [5].

Finally, the pia mater, the deepest layer of the meninges, is composed of the epinial layer, that contains mesothelial cells and collagen fibbers, and the intima pia, which consists of elastic and reticular fibbers [6]. The mesothelial cells connect the pia mater to the arachnoid matter and the intima pia adheres to the outermost layer of neural tissue, known as the glial membrane [3]. Moreover, the cerebral pia mater forms sheaths around the blood vessels that enter and exit the brain perpendicularly to the meninges [7].

1.2   Brain components and function

The nervous system is divided into the central nervous system (CNS) and the peripheral nervous system (PNS). The CNS is composed of the brain, its cranial nerves and the spinal cord, whereas the PNS is composed of the spinal nerves that branch from the spinal cord and the autonomous nervous system [8].

The brain can be divided mainly in three parts: forebrain, midbrain and hindbrain (Figure 2). The forebrain is divided into the diencephalon, which contains the *thalamus* and hypothalamus that control sensory and autonomic processes, and the telencephalon, which comprises the cerebrum [9]. The cerebrum takes up the majority of the space and controls somatosensory and motor functions, language, cognition, memory, emotions, hearing, and vision [10].
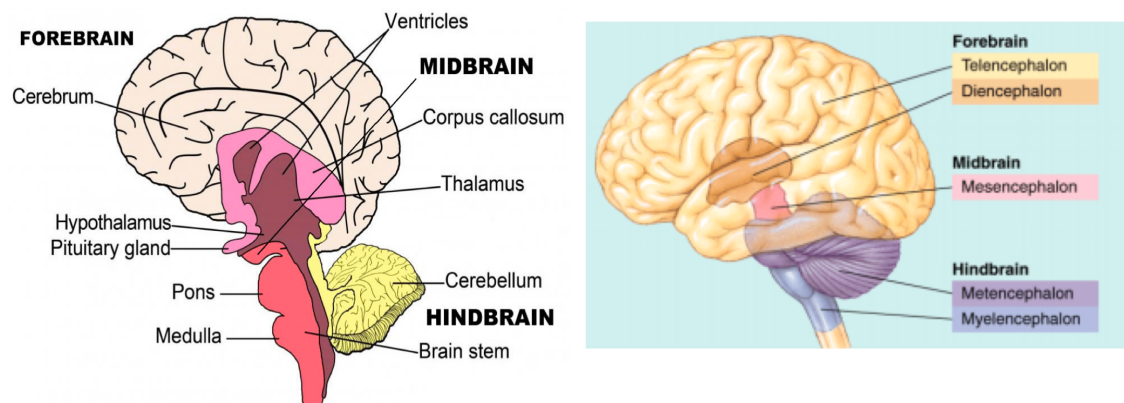
Figure 2 – Human brain components
The brain can be divided in 3 main components: forebrain, midbrain and hindbrain.
The cerebrum can be further subdivided in 4 lobes: frontal, occipital, parietal and temporal.
Adapted from https://www.wisegeek.com/what-is-neuropsychology.htm# and http://brainvisor.com/structure-function%20(1).html .

The midbrain ensures the connection between the forebrain and the hindbrain, transmitting signals between them [9]. Moreover, it is where the basal ganglia and related nuclei are located (Figure 3). These structures are involved in motor control, motor learning, executive functions and behaviour, as well as emotions [11].
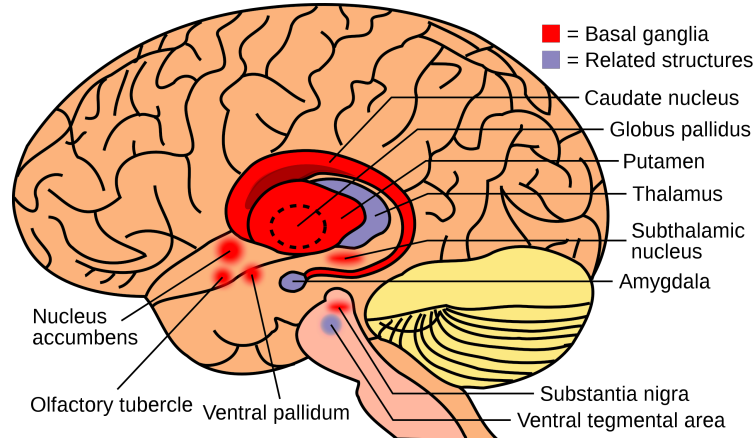
Figure 3 – Basal ganglia and its related nuclei
Representation of the basal ganglia and its related nuclei location in the human brain.
Source:https://commons.wikimedia.org/wiki/File:Basal_ganglia_and_related_structures_(2).svg

Basal ganglia stands for the nuclei deeply embedded in the brain hemispheres (*striatum* or caudate-*putamen* and *globus pallidus*) and the related nuclei consist of structures located in the diencephalon (subthalamic nucleus), mesencephalon (*substantia nigra*) and pons [11]. The basal ganglia and related nuclei can be

additionally categorized as input, output and intrinsic nuclei. The input nuclei are composed of the caudate nucleus, the *putamen* and the *accumbens* nucleus and are responsible for receiving incoming information mainly from the cortex, *thalamus* and the *substantia nigra* [11]. The internal segment of the *globus pallidus* and the *substantia nigra pars compacta* are the output nuclei and thus send basal ganglia information to the *thalamus* [11]. The intrinsic nuclei are composed of the external segment of the *globus pallidus* and relay the information between the input and output nuclei [11].

The hindbrain can be divided into three sections: medulla oblongata, pons and cerebellum. Its main function is to control certain physiological functions of the body such as heart rate, breathing and blood pressure [12].

1.2.1 Brain lobes

The human brain is divided by a deep longitudinal fissure into the left and right hemispheres, that are kept in contact with one another by the corpus callosum [10]. Each individual tends to use more a hemisphere than the other and usually the left hemisphere is the dominant one [10]. Each hemisphere can be then subdivided into the frontal, parietal, occipital and temporal lobes, with each lobe carrying out different functions [10] (Figure 4).
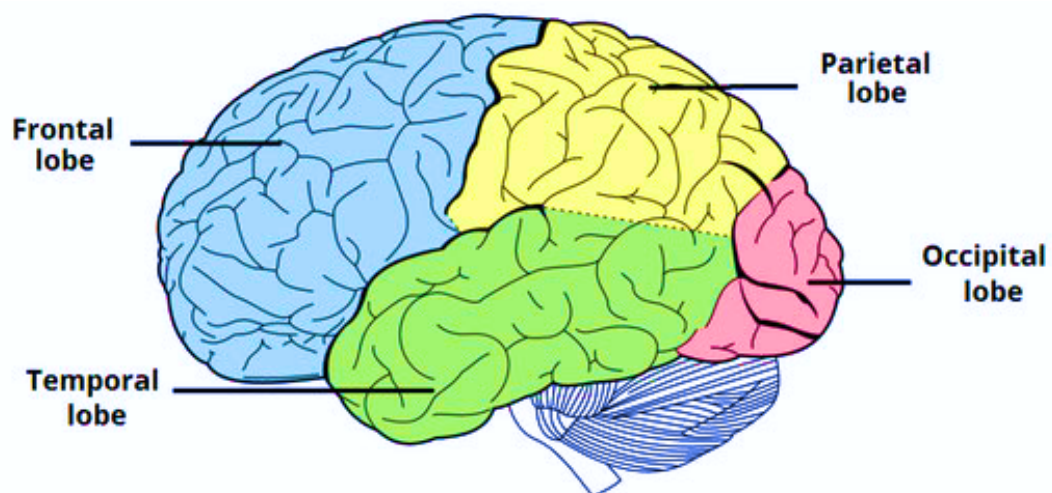
Figure 4 – Human brain lobes
Representation of the location of the 4 different lobes in the human brain.
Adapted from © By TeachMeSeries Ltd (2020).

4

The frontal lobe is the largest of the four lobes and is responsible for several functions such as motor skills, judgement, abstract thinking, creativity and maintaining social appropriateness. It includes the primary motor and prefrontal cortices [13]. The primary motor cortex, or percental gyrus, is the area responsible for movement [10]. The prefrontal cortex is considered the "personality centre" where we process moment-to-moment inputs from our surroundings and manifest our insight, foresight and planning capabilities into the actions that define who we are [14]. Lesions in this area often cause neuropsychiatric disorders such as disinhibition, apathy, loss of initiative and personality changes [14].

The parietal lobe controls perception and sensation such as the sense of touch, temperature and pain in parts of the contralateral body, i.e. the body side opposite to that of the parietal lobe's hemisphere [10]. Injury in the parietal lobe can therefore cause loss of sensations that depend on which hemisphere the injury takes place. For instance, damage in the dominant hemisphere would cause agraphia, acalculia, finger agnosia and left-right disorientations [10]. Damage in nondominant parietal lobe hemisphere would cause agnosia of the contralateral side of the field of vision, also known as the hemispatial neglect syndrome [10].

The occipital lobe is the smallest lobe and forms the caudal part of the brain [15]. It is responsible for its visual processing area, being associated with visuospatial processing, distance and depth perception, colour determination, object and face recognition and memory formation [15].

The temporal lobe can be divided into superior, middle and inferior temporal gyruses (Figure 5) [10]. It controls language comprehension, hearing and memory [10].
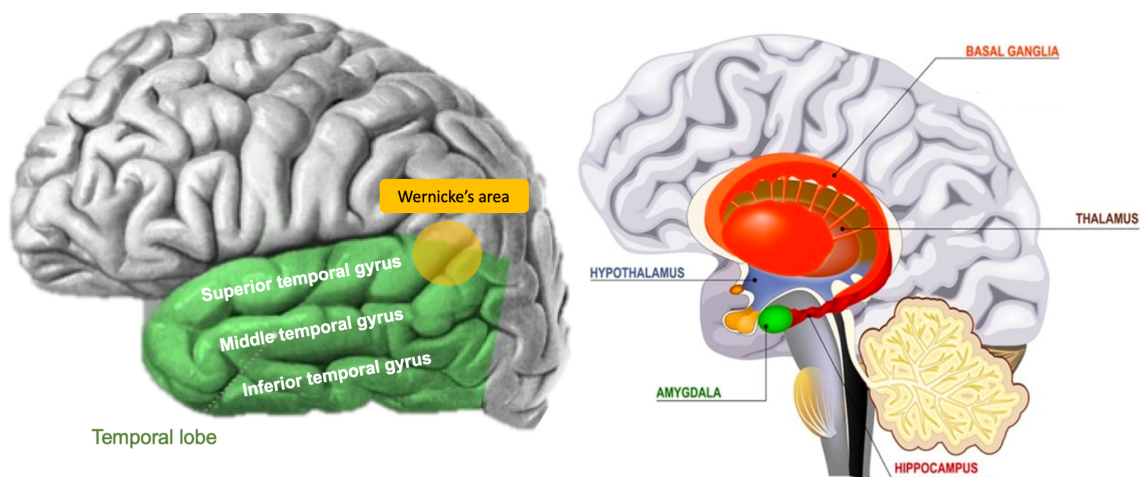
Figure 5 – Temporal lobe
Representation of the temporal lobe division as well as the location of the hippocampus and amygdala.
Adapted from © Assoc Prof Frank Gaillard, Radiopaedia.org, rID: 46670 and ID 139569785 © Designua | Dreamstime.com.

Wernicke's area, responsible for language comprehension, is located in the superior temporal gyrus of the dominant hemisphere [16]. Damage in this specific area causes receptive aphasia where one is unable to comprehend or express written or spoken language [16].

The primary auditory cortex area, which is responsible for processing most auditory information from the contralateral ear, is also located into the superior temporal gyrus [10]. Moreover, the hippocampus and amygdala can be found in the medial temporal lobe, with the amygdala located just in front the hippocampus (Figure 5) [17]. Those two regions play a key role in emotional learning and memory [17].

1.3 Brain cell types

The human brain is considered a complex organ, being composed of several different cell types. It is estimated that the entire brain is made of 67-86 billion neurons, around 40-50 billion glial cells and 20-25 billion endothelial cells [18]. For decades, it was thought that the glia-neuron ratio (GNR) for the entire human brain was 10:1 but, since 2009, it has been established that the GNR is, in fact, closer to 0.7:1 [18]. Additionally, this ratio can vary between brain areas and with age. For

instance, the grey matter of the human cerebral cortex evolves from a GNR of 0.3:1 in the new-borns to a GNR of 2:1 in adulthood [18].

1.3.1 Neurons

Given the very high number of estimated neurons in the human brain, it is not surprising that several different neuronal cell types exist. Although the best neuronal classification is still debated in the neurobiology field, there are three main categories, namely, morphological, functional and molecular, that can be used for that purpose [19].

The neuronal classification based on the function considers the direction of the action potential (neuronal electric impulses that send signals around the body) being classified as sensorial, motor or interneurons [8]. The sensorial neurons (also known as afferent neurons) are responsible for conducting the action potentials to the CNS, while the motor neurons (also known as efferent neurons) conduct the action potentials from the CNS to the muscles or glands, and the interneurons conduct the action potential from one neuron to another in the CNS [8].

The morphological properties of a neuron are based on its dendritic and axonal shapes, soma size and spine density [19]. Indeed, neurons can be classified as multipolar, bipolar or unipolar [8] (Figure 6).
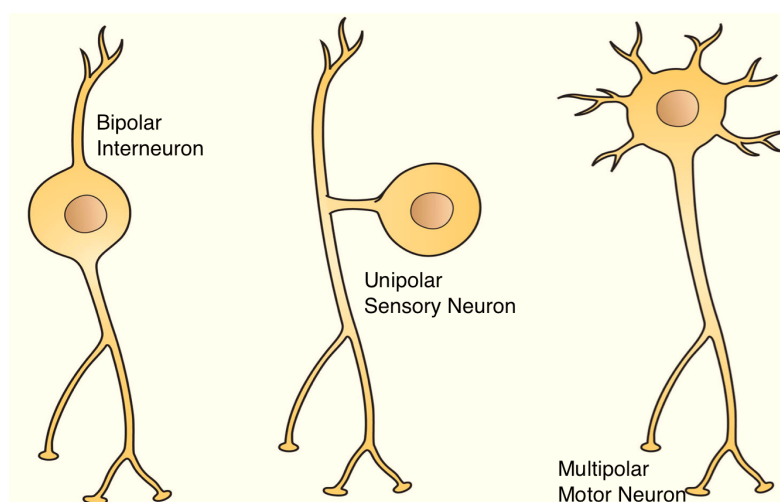
Figure 6 – Neuronal morphological types
Morphologically, neurons can be classified as multipolar, bipolar or unipolar.
Adapted from
https://commons.wikimedia.org/wiki/File:Three_Basic_Types_of_Neuronal_Arrangements.png .

Multipolar neurons have several dendrites and only one axon, being found mainly in the CNS, while motor neurons are also multipolar [8]. Bipolar neurons have one dendrite and one axon, and are usually found in some sensorial organs such as the retina, the eye and the nasal cavity [8]. As for unipolar neurons, these are in fact pseudo-unipolar. They have an extension that divides in two branches: one axonal that goes to the CNS and one peripheric that goes to the periphery where it ramifies into sensorial receptors, similarly to the dendrites [8]. The two branches function as a unique axon [8].

The most commonly used molecular properties to classify neurons are based on their protein and mRNA composition [19].

1.3.2 Glial cells

Although glial cells are not as diverse as neurons, they are essential for normal body function. In the PNS, glial cells can be divided into Schwan cells, satellite cells and enteric glia [20]. This thesis will focus on the CNS glia and as such these cells will be introduced in more detail.

The glia in the CNS is composed of astrocytes, microglia and oligodendrocytes. Their relative abundance can vary between brain regions but oligodendrocytes are the most abundant glial cell type, reaching up to 45-75% of total human brain glial cells, followed by astrocytes with 19-40%, and microglia contributing with 10% or less [19].

Astrocytes are present in the entire CNS and are responsible for many physiological functions, such as synaptic transmission and information processing by neural circuits, as well as maintenance of water and blood-brain-barrier (BBB) homeostasis [21]. They respond to all forms of CNS insults by a process referred to as astrogliosis, considered to be a pathological hallmark of CNS structural lesions [21].

Microglia are the most abundant mononuclear phagocytes in the CNS [22]. They are responsible for several important processes in the brain, such as elimination of

microbes, dead cells, redundant synapses, protein aggregates and other antigens that might harm the CNS [23]. In a healthy adult brain, microglia are ramified, maintaining an immunological stable environment, although they are not able to do phagocytosis or present antigens [22]. Only when sensing an injury in the CNS, they become activated and acquire a fully active phagocytic form, secreting proinflammatory mediators and neurotoxins [24] and giving rise to the microgliosis process. As such, they also participate in the removal of damaged neurons and foreign substances and are responsible for immunological surveillance, secreting growth and pro-inflammatory factors such as prostaglandins, TNF-α and free radicals [25]. These factors are needed for normal biological functions but have to be tightly regulated to avoid over-activation that triggers a neurotoxic response [25].

Oligodendrocytes' primary function is to produce the myelin sheath that wraps the axons of many nerve cells. This process facilitates neuronal transmission via saltatory action potential that takes advantage of the conductance over the nodes of Ranvier, forming the white matter of the CNS [26]. Oligodendrocytes are considered the largest non-neuronal cell population in the brain [27]. Oligodendrocyte precursor cells (OPCs) represent up to 5% of cells in the mature brain and are characterized by the expression of the proteoglycan nerve-glial antigen NG2. These cells are the main class of proliferating cells that can differentiate into oligodendrocytes, astrocytes and possibly neurons, although this ability to differentiate remains debatable [28].

1.3.3 Neuron-glia interaction

Although astrocyte and microglia populations have very specialized roles and show heterogeneous distributions across brain tissue, their functional interplay and interaction with neurons are also relevant for the maintenance of a healthy brain [29,30]. Neuron-glia interactions are responsible for several developmental processes in the brain: neurogenesis; myelination; synapse formation, maturation and plasticity; neuronal migration, proliferation, differentiation and signalling [31,32]. Moreover, soluble factors, like neurotransmitters, hormones and growth factors secreted by glial and neuronal cells, also play a role in the nervous system's morphogenesis [32].

Another important feature of neuron-glia interaction is the BBB. It is mainly composed of endothelial cells and perivascular end feet of astrocytic glia and acts as a selective physical barrier by facilitating the entrance of required nutrients to the brain and excluding potential harmful compounds [33]. Besides, many features of the BBB can be modulated under physiological conditions through the release of transmitters and modulators by neurons, astrocytes and endothelium cells [33]. For example, the BBB can allow the passage of growth factors and antibodies needed into the brain by opening its endothelial cells' tight junctions [33].

1.4 Brain diseases

The brain is a very tightly regulated and complex organ. As such, when its function is impaired, it can lead to several types of disease. Neurological disorders contribute to 11.6% of global disability-adjusted life years (DALYs) and 16.5% of deaths from all causes, being the leading group cause of DALYs and the second leading group cause of deaths in the world [34]. Since 1990, there was an increase of 39% in the number of deaths and an increase of 15% of DALYs from neurological disorders [35].

Stroke is the largest contributor to global neurological DALYs, being responsible for 47.3% of DALY and 67.3% of deaths in 2015 [36] (Figure 7). Migraine is the second largest contributor, followed by Alzheimer's and other dementias and meningitis [36]. Indeed, migraine and Alzheimer's disease (AD) and other dementias were ranked among the top four contributing neurological conditions in all the 21 world regions where the Global Burden of Diseases, Injuries, and Risk Factors Study (GBD) was performed [35].
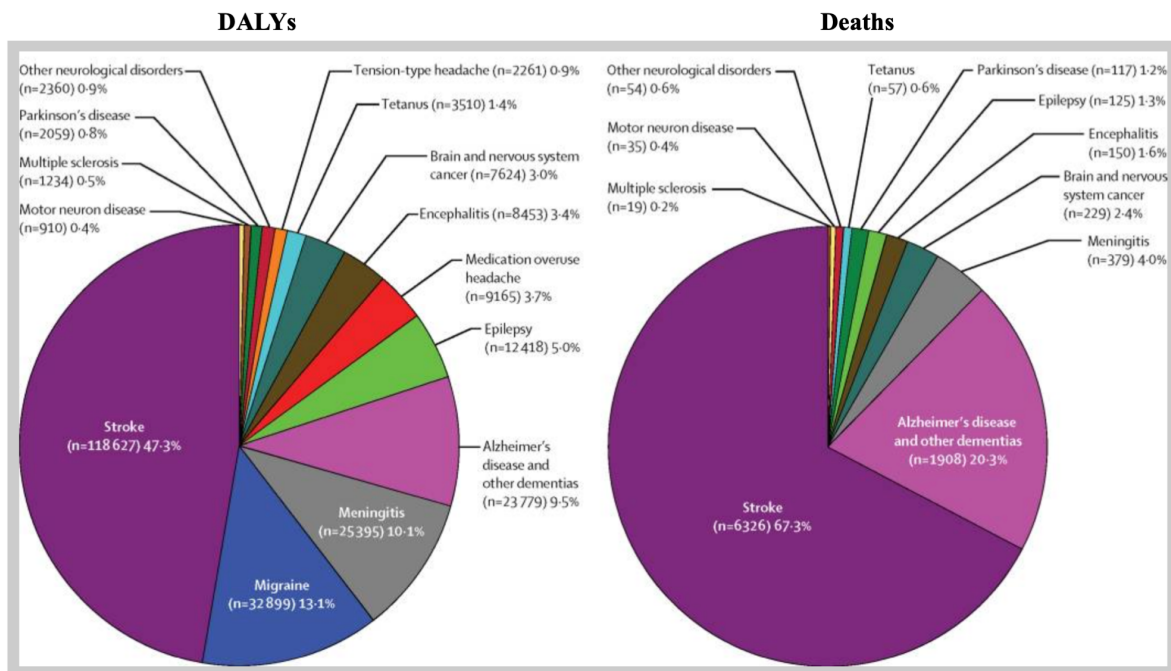
Figure 7 – Relative contribution of different neurological disorders to their overall burden
Estimates of the disability-adjusted life years (DALYs) and deaths caused by several neurological disorders in 2015.
Figure adapted from [36].

The burden of neurological disorders is large and increasing, challenging the sustainability of health systems. It is therefore imperative to discover new leads for the design of more effective treatments and preventive measures. Hence, in this PhD thesis we will focus on the molecular aspects of Alzheimer's and Parkinson's diseases.

2. Alzheimer's disease

2.1 Epidemiology

Worldwide, a new case of dementia is diagnosed every three seconds and, by 2018, around 50 million people were known to be living with dementia, a number that is expected to more than triple by 2050, as the population ages [37]. Alzheimer's disease (AD) is the biggest single cause of dementia, accounting for up to 80% of cases diagnosed, and its prevalence is expected to double every 5 years after the age of 65 [38].

Considering that the population older than 60 years is expected to increase by 2050 [39] (Figure 8) and that age is a major risk factor for AD [40], it is expected that AD's incidence and prevalence will also increase [41,42]. Moreover, more women than men are diagnosed with AD, which can be partially driven by more women surviving until older ages, when dementia becomes more prevalent [43].
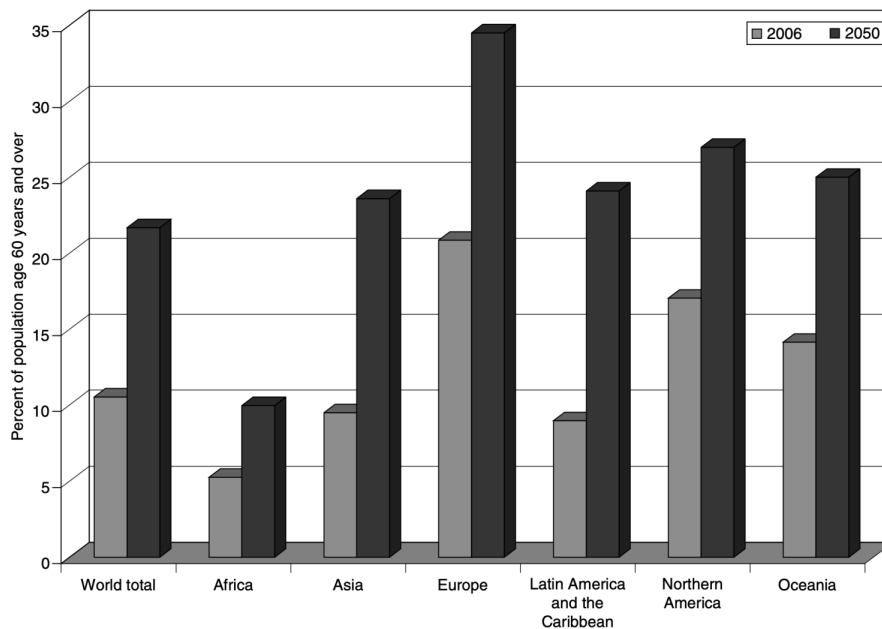
Figure 8 – Percentage of population aged 60 years and over worldwide
It is expected that, by 2050, the world population with 60 years of age or above will double compared with 2006.
Figure adapted from [39].

2.2 Aetiology

AD can be classified according to age of onset and genetic predisposition. Most AD cases (~ 95%) are diagnosed as late onset AD (LOAD), around the age of 65, and are considered to be mainly sporadic [44]. Conversely, early onset AD (EOAD), manifesting in individuals between 30 and 60 years old, is mostly familial AD (FAD) and accounts for 1 to 6% of all cases [40]. Although both EOAD and LOAD can be found in patients with a family history of AD [40], around 60% of EOAD patients have several relatives with AD diagnosed and, from the cases within these families, 13% are inherited in an autosomal dominant manner with at least three generations affected [45,46].

Progressive problems centred on episodic memory are the commonest symptoms of AD in elderly individuals and can be related to amnestic mild cognitive impairment (MCI) [47]. Difficulties related with self-orientation and multitasking, as well as loss of confidence, are other symptoms that appear in AD [38]. As the disease progresses, cognitive problems become more profound and can widespread and interfere with daily living activities, increasing the patient's self-care dependency [38]. Later on, symptoms such as behavioural changes, impaired mobility, hallucinations and seizures might appear [38]. AD patient's death will occur, on average, 8.5 years after those symptoms' appearance [48].

The most common autosomal dominant inherited mutations in FAD cases are mainly found in three genes, namely, amyloid precursor protein (*APP*) where 221 mutations were reported, presenilin 1 (*PSEN1*) with 32 mutations described and presenilin 2 (*PSEN2*) with 19 mutations reported [49,50]. Moreover, *PSEN1* and *APP* mutations are linked to dementia cases with an earlier onset, contrasting with *PSEN2* mutations that account for the rarest FAD cases and are associated with a later age of onset (> 60 years in 52% of cases) [49,50]. FAD cases associated with mutations in both *APP* and *PSEN1* genes are generally characterized by a faster course of the disease and by frequent atypical clinical manifestations such as weakness and stiffness of the legs and prominent language impairment [49].

LOAD is considered to be likely driven by a complex interplay between genetic and environmental factors. Apolipoprotein E (APOE) genotype is the strongest risk factor for LOAD. *APOE* has three common alleles (ε2, ε3, ε4), where one *APOEε4* allele increases AD risk by 3-fold and two *APOEε4* alleles increase AD risk by 12-fold [51,52]. Thus, *APOEε4* is also associated with a dose-dependent decrease in age at onset [51]. Contrastingly, *APOEε2* is associated with a decreased risk for AD at late age onset [51,52]. Recently, a variant in the *TREM2* gene, that encodes a receptor expressed in myeloid cells that mediates inflammatory responses, was also shown to confer the same AD risk as one copy of the *APOEε4* allele [53,54]. Despite first-degree relatives of patients with LOAD having approximately twice the expected lifetime risk of the disease, there is no Mendelian inheritance pattern of transmission [40].

Genome-wide association studies (GWAS) have identified several common and rare variants as genetic AD risk factors (Figure 9), not only related with amyloid-beta (Aβ) production and clearance but also with lipid metabolism, inflammatory response and endocytosis [55]. Additionally, common risk variants that individually confer only a very small increase in AD risk can almost double the risk if combined and have been used as a polygenic risk factor [56].
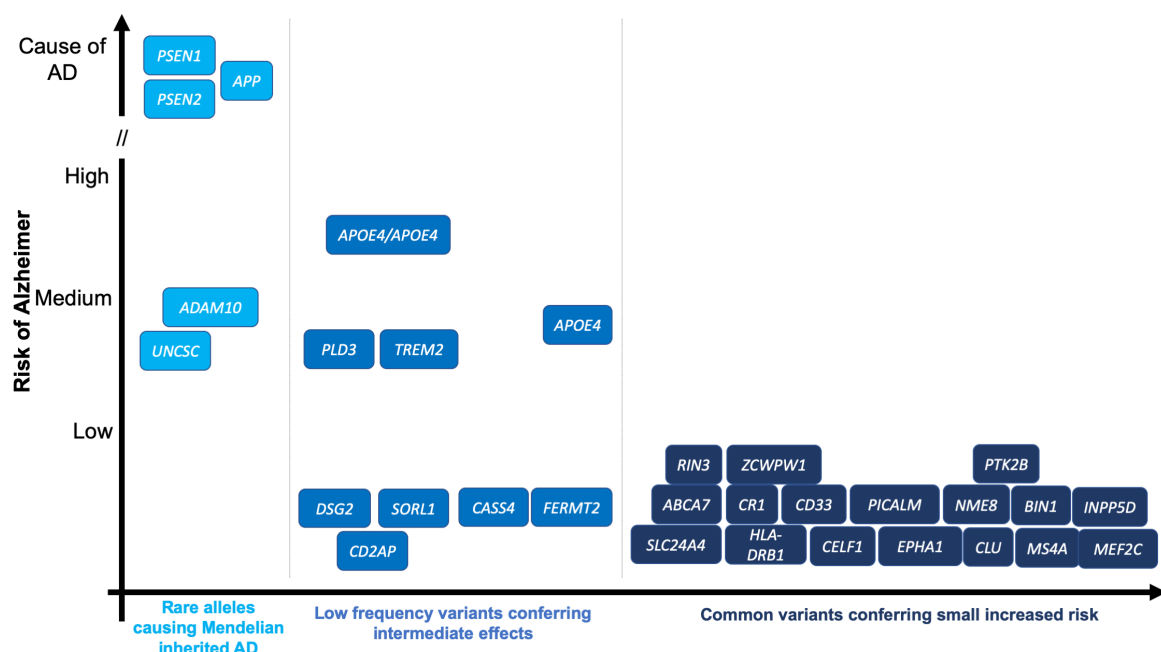
Figure 9 – Genetic variants associated with AD risk
Summary of genes implicated in AD by GWAS.
Figure adapted from [38] and [55].

Despite 70% of AD risk being thought to be related to genetic factors [38], several non-genetic factors have also been associated with increased risk of AD, the most consistently reported being the presence of a cerebrovascular disease and its antecedents [41]. Clinical history of diabetes, hypertension, smoking, obesity, and dyslipidaemia have all also been reported to increase AD risk [41,47,57]. However, other factors, such as undertaking oestrogen, statins, antihypertensive medications and non-steroidal anti-inflammatory drug therapy, having a diet rich in folate, vitamin E/C and coffee, as well as being intellectually and/or physically active, have shown to be protective against AD [41,57].

2.3 Pathology

AD brains do not show any gross macroscopic alteration that can be considered as diagnostic [58]. They show a moderate degree of cortical and medial temporal atrophy affecting the amygdala and the hippocampus, usually together with an enlargement in the frontal and temporal horns of the lateral ventricles [59]. This dilation of the temporal horns can be detected by magnetic resonance imaging (MRI), early in the clinical course of the disease [60,61]. Other macroscopic features that can be observed in AD brains include loss of neuromelanin pigmentation in the *locus coeruleus*, white matter volume loss and decrease in brain weight [59]. However, these changes are not specific enough to diagnose AD with certainty since similar alterations can be observed in the brains of non-AD elderly individuals or associated with other age-related disorders [58,59,62].

A microscopic examination of multiple brain regions is needed in order to properly diagnose AD [63]. The main characteristics for AD pathologic diagnosis are amyloid plaques deposition and neurofibrillary tangles (NFTs) [64].

Amyloid plaques are extracellular accumulations, specific of AD, composed primarily of abnormally folded amyloid-beta (Aβ) peptides with 40 or 42 amino acids (Aβ40 and Aβ42, respectively), two natural byproducts from the APP metabolism, after APP's sequential cleavage by the enzymes β- and γ-secretases in neurons [64]. Although the normal function of APP is not fully understood yet, Aβ production and secretion are known to be stimulated upon synaptic activity [65]. The Aβ42

peptide tends to be more abundant in amyloid plaques than Aβ40 due to its higher rate of fibrilization and insolubility [38].
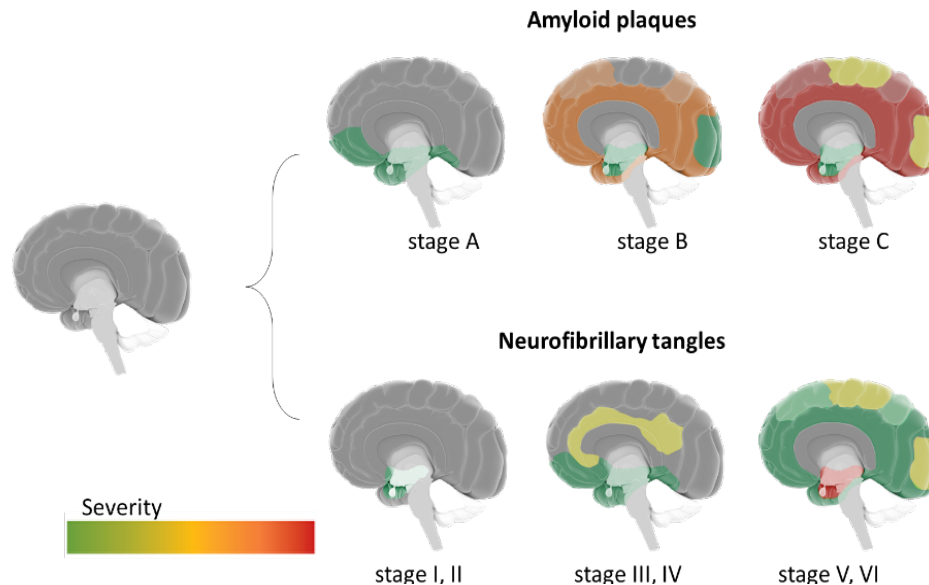
Figure 10 – Amyloid plaques and neurofibrillary tangles in AD progression
Schematic representation of amyloid (top) and tau (bottom) pathologies' progression through the brain.
Figure kindly provided by Sara Mendes [70], inspired by [47].

Most mutations in *APP*, *PSEN1* and *PSEN2* result in the overproduction of Aβ, specially Aβ42 [47]. Indeed, patients carrying mutations in those genes have lower Aβ42/Aβ40 ratios in plasma and higher Aβ42 production in the central nervous system (CNS) [66,67].

Accumulation of amyloid plaques can be summarized into three stages (Figure 10): isocortical (amyloid deposits mainly found in the basal portions of the frontal, temporal, and occipital lobes), allocortical or limbic (hippocampal formation is only mildly involved, and the primary sensory, motor, and visual cortices are devoid of amyloid), and subcortical (deposition of amyloid in the primary isocortical areas and, in some cases, the appearance of amyloid deposits in the molecular layer of the cerebellum and subcortical nuclei such as the *striatum*, *thalamus*, hypothalamus, subthalamic nucleus, and red nucleus) [68–70].

Although amyloid plaque deposition is part of AD diagnosis, it does not correlate with the severity nor the duration of the associated dementia [64]. The amyloid burden reaches a plateau early after the onset of the cognitive symptoms or at the

preclinical phase of the disease and even the size of the plaques does not correlate with its course [71,72]. Conversely, due to neuronal and synapse loss typically paralleling tangle formation, NFTs are better correlated with clinical features and severity of AD [71].

NFTs are mainly composed of the microtubule-associated tau protein in an aberrantly misfolded and abnormally hyperphosphorylated state [64]. Often, neuropil threads, thought to result from the breakdown of dendrites and axons of the tangle-bearing neurons, can be found along NFTs [64]. Essentially, the accumulation of NFTs starts in the medial temporal lobes and hippocampus and spreads progressively to other areas of the neocortex [47] (Figure 10). Thus, NFTs' presence, in contrast with amyloid plaques', is less AD-specific since it is also observed in several other neurodegenerative diseases such as progressive supranuclear palsy, corticobasal degeneration, and subtypes of frontotemporal dementia [65].

Other features of AD brains can be microscopically analysed. For instance, besides Aβ being the main component of amyloid plaques, it can also be deposited in the cerebral blood vessels leading to cerebral amyloid angiopathy [73]. In fact, 85-95% of AD cases have some degree of cerebral amyloid angiopathy [59]. Another microscopic characteristic found in the cytoplasm of hippocampal pyramidal neurons of AD brains is the granulovacuolar degeneration and Hirano Bodies [64]. The origin and significance of granulovacuolar degeneration is still unknown and consists in the accumulation of large double-membrane bodies. The Hirano Bodies are eosinophilic rod-like cytoplasmic inclusions that are also detected in the hippocampal CA1 region of elderly brains but show a higher number and a translocation towards the neurons of the stratum pyramidal in AD brains [64]. Their role is not fully understood. Finally, neuronal and synapse losses, as well as glial responses, are also cellular AD-related markers [59]. Indeed, synapse loss, that is probably triggered by amyloid and tau pathology [74,75], seems to precede neuronal loss as well as being strongly correlated with cognitive decline in AD, even surpassing the associations with neuronal loss and tau burden [76].

2.4   Pathogenesis

AD pathogenesis remains not fully clear. Several hypotheses have been proposed, namely, the amyloid cascade, the cholinergic and the mitochondria-associated endoplasmic reticulum membrane (MAM) hypotheses.

2.4.1 Amyloid cascade hypothesis

The amyloid cascade hypothesis is the most commonly accepted theory. It states that AD pathogenesis starts as a series of abnormalities in the processing and secretion of APP through its sequential cleavage by β- and γ-secretases in the brain and the unbalance between production and clearance of Aβ is its trigger event and most important factor [77]. Although its function remains unclear, APP was already suggested to play a role as a surface receptor, an adhesion molecule, a regulator of neuronal processes such as neurite outgrowth and synaptogenesis, a signalling molecule and a regulator of cell survival and death [78]. The fact that Aβ depositions are found in AD brains, their known neuronal toxic properties *in vitro* and that FAD cases have mutations linked either to Aβ production or processing leading to overproduction of toxic forms of β-amyloid, support the amyloid cascade hypothesis [79]. However, nowadays it is thought that Aβ oligomers, instead of Aβ plaques, are the most toxic and pathogenic form of Aβ and that Aβ plaques may indeed act as a protective reservoir [80,81].

2.4.2 Cholinergic hypothesis

The cholinergic hypothesis was presented over 35 years ago and suggests that a selective dysfunction of cholinergic neurons is the major responsible for the cognitive decline observed in elderly and AD brains [82]. Thus, the major alterations in cholinergic neurons are considered to be the choline uptake, impaired acetylcholine release, deficits in the expression of nicotinic and muscarinic receptors, dysfunctional neurotrophin support, and deficits in axonal transport [82–84]. Additionally, some studies have already shown that Aβ can interact with cholinergic receptors, affecting their function [85]. Although the relationship between

cognitive impairment and decreased cholinergic transmission is known to play a role in AD, it does not establish a definitive AD causation by itself [64].

2.4.3 MAM hypothesis

Besides plaques and tangles, other biochemical and morphological features, such as altered calcium, glucose, cholesterol and phospholipid metabolisms, increased endoplasmic reticulum (ER) stress and changes in dynamics and reduction of bioenergetic functions of mitochondria, are present in AD brains [86]. Since all these features are associated with functions occurring within a subdomain of the ER, known as mitochondria-associated ER membranes (MAMs), and MAM-localized functions are significantly increased in cellular and animal models of AD and in cells from AD patients, Area-Gomez and colleagues suggested the MAM hypothesis [87]. MAM is a dynamic and highly specialized subdomain of the ER that is physically and biochemically connected to mitochondria, formed directly by the apposition of bulk ER with mitochondria [88]. The abnormal increase of MAM function in AD affects cellular processes such as calcium homeostasis, cholesterol and phospholipid metabolism. That leads to cellular consequences such as altered APP processing and tau phosphorylation, causing formation of Aβ plaques and tangles, among other phenotypes, that all together contribute to AD onset [88].

2.5   The specific roles of brain cell types in AD

AD brains are characterized by extensive neuronal cell death that can occur through apoptosis, necrosis, autophagy or cytoplasmic disfunction [89,90] and an intense glia reaction (gliosis) response [89].

2.5.1 Neurons

Neuronal survival and function are compromised in the presence of exogenous Aβ [91–96]. For instance, glutamatergic neurons expressing a mutated *APP* exhibit altered APP subcellular distribution and differential cleavage by β- and γ-secretases, perturbing Aβ production and causing an elevated tau phosphorylation

[97]. Additionally, neurons carrying *APP* mutations exhibit a functional impairment in cellular uptake, trafficking and degradation pathways, as well as ER and oxidative stress [98].

Studies have highlighted that neurons harbouring homozygous *APOEε4* alleles, the major risk factor of AD, derived from iPSCs (induced pluripotent stem cells), besides producing more Aβ and having higher phosphorylated tau than iPSC-derived neurons with *APOEε3* alleles [99,100], also present endosome abnormalities and defects in autophagy and mitophagy [98]. Moreover, glutamatergic neurons with *APOEε4* alleles showed more synaptic sites and increased frequency of spontaneous synaptic transmission [99]. GABAergic *APOEε4* interneurons tend to degenerate in culture as opposed to glutamatergic and dopaminergic *APOEε4* neurons, whereas the *APOEε4* cholinergic neurons exhibited elevated sensitivity and altered Ca^{2+} signalling in response to glutamate toxicity [98]. Essentially, there are differences in neuron sub-type Aβ secretion and susceptibility to Aβ-induced toxicity, especially between glutamatergic and GABAergic neurons [101,102].

2.5.2 Astrocytes

Astrogliosis is detected in *post-mortem* AD brains by the presence of reactive astrocytes with a marked cellular hypertrophy and increased glial fibrillary acidic protein (GFAP) and S100B expression [103]. Reactive astrocytes are also found near amyloid plaques and perivascular β-amyloid deposits, contributing to the local inflammatory response and modulation of calcium signalling [104–106].

Although astrogliosis could be considered a protective reaction, since it is triggered upon a CNS injury, in AD cases it seems to contribute directly to defective clearance of potential harmful metabolites such as Aβ due to the downregulation of Aquaporin 4, that plays an important role in the normal glymphatic flow [27,107]. Besides, upon Aβ exposure, astrocytes become activated, expressing inflammatory markers earlier and displaying abnormal synchronous Ca^{2+} transients over long distances, showing their relevance in Aβ catabolism [27]. Reactive astrocytes are capable of accumulating large amounts of Aβ and neuronal nicotinic cholinoreceptor, known to

have high affinity to β-amyloid [104,105]. Indeed, astroglial β-amyloid deposits were already shown to participate in plaques formation [108]. Besides, PET studies confirmed that astrogliosis is an early event in patients, being the strongest signal seen in prodromal AD [109].

Despite these observations, it is still unclear whether astrogliosis is beneficial or harmful in AD. For instance, in APP/PS1 mice, the attenuation of astrocyte activation through deletion of *GFAP* and *Vimentin* genes showed an acceleration in plaque pathogenesis and a marked increase in dystrophic neurites [110]. However, another group showed the opposite effect in similar models [111]. Those contradictory findings might be explained by the stage of AD and the brain region affected [112].

Nonetheless, the relationship between amyloidosis, tau pathology, and astrogliosis remains to be elucidated.

2.5.3 Microglia

In AD, microglia are often found near Aβ plaques [113,114] and were shown to play a dual role in the disease. On the one hand, they help eliminate the Aβ aggregation through phagocytosis and, on the other hand, they facilitate Aβ accumulation via the release of neurotoxic proteases and inflammatory factors [24]. Moreover, activated microglia can secrete various inflammatory molecules such as IL-1, IL-6, TNF-α, free radicals and chemokines, all associated with the Aβ cascade during the start and development of AD [24]. Essentially, under neurodegeneration conditions, microglia detect damage-associated patterns that are created through defective cells releases, including misfolded proteins and aggregated peptides, which activate the pattern recognition receptors of microglia, leading to a sustained release of neuroinflammatory factors that promotes neurodegeneration and disease progression [115].

Besides microgliosis, the majority of identified AD risk genes being selectively or preferentially expressed in microglia also points to the importance of microglia in AD brains [116]. TREM2, a cell surface receptor selectively and highly expressed in microglia, has been specially driving attention to microglia's role in AD. Its most

clearly associated mutation with AD appears to be a loss-of-function mutation, impairing TREM2 ligand binding and phagocytosis by microglia [117,118]. In physiological conditions, TREM2 interacts with the activation adaptor DAP12 and initiates signal transduction pathways that promote microglial chemotaxis, phagocytosis, survival and proliferation [119–121]. Thus, TREM2 extracellular ligands include a variety of phospholipids and glycoproteins, namely APOE and CLU, two proteins encoded by well-known AD-risk genes [116]. Other extracellular ligands of TREM2 are apoptotic neurons [122]. Indeed, microglia maintain tissue homeostasis through clearance of debris and TREM2 is required for microglial phagocytosis of a variety of substrates including apoptotic neurons and Aβ [116]. Moreover, TREM2-deficient microglia showed a reduced uptake of Aβ-lipoprotein complexes *in vitro* [123] and less evidence of Aβ internalization *in vivo* [124], suggesting that TREM2 loss-of-function increasing risk of developing AD might be related to these impairments in Aβ uptake and clearance.

2.5.4 Oligodendrocytes

In 1996, Braak suggested a link between the neurons' vulnerability and their myelination stage, as the spreading of NFTs seemed to recapitulate the pattern of myelination in reverse order [125]. Thus, white matter loss is one of the earliest brain changes in AD, preceding even the appearance of tangles and plaques [126]. A variety of structural, histopathological and biochemical pathologies take place in the AD patients' white matter. For instance, radiological markers of white matter damage, believed to reflect demyelination and axon damage, can be observed in patients as young as 22 years old, an even earlier onset than expected in patients carrying AD mutations [127]. Moreover, oligodendrocytes and OPCs are thought to be either altered in number and in the stability of their DNA or functionally less efficient in the presence of genetic changes, oxidative stress, increased iron levels and vascular pathology [128,129]. Additionally, some AD mouse models show white matter disruption and changes in the expression of myelin markers as the first pathological changes and only show cognitive impairments between 3 and 6 months of age [130].

In summary, white mater loss in AD is thought to be caused by several factors namely oxidative stress, apoptosis, neuroinflammation and excitotoxicity, associated with accumulation of Aβ and tau hyperphosphorylation [126,131].

2.6   Diagnosis

According to the latest diagnostic criteria, AD's clinical onset can be divided in three broad periods: preclinical, MCI and AD dementia, with the time elapsed between each period being in the order of decades [132]. Although AD can only be certainly diagnosed after a detailed *post-mortem* microscopic examination, a combination of tools and clinical tests can be used to diagnose living AD patients with more than 95% accuracy [133].   These include the clinical review of the patients' familiar history, as well as cognitive functions' evaluation through neuropsychological tests [134]. Blood tests are also performed to exclude conditions other than AD that might cause or contribute to cognitive symptoms, including assessment of full blood count, renal function, thyroid function, vitamin B12, infections, cancer, depression and folate levels [38,133].

MRI is also recommended for patients with cognitive impairment to exclude structural abnormalities and to provide positive diagnostic information [135]. For instance, the detection of focal symmetrical medial temporal atrophy has predictive value for AD [136]. Thus, MRI can also be used for differential diagnosis, helping in the exclusion of other neurodegenerative diseases and the evaluation of the presence and extent of cerebrovascular diseases that might mimic or co-occur with AD [38]. Additionally, amyloid positron-emission tomography (PET) is also used in the clinical context, with florbetapir, flutemetamol and florbetaben being the agents approved by the European Medicines Agency (EMA) and the US Food and Drug Administration (FDA) to be used in PET scans for AD diagnosis. These compounds have been shown to bind to fibrillary β-amyloid and highly correlated with the β-amyloid burden at *post-mortem* [137–139]. However, the cost of amyloid PET scan is not reimbursed by the public health systems in most countries and, as such, its use is still being evaluated in terms of clinical utility and cost-effectiveness [38].

Cerebrospinal fluid (CSF) examination is also used to diagnose AD, given CSF's higher levels of tau and phosphorylated tau and decreased levels of Aβ42 in AD cases [140]. Moreover, those CSF biomarkers can also help to predict the development of AD by MCI individuals [140], which is clinically important since 15% of MCI cases progress to AD [141]. This evaluation is included in the AD diagnosis criteria [142].

Finally, although routine testing of genetic risk factors such as the *APOE* status is not prescribed, genetic testing can be used to identify autosomal dominant causes of AD when these are suspected [38].

2.7   Treatment

At the moment there is no cure for AD. The drugs currently prescribed for this disease are only symptomatic and can be divided in three groups: inhibitors of acetylcholinesterase, antagonist of a N-methyl-d-aspartate (NMDA)-type receptor for the neurotransmitter glutamate and psychiatric drugs to control depression and behavioural abnormalities [133].

AD patients are known to have impaired cerebral cholinergic functions implicated in cognitive losses [143]. Therefore, acetylcholinesterase's inhibitors are used to compensate for the depletion of the neurotransmitter acetylcholine in AD brains by inhibiting its degrading enzyme, acetylcholinesterase, thus improving the cholinergic transmissions [133]. Three commonly prescribed cholinesterase inhibitors are donepezil, galantamine and rivastigmine. Although they showed small beneficial effects in functional and/or cognitive scores, they do not translate in consistent benefits in patient-oriented outcomes such as the quality of life or institutionalization need [144].

Although excitatory glutamatergic neurotransmission via NMDA receptors is critical for neuronal survival and synaptic plasticity, its excessive activity causes excitotoxicity, promoting cell death [145]. In AD, since neuronal cell death correlates with the progressive decline in cognition/memory and the development of

pathological neural anatomy, Memantine, an NMDA receptor antagonist drug, is also prescribed [145]. It is the only drug targeting NMDA receptors approved by FDA in 2003 [144]. However, despite randomized clinical trials showing small benefits in cognition, global and functional status in moderate to severe dementia, these were not consistently seen in less severe AD cases [144]. Overall, Memantine is currently used to treat cognitive and functional symptoms in patients with moderate to severe AD [144]. In the clinic, the combination of Memantine with a cholinesterase inhibitor may be used to treat the symptoms of patients with moderate to severe AD since Memantine is tolerable and there is no other beneficial treatment for cognitive and functional decline [144].

Many AD patients also suffer from psychiatric or behavioural problems contributing to a reduction of their life quality and, by consequence, an increasing burden to their families and community. The antipsychotics commonly prescribed for AD patients are risperidone and olanzapine. However, their use is controversial given that they are related with elevated mortality rate and risk of cerebrovascular adverse events whereas only showing small benefits for psychotic symptoms in AD [146]. Anticonvulsant mood stabilizers and antidepressants such as benzodiazepines are also commonly used for treating psychiatric or behavioural symptoms, although their usage is controversial since several AD clinical trials showed none or very small benefits with potential high adverse effects such as sedation, falls and gastrointestinal problems when taking those drugs [146].

Nonpharmacological therapies are also used to improve cognitive and functional symptoms in AD. Those therapies include: participating in leisure activities, leading to decreased neuropsychiatric symptoms and higher functional capacity as well as slowing memory loss; participating in mental stimulation programs, such as puzzles, that can improve cognition and self-reported quality of life and well-being; doing occupational therapy training in coping strategies and getting help from cognitive aides; performing structured physical exercise programs to improve physical function, reduce neuropsychiatric symptoms such as depression and slow the functional decline rate [144].

3.1 Epidemiology

Parkinson's disease (PD) is the second most common neurodegenerative disorder in the world, affecting 1 to 2% of individuals with over 60 years of age [147]. In 2016, it is estimated that there were 6.1 million individuals affected with PD and that this number will continue to increase due to demographic changes [148,149] (Figure 11).

Considering that the percent of population older than 60 years is expected to increase by 2050 [39] and age is a major risk factor for PD [150], it is expected that its incidence and prevalence will also increase [148]. Moreover, men have twice the risk of developing PD than women, although women have a higher mortality rate and faster progression of the disease [151].
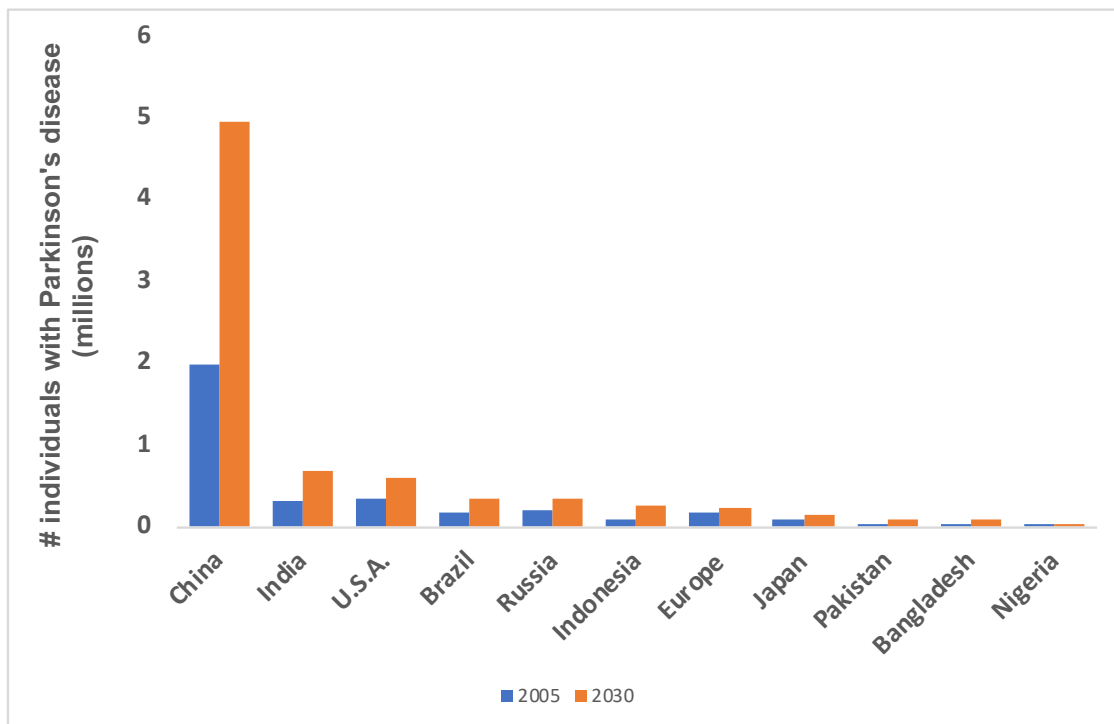
Figure 11 – Projected number of individuals with PD per country
Estimated numbers of individuals over the age of 50 with PD in different countries. The values for Europe are for the five most populous nations in Western Europe (Germany, France, the United Kingdom, Italy, and Spain).
Adapted from [149].

3.2 Aetiology

The majority of PD cases are idiopathic, that is, they have unknown aetiology, although 5-10% of the cases have a strong genetic component [152]. PD is indeed considered a multifactorial disease in which both genetic and environmental factors play a role [153].

The first PD-related symptoms usually do not develop until 70-80% of dopaminergic neurons are lost [154]. They usually consist in bradykinesia, muscular rigidity, resting tremor and postural instability not caused by primary visual, vestibular, cerebellar or proprioceptive dysfunction [155]. Bradykinesia is the most common symptom and may be apparent as soon as the patient enters the consulting room or when the patient undresses in order to be examined, although it can also be assessed through its facial immobile and rigid expression or its slow, quiet and lacking rhythm and melody speech [150]. A common test to analyse the patient's bradykinesia is by asking him/her to perform a rapid and repetitive finger taping of the index finger on the thumb for about 20 seconds on each hand [150]. Bradykinesia can also be assessed for the lower limbs by observing the patient doing fast foot taping and walking [150]. Bradykinesia is confirmed when there is a demonstration of slowness and a progressive reduction of speed and amplitude on sequential motor tasks.

Cigarette smoking and coffee drinking have been shown to reduce the risk of developing PD [156,157], although the underlying reasons are not fully understood. Additionally, the association between caffeine and PD differs between gender, being stronger in men than in women [158]. Other lifestyle factors, such as having a diet rich in fruits, vegetables and grains, as well as frequently practicing high intensity physical activity, were also shown to decrease the risk of PD [159].

The usage of injectable drugs contaminated with MPTP (1-methyl-4-phenyl-1,2,3,6-tetrahydropyridine) cause typical PD signs via the metabolization of MPTP into the neurotoxin MPP+ (1-methyl-4-phenylpyridinium), a mitochondrial complex I inhibitor that selectively damages dopaminergic cells in the *substantia nigra* [160]. After this

study in 1983, several others have shown an association between PD and the usage of pesticides and herbicides, namely Paraquat, an herbicide structurally very similar to MPP+, and rotenone [161]. Both of these are also selective inhibitors of mitochondria complex I and have been shown to induce dopaminergic depletion in animal models of PD [162].

To date, several common and rare gene variants have been linked as genetic PD risk factors [163] (Figure 12). Moreover, 5% of the minority of PD cases that have reported family history of the disease have Mendelian inheritance [153]. *SNCA*, *LRRK2* and *MAPT* are the genes most significantly associated with PD in GWAS and candidate gene association studies and they all present an autosomal dominant inheritance of the disease [164].
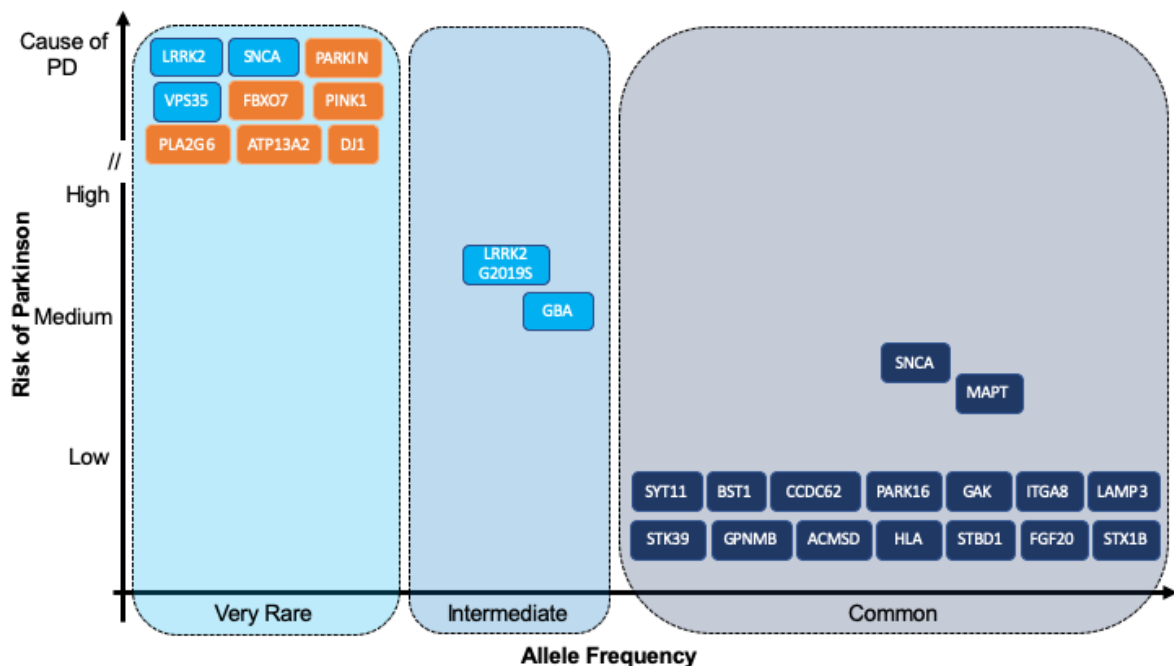
Figure 12 – Genetic variants associated with PD risk
Summary of genes implicated in PD by GWAS and candidate gene association studies. Light blue genes are dominantly inherited, orange genes are recessively inherited and dark blue genes lay on PD risk loci.
Figure adapted from [163].

The α-synuclein (*SNCA*) gene was the first to be linked to the disease in 1997, in a large family of Southern Italy, where a missense mutation (A53T) was found to segregate with the disease [147]. This mutation was found in several other families of Greek and Italian origins as well as with rare frequency in patients from Korea,

Sweden, Poland, Spain, United Kingdom, France, Japan and China [165]. Later, other *SNCA* point mutations and whole-locus multiplications (duplications, triplications and quadruplications) were also found to be associated with PD [165]. This gene is considered pleiomorphic in the context of PD risk given that both rare mutations and common variation at its locus alter the risk of the disease. For instance, there seems to be a *SNCA* genomic dosage-related PD phenotype since patients with homozygous duplications and four copies of *SNCA* have earlier and more severe symptoms than those with a single *SNCA* mutation [166]. Non-coding genetic variability in the *SNCA* locus confers risk and predisposes to genetically complex PD [164].

Genetic variants in *LRRK2* account for the majority of known heritable PD cases, with the most pathogenic variant, G2019S, being responsible for about 1% of PD patients with genetically complex PD and 4% with a family history of PD [165]. This specific variant has the highest frequency among the North African Arab and Jewish population, as well as in the Middle East and in Southern Europe, compared to Northern Europe [164]. Additionally, six other mutations were proven to be pathogenic [167]. *LRRK2* mutations have an age-related penetrance and clinical features identical to late-onset idiopathic PD [168].

Although *MAPT* mutations have been predominantly associated with dementias, they have also been shown to be associated with PD. There are two major haplotypes at the *MAPT* locus: the directly oriented haplotype H1 and the inverted sequence containing H2 [164]. *MAPT* H1 sub-haplotypes were found to be preferentially associated with PD, suggesting that haplotype-specific differences in the expression, and potentially in the alternative splicing of *MAPT*, affect cellular functions at different levels, increasing susceptibility to PD [169].

VPS35, the vacuolar protein sorting 35 ortholog gene, that encodes a core component of the retromer complex, has recently emerged as a novel cause for autosomal dominant familial PD, although the molecular mechanism by which it induces progressive neurodegeneration in PD is still unknown [170]. The D620N mutation, initially found in a Swiss PD family, was also reported in families from other origins such as the United States, Tunisia and Israel [171]. This mutation seems

predominantly linked to families of Caucasian descent with autosomal dominant PD and rare in the Asian population, except for the Japanese [170]. It is estimated that the *VPS35* D620N frequency in patients with familial PD is between 0.1 to 1% [172].

It was observed in the clinic that first- and second-degree relatives of patients with Gaucher's disease, a lysosomal storage disorder, had an increased PD incidence [173,174]. Thus, some patients with Gaucher's disease presented parkinsonism features suggesting a strong link between *GBA* and PD [175,176]. Heterozygous *GBA* mutations are actually the largest genetic risk factor for developing PD, conferring an approximately 5-fold risk increment [177]. Moreover, it is estimated that 5-10% of PD patients carry a *GBA* mutation and that their penetrance and lifetime risk of developing PD varies with age, from around 20% at 70 to 30% at 80 years old [178]. Despite being considered a substantial common risk in PD, its frequency varies according to ethnicity, being particularly more frequent in Ashkenazi Jewish individuals [164].

Other genes with an autosomal recessive transmission were also found to play a role in PD. Unlike the autosomal dominant forms of PD that tend to have an age of onset similar to idiopathic PD, the autosomal recessive forms present an earlier onset, typically less than 40 years old [179].

Mutations in Parkin (*PRKN*) are the most common cause of autosomal recessive PD, being present in up to 50% of all early-onset PD cases [180]. Mutations in *PRKN* were found in familial and idiopathic PD patients across populations from all ethnic origins and seem to be linked to loss of function of PRKN [180]. In physiological conditions, *PRKN* encodes an E3 ubiquitin ligase that helps to eliminate dysfunctional mitochondria and unwanted proteins in the cell. These processes can be impaired when *PRKN* is mutated, leading to an excessive accumulation of protein and mitochondria, resulting in cell death [176].

PINK1 is the second most common gene that, when mutated, can cause autosomal recessive PD and it is also involved in mitochondrial maintenance and quality control [163]. Remarkably, *PINK1* shares the same mitochondrial pathway as *PRKN* [150]. Moreover, both *PINK1* and *PRKN* are ubiquitously expressed and, when their

function is lost, lead to selective loss of dopaminergic neurons and manifestations of PD symptoms such as tremor and bradykinesia [181]. Mutations in *PINK1* are estimated to account for 1-8% of all early-PD onset cases [182].

Mutations in *DJ-1* are very rare causes of autosomal recessive PD. They are estimated to account for 1-2% of all early onset PD cases [182]. *DJ-1* is known to also be important for mitochondrial health, although its function remains to be characterized [179]. *PRKN*, *DJ-1* and *PINK1* mutations are all associated with an early onset of PD, a slow progression of the disease and a positive response to levodopa treatment that compensates for the loss of dopamine [180].

ATP13A2, *PLA2G6* and *FOXB7* are autosomal recessive genes shown to cause parkinsonism with atypical features [147]. For instance, specific mutations in *ATP13A2*, that encodes a lysosomal membrane protein with an ATPase domain predominantly expressed in the brain, cause an atypical parkinsonism also known as the Kufor-Rakeb syndrome [183]. Patients with mutations in that gene have a very early onset, at 11 to 16 years old, and a rapid progression of parkinsonian symptoms [180]. Mutations in *PLA2G6* and *FBXO7* have also been found in autosomal recessive families, although their frequency is very low, with individuals also presenting a very early onset of the disease [180].

The PD risk factor genes can be summarized as belonging to major biological pathways such as autophagy, endocytosis, mitochondrial biology, immune response and lysosomal function [164]. All these pathways have already been shown to be implicated in PD [164].

3.3   Pathology

PD can be divided into six neuropathological stages (Figure 13). It starts by affecting the olfactory bulb and/or the dorsal motor nucleus of the glossopharyngeal and vagal nerves (stage I) and ultimately reaches the neocortex (stage VI), with several years mediating between those stages [184].
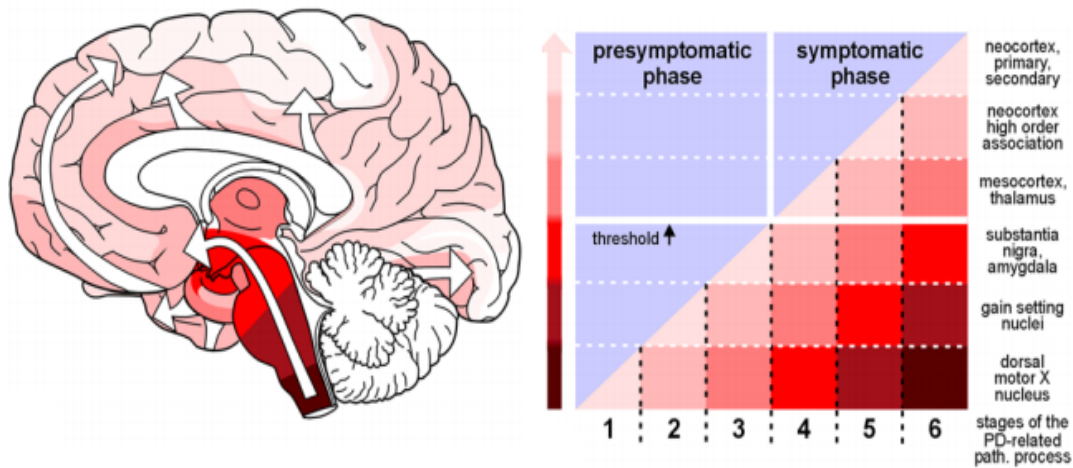
Figure 13 – The six neuropathological stages of Parkinson's disease
The severity of the pathology is indicated by darker degrees of shading in the coloured arrow in the middle. The white arrows in the left panel indicate the ascending pathological process.
Adapted from [184].

However, macroscopically, the idiopathic PD brain does not show any gross alteration, only mild atrophy of the frontal cortex and ventricular dilation in some cases [153]. Sections of PD brainstems often show a loss of the normally dark pigment in the *substantia nigra* and *locus coeruleus* that is correlated with the loss of dopaminergic and noradrenergic neurons, respectively [185]. The most profoundly affected area in the *substantia nigra* is the ventrolateral tier, that contains neurons projecting to the dorsal *putamen* of the *striatum* [179]. Moreover, other brain regions suffer neuron loss in PD such as the amygdala and hypothalamus [185].

Microscopically, the main hallmark of PD is the presence of Lewy bodies (i.e. intracellular aggregations of lipids and proteins, namely α-synuclein) in neuronal cell bodies and axons [152]. Besides being present in the *substantia nigra*, this manifestation can also be found in the spinal cord and in the peripheral nervous system [179].

In humans, α-synuclein belongs to a three-protein family composed by α-, β- and γ-synucleins and is distinguishable from β- and γ-synucleins by the non-amyloid-β component (NAC) region of its plaques [186]. Alpha-synuclein exists in several conformations in a dynamic equilibrium, modulated by internal and external factors that can both either promote or inhibit its fibrillation [187]. Moreover, α-synuclein is abundantly expressed in the nervous system, comprising 1% of total cytosolic

proteins, although it can also be found in erythrocytes and platelets [188]. Despite α-synuclein's function not being fully understood yet, it seems that it modulates synaptic transmission and controls neurotransmitter release [188]. Moreover, α-synuclein can bind to anionic lipids, which suggests that it can interact with biological membranes *in vivo* [187], by adopting an atypical α-helical structure (Figure 14). It is though that α-synuclein exists in equilibrium between its unstructured monomeric forms and its tetrameric α-helical oligomeric structure that is resistant to fibrillization [189,190].
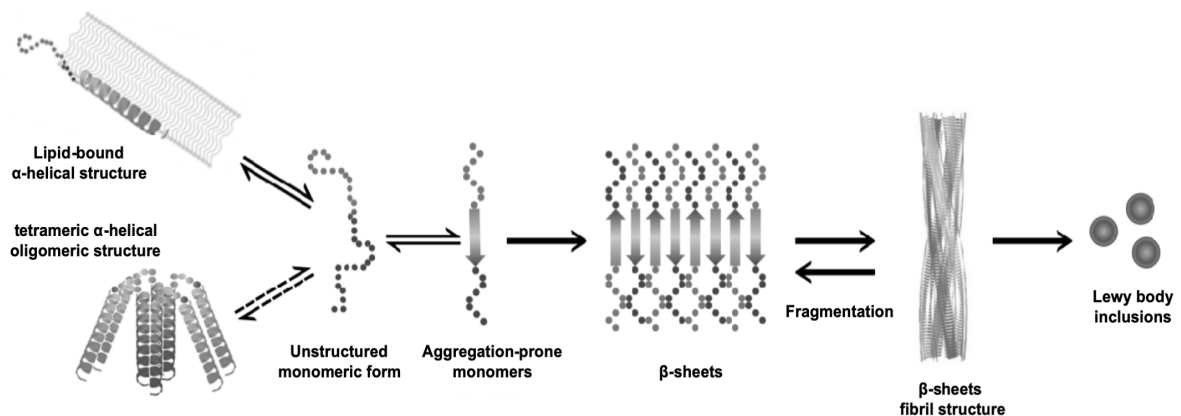
Figure 14 – α-synuclein's fibrillization process
Unfolded α-synuclein exists as a monomer but, when interacting with lipids, forms an α-helical structure. There is an equilibrium between α-synuclein's unstructured monomeric form and its tetrameric α-helical oligomeric structure. Unfolded α-synuclein can also start to aggregate and give rise to β-sheets that can then be elongated and create β-sheet fibril structures. These fibril aggregates can then be sequestered into Lewy bodies.
Figure adapted from [190].

However, α-synuclein fibrilization can occur, leading to Lewy body formation. In fact, fibril formation requires α-synuclein's structure to suffer a conformational change from unstructured monomers to β-sheets. Once this becomes the predominant form, monomeric α-synuclein can begin to stack and form β-sheet fibril structures [189]. Besides being composed by those fibril forms, Lewy bodies also have partially truncated α-synuclein and aggregates of both full length and truncated protein [191]. Moreover, α-synuclein seems to be modified by several processes such as phosphorylation, oxidation, nitrosylation, glycation or glycosylation [188]. Although α-synuclein was found to be phosphorylated at S19 in Lewy bodies, it is not yet known the role, if any, this modification is playing in the neurotoxicity context [188]. All rare point mutations in α-synuclein that result in autosomal dominant familial PD

are in the N-terminal region and presumably cause the misfolding and/or aggregation of the mutant α-synuclein protein [187]. However, how these mutations accelerate aggregation remains unclear.

Besides α-synuclein aggregates, inclusions composed by other proteins such as β-amyloid and tau-containing neurofibrillary tangles, which are hallmarks of AD, can also be found in PD brains [179]. In fact, concomitant AD pathology is associated with a greater burden of Lewy body pathology, correlates with a shorter latency to onset of dementia in PD [192] and occurs in up to 50% of patients with PD and dementia [193]. Neuroinflammation is another feature found in PD pathology, as astrogliosis and microgliosis are found within areas of neurodegeneration in PD [179].

3.4   Pathogenesis

Several mechanisms have been implicated in PD pathogenesis. A-synuclein aggregation, however, seems to be central to the development of the disease, although other processes, such as abnormal protein clearance and mitochondrial dysfunction, have also been reported.

3.4.1 The spread of alpha-synuclein

Braak and colleagues developed an α-synuclein spread hypothesis based on the presence of pathological aggregates in different brain regions. As such, they suggest that PD might progress in six stages following a caudo-rostral pattern (Figure 13) [194]. However, not all PD cases follow this theoretical pattern neither does this hypothesis explain the absence of clinical symptoms in individuals whose autopsy reveals widespread α-synuclein pathology [195].

Two groups independently reported that PD patients subjected to embryonic mesencephalic neuronal engraftment into their *striatum* developed Lewy bodies many years after grafting [196,197], giving rise to the "prion-like" hypothesis to describe the mechanism of α-synuclein propagation. Essentially, this hypothesis states that α-synuclein would be released by living or dying cells into the surrounding extracellular milieu [195]. The released α-synuclein would then be absorbed by the

grafted neurons and serve as a template to promote the misfolding of the endogenously produced α-synuclein, leading to the formation of Lewy bodies [195]. Moreover, intracerebral injections of synthetic α-synuclein fibrils or homogenates of brain derived from α-synuclein-transgenic PD mouse models exhibiting Lewy pathology into young asymptomatic α-synuclein-transgenic mice stimulate both the formation of Lewy body-like inclusions and the onset of motor signs [198]. Although all these studies support the "prion-like" model for the spread of α-synuclein, it is worth to note that Mendez and colleagues reported lack of Lewy body pathology in five patients with PD, 9 to 14 years after transplantation of foetal midbrain cell suspensions [199]. However, these difference in results might be linked to differences in the incubation period, pattern of α-synuclein pathology, the graft environment, the number of years post-grafting, the animal model used, and individual differences between patients [200].

The detection of α-synuclein in the human plasma and in the cerebrospinal fluid (CSF), as well as in the medium of several types of cultured neurons, supports the idea that α-synuclein can be secreted [201–203]. However, the exact mechanisms by which α-synuclein is released and how the cells can internalize are not fully understood yet. It is hypothesized that α-synuclein can be passively released but only monomeric α-synuclein can pass through the cell membrane via a yet unidentified membrane translocator, suggesting that α-synuclein multimers are prevented from passively exiting the cell [200]. Additionally, it was hypothesized that cells might have mechanisms to recognize misfolded α-synuclein and selectively translocate such proteins into vesicles, reducing its intracellular neurotoxicity, and secrete the vesicular α-synuclein through non-canonical endoplasmic reticulum/Golgi-independent exocytosis [204].

LAG3 and neurexin 1a were also identified as receptors for preformed fibrils, but not monomers, able to initiate transmission of α-synuclein and accelerate its spread throughout mouse brains [205,206]. Exosomes are also considered to play a role in the spread of α-synuclein in PD. For instance, exosomes isolated from plasma of PD patients showed a higher concentration of α-synuclein when compared with those of non-PD individuals [207]. Moreover, exosomes may contain α-synuclein aggregates that can act as seeds for their spreading in the brain [208]. PD CSF

exosomes have indeed been shown to initiate oligomerization of soluble α-synuclein in targeted cells in a dose-dependent manner and confer disease pathology [209]. Furthermore, there is also the hypothesis that the pathogenesis of PD involves trans-synaptic cell-to-cell α-synuclein transmission from the olfactory bulb to the *substantia nigra* [210].

Several PD patients report gastrointestinal symptoms, which highlights the link between the gut and the brain in PD [211]. Indeed, it has been suggested that PD may be triggered by an unknown agent that breaches the intestinal epithelial barriers to induce α-synuclein aggregation in the enteric nervous system [212]. This hypothesis rises from the strong correlation of increased intestinal gut permeability with intestinal α-synuclein, as well as with staining of gram-negative bacteria and tissue oxidative stress, suggesting a role of gut leakiness in PD [213]. Essentially, it is proposed that α-synuclein misfolding might begin in the gut and spread to the brain in a "prion-like" manner via the vagus nerve into the lower brainstem and ultimately to the midbrain [212]. Plus, Lewy bodies and Lewy neurites were also found in the peripheral nervous system of the gut and in the sympathetic and parasympathetic ganglia in PD patients but also in apparently healthy individuals without typical motor symptoms or CNS pathology of PD [210].

Other putative mechanisms such as transmission through direct penetration, axonal transport or via trans-synaptic means, have also been proposed to be involved in α-synuclein cell-to-cell propagation [200].

3.4.2 Abnormal protein clearance

There are two main processes by which a cell can remove its dysfunctional proteins: the autophagy-lysosome pathway, responsible for the vesicle-mediated degradation of long-lived proteins and degradation of cellular organelle, and the ubiquitin-proteasome system (UPS) [214]. The mechanisms responsible for α-synuclein degradation are not identified yet and neither is how the cell decides if the degradation should be mediated by the UPS or the autophagy pathway.

Autophagy is responsible for maintaining homeostasis for intracellular recycling and metabolic regulation [215]. It mainly occurs in three forms: microautophagy, where the lysosomal membrane extends to invaginate the cellular contents for degradation; chaperone mediated autophagy (CMA), where a chaperone protein recognizes and directs proteins with a specific consensus sequence to the lysosome for degradation; and macroautophagy, where special structures called autophagosomes entrap the cellular contents and targeted proteins and then fuse with the lysosome for degradation (Figure 15) [215–217].
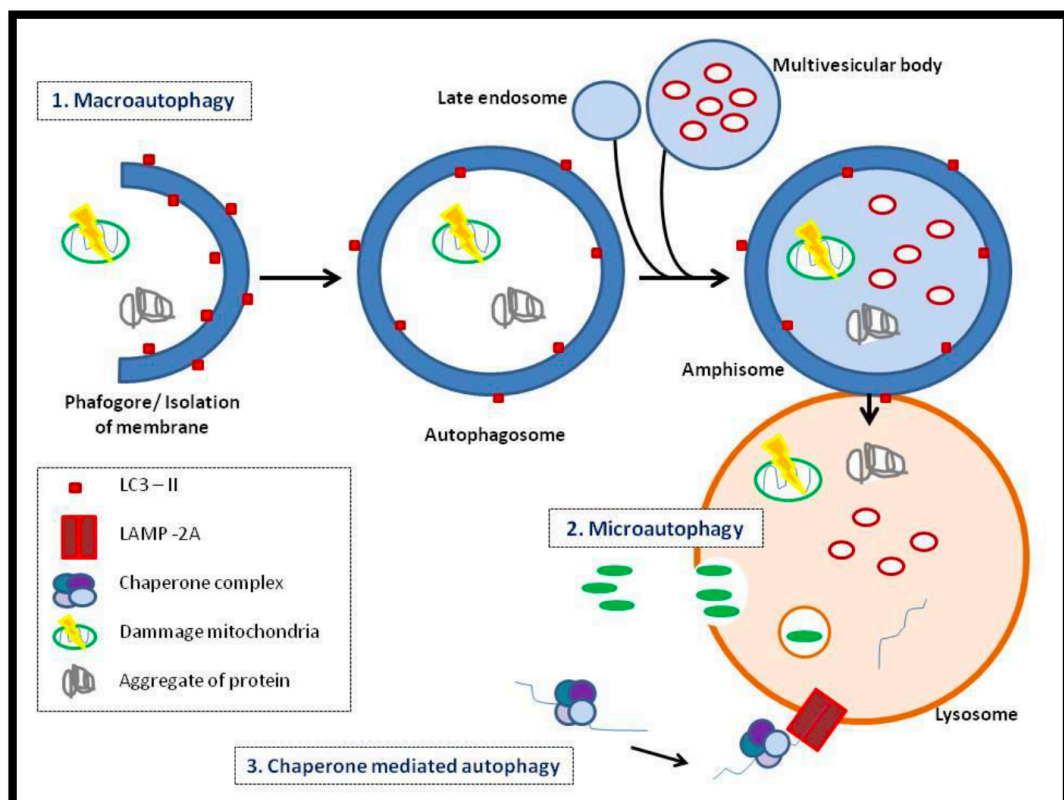
Figure 15 – The three autophagy processes
There are three different types of autophagy in the cell: macroautophagy (1) where the cytosolic components are delivered to the lysosome by vesicles; microautophagy (2) where the lysosomes capture small volumes of cytosol; and chaperone-mediated autophagy (CMA) (3), where the soluble substrates that present a specific chaperone complex are translocated into the lysosome through the LAMP-2A lysosomal receptor. Figure from [217], adapted from [216].

The first evidence postulating the involvement of autophagy in PD came when autophagic vacuoles were described in the *substantia nigra* of PD patients [218]. An increment in the autophagosome marker LC3-II protein and a decrease in the lysosomal markers LAMP1 and LAMP2A, as well as increases in several molecular chaperones such as HSC70 and HSP35, are also consistently found in PD brain

tissue and suggest the presence of abundant and dysfunctional autophagosomes and lysosomes [219]. Additionally, several genes whose mutations are known to confer PD risk are linked to autophagy, strengthening the hypothesis that this process may be contributing to PD pathogenesis. This is the case of mutations found in the *ATP13A2* gene which encodes for a lysosomal protein, the *PRKN* and *PINK1* genes that are involved in the autophagic turnover of mitochondria, or even the *GBA1* mutations that result in a dysfunction of the lysosome-autophagy system [153]. Moreover, wild-type monomeric α-synuclein has been shown to contain the specific consensus motif that is targeted and degraded by the CMA, whereas macroautophagy has been implicated in the clearance of α-synuclein oligomers as well as in mutant and post-transcriptionally modified forms of α-synuclein in cellular models of PD [220]. Furthermore, there seems to be a sensitive balance between α-synuclein intracellular accumulation and autophagy-regulated secretion that, if disturbed, can either promote aberrant intracellular accumulation or excessive secretion that can later contribute to the spread of PD through the nervous system [221].

The UPS is also an intracellular protein degradation system important for the turnover of the majority of short-lived proteins [222]. To be UPS-degraded, proteins have to be covalently tagged with ubiquitins, which are 76 amino acid proteins [223]. This tagging occurs via an iso-peptide bond ligated through a reaction that requires the sequential actions of ubiquitin activating (E1), conjugating (E2) and ligating (E3) enzymes [223]. These actions are usually repeated multiple times, allowing the formation of a polyubiquitin chain on the substrate that marks the protein for degradation by the 26S proteasome in association with two 19S regulatory caps [223]. These regulatory caps are mainly important for the initial steps of substrate proteolysis, namely recognition, unfolding and translocation of substrate proteins into the lumen of the proteolytic core [224]. After degradation, individual monomers are regenerated by the action of deubiquitylating enzymes [223].

The first evidence suggesting UPS' impairments are linked to PD came from UPS having a significantly reduced catalytic activity in PD compared with non-PD *substantia nigra* [225]. The same type of impairments were then also found in peripheral blood mononuclear cells of PD patients [226], together with lower

expression of different proteasomal components important for the normal function of the UPS [227]. Furthermore, *PRKN* and *UCH-L1*, both linked to monogenic PD, were shown to play a role in UPS function. PRKN seems to work as an E3-uniquitin protein ligase through its ring domains and may control protein levels via ubiquitination [228] whereas an *UCH-L1* missense mutation, found in a German family with PD, caused a partial loss of catalytic activity in this deubiquitylating enzyme [229]. Additionally, pharmacological inhibition of the proteasome in wild-type rats and transgenic mice was shown to lead to dopaminergic cell death as well as Lewy body-like inclusions in the *substantia nigra* of their brains [230,231]. All those findings suggest that UPS might play a role in PD pathogenesis.

3.4.3 Mitochondrial dysfunction

Mitochondria play a vital role in the regulation of cellular energy production, calcium homeostasis, bioenergetic quality control and cell death regulation [232]. Dopaminergic neurons in the *substantia nigra* are responsible for the highest cellular energy demand (~20%) of the human body and are also known to have a high rate of mitochondrial oxidative metabolism [232]. As such, it is not surprising that mitochondrial dysfunction is central for PD pathogenesis since the *substantia nigra* is the most affected area in PD brains. Thus, primary mitochondrial defects such as mutations in the polymerase gamma gene (*POLG*) are sufficient to cause not only loss of neurons in *substantia nigra*, among other neuronal populations in other regions, but also PD-like symptoms [233]. However, it is still unknown whether mitochondrial dysfunction is a cause of PD or a consequence of disease progression.

As mentioned before, α-synuclein can interact with membranes, namely the mitochondrial ones. A-synuclein possesses a non-canonical mitochondrial targeting sequence and seems to influence mitochondrial structure and function [234]. Moreover, increased levels of wild-type and mutated α-synuclein were shown to induce mitochondrial fission and production of reactive oxygen species (ROS) *in vitro* and *in vivo* [235]. Additionally, pathogenic mutations in α-synuclein were found

to reduce α-synuclein binding to the mitochondria-associated membranes important for Ca^{2+} signalling and cellular apoptosis [236].

PINK1, *PRKN* and *DJ-1*, genes linked to autosomal recessive PD, are also found to be key mediators of mitochondrial homeostasis and mitophagy (degradation of mitochondria by autophagy), further supporting the role of mitochondrial dysfunction in PD [233]. For instance, failure in the activation of *PRKN* through *PINK1*, known to be responsible for mitophagy and to be an essential pathway for mitochondrial quality control, causes persistence of damaged and ROS-producing mitochondria that lead to cellular stress [235]. Several studies already reported deficiencies in mitochondrial complex I, the first enzyme of the mitochondrial electron transport chain, in *PINK1* knockouts and mutants [235]. Mitochondrial localization of DJ-1 is neuroprotective and dependent on oxidation by ROS that can be inhibited when *DJ-1* is mutated [237]. Although DJ-1 can directly interact with both monomeric and oligomeric α-synuclein, it is still unclear if it happens at the mitochondrial level or in response to a stimuli such as DJ-1 oxidation [235].

Moreover, *LRRK2*, the most common mutated gene in familial PD cases, is also known to interact with a number of key regulators of mitochondrial fission/fusion, with its protein product shown to be co-localized with these in either in the cytosol or in the mitochondrial membranes [238]. In fact, increasing wild-type *LRRK2* expression was shown to cause mitochondrial fragmentation along with an increment in DLP1, a mitochondrial dynamin-like fission protein, that is even further exacerbated when *LRRK2* is mutated (G2019S) in SH-SY5 and differentiated primary cortical neuron cell lines [238]. Additionally, LRRK2 was also found to modulate the activities of Mfn1/2 and OPA1, both mitochondrial fusion regulators. Also, PD patients harbouring the *LRRK2* G2019S mutation present decreased levels of mature OPA1 [239]. Thus, the expression of mutant *LRRK2* and/or its wild-type overexpression in iPSCs from PD patients induces fragmented mitochondria that produce more ROS and less ATP and show an increased vulnerability to stressors [235]. For instance, iPSC-derived *LRRK2* G2019S dopaminergic neurons are much more vulnerable to H_2O_2, 6-hydroxydopamine (6-OHDA), rotenone, and proteasome inhibitors, than wild type iPSC-derived *LRRK2* dopaminergic neurons

[240,241]. In summary, the kinase activity of LRRK2 may be important to modulate mitochondrial fusion and fission in PD dopaminergic neurons.

All the aforementioned findings support the idea that mitochondrial dysfunction plays indeed a central role in the pathogenesis of PD. Noteworthily, alterations in pathways related with autophagy and lysosomes can also allow the accumulation of defective mitochondria, exacerbating mitochondrial dysfunctions that can then increase the oxidative damage to proteins and organelles in PD brains, leading to neuronal loss [233].

3.4.4 Autoimmunity

The immune system has been implicated in PD pathogenesis either through inflammation or as an autoimmune response [242]. However, it is not yet fully understood if this immune activation is a cause or a consequence of the observed neuronal loss.

An autoimmune disease is characterized by the presence of self-antigens and its associated auto-antibodies or specific autoreactive cells that are related to the observed pathology [243]. There are several studies that suggest PD to be an autoimmune disease given that the complement system, chemokines and cytokines, related with the innate immune system activation, were found highly increased in *post-mortem* brains [244]. Additionally, gamma delta (γ/δ+) T cells were also found increased in the peripheral blood and CSF of PD patients [245]. Moreover, serum levels of anti-α-synuclein antibodies were shown to be associated with the familial variants of PD and anti-GM1-ganglioside antibodies were associated with the tremor-dominant form of PD [246]. In another study that reinforces autoimmunity as playing a role in PD pathology, a CSF-derived auto-antibody that reacts with dopaminergic neurons in the *substantia nigra* was present in 78% of the tested PD patients but only in 3% of non-PD patients [247]. Furthermore, the cytotoxic effect of this CSF antibody on the dopaminergic neurons was also measured via immunoglobulin G (IgG), correlated with the degree of neurodegeneration in PD [248]. Consistently, purified IgG from PD patients injected in *substantia nigra* of adult

rats caused more degeneration of its neurons and selective damage to the nigrostriatal pathway when compared to injection of non-PD IgG [249].

Moreover, PD patients seem to have fewer naïve T cells and more activated T cells, as well as a lower number of T helper cells [250]. Besides, the presence of T cells was shown to be increased in the *substantia nigra* of PD patients, one of the brain regions most affected by the disease, suggesting that those cells underwent a targeted extravasation [250]. Additionally, T cells of PD patients were also found capable of generating an autoimmune response to α-synuclein [251], which could support the hypothesis of PD resulting from an autoimmune response triggered by the recognition of aggregated and misfolded α-synuclein as a foreign identity.

GWAS also reported a strong association between the human leucocyte antigen (HLA) class II region, a key molecule of the immune system, and the risk of developing PD [252]. Besides, the usage of ibuprofen, a nonsteroidal anti-inflammatory drug, was linked with a lower PD risk [253].

All these findings highlight the relevance of the immune system in PD, independently of it being considered a trigger of or a response to neurodegeneration in PD.

3.5   The specific roles of brain cell types in PD

As in AD, PD brains are also characterized by extensive neuronal cell death that can occur through apoptosis, necrosis, autophagy or cytoplasmic disfunction [89,90] and an intense glia reaction (gliosis) response [89].

3.5.1 Neurons

Dopaminergic neurons are those most prone to neurodegeneration in PD and the cellular basis of the first PD symptoms such as tremors. Some studies show that dopaminergic neurons might die through apoptosis and others find no signs of apoptosis in the nigral dopaminergic neurons [254,255]. Additionally, *substantia nigra* neurons contain neuromelanin, a pigment that is the oxidized product of

dopamine, that has also been considered a contributor to neuronal death in PD. Neuromelanin can capture iron and absorb pesticides, such as rotenone, that will promote an increase in oxidative stress resulting in the selective neuronal death in the *substantia nigra* [256]. Moreover, those neurons in transgenic mice can also degenerate upon high concentrations of melanin, producing PD-like symptoms as well as protein turnover dysfunction [257,258]. Furthermore, vulnerability of the *substantia nigra* to dopamine-induced oxidative stress and neuronal cell death might also be related to the diminished expression of the dopamine transporter therein in PD. This decrease leads to impaired dopamine storage and enhanced dopamine reuptake, causing cell death [259]. However, the *striatum* being not degenerated in PD and acting on dopamine might suggest that the location of dopamine concentration, i.e., cytoplasm vs. synapse, influences the selective vulnerability of the *substantia nigra* [260]. Besides dopaminergic neuronal death, PD brains also present neuronal degeneration in other regions [261].

Lewy bodies are another feature that can be found in PD neurons, although their contribution for promoting or preventing neuronal death is not yet established. Greffard and colleagues, for instance, showed that the percentage of Lewy body-bearing neurons and immunoreactive α-synuclein in the *substantia nigra* were not correlated with the symptoms or the disease duration [262]. Given this observation, they hypothesized that Lewy bodies are eliminated when the neurons that bear them die, suggesting that the destruction rate of Lewy bodies is equal to their production [262].

As mentioned before, *SNCA* has been found mutated in autosomal familial dominant PD, leading to the assumption that α-synuclein accumulation and misfolding could be the cause of neuronal death. There are studies that suggest that overexpression of α-synuclein, especially the mutant forms found in PD familial cases, exacerbate the vulnerability of neurons to dopamine-induced cell death through excess ROS generation [263,264]. Moreover, it has also been reported that dopamine and neuromelanin can directly affect α-synuclein aggregate propensity, helping to generate more toxic forms of α-synuclein [265,266], and that α-synuclein can alter enzymes involved in the dopamine metabolism, generating toxic dopamine metabolites [267].

3.5.2 Astrocytes

It is known that PD patients have a more permeable BBB, suggesting a potential role of astrocytes in PD [268]. Moreover, astrocytes produce several molecules that are important for the development and survival of dopaminergic neurons, namely the glia-derived neurotrophic factor (GDNF) [269]. Expectedly, astrocytes have been associated with dopaminergic neuron degeneration in PD [269]. Furthermore, a comparative transcriptomic analysis across different types of human and mouse brain cells showed that many of the genes that have a monogenic mutation associated with familiar PD (e.g. *PARK7*, *SNCA*) are equally or even more expressed in astrocytes than in neurons [270,271]. Proteins encoded by some of those genes are indeed already known to play a role in astrocyte physiology [270]. One such example is *DJ-1*, important not only for the maintenance of mitochondria in astrocytes, but also for neuroprotection against rotenone [272,273].

In pathological conditions, such as brain injury and oxidative stress, astrocytes undergo astrogliosis, characterized by several morphological and functional changes [274]. This is, together with inflammation, a common feature of all neurodegenerative disorders [275]. Both cellular and animal PD models generated with the administration of rotenone or MPTP present astrogliosis, together with neuronal death, mitochondrial dysfunction and nuclear fragmentation [276].

3.5.3 Microglia

Upon a compromise of brain homeostasis, such as an injury, infection or a neurodegenerative disorder, microglia shift their phenotype from a "resting" to an "activated" state [274]. Once activated, microglia proliferate and migrate towards chemoattractants. This process has been postulated to play an important role in PD, since there is a dense population of microglia in the *substantia nigra* that, when becoming activated, can influence the midbrain dopaminergic neurons that are extremely sensitive to cytokines [277]. Thus, even though microglial activation can enhance neuronal survival by releasing trophic and anti-inflammatory factors, the constant release of harmful molecules by microglia in the *substantia nigra*

overshadows, in the context of PD, this beneficial effect, becoming overall detrimental [278].

Moreover, a study, performed in rhesus monkeys treated with MPTP to recapitulate to some extent the PD phenotype, suggested that microglia are important for the selective vulnerability of dopaminergic neurons to MPTP [279]. Additionally, a GWAS study identified a genetic risk factor for late-onset PD in the human leucocyte antigen gene (*HLA-DRA*) that is specifically expressed in microglia, strengthening the role of microglia in PD [280]. Besides, PET studies also identified microgliosis as being an early and sustained response in PD [281,282].

One type of pattern recognition receptor, known to respond to pathogen-associated molecular patterns and recognize invading pathogens for host defence immune mechanisms, are the tool-like receptors (TLRs). Microglial TLR1/2 has been shown to play a role in the α-synuclein pathogenesis, with microglial TLR2 found overexpressed in PD patients [283] and activated by α-synuclein in different experimental systems [284]. Upon TLR1/2 activation, microglia start to release pro-inflammatory cytokines, such as TNFα and IL-1β, in a My88 dependent manner, as well as anti-inflammatory cytokines, demonstrating the dual role that microglia can have upon this activation [284]. A-synuclein can also interact with other microglial receptors, such as EP2, that regulate its phagocytosis, CD11b, that will cause microglial migration downstream, or even the CD36 receptor, that regulates microglial activation and TNFα release [284]. Although all these receptors can activate different pathways upon α-synuclein signal, they activate microglial inflammatory response. Additionally, genes related with PD risk, such as *DJ-1*, *LRRK2* and *SNCA*, were shown to be able to mediate microglia inflammation and microglial phagocytosis [284].

3.5.4 Oligodendrocytes

A-synuclein has been found in OPCs isolated from rodent brains, as well as in oligodendrocytes originated from human embryonic stem cells and iPSCs derived from PD patients' fibroblasts [285]. Moreover, α-synuclein was also observed to be decreased in pre-myelinating oligodendrocytes regardless of the iPSCs being healthy or diseased [285]. Conversely, α-synuclein overexpression in OPCs could

delay their maturation into oligodendrocytes expressing the mature marker MBP, suggesting a tight link between the intracellular levels of α-synuclein and the maturation capacity of primary OPCs [286]. An age and disease-dependent loss of MBP signal was indeed observed in the *striatum* of PD mouse models and α-synuclein seemed to be involved in the regulation and/or the maintenance of myelin phospholipids [287].

Although there have been reports pointing out to microstructural differences in white matter between PD and control brains, it is still unknown if they are due to alterations in the brain's myelin content [288–291]. In a neuroimaging study, Dean and colleagues reported a higher myelin water fraction in PD brains compared with age-matched controls and its positive correlation with levodopa dosage, suggesting an adaptive mechanism or a side effect of levodopa supplementation [292]. It seems that PD pathological changes progress inversely to brain myelination, contributing to the hypothesis that oligodendrocytes might be involved in PD [292].

3.6   Diagnosis

PD diagnosis is done by clinical observation of the patient but is not straightforward. It is estimated that 25% of the patients diagnosed with PD have an alternative diagnosis such as Alzheimer-type pathology or vascular encephalopathy, when their brain samples are analysed *post-mortem* [293]. However, in the past three decades, the criteria and guidelines have been optimized, achieving a diagnostic accuracy of 82% [294]. The most widely used clinical criteria for PD diagnosis refer to the Queen Square Brain Bank (QSBB) that provides a three-step method for evaluating a patient [295].

The first step details PD-related symptoms and the second step is to check if the patient does not have any exclusion criteria such as history of repeated strokes, head injuries, supranuclear gaze palsy or cerebellar signs [295]. The third step is to assess if the patient has three or more required criteria defined by QSBB (e.g., unilateral onset, excellent response to levodopa, hyposmia) [295]. Noteworthily, an

important and diagnostic feature of PD is the responsiveness of motor symptoms to levodopa administration [296].

One of the reasons hampering PD diagnosis is the amount of diseases with very similar symptoms that incite the performance of differential diagnosis, that is, to distinguish PD from other diseases. For instance, abuse of PD-inducing drugs, such as MPTP, is considered secondary parkinsonism; multisystemic atrophy, progressive supranuclear palsy and corticobasal syndromes are disorders deemed as atypical parkinsonism; and other neurodegenerative diseases, such as dementia with Lewy bodies, AD with parkinsonism, prion disease or frontotemporal dementia, also share several symptoms with PD [296].

Imaging techniques are usually employed for differential diagnosis. Patients that are thought to have PD but fail to respond to levodopa administered for 12 weeks undergo an MRI scan to exclude other rare secondary causes such as supratentorial tumours, normal pressure hydrocephalus and extensive subcortical vascular pathology [150]. PET or single-photon emission computed tomography (SPECT) of dopaminergic regions can also be used to distinguish PD from conditions with no dopaminergic denervation such as drug-induced parkinsonism [296]. The demonstration of normal striatal dopamine-transporter uptake with dopamine transporter SPECT can avoid inappropriate anti-parkinsonian treatment and is also helpful in identifying juvenile parkinsonism when the differential diagnosis lies between levodopa-responsive dystonia and monogenetic parkinsonism [150].

3.7   Treatment

At the moment, there is no cure for PD and the available treatments are only symptomatic.

The most commonly prescribed drugs for PD include levodopa, dopamine agonists and monoamine oxidative type B inhibitors that enhance intracerebral dopamine concentrations or stimulate dopamine receptors [297]. Most of those drugs help PD

patients with bradykinesia and rigidity and, to some extent, tremors [179]. Anticholinergic drugs, such as clozapine, are also used to control the tremors [179].

Although levodopa and dopamine agonists are the most frequently prescribed drugs, they also present several side-effects such as nausea and daytime somnolence [179]. Long-term dopaminergic treatments lead to complications in the course of PD, including dyskinesia, motor and non-motor fluctuations and psychosis, that can reduce the patient's quality of life [298]. To reduce the wide fluctuations in dopamine concentrations, monoamine oxidative type B or catechol-O-methyltransferase inhibitors are also used [298]. Additionally, non-dopaminergic treatments can also be useful to treat motor complications. For instance, amantadine or clozapine have been shown to affect multiple neurotransmitter systems and are effective in treating dyskinesia [298].

PD patients also suffer from treatable non-motor symptoms such as psychiatric symptoms, sleep disorder autonomic dysfunction and fatigue [297]. Depression can also be present in PD patients and is typically treated with antidepressants based on selective serotonin uptake inhibitors such as citalopram, fluoxetine and sertraline [179].

In the late stage of PD, the motor and non-motor symptoms usually start to respond poorly to levodopa, which may be explained by the involvement of other neurotransmitter systems. For instance, gait dysfunction and falls in late-stage PD patients seem to be related to a reduction of acetylcholine due to the degeneration of the cholinergic structures [299]. As such, acetylcholine inhibitors, such as donepezil or rivastigmine, are also used to manage these type of symptoms [179].

Deep brain stimulation (DBS) is another therapy that is nowadays used to treat PD patients with motor fluctuations and dyskinesias. Although the most common modality used is the subthalamic nucleus stimulation, stimulation of nodes in the cortico-basal ganglia-thalamo-cortical network can also be targeted [300]. The precise mechanism responsible for the clinical effects of DBS on the motor symptoms of PD is not fully elucidated yet. However, it has been suggested that DBS dissociates input and output signals from the basal ganglia, resulting in the

disruption of abnormal flow through the stimulation site [301]. Other hypotheses postulate that DBS of the subthalamic nucleus is excited while inhibiting some specific pathways or even altering neurotransmitter release at synapses that provide clinical benefits for PD patients [300]. Nevertheless, DBS treatment is not suitable for all PD patients and its accessibility can vary by country. According to the United Kingdom National Health Service Commissioning Board, patients that have a clear levodopa response, not cognitively impaired and do not fall frequently would be suitable candidates for DBS if the drug therapy has not provided good symptom control [300]. Besides, to apply this therapy, a brain surgery is needed and complications can occur during the procedure. Although the overall adverse events are at low rates, 1-15% of DBS procedures report hardware infection resulting in multiple hardware savage attempts, hospitalizations and long-term antibiotic therapy [302].

Although, over the past few decades, animal and clinical research have improved our understanding of the pathophysiological courses of AD and PD, their intricate molecular mechanisms have not yet been fully elucidated, hampering the discovery of effective drugs for reversing or slowing down AD or PD progression. The advent of high-throughput molecular profiling, at a genome-wide scale, of biological samples has been instrumental in attempting to unveil which specific molecular mechanisms underlie AD and PD.

Transcriptomics is the study of the transcriptome, i.e., the complete set of RNA molecules present in one cell or in a population of cells [303]. Although the genome is considered static, since it is mostly the same in nearly every cell of the same organism, the transcriptome is variable and dynamic, assuring the functional diversity of cells and tissues. The transcriptome can thus be used as a snapshot of genes' activity and thereby a signature of the cellular activity, providing insights into the molecular mechanisms underlying several processes in the cell or tissue, from development to disease [304]. Several technologies have been developed over the years to profile the transcriptome, with the most used being microarrays, an hybridization-based approach, and high-throughput RNA sequencing (RNA-seq) [304].

The most commonly studied RNA molecules are messenger RNAs (mRNAs), that can serve as blueprints for protein synthesis. To study this type of molecule in a sample, RNA isolation is required. This process can be summarized in the following steps: mechanical disruption of cells or tissue; ablation of RNAses, macromolecules and nucleotide complexes; separation of RNA from other biomolecules and precipitation of the RNA via solution or elution from a solid matrix [303]. Afterwards, there is an enrichment of the extracted RNA population in mRNA, by positive selection of polyadenylated (poly-A) RNAs using poly-A affinity methods [305].

4.1 Transcriptomics of AD and PD brain samples

There have been several efforts involving the profiling of transcriptomes of *post-mortem* AD brain samples with microarrays but they seemed to lack reproducibility when their results were compared across studies. Moreover, many molecular and pathways changes identified therein were apparently not AD-specific, having been related also with other neurodegenerative and mental health disorders [306]. Patel and colleagues therefore performed a meta-analysis of human brain transcriptomes using publicly available microarray data from multiple brain-related disorders, including AD [306]. Through this metanalysis, they were able to identify, consistently across several brain regions, 3 AD-specifically downregulated (*NDUFS5*, *SOD1* and *SPCS1*) and 4 AD-specifically upregulated (*OGT*, *PURA*, *RERE* and *ZFP36L1*) genes, as well as six AD-specific pathways, all related with metabolism of proteins [306]. Moreover, other studies used RNA-seq to profile *post-mortem* transcriptomes from total brain, frontal and temporal lobe [307], parietal cortex [308] and hippocampi [309] of AD and non-AD individuals. Several pathways were therein reported as being changed in AD brains, such as those involved in lipid metabolism [308], neuronal communication [309] and synapse function [307]. Additionally, Annese and colleagues analysed *post-mortem* hippocampal transcriptomes from LOAD and non-AD patients where most of the AD-associated gene expression changes were related with the regulation of important neural processes such as neurogenesis, synaptic vesicle trafficking, long-term potentiation, neurite outgrowth and hyperphosphorylation of Tau [310]. Furthermore, very recently, Wan and colleagues, performed a meta-analysis of differential gene expression over two thousand human *postmortem* brain samples and 96 different mouse studies relevant to AD, other neurodegenerative disorders, aging and related mechanisms [311]. They were able to identify five human dominant consensus clusters with robust and reproducible patterns of co-expression patterns in seven brain regions affected by AD [311]. Additionally, they showed that most AD mouse models have poor correspondence to human disease at the brain transcriptome level, with the exception of neuronal and microglial-enriched co-expression modules [311]. Their cross-species approach also demonstrated the impact of sex on AD brains, with AD apparently progressing more rapidly in female than in male mice and female human

AD brains showing quantitatively greater transcriptional changes than males [311]. Although this cross-species resource can be very valuable for highlighting AD-associated transcriptional network changes in human brains and identifying their correspondence in mouse models for AD preclinical studies, it does not consider differences between samples' cell compositions across datasets. Indeed, most of the human co-expression modules found were strongly enriched for cell-type-specific genes and were not specific of AD, since they were also found in mouse studies on other neurodegenerative disorders and aging [311].

PD-specific changes in gene expression remain poorly understood and elucidating them is crucial in the search for PD biomarkers and novel therapeutic strategies. Kelly and colleagues have conducted a meta-analysis study of the largest PD cohort to date of publicly available microarray data, to identify PD-specific gene expression changes and compare them with AD [312]. The authors were able to identify changes in signalling, protein-protein interaction, mitochondrial and oxidative stress pathways [312]. Moreover, they state that most of the genes found differentially expressed in this PD cohort were also found in AD and identified *REST* as a potential upstream regulator in both disorders [312]. Another study profiled the mRNA of *substantia nigra*, *striatum* and the cortex in control and PD *post-mortem* brains and found changes related to oligodendrocytic function and synaptic vesicle release in all those regions [313]. The prefrontal cortex mRNA was also profiled in PD *post-mortem* brains along the proteome of the same samples [314]. In this study, the authors found a modest comparability between the mRNA and proteomic changes, although they observed consistent changes in functional pathways such as mitochondrial-related, protein folding and metallothionein pathways, all previously described in PD [314]. In 2020, Benoit and colleagues did a pioneer study where they profiled brain biopsies from the frontal lobe of PD and healthy living patients that had undergone neurosurgical procedures [315]. Their study revealed changes in genes related with trophic signalling, apoptosis, inflammation and cell metabolism pathways as well as 123 gene expression changes that had not been previously reported in other PD studies involving *post-mortem* brain samples [315].

Although many AD and PD studies have investigated transcriptional regulation in the brain, it is important to state that they are usually restricted to *post-mortem*

material (except the Benoit *et al.* study [315]), representing an end-stage reflection of the neurodegenerative diseases. Moreover, the reported changes in gene expression could be reflective of differences in cellular composition between affected and healthy tissue or different disease stages, rather than being indicative of disease-causing differences in transcription regulation [316].

4.2   Single cell transcriptomics

Traditionally, cells are classified according to their morphology and certain proteins' expression levels in different functional settings [317]. With the advent of single-cell RNA-seq (scRNA-seq), it became possible to classify and characterize cells at the transcriptional level on a genome-wide scale [317]. From 2015 to 2019, more than 80 papers described using scRNA-seq to characterize brain cell types in different regions, at different developmental stages or disease statuses [318]. Moreover, the number of cells sequenced per study has been increasing, thereby helping the scientific community to construct a more comprehensive landscape of neural cell types [318].

The first scRNA-seq study related with the human brain was published in 2014. This study revealed the intratumoral heterogeneity of human primary glioblastoma and its diverse regulatory programs, central to glioblastoma's biology, prognosis and therapy [319].

By 2015, Darmanis and colleagues were the first to isolate and sequence whole transcriptomes of the six major cell types (neurons, astrocytes, microglia, oligodendrocytes, OPCs and endothelial cells) from adult and foetal human cortical tissues [320]. By using scRNA-seq, they identified a new subset of adult neurons presumably not immune-privileged (i.e. the introduction of an antigen therein would trigger an inflammatory immune response), as well as neuronal changes from early developmental to late differentiated stages [320]. In the same year, individual neural stem cells from the human neocortex were also sequenced, contributing to a better understanding of its development and evolutionary expansion [321].

In 2016, Lake and colleagues developed a single-nucleus sequencing (snRNA-seq) technology that was applied in *post-mortem* human brains [322], contrarily to previous scRNA-seq methods that required freshly isolated neurosurgical tissues. Being able to analyse *post*-mortem samples is advantageous when studying non-accessible tissues in living patients such as brain tissue [322]. However, snRNA-seq is less sensitive, i.e. has a much lower transcript detection rate, than scRNA-seq [323]. To enhance the snRNA-seq technology, Habib and colleagues developed in 2017 the DroNc-seq method to perform massive parallel snRNA-seq with droplet technology [324]. This method was applied to both human and mouse prefrontal cortex samples and enabled the classification of their cell types. Later on, another study used the same approach to sequence single nuclei from human visual cortex, frontal cortex and cerebellum [325].

Nowakowski and colleagues managed to perform scRNA-seq in human telencephalon, highlighting human brain development at the molecular level [326]. The authors developed a mixed model of topographical, typological and temporal hierarchies that govern cell-type diversity and also distinguished excitatory lineages emerging in rostral and caudal cerebral cortices [326]. scRNA-seq has also been used to study the development of other human brain regions such as prefrontal cortex and cerebral cortex [327,328].

Spaethling and colleagues developed a culture system for resected adult human brain tissue extracted during neurosurgery and performed scRNA-seq on cells after 3 weeks in culture, thus demonstrating a potentially relevant system for personalized precision medicine [329].

Despite all the previous studies referring to non-diseased brains, scRNA-seq has been more recently applied in the context of brain disease. There are several studies using single-cell sequencing of brain cancers such as primary and non-primary gliobastomas [319,330–334], oligodendroglioma [335], oligodendrocytoma [336], astrocytoma [336] and medulloblastoma [337]. Single nuclei from cells of prefrontal and anterior cingulate cortex of autistic and non-autistic patients were also sequenced [338]. The authors identified specific sets of genes enriched in upper-layer projection neurons and microglia that correlate with clinical severity,

suggesting that these molecular changes are linked with behavioural manifestations of autism [338].

Single-cell technologies are also starting to be used in the context of neurodegenerative diseases. For instance, in 2019, Lang and colleagues performed scRNA-seq of dopamine neurons derived from non-PD iPSCs and iPSCs harbouring a genetic risk variant for PD, where they identified a progressive axis of gene expression variation leading to endoplasmic reticulum stress that could be potentially regulated by *HDAC4* [339]. Also, there was a study where the authors performed snRNA-seq of multiple cell lineages in Multiple Sclerosis (MS) lesions and found lineage- and region-specific transcriptomic changes associated with selective cortical neuron damage and glia activation that contribute to the progression of MS lesions [340]. Finally, there was a pioneer study coming out in 2019 that performed snRNA-seq to analyse transcriptional changes in early and late disease stages of AD, as well as gender-associated transcriptional differences in AD patients [341]. Additionally, another study came out very recently, where snRNA-seq of an AD mouse model and human AD samples showed specific transcriptomic signatures for AD oligodendrocytes, astrocytes and microglia, and unveiled a new population of reactive oligodendrocytes in mouse [342].

It is clear that single-cell technologies will keep evolving and massively contribute to the creation of a human brain cell atlas. Hopefully, the specific transcriptomic signatures of each neural cell type will be well defined to contribute to a better understating of the brain as a whole. Furthermore, it will also be possible to address the contribution of specific cell-type transcriptomic changes to a particular brain disease and how those changes can be manipulated.

5.1 Microarrays

Microarrays were first introduced in 1995 [343] and are an hybridization-based tool that measures the relative expression level of a gene by determining the amount of cognate mRNA present in a sample [344]. Through a single experiment, microarrays allow for a quick and efficient analysis of the expression of thousands of genes, which is an advantage over single gene-centred laboratory quantification methods such as northern blotting and reverse transcriptase quantitative polymerase chain reaction (RT-qPCR) [303,344].

A microarray can be a glass slide, a nylon membrane or a silicon chip, containing spots of each gene's DNA at known location [345]. Those spots are also known as probes and, for mRNA measurement, they are usually sequences of complementary DNA (cDNA) or oligonucleotides, which are short fragments of a single-stranded DNA with specific complementarity to the gene's target sequence [345]. Once mRNA is isolated from a sample and converted into cDNA with a fluorescent tag, it is placed over the array in order to hybridize with the probes, in case they share sufficient sequence complementarity [346] (Figure 16). Afterwards, the array is washed to eliminate non-hybridized transcripts [346].

After the washing step, each probeset (a collection of probes targeting the same molecule) will be bound to a certain quantity of labelled cDNA [347]. The amount of sample hybridization is estimated after a laser is beamed to excite the dye of the labelled cDNA, whose intensity is proportional to the transcript quantity [344]. This fluorescence is then captured by a scanner that gives an image of a grid of bright spots, each corresponding to a probe [344]. The image is then transformed into a matrix of intensity values and the gene expression analysis can start [347].
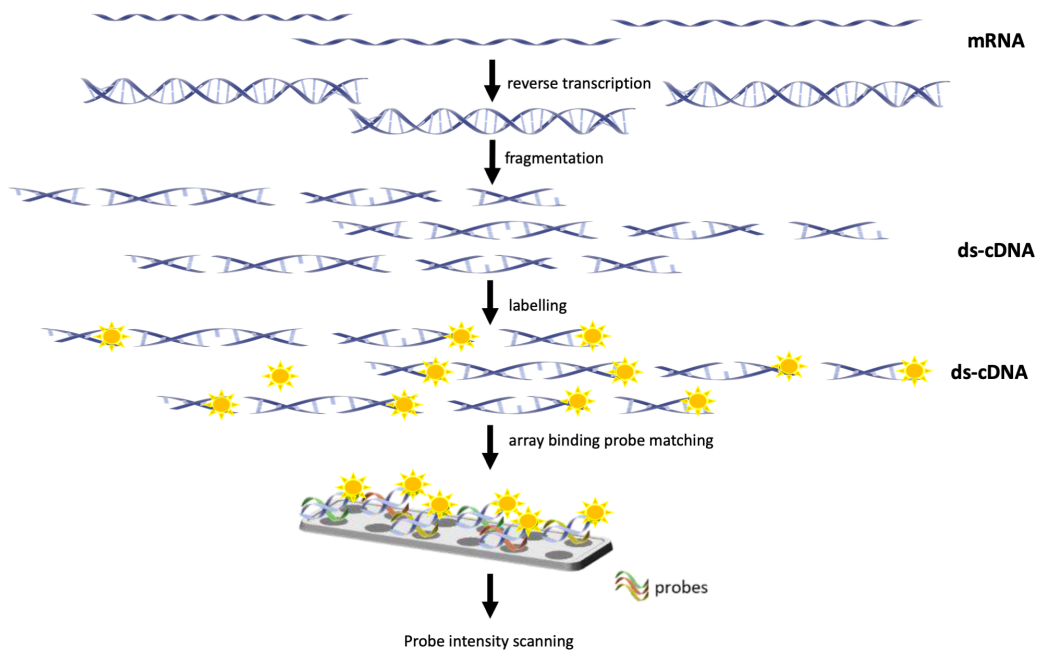
Figure 16 – mRNA quantification with microarrays
Microarrays are based on fluorescently labelled cDNA that hybridizes with complementary pre-defined probes.
Figure inspired by [303].

5.2   RNA-seq

RNA-seq is a more recent technique that uses high-throughput technologies to sequence RNA, namely the mRNA [304]. Briefly, mRNA of cells or tissue is fragmented and converted into a library of cDNA fragments to which adaptors are attached in one or both ends [304]. Then, each molecule can be amplified followed by high-throughput sequencing to obtain short nucleotide sequences (computationally represented by text strings known as reads) from one end (single-end sequencing) or both ends (paired-end sequencing) [304]. Single-end sequencing is cheaper than paired-end and is enough to quantify gene expression levels [303]. However, paired-end sequences can provide more robust alignments, being potentially beneficial for gene annotation and discovery of new transcript isoforms [348]. The reads generated by RNA-seq are usually around 100 base pairs but can vary between 30 and 10 000 base pairs [303]. Additionally, RNA-seq can be stranded or unstranded. If stranded, reads can be specifically assigned to their cognate RNA molecules' transcriptional strand, allowing to discriminate the transcription of genes that overlap in different genomic strands [349].
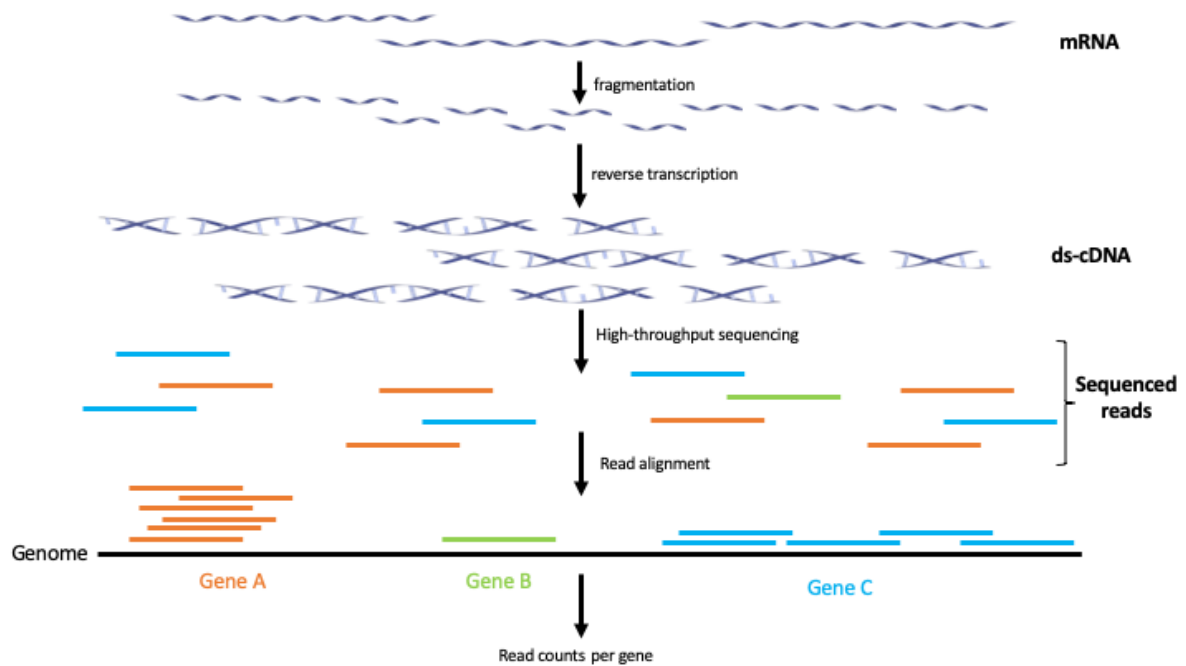
Figure 17 – mRNA quantification by RNA–seq
mRNA is fragmented and then reverse transcribed, creating double-stranded cDNA. Afterwards it is high-throughput sequenced, generating reads that can then be aligned, for instance, against the reference genome sequence.
Figure inspired by [303].

With this technique, an expressed gene is represented by several reads associated with sequenced fragments of its mRNA (Figure 17). Since RNA-seq is not based on probe design but rather on the detection of molecules at single-nucleotide resolution, it does not have issues related with probe redundancy and annotation, allowing a better coverage of all transcripts in the sequenced sample, even novel unknown (i.e. never annotated before) ones, reaching therefore higher specificity [350–352]. Also, due to background noise and cross-hybridization, microarrays are not so effective in detecting genes with low expression levels as they cannot distinguish them from non-expressed ones, being therefore less sensitive [351]. RNA-seq therefore also outperforms microarrays in the detection of differentially expressed genes because it allows for a more accurate quantification of low-abundant transcripts [353]. Additionally, the RNA quantity needed for RNA-seq is much lower (nanograms) than what is required for microarrays (micrograms), which also helps RNA-seq to be a more convenient technique [303].

Once the reads are obtained, the reconstruction of the original transcriptome can be achieved through either computational *de novo* assembly or by aligning the reads

against a reference genome or transcriptome [304]. Gene expression is then quantified based on the amount of reads that align to a given gene.

5.3 Single-cell RNA-seq

With the advent of scRNA-seq, it became possible to molecularly classify and characterize individual cells at a genome-wide level [317]. The first scRNA-seq experiment happened in 2009, when a single mouse blastomere was sequenced [354]. Nowadays, with the improvement of high-throughput single-cell technologies, hundreds to thousands of cells can be sequenced in parallel (Figure 18), allowing for an unbiased view of the heterogeneity of transcriptomes across individual cells within a population [317].
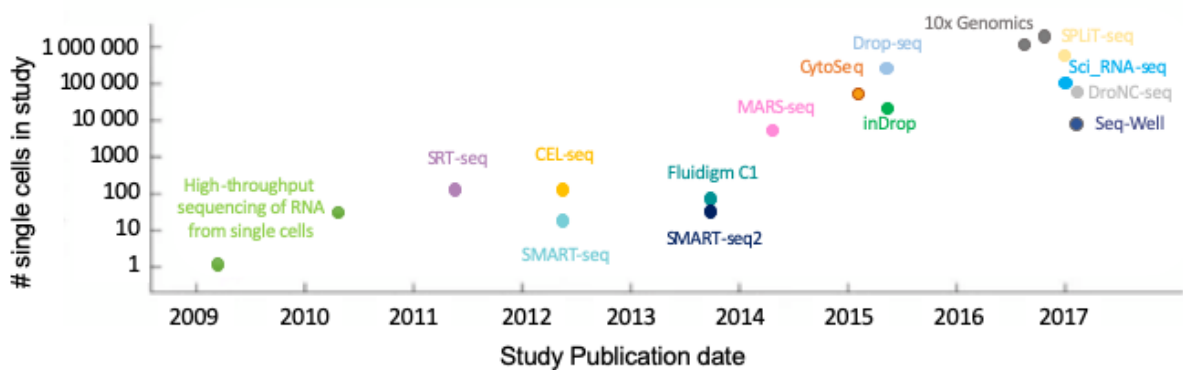
Figure 18 – Key single-cell mRNA-seq technologies
Timeline of available key single-cell RNA sequencing as of 2017.
Figure adapted from [317].

All scRNA-seq protocols share as common initial steps the conversion of the cell's transcriptome into cDNA. Then, the cDNA is amplified and sequenced to quantify gene expression levels therein [317]. However, two challenges have to be overcome to sequence mRNA from single cells: capturing them and amplifying their minute amount of mRNA [355].

To isolate cells, methods such as micromanipulation and laser capture microdissection (LCM) provide a small, yet precise, number of cells, whereas automatic methods, such as microfluidics, are mainly focused on high-throughput cell isolation (Figure 19). Micromanipulation techniques tend to be very time

consuming and laborious but the microscopic supervision ensures that a single cell is captured at each isolation attempt. LCM is normally employed to isolate cells from tissues, where a laser is used to attach individual cells to a removable thin film [356,357].
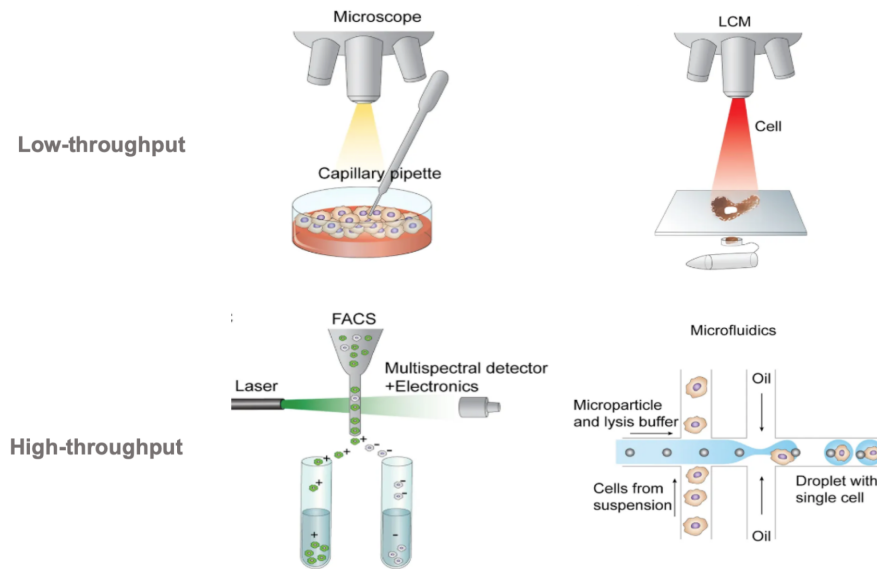
Figure 19 – Single cell isolation methods
Examples of high- and low-throughput methods for single cell isolation. LCM – laser capture microdissection; FACS – fluorescence-activated cell sorting.
Figure adapted from [291].

High-throughput isolation methods require cells to be dissociated from a tissue and suspended in a buffer. This step can be very challenging because dissociating cells from a tissue using enzymes like trypsin or collagenase might affect cell viability as well as each cell's transcriptional profile [355]. Once cells are suspended, they can be sorted into individual wells by fluorescence-activated cell sorting (FACS) or microfluidic platforms, such as the Fluidigm C1 robot or microdroplet methods. FACS is usually a fast and accurate method to sort cells that can also give information on the amount of fluorescence of specific labelled proteins in each cell but has a higher reagent cost per cell [355]. Fluidigm C1 has some limitations, although its reagent costs per cell are cheaper and it allows a precise fluid control. For instance, it can only be used with cells of a relatively homogenous size because its capture sites have only three size ranges: 5-10, 10-17 and 17-25 microns in

diameter [355]. Thus, the capture efficiency for sticky or non-spherical cells is low. In addition, this technique requires a large amount of input cells (~ 1 000 cells) per capture, being inadequate if the starting sample contains few cells [358]. Besides Fluidigm C1, some microfluidic methods are based on microdroplets with the potential of capturing thousands of cells in a single experiment as well as of enabling high-throughput delivery of reagents to each droplet, further reducing costs [359].

As mentioned above, the other single-cell sequencing challenge regards the amplification of the low mRNA amount per cell. Only 10-20% of transcripts are reversely transcribed into cDNA: one of the caveats that scRNA-seq protocols need to improve [358]. Next, the resulting small amounts of cDNA need to be amplified and both the most commonly used techniques, PCR and *in vitro* transcription (IVT), have biases. PCR is a nonlinear amplification process with sequence-dependent efficiency [355]. The IVT method provides a linear amplification but the requirement of an additional round of reverse transcription of the amplified RNA results in additional 3′ coverage biases [355].

Another way to increase the single-cell RNA-seq throughput is by multiplexing samples. In scRNA-seq this can be achieved through barcoding samples either before reverse transcription or during library preparation [355]. Additionally, each individual mRNA molecule can also be barcoded within a cell during reverse transcription with a unique molecular identifier (UMI) [360,361]. In summary, the number of copies of a transcript from a given cell lysate is equivalent to the number of UMIs associated with all tags that map to the transcript, considering the initial RNA capture rate of the protocol [355].

Since scRNA-seq technology is very recent, there is no gold-standard pipeline to analyse this type of data yet. Although scRNA-seq analyses are similar to those of bulk RNA-seq, there are nevertheless some particularities [362]. For instance, in cell populations, there might be dropouts, that is, a gene can be moderately or lowly expressed in one cell but not detected in another cell of the same type [363]. These dropouts happen due to the low amounts of mRNA and its inefficient capture in individual cells as well as the stochasticity of mRNA expression [363]. This

characteristic implies the application of a different RNA-seq normalization method that accounts for high-dimensional zero inflated count data [364].

Moreover, scRNA-seq experiments often generate large amounts of data containing thousands of gene expression measurements over thousands individual cells, presenting challenges in computational analysis such as high dimensionality [363]. Additionally, different scRNA-seq datasets can also present a high variability regarding the number of cells sequenced, the sequencing depth or even the experimental procedure used. Therefore, scRNA-seq pipelines should have a quality control step to determine if the individual-cell experiment succeed or failed, a normalization and scaling step to eliminate batch effects, followed by dimension reduction and visualization methods [365], adapted for each individual RNA-seq dataset.

6. Inference of cellular composition of tissue samples

Although transcriptomic analyses of bulk tissues shed light on several biological processes, they overlook cell type composition. When working with bulk gene expression data, one cannot assess if the observed pattern of expression is driven by a particular cell type since it reflects the average expression across the entire tissue's cell population. Essentially, by not considering cellular composition as a potential confounding factor, especially in cellular heterogenous tissues such as the brain, it is not possible to know if gene expression differences between samples are due to cell type proportion differences, systemic or cell type-specific changes in expression, or even a combination of some or all of them [366].

With the advent of scRNA-seq, the ability to measure the gene expression levels of each individual cell enabled the development of approaches to estimate the cell type composition of a heterogenous sample. Although most of those tools have been used in estimating the proportion of normal, tumour or immune cells in heterogenous tumours [367–371], others have been applied to different scenarios [372–378]. For instance, Kuhn and colleagues developed population-specific expression analysis (PSEA) and applied it to Huntington disease's brains [379]. However, scRNA-seq has very labour-intensive protocols that require expensive and specialized resources, making it, for the moment, not easy to implement in a clinical setting [380].

Cell type deconvolution stands for a procedure that estimates the proportion of each cell type in a bulk/mixture sample from their corresponding cell-type-specific gene expression profiles [381]. Most existing methods require cell-type-specific gene expression profiles (also known as signature matrixes) as input to estimate the sample's cell-type proportions or vice-versa and typically use regression techniques to estimate the unknowns of interest [382]. It is the case, for instance, of MuSic (Multi-subject Single Cell deconvolution), a weighted non-negative least squares linear regression-based method, that estimates cell type proportion in bulk samples by giving low leverage to genes showing less cross-cell type variation and high leverage to the most influential genes of cell-type-specific gene expression profiles

as input [380]. Cell Population Mapping (CPM) uses a support vector regression approach to combine the bulk profile of a complex tissue with a collection of CPM's reference scRNA-seq profiles, to infer the cellular composition of the input complex tissue [383]. Other methods, such as CDSeq (Complete Deconvolution for Sequencing data), perform deconvolution approaches without requiring cell-type-specific gene expression profiles or specific sample cell-type proportions by decoupling the bulk RNA-seq profile into weighted averages of expression profiles of possible constituent cell types [381]. The CDSeq pipeline introduces a "complete" deconvolution method that estimates both cell-type proportions and cell-type-specific gene expression profiles. While gene expression profiles of tissue samples are assumed to be weighted averages of the gene expression profiles of pure individual cell types, the tool is based on a probabilistic model inspired in the way RNA-seq reads are generated from genes. More specifically, deconvolution is achieved with random variable modelling of the probability of a given read being assigned to a given gene in a given cell type. This probability depends on the proportion of this cell type in the sample and on the typical amount of RNA produced by cells of this type, accommodating the possibility of different cell types producing different amounts of RNA [381]. However, afterwards, reference gene expression profiles or marker genes are still required to match cell types gene expression profiles constructed by the algorithm with actual biological cell types [381]. CIBERSORTx [384], a computational framework to estimate cell type proportions in bulk samples, uses the CIBERSORT [377] deconvolution algorithm that is based on linear support vector regression. This algorithm performs a feature selection where genes from the signature matrix are adaptively selected to deconvolute a given bulk mixture [377]. Additionally, CIBERSORTx is able to overcome technical variation across different platforms (i.e. scRNA-seq, RNA-seq, microarrays) and tissue preservation techniques (fresh/frozen) by performing batch correction methods, namely B-mode or S-mode [385]. B-mode batch correction is used for deconvolution when the signature matrix was derived from bulk RNA-seq of populations of sorted cells of the same type or from scRNA-seq data generated without UMIs (i.e. SMART-Seq2) [385]. This batch correction method will adjust the mixture dataset, so that it is in the same space as the signature matrix, and will be then used for estimating the cell type proportions [385]. S-mode batch correction is used when the single cell-derived signature matrix comes from droplet-based protocols or protocols

that use UMIs (i.e. 10x Chromium, Drop-Seq). Unlike B-mode, S-mode adjusts the signature matrix to be in the same order of magnitude of expression as the mixture dataset and then use the adjusted signature matrix to estimate the cell proportions [385]. CIBERSORTx has already been used in different studies to estimate cell type proportions. For instance, it was used to estimate the composition in non-cancer cells of tumours from their bulk transcriptomes, focusing on immune cells, thereby allowing to analyse the tumour microenvironment in solid cancers [386]. Moreover, Zeran and colleagues used CIBERSORTx to estimate the neuronal proportions of *post-mortem* brain samples from patients with and without neurodegenerative disorders and were able to identify an association between a frontotemporal lobar degeneration-protective *TMEM106B* variant and an increased neuronal proportion, suggesting that this gene variant may have a neuronal protection effect against normal physiological aging, independent of the disease status [387].

Alzheimer's and Parkinson's diseases are the two most common neurodegenerative disorders worldwide [36]. Although aetiological processes, affected brain regions and clinical features are disease-specific, they share common mechanisms such as mitochondria dysfunction, neuronal loss and tau protein accumulation [388,389]. Their associated major risk factor is ageing [390]. The increasing worldwide life expectancy [391,392], together with the scarcity of available treatment choices, makes it thus pressing to find the molecular bases of AD and PD so that the causing molecular mechanisms can be targeted. A common strategy to study the mechanisms underlying neurodegenerative disorders is to compare the gene expression profiles of diseased and control brain tissues, thereby identifying biological pathways and cellular processes putatively altered in disease [393]. However, the specificities of diseased whole-brain gene expression profiles mainly reflect altered cellular composition, therefore masking disease-associated systemic or cell-type-specific molecular alterations [393].

Therefore, the work described herein had the following aims:

1) Define the gene expression signatures of the major human brain cell types.
2) Identify pathology-associated molecular effects in AD and PD by decoupling them from neurodegeneration (i.e. the loss of neurons), accounting for cell type composition when comparing transcriptomes of healthy and diseased brain samples.
3) Identify, through computational chemo-transcriptomics tools, candidate small molecules for specifically targeting the profiled condition-associated molecular alterations.

Characterising those molecular alterations has allowed us to tackle pertinent questions on the molecular nature of the alterations that AD and PD induce in the brain. Our approach could therefore not only bring new insights into the molecular aetiology of AD and PD but also foster the discovery of more specific targets for functional and therapeutic exploration.

1. Datasets used

We obtained, through NCBI Gene Expression Omnibus (GEO), two single-cell RNA-seq datasets that we employed to derive gene expression signatures for the major brain cell types (i.e. astrocytes, microglia, neurons and oligodendrocytes), one from human temporal lobe (GSE67835 [320] - only cells from adult samples were used) and the other from mouse cortex (SRP135960 [394]). We used a third single-cell RNA-seq dataset (GEO GSE73721 [271]) to independently validate those signatures, considering only cells from the human cortex (12 astrocytes, 1 neuron, 4 oligodendrocytes and 2 endothelial cells), for consistency.

The AD analysis was based on the temporal cortex RNA-seq dataset from the AMP-AD Knowledge Portal with accession syn3163039 [395]. We used the table available therein, containing the pre-processed raw read counts for each gene in each sample, for the downstream analyses. We selected only the samples diagnosed as AD and non-AD with RNA integrity number (RIN) ≥ 8 [396].

We used AD dataset GEO GSE104704 [397] for independent validation, less stringently requiring RIN ≥ 6 to keep enough samples for analysis.

We fetched the PD RNA-seq dataset from GEO GSE68719 [314] and kept samples with RIN ≥ 7 and from donors older than 60 years, for a better age match between control and diseased samples and given the reported onset of idiopathic PD at around 65 years of age [398].

For independent validation, we used PD gene expression microarray dataset GEO GSE20168 [399]. Since the PD RNA-seq dataset only comprised males, we selected the 10 non-diseased and 8 PD male samples from the microarray dataset. Although RINs were not provided for this dataset, we were able to detect possible RNA degradation by using function *AffyRNAdeg* from the *xps* R package [400].

All datasets used are summarized in Table 1.

Table 1 – Summary of transcriptomic datasets analysed

	Accession	Species	Type	Condition	Technology	Pre-processed data
Darmanis (Darmanis et al., 2015b)	GEO GSE67835	Human	Single cell	Normal	RNA-seq	No
Mouse (Zeisel et al., 2018)	http://mousebrain.org/downloads.html	Mouse	Single cell	Normal	RNA-seq	Yes
Zhang (Zhang et al., 2016)	GEO GSE73721	Human	Single cell	Normal	RNA-seq	No
MayoClinic (Allen et al., 2016)	https://www.synapse.org/#!Synapse:syn3163039	Human	Bulk	AD + Normal	RNA-seq	Yes
Nativio (Nativio et al., 2018)	GEO GSE104704	Human	Bulk	AD + Normal	RNA-seq	No
Dumitriu (Dumitriu et al., 2016)	GEO GSE68719	Human	Bulk	PD + Normal	RNA-seq	No
Zhang bulk (Zhang et al., 2005)	GEO GSE20168	Human	Bulk	PD + Normal	Microarray (Affymetrix Human Genome U133A)	No

1.1   Samples discarded

We discarded respectively one and three non-AD samples from the MayoClinic and Nativio datasets because they presented a very low (< 0.40) estimated proportion of neurons (Figure 20, Table S1). Therefore, we used totals of 71 AD and 32 non-AD samples from the MayoClinic dataset and 9 AD and 14 non-AD samples from the Nativio dataset.
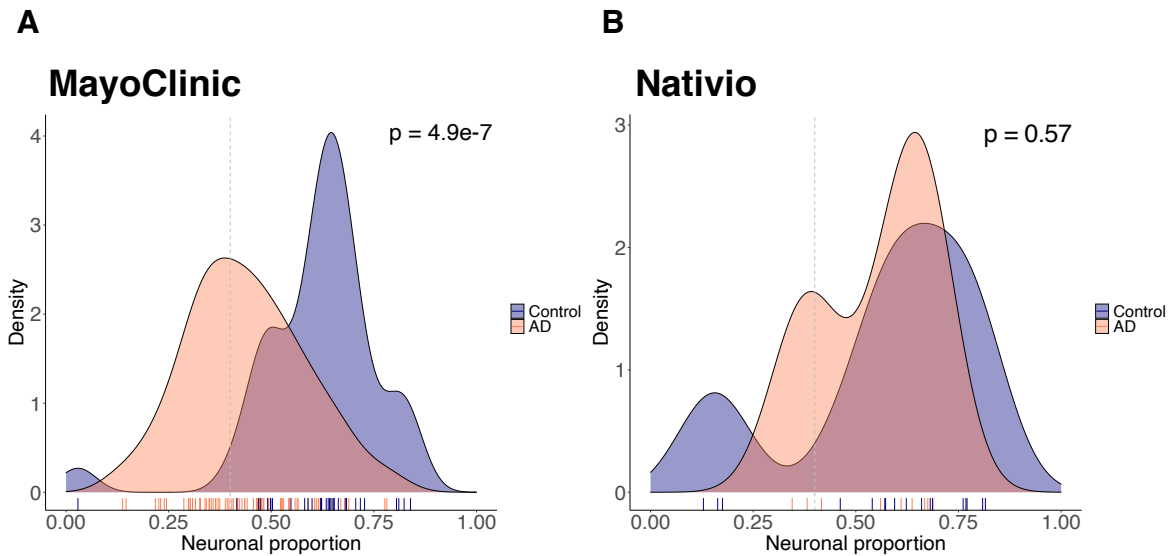
Figure 20 – Smoothed histograms of distribution of neuronal proportions of AD and non-AD samples
Smoothed histograms of distributions of neuronal proportions of diseased (AD) and non-diseased (Control) samples from the **(A)** MayoClinic and **(B)** Nativio datasets. One MayoClinic and three Nativio Control samples were removed from further analyses due to their very low (< 0.4, vertical dashed lines) neuronal proportions. The significances (p) of Wilcoxon signed-rank tests used to compare differences in proportions between diseased (AD) and non-diseased (Control) samples are shown.

When performing principal component analysis (PCA) of the normalized gene expression data (see sections "Statistical tests" and "Data processing" below) from the Dumitriu dataset, we identified 2 samples (SRR2015728 and SRR2015748) with an outlying behaviour (Figure 21).
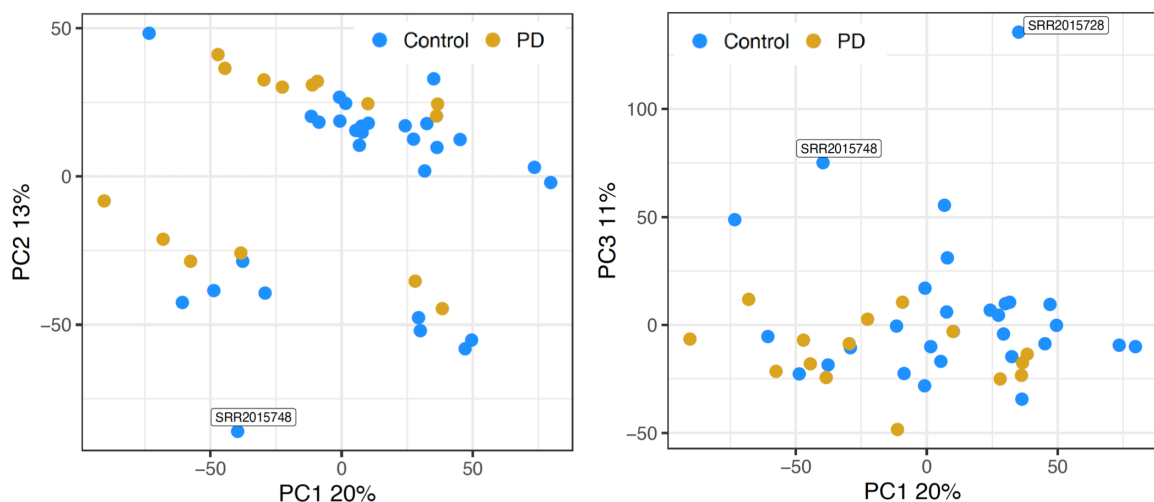
Figure 21 – Identification of outlying samples in the Dumitriu dataset
Sample factorial maps of components 1 (PC1) and 2 (PC2) (left), and 1 and 3 (PC3) (right), of Principal Component Analysis (PCA) of the gene expression in Dumitriu samples. Indicated in the respective axes' labels are the percentages of data variance explained by the components. Labelled are the two samples deemed as outliers and removed from further analyses.

When clustering samples based on the correlation between their normalized gene expression profiles (see section "Statistical tests" below), SRR2015728 and SRR2015748 are again shown to be outliers (Figure 22).
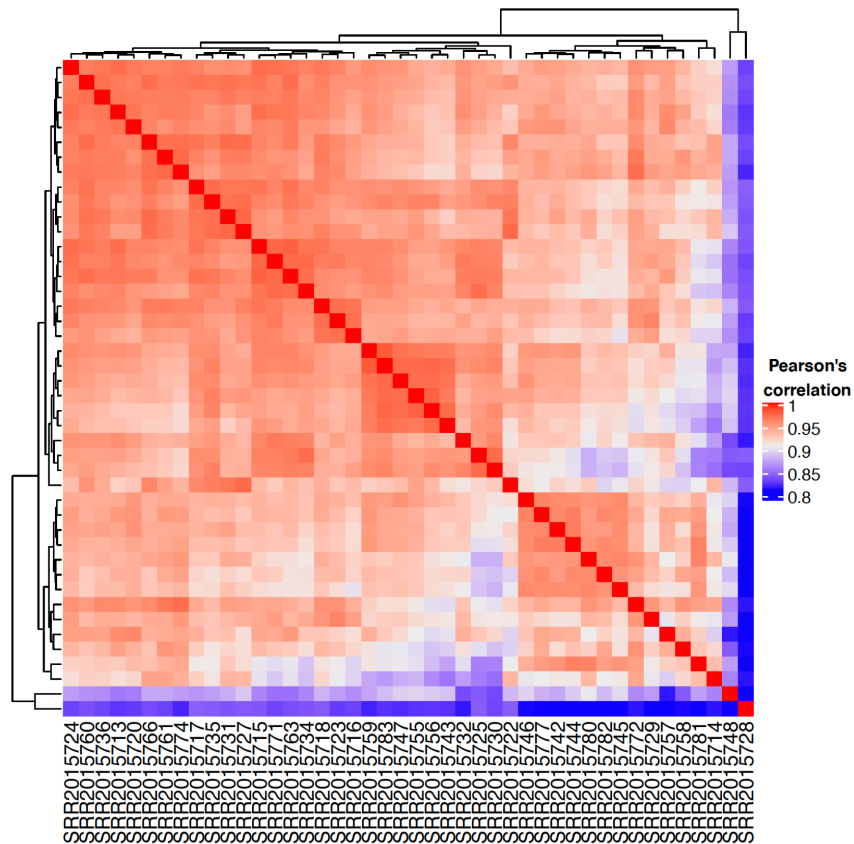
Figure 22 – Identification of outlying samples in the Dumitriu dataset
Heatmap of gene expression correlation between Dumitriu samples, with associated hierarchical clustering, confirming the outlying behaviour of the two excluded samples.

Moreover, non-PD samples SRR2015714 and SRR2015728 are also those showing an abnormally low (< 0.40) estimated neuronal proportion (Figure 23 A, Table S1). As such, we conservatively discarded those 3 samples from the Dumitriu dataset, leaving 15 PD and 26 non-PD samples. Regarding the Zhang dataset, although one non-PD sample had a low (< 0.40) estimated neuronal proportion (Figure 23 B), we decided to keep it due to the small number of samples in the dataset (Table S1).
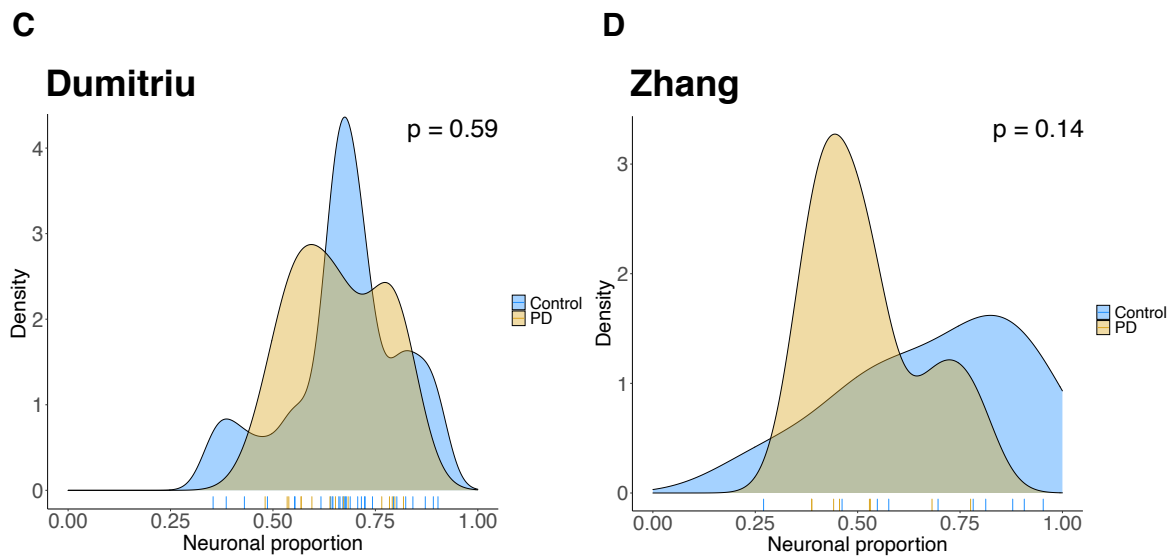
Figure 23 – Smoothed histograms of distribution of neuronal proportions of PD and non-PD samples

Smoothed histograms of distributions of neuronal proportions of diseased (PD) and non-diseased (Control) samples from the **(A)** Dumitriu and **(B)** Zhang datasets. The significances (p) of Wilcoxon signed-rank tests used to compare differences in proportions between diseased (PD) and non-diseased (Control) samples are shown.

2. Statistical tests

We performed all statistical analyses in R (programming language for statistics and graphics) [401], extensively using packages from Bioconductor (repository of R tools for the analysis of high-throughput biological data) [402]. We used t-tests [403] to compare differences in expression of specific marker genes, as well as differences in age distributions between diseased and non-diseased groups. To compare differences in proportions of neural cell types between diseased and non-diseased brains, we used Wilcoxon-signed-rank tests [404], and to compare the neuronal proportion densities between diseased and non-diseased brains, we used the Kolmogorov-Smirnov test [405]. For correlation analysis, we used Pearson's correlation, unless stated otherwise. We chose Euclidean distance for clustering samples based on gene expression correlation, having used the *ComplexHeatmap* package [406] for the purpose and to generate the associated heatmap in Figure 22.

Principal component analysis (PCA), enabling the identification of the linear combinations of variables that contribute the most to data variance [407], was implemented through the singular value decomposition (SVD) algorithm provided by

the *PCA* function from R package *FactoMineR* [408].

Where applicable and not indicated otherwise, p-values were corrected for multiple testing using Benjamin-Hochberg's False Discovery Rate (FDR)

3. Data processing

For all the RNA-Seq datasets with no pre-processed data available (Table 1), we aligned the reads against the human transcriptome (hg38 Gencode annotation [409]) with Kallisto [410] using the default parameters.

For both single-cell datasets, we performed state-of-the-art procedures for quality assessment [411], such as checking for library size discrepancies between cells, the number of expressed genes per cell and the proportion of reads aligning to mitochondrial genes [411] (Figure 24). We removed low-quality cells that presented
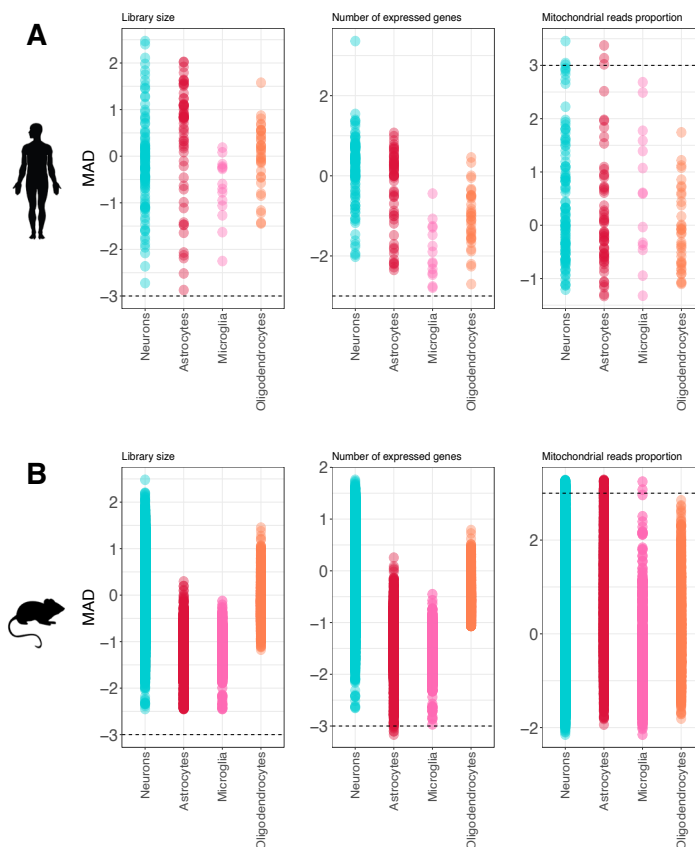
Figure 24 – Quality assessment of single-cell datasets
Dot plots of median absolute deviations (MADs) of library size (i.e. total number of RNA-seq reads), gene counts (i.e. number of genes detected) and proportion of mitochondrial reads (i.e. RNA-seq reads of transcripts from mitochondrial genes) of cell samples from the **(A)** Darmanis and **(B)** Mouse datasets. Cells with MADs below -3 for either library size or gene counts or above 3 for mitochondrial proportion (horizontal black dashed lines) were removed from subsequent analyses.

a median absolute deviation (MAD) < -3 for the library size, MAD < -3 for the number of expressed genes or a MAD > 3 for the proportion of mitochondrial reads.

Additionally, we kept for downstream analysis only genes whose log10(average read counts per million (CPM)) > 0 (Figure 25) and whose variance in expression was significantly associated with the biological component (i.e., the cell type) as assessed through the usage of the *decomposeVar* function from the *scran* R package [411]. Briefly, the variance in expression for each gene was decomposed into their biological and technical components. The technical component is estimated by fitting the mean-dependent trend of the variance. The biological component of the variance is then calculated by subtracting the technical component from the overall variance [411].
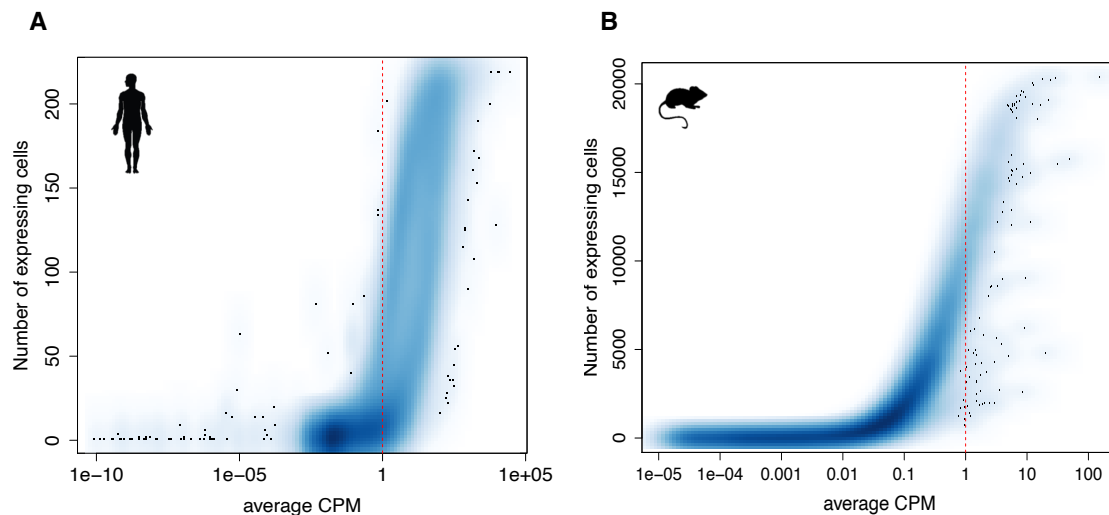
Figure 25 – Selection of informative genes
Smoothed scatter plots relating, for each gene, its average expression across cells with the number of cells in which its expression was detected for the **(A)** Darmanis and **(B)** Mouse datasets. Only genes with average expression higher than 1 CPM (vertical red dashed lines) were kept for subsequent analyses.

This last step avoids prioritizing genes whose expression is highly variable due to technical factors such as sampling noise during RNA capture and library preparation [411].Furthermore, the t-Distributed Stochastic Neighbour Embedding (tSNE) [412] plot of human single-cell (Darmanis) gene expression shows a few cells not clustered together with those of their respective annotated type (Figure 26A). Moreover, all of them appear to have been misclassified also based on single-cell trajectories (i.e. cells' ordering according to their inferred biological state [413]) obtained with the *monocle* package [413–415] (Figure 26B) or the nearest shrunken

centroid classification, implemented in R package *pamr* [416] (Figures 26C-D). Therefore, they were discarded from our analysis (Figure 26E). No potentially misclassified cells were detected in the mouse dataset (Figure 26F).
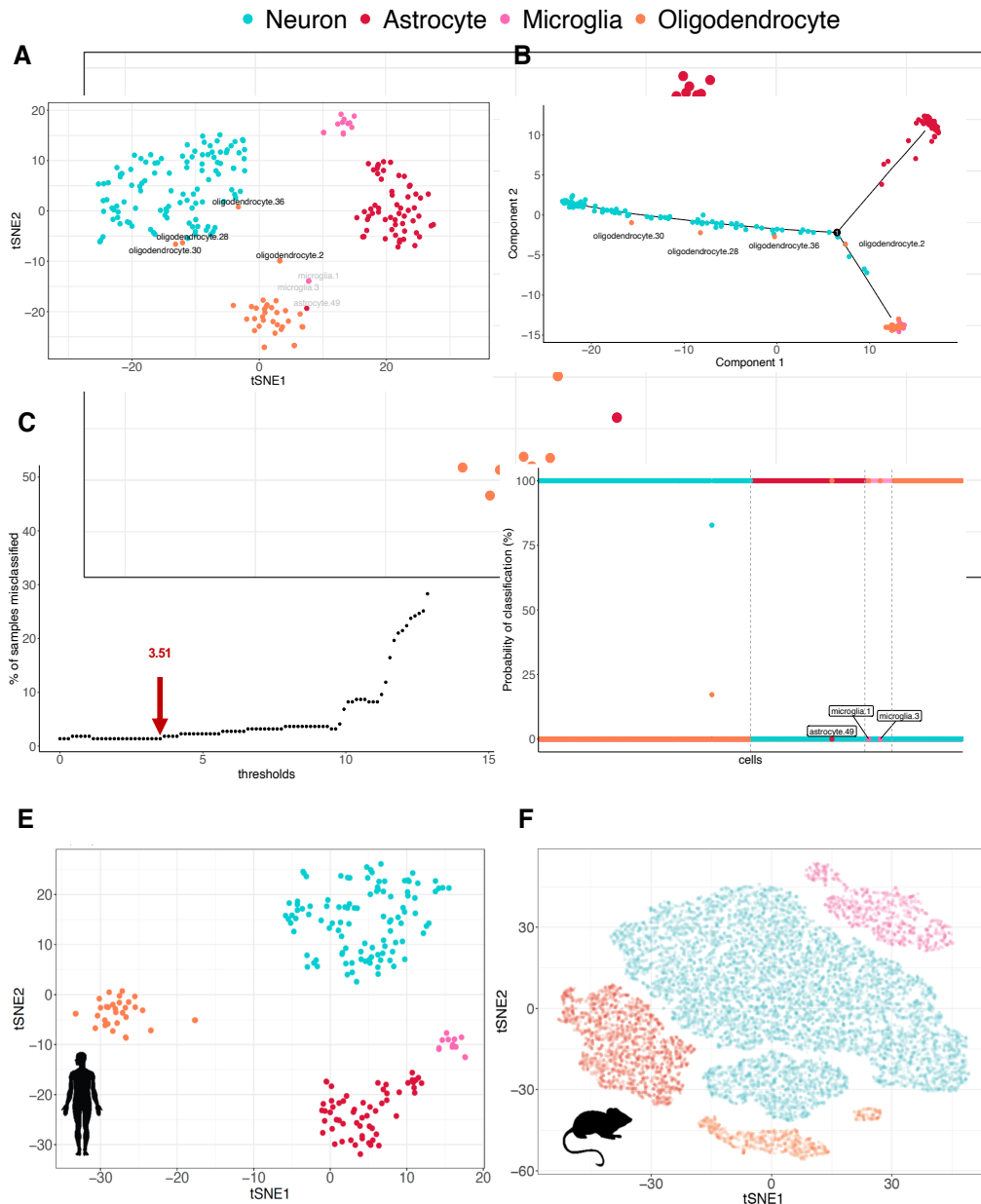
Figure 26 – Identification of misclassified cells
(A) t-Distributed Stochastic Neighbour Embedding (tSNE) plot of gene expression of Darmanis brain cells. Labelled samples do not cluster with those of their respective annotated cell types, according to *pamr* (gray) or *monocle* (black). **(B)** *monocle*-derived single-cell trajectory analysis in the Darmanis dataset. Labelled are cells that do not map to the same states as those of their annotated cell types. **(C)** Percentage of samples misclassified by *pamr* across centroid shrinkage tresholds. 3.51 was selected, amongst the thresholds with the lowest misclassification error, as that yielding a classifier simultaneously with fewer genes and lower false discovery rate. **(D)** Probability of classification by *pamr* of each Darmanis cell sample in each of the four main brain cell types. Labelled are misclassified cells. **(E)** tSNE plot of gene expression of Darmanis cells without the misclassified samples. **(F)** tSNE plot of gene expression of Mouse cells used to derive the murine cell type signature.

After the filtering steps mentioned above, summed expression values across pools of cells were deconvolved in cell-based factors for normalization of the Darmanis and the mouse single-cell gene expression datasets [417]. All bulk RNA-seq datasets were quantile-normalized using the *voom* function, from the *limma* R package [418]. The *rma* function from the *affy* R package [419] was used to normalize and summarize the PD microarray dataset.

Moreover, we used the *ComBat* function from the *sva* package to correct for batch effects. This function requires possible technical effects to be encoded as categorical variables [420]. Thus, for the AD MayoClinic dataset, RIN was defined as high if > 8.5 and low if ≤ 8.5, in the AD Nativio dataset high if > 7.3 and low if ≤ 7.3, and in the PD Dumitriu dataset it was defined as high if > 7.8 and low if ≤ 7.8. For the PD Zhang dataset, the RNA degradation slope, derived from the average intensities per relative 5′ - 3′ position of probes in their target transcripts across probe sets [421], was used and defined as low if ≤ 5 and high if > 5.

We quantified gene expression from RNA-seq data in counts per million (CPM) and kept only genes with an average CPM higher of 10*/L*, where *L* is the minimum library size in million reads [422], in at least *N* samples, where *N* is the smallest sample

Figure 27 – Selection of informative genes
Smoothed scatter plots relating, for each gene, its average expression across samples with the number of samples in which its expression was detected for the **(A)** MayoClinic, **(B)** Nativio, and **(C)** Dumitriu datasets. Genes kept for analysis have an average expression of at least 0.34, 0.83, and 0.66 CPM and are expressed in at least 33, 9, and 15 samples (red dashed lines) respectively for the MayoClinic, Nativio, and Dumitriu datasets.

size in our analyses (Figure 27). For the microarray dataset, gene expression was quantified by normalized intensities.

4. Estimation of cellular composition of bulk AD, PD and non-diseased brain samples

We used CIBERSORTx deconvolution [423], relying on human and mouse gene expression signatures for the major brain cell types derived as described above, to estimate the cellular composition of all AD, PD, and non-diseased brain samples from their bulk transcriptomes. Moreover, as CIBERSORTx options, we enabled batch normalization, disabled quantile normalization and used 100 permutations for significance analysis. Following CIBERSORTx's user guidelines, the B-mode batch normalization was chosen to perform deconvolution when using the human signature, since the single cell data used to derive it were generated with SMART-seq2 [424], and the S-mode batch normalization when using the mouse signature, since it is tailored for signatures derived from data generated with the 10x Genomics Chromium platform, as was the case [423].

5. Differential gene expression

We performed differential gene expression using the *limma* [418] and *edgeR* [425] packages.

For each coefficient in the linear model, the magnitude of differences in gene expression was measured in $\log_2$ fold-change and their significance was given by the FDR-adjusted p-value of the moderated t-statistic (an ordinary t-statistic with its standard errors moderated across genes), along with the empirical Bayes statistic (B statistic - log-odds ratio of a gene being differentially expressed) [426]. Moreover, we also used the moderated t-statistic to assess the differential gene expression coherence between different datasets.

We linearly modelled gene expression in the AD datasets according to the following:

$$GE_x = \beta_0 + \beta_{Disease} \cdot Disease + \beta_{RIN} \cdot RIN + \beta_{Neurodegeneration} \cdot Neurodegeneration$$
$$+ \beta_{Age} \cdot Age + \beta_{Sex} \cdot Sex + \beta_{Interaction} \cdot Interaction + \varepsilon$$

Here GE_x is the expression of gene x; *Disease* is the sample's centered disease status; *RIN* is the categorized sample's RNA Integrity Number (1 for high and 0 for low); *Neurodegeneration* is given by the sample's estimated proportion of neurons centered; *Age* is the age of the sample's donor in years; *Sex* is the biological sex of the sample's donor (1 for male and 0 for female); *Interaction* is the interaction between *Disease* and the *Neurodegeneration* effects, given by the product of the two and interpretable as the differential effect of the loss of neurons between AD and non-diseased samples or, equivalently, the part of AD effect that is dependent of the sample's neuronal contents; βs are the unknown coefficients, to be estimated from fitting that linear model to the gene expression data, for each of the aforementioned variables hypothesized to impact gene expression; ε states the error of the model, that is the remaining variance not explained by the model. *Disease* and *Neurodegeneration* were centered to diminish the correlation between their associated estimated coefficients, thereby using a model more consistent with the purpose of estimating independent effects [427]. We thus shifted the "prediction center" (i.e. the virtual reference) to the average sample [427] by turning the variables' means to 0 through the usage of the *scale* function from the built-in R package *base* [428], with the *scale* argument turned to "false".

Likewise, we modelled gene expression in the PD Dumitriu dataset as following:

$$GE_x = \beta_0 + \beta_{Disease} \cdot Disease + \beta_{RIN} \cdot RIN + \beta_{Neurodegeneration} \cdot Neurodegeneration$$
$$+ \beta_{Age} \cdot Age + \beta_{Unknown\ Batch} \cdot Unknown\ Batch + \varepsilon$$

Unknown batch corresponds to a batch effect of unknown source detected by PCA (Figure 28A) that was thereby adjusted for (Figure 28B).

For validation with the independent PD microarray dataset (Zhang), we used the following linear model:

$$GE_x = \beta_0 + \beta_{Disease} \cdot Disease + \beta_{Neurodegeneration} \cdot Neurodegeneration + \beta_{Age} \cdot Age + \beta_{RNA\ degradation} \cdot RNA\ degradation + \varepsilon$$

RNA degradation is given by its slope grouping for each sample (1 for high and 0 for low).

We considered a gene differentially expressed if FDR < 0.05, except for the Zhang PD microarray dataset, where we considered FDR < 0.11. This arbitrary cut-off was used to "rescue" a reasonable number of genes for further analyses, given the small sample size of the Zhang dataset and the consequent lower statistical power of the associated differential expression analysis. This arbitrary looseness in specificity is dealt with by subsequent filtering (v. section on permutation analyses below).
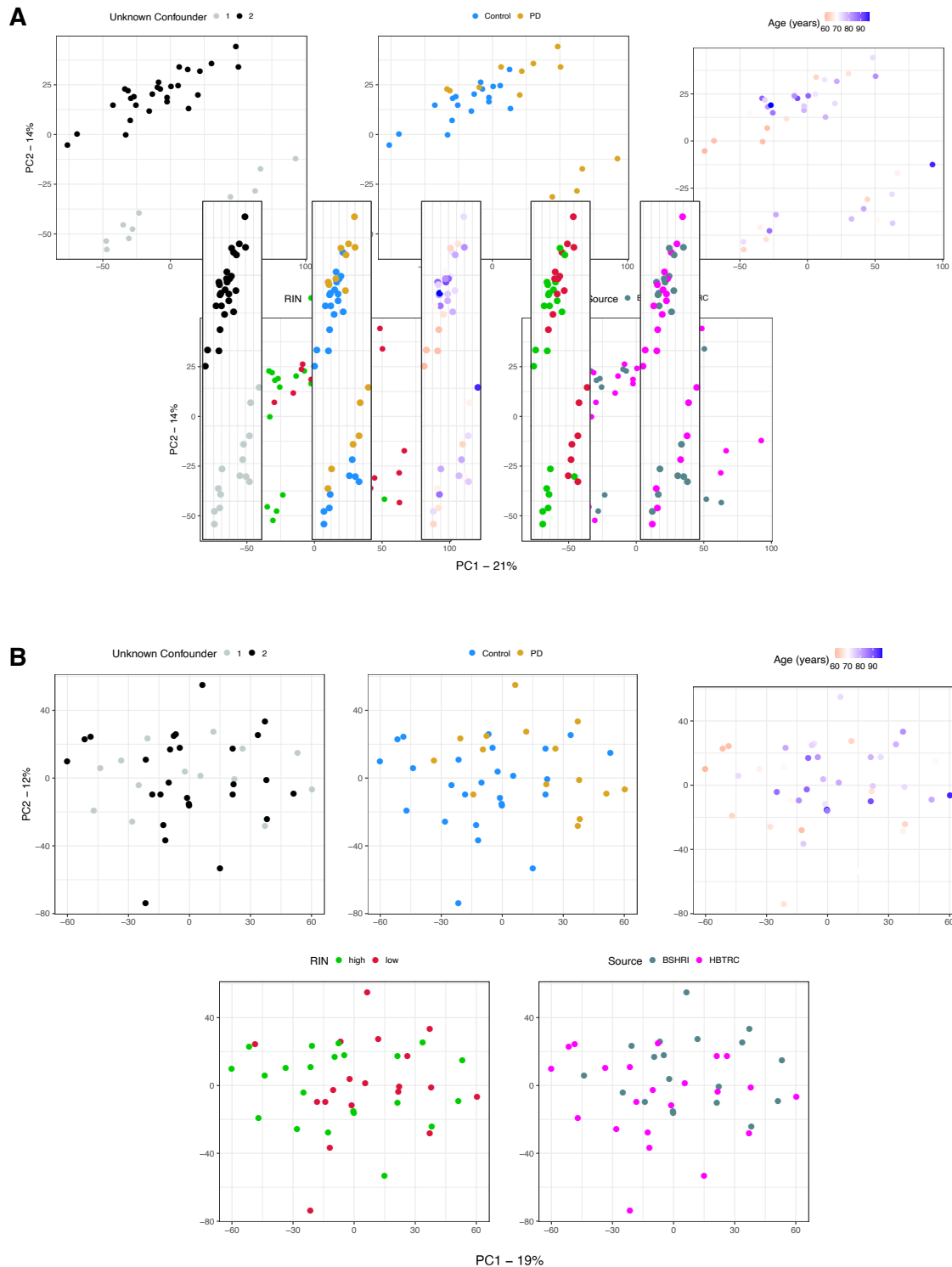
Figure 28 – Unknown confounder in the Dumitriu dataset
Sample factorial maps of components 1 (PC1) and 2 (PC2) of Principal Component
Analysis (PCA) of the gene expression in Dumitriu samples before adjusting for the
unknown confounder **(A)** and after adjusting for it **(B)**, with samples coloured according to
a different variable in each panel. Indicated in the respective axes' labels are the
percentages of data variance explained by the components. The confounder effect
highlighted in the first panel **(A)** could not be explained by any known variable, namely,
condition (disease) status, age, RIN or source of the samples (second to fifth panels from
(A)).

6. Identification of genes reportedly associated with AD and PD

Genes already reported to play a role in AD and PD were gathered from the DisGeNET database [429]. Only genes with a human gene-disease association (GDA) score > 0.1 and an evidence index ≥ 0.9 (180 genes for AD and 112 genes for PD) were considered as such in our analyses.

7. Permutation analyses

We performed permutation tests to identify genes with consistent differential expression ranking between datasets. For each gene, we multiplied its t-statistic values for the intrinsic disease effect (*Disease* in the linear models) in each of the two datasets (MayoClinic and Nativio for AD; Dumitriu and Zhang for PD) and compared that product with the distribution of those resulting from 5000 random permutations of the disease status labelling of samples. The proportion of random products more extreme than the empirical one was taken as its False Discovery Rate (FDR).

To assess the similarity between the intrinsic AD and PD *Disease* effects on gene expression, we compared the aforementioned FDRs. For each disease, when t-statistics for both datasets were positive, we used $-\log_{10}(\text{FDR})$, when both negative, we used $\log_{10}(\text{FDR})$, and when contradictory (i.e. showing different signs) we set this value to 0. When FDRs were originally zero, we equaled them to 1e-5 (half of the FDR resolution) to avoid infinite values when computing their logarithms. Then, for each gene, we multiplied those scores of AD and PD and compared this product with the distribution yielded by 1 000 000 permutations of randomly shuffled product scores. The proportion of random products more extreme than the empirical one was taken as its FDR.

8. Gene set enrichment analysis

We identified KEGG [430] pathways dysregulated in AD and PD datasets using the *Piano* R package [431] to perform gene set enrichment analysis (GSEA) [432,433],

by default on t-statistics, but also on B-statistics of differential gene expression for the AD *Disease* and *Neurodegeneration* effects. We also used the AD cell-type marker genes defined by Kelley *et al.* [434] as a gene set. For GSEA on genes commonly changed in AD and PD, we used -log10(FDR) when both AD and PD scores were positive, log10(FDR) when both negative, and zero when signs were contradictory.

9. Identifying candidate compounds for reverting disease-associated gene expression alterations

We used *cTRAP* [435] to compare the changes in gene expression induced by thousands of drugs in human cell lines, available in the Connectivity Map (CMap) [436], with those in human brains that we have inferred to be related to the intrinsic (i.e. systemic) AD and PD effects. As input for *cTRAP*, we used the aforementioned scores for the *Disease* and *Neurodegeneration* effects, thereby ranking changes that are coherent between the MayoClinic and Nativio datasets for AD and the Dumitriu and Zhang datasets for PD, as well as those coherent between AD and PD. The compounds, in clinical trials or launched, with their perturbation z-scores [436] exhibiting the 20 most negative and the 20 most positive average (across different cell lines) Spearman's correlation with the *Disease* effect scores across common genes, and with an average absolute Spearman's correlation with the *Neurodegeneration* effect scores < 0.05 (to avoid confounding between effects), were selected for AD (Figure 29A) and PD (Figure 29B) as the top candidates for reversal or induction of disease-associated gene expression alterations for discussion. Noteworthily, cMap includes data for the same compounds tested with different concentrations and at different time points, as well as run in different plate types (ASG, CPD, HOG, etc) (Tables S16-S18).
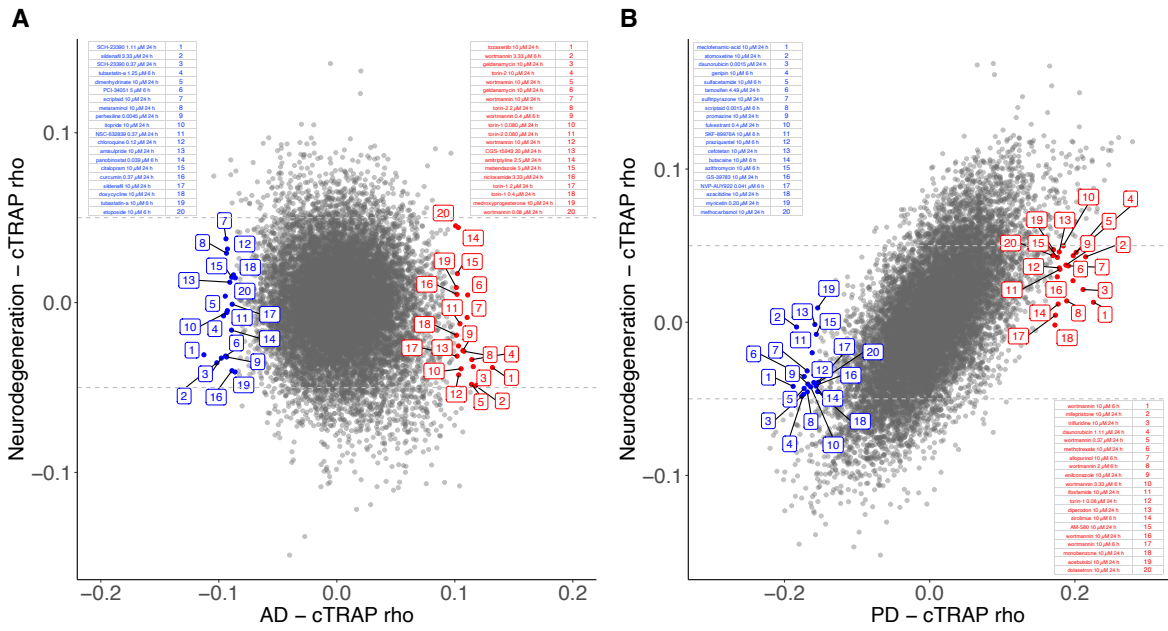
Figure 29 – Selection of top compounds for reversal or induction of AD- and PD- specific gene expression alterations
(A) Scatter plot comparing, between the AD and the Neurodegeneration effects, the cTRAP-derived cross-gene Spearman's correlation coefficients (rho) of their differential expression combined scores with perturbation z-scores for cMap compounds. Labelled compounds are those selected as top candidates for reversal (blue) and induction (red) of AD-associated gene expression alterations (v. Materials and Methods) and with |rho| < 0.05 for Neurodegeneration (dashed light gray lines). **(B)** Scatter plot comparing, between the PD and the Neurodegeneration effects, the cTRAP-derived cross-gene Spearman's correlation coefficients (rho) of their differential expression combined scores with perturbation z-scores for cMap compounds. Labelled compounds are those selected as top candidates for reversal (blue) and induction (red) of PD-associated gene expression alterations (v. Materials and Methods) and with |rho| < 0.05 for Neurodegeneration (dashed light gray lines). Note: identical labels correspond to the same compound tested with the same concentration and at the same time point but in a different plate (v. Materials and Methods).

The results presented below were published in the Frontiers in Neuroscience, Neurogenomics section, peer-reviewed journal. The author of this thesis was responsible for all the analyses, interpretation of data and the writing of the manuscript, under the supervision of Prof. Dr. Nuno Luis Barbosa Morais.

1. Derivation of gene expression signatures for the major brain cell types

We employed CIBERSORTx [423] to infer, with machine learning, both human and mouse gene expression signatures for each of the major brain cell types (Tables S2, S3) and subsequently used them to estimate the cellular composition of brain samples from their bulk transcriptomes.

We followed three different approaches to assess the accuracy of human and mouse CIBERSORTx-derived signatures in correctly identifying the major cell types in human brain samples, that we describe below.

1.1 Estimating cell-type proportions of artificial mixture samples derived from the Darmanis dataset

We split the Darmanis human dataset such that 80% of cells were used to infer cell type-specific gene expression signatures with CIBERSORTx. We used the
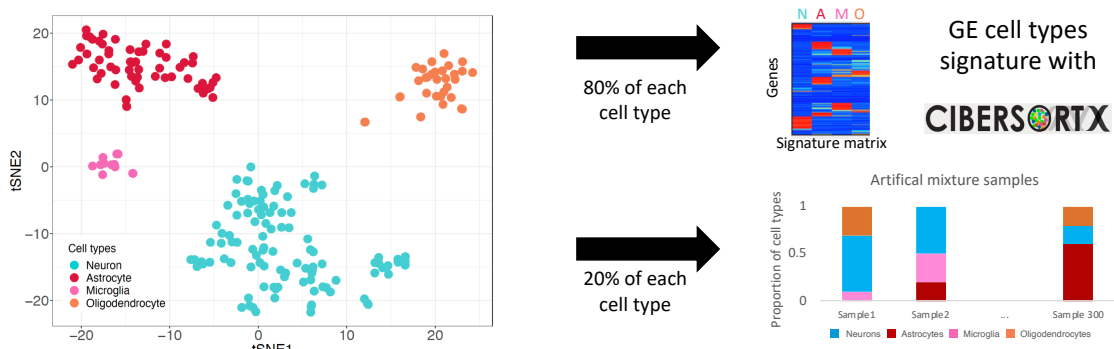
Figure 30 – Pipeline to derive the human cell type signature and the artificial mixture samples from the Darmanis single-cell dataset.
CIBERSORTx derived the human cell type signature matrix from gene expression from 80% of the cells of each type. The remaining 20% of cells of each type were used to generate artificial mixture samples with different cellular compositions that were then used to test the signature.

remaining 20% of cells, with the same proportion of each cell type, to create 300 artificial mixture samples with a diverse range of known (i.e. pre-defined) cell-type proportions (Figure 30) by generating chimeric libraries of 35 million reads. In brief, all the reads from all cells of each cell type were pooled together. For each artificial sample, reads were randomly sampled from cell-type-specific pools according to its defined cell type proportion as in Table S4. We treated the artificial mixture samples as bulk RNA-seq samples.

CIBERSORTx estimated the cell type proportions of the artificial mixtures, using the
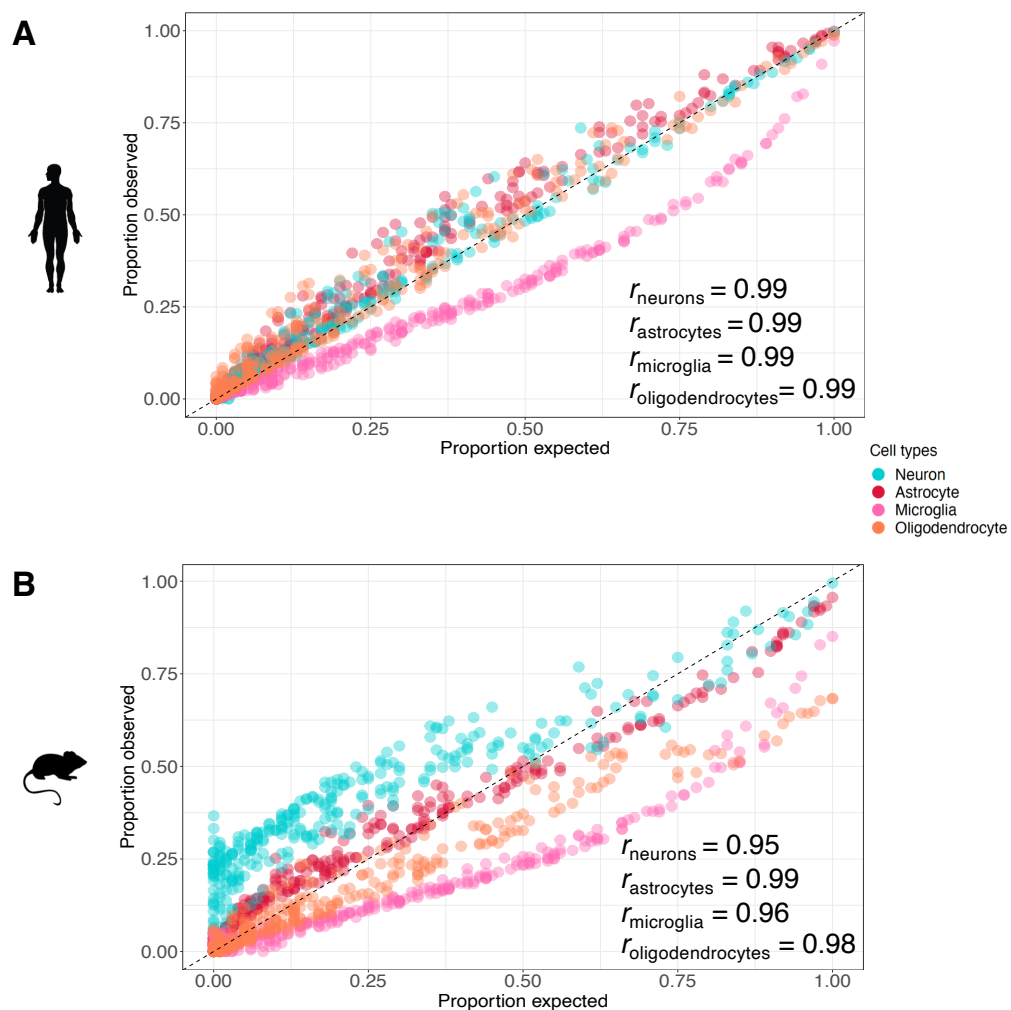
Figure 31 – Comparison between estimated and expected cellular compositions of artificial mixture samples (Darmanis)
(A) Comparison between the proportions estimated by CIBERSORTx (observed) and those expected in the artificial mixture samples generated as in Figure 30. **(B)** Comparison between the proportions estimated by CIBERSORTx (observed) and those expected in the artificial mixture samples generated as in Figure 30 using the CIBERSORTx-derived mouse cell type signature. Pearson's correlation coefficients (r) between observed and expected proportions are shown for each cell type.

human (Darmanis) cell-type-specific gene expression signatures. Those estimates are generally concordant with the expected proportions, except for the systematic underestimation of microglia's relative abundance (Figure 31A). We repeated the deconvolution analysis in the same artificial mixtures but using the mouse cell-type signatures and got a similar, albeit noisier, concordance (Figure 31B).

1.2 Classifying samples from the Zhang single-cell dataset

We ran CIBERSORTx using the same human and mouse cell-type signatures, to classify samples from an independent human brain single-cell RNA-seq dataset (Zhang). Most cells were correctly classified with the human signature (Figure 32A).
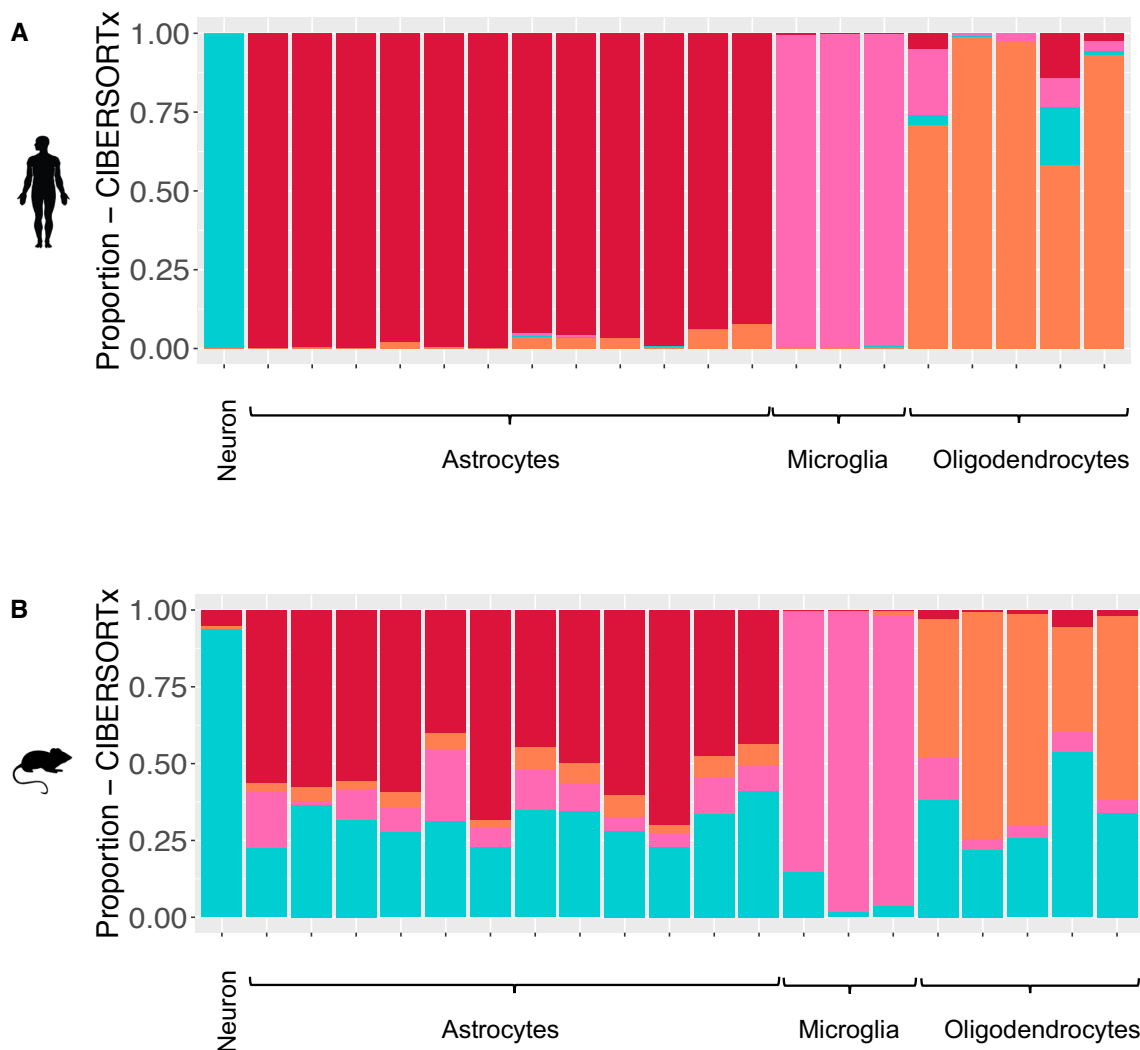
Figure 32 – Classification of Zhang human brain single-cell samples
Barplots of CIBERSORTx estimates of cellular composition of the Zhang single-cell samples based on the **(A)** human and **(B)** mouse cell type signatures.

With the mouse signature, most cells are classified as a mixture of cell types but with a dominant proportion of that expected (Figure 32B).

1.3 Estimating cell-type proportions of artificial mixture samples derived from the Zhang single-cell dataset

We generated artificial mixtures from the Zhang dataset as described in 4.1.1 section. Those artificial mixtures were then deconvoluted with CIBERSORTx relying again on the derived human and mouse signatures. Both signatures yield significant
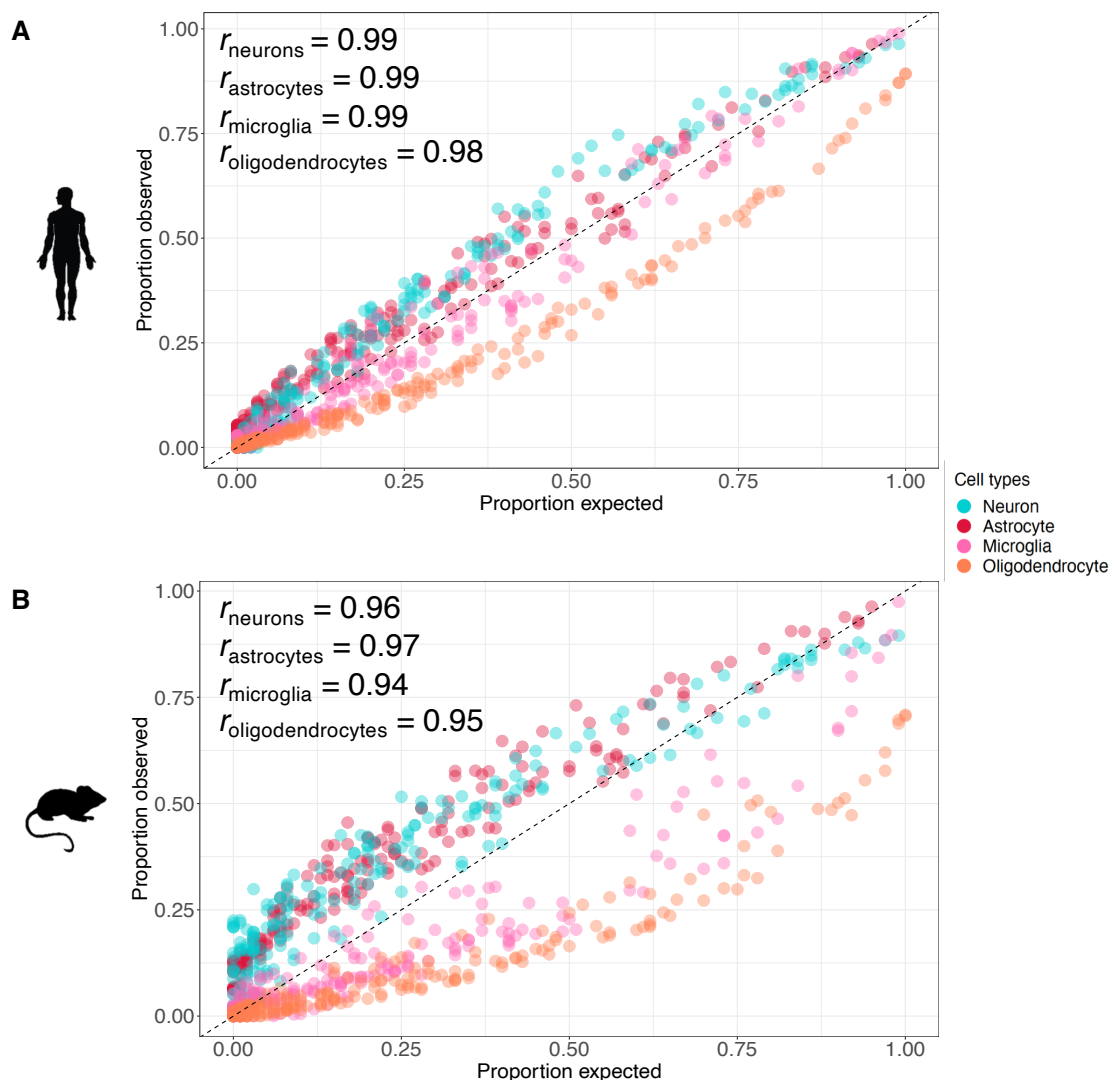
Figure 33 – Comparison between estimated and expected cellular compositions of artificial mixture samples (Zhang)
Comparisons between the proportions estimated by CIBERSORTx (observed) and those expected in the artificial mixture samples derived from the Zhang single-cell dataset, using the **(A)** human and **(B)** mouse cell type signatures. Pearson's correlation coefficients (r) between observed and expected proportions are shown for each cell type.

concordances (all with p < 2.2e-16) between the expected and observed proportions, with the human signature being a[...]e (Figure 33).

2. The cellular composition of AD

Most neuronal markers (*DCX* [437], *MAP2* [437][...]*L* [437], *RBFOX3* [437], *SYP* [437]) are significan[...]al cortex samples from the MayoClinic dataset (Fig[...] (*ALDH1L1* [438]), *GFAP* [438]), *SLC1A3* [4[...]ic oligodendrocytic markers (*CD40* [439], *OLIG*[...]d significantly upregulated in AD brains.
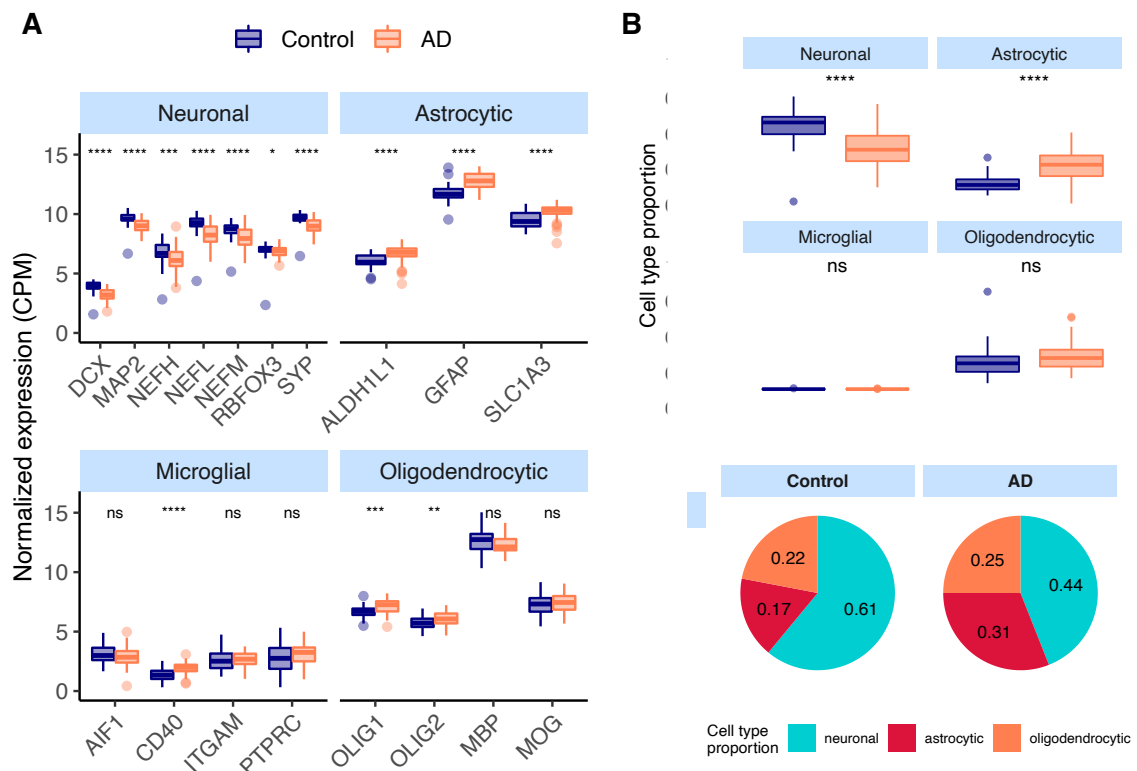
Figure 34 – Estimated cellular composition of MayoClinic brain samples
(A) Neuronal, astrocytic, microglial, and oligodendrocytic known markers' expression in the MayoClinic samples. T-tests were used to compare gene expression mean differences between diseased (AD) and non-diseased (Control) samples. **(B)** Estimates of the composition of MayoClinic samples in each main cell type based on the human cell type gene expression signature. Wilcoxon signed-rank tests were used to compare differences in proportions between diseased (AD) and non-diseased (Control) samples. Legend: ns: non-significant, ****: p <= 0.0001, ***: p <= 0.001, **: p <= 0.01, *: p <= 0.05.

CIBERSORTx [423] was used to derive the composition in major cell types (astrocytes, microglia, neurons and oligodendrocytes) of AD brain samples. These estimates (Figure 34B) are concordant with the observations in Figure 34A, including significant increase and decrease respectively in the proportions of astrocytes and neurons in AD brain samples.

Despite the known differences in gene expression between mouse and human brain cells [441], the same trends can be seen using the mouse signature (Figure 35).
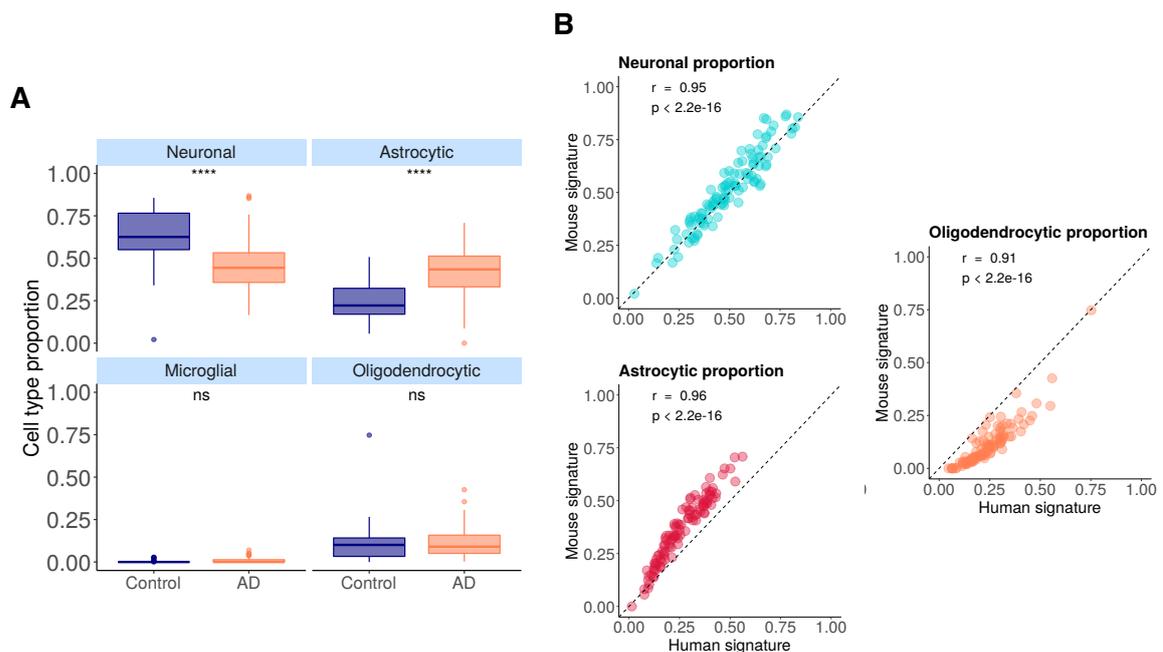
Figure 35 – Estimated cellular composition of MayoClinic brain samples using the mouse cell type gene expression signature
(A) Estimates of the composition of MayoClinic samples in each main cell type based on the mouse cell type gene expression signature. Wilcoxon signed-rank tests were used to compare differences in proportions between Control and AD samples. ns: non-significant, ****: p <= 0.0001. **(B)** Comparison between estimated proportions of different cell types in MayoClinic samples obtained from the human and mouse cell type signatures. Their Pearson's correlation coefficient (r) and respective p-value (p) are shown.
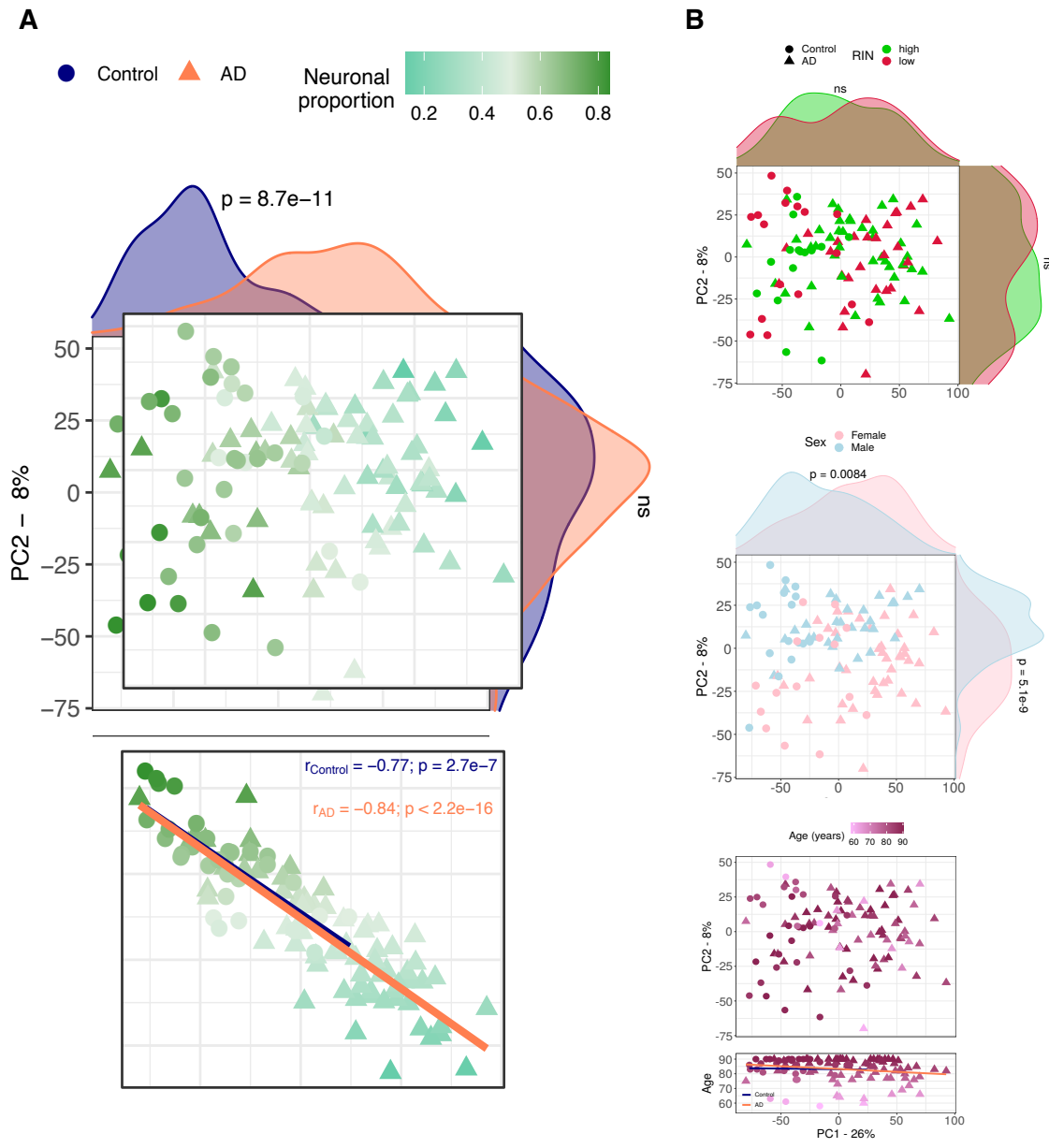
Figure 36 – Principal Component Analysis (PCA) of the gene expression in MayoClinic samples

(A) Sample factorial map (upper plot) of components 1 (PC1) and 2 (PC2) of Principal Component Analysis (PCA) of the gene expression in MayoClinic samples, and their neuronal proportion related to PC1 loadings (lower plot). Indicated in the respective axes' labels are the percentages of data variance explained by PC1 and PC2. In the lower plots, the coloured solid lines represent the linear regressions between neuronal proportions and PC1 loadings for AD and Control Samples. The respective Pearson's correlation coefficients (r) and associated significance (p) are also indicated. **(B)** Same as (A) but samples are coloured according to the RIN (top), Sex (middle) and Age (bottom). Indicated in the respective axes' labels are the percentages of data variance explained by PC1 and PC2. In the lower right plot, the coloured solid lines represent the linear regressions between age and PC1 loadings for AD and Control Samples.

Kolmogorov-Smirnov tests were used to compare the distributions of PC1 and PC2 loadings between AD and Control samples (A), RIN groups (B) and Sexes (B), illustrated by the smoothed histograms along the respective axes of the PCA plots (ns: non-significant).

A

B
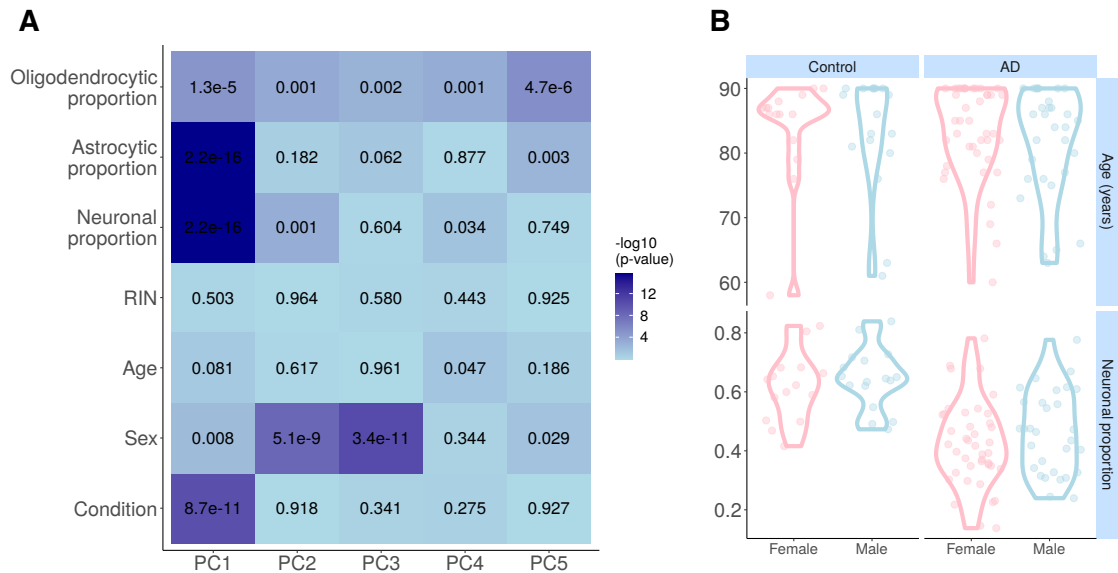
Figure 37 – Relationship between known effects on gene expression in MayoClinic samples
(A) Heatmap of significance, given by p-values, of the association between the loadings of each of the first 5 components of PCA and the seven annotated potentially explanatory sample variables. Spearman's correlation and Kolmogorov-Smirnov tests were used respectively for categorical (Condition, Sex and RIN) and continuous (proportions of astrocytes, neurons and oligodendrocytes, and Age) variables. **(B)** Violin plots of distributions of age and neuronal proportion of samples, discriminated between sexes and disease status.

3. AD alters cortical gene expression independently from neurodegeneration

We linearly modelled gene expression in the MayoClinic brain samples as a function of technical (RIN) and biological variables, such as neuronal proportion (reflecting neurodegeneration), systemic AD, Age, Sex and interaction between neurodegeneration and AD (Table S6, Figure 38).
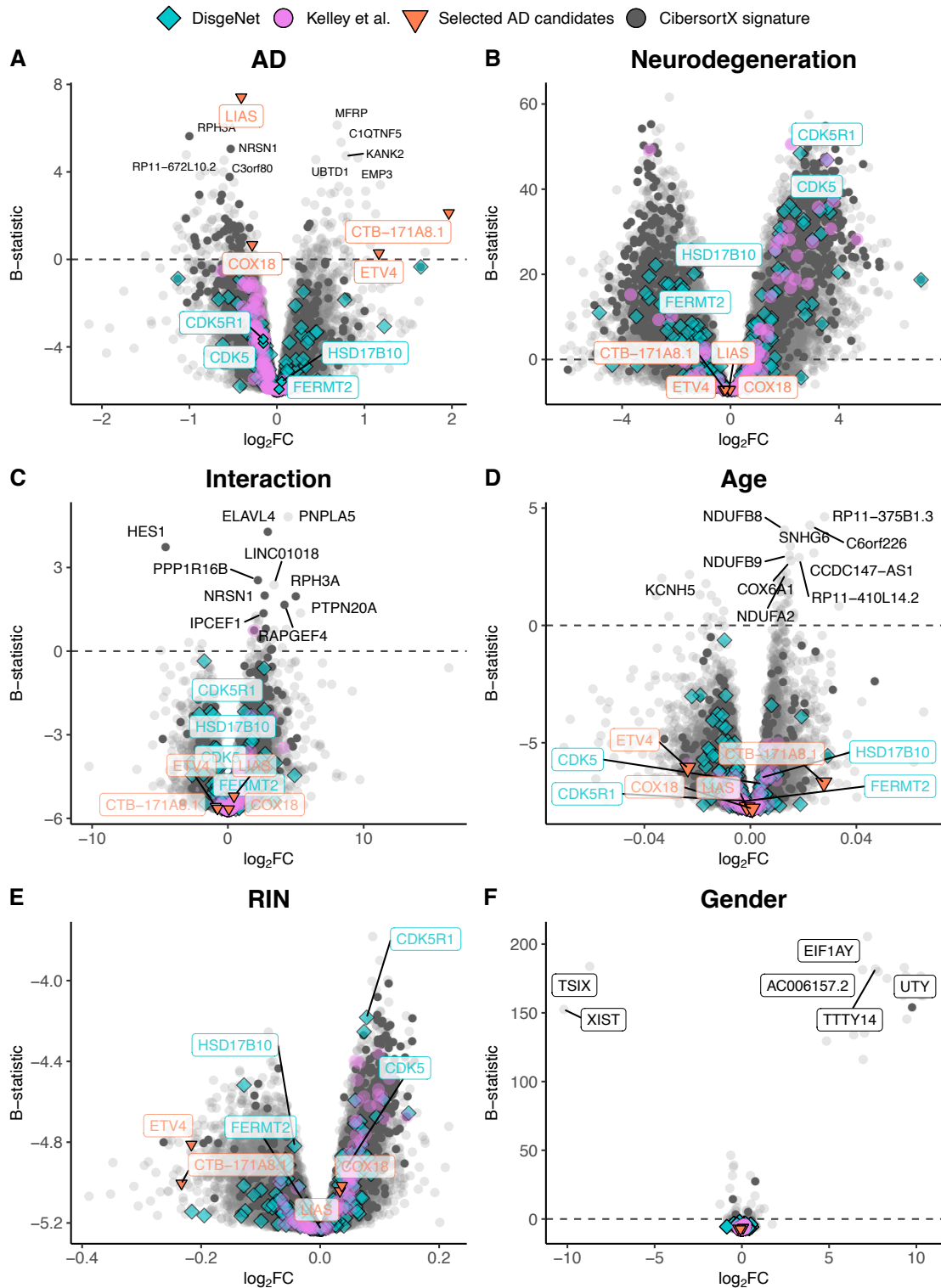
Figure 38 – Volcano plots of differential gene expression in MayoClinic samples

Volcano plots, relating log2 fold-changes (log$_2$FC) and B-statistics, of differential gene expression associated with the **(A)** AD, **(B)** Neurodegeneration, **(C)** Interaction, **(D)** Age, **(E)** RIN and **(F)** Gender effects in MayoClinic samples. Highlighted with larger coloured dots are disease-associated genes from DisgeNet [429] (light blue), genes reported by [434] as undergoing cell-type-specific changes in AD (pink), manually selected gene candidates for AD-specific alterations (orange), and genes included in the CIBERSORTx-derived expression signature for the major brain cell types (dark grey). Amongst all these, labelled are genes of particular interest, with individual expression profiles plotted in Figure 39 and 40. The other labelled genes are the top 10 differentially expressed genes.

We w

syste

a stro

LIAS, CTB-171A8.1, COX18 and ETV4 exemplify genes that show a strong intrinsic

AD effect, independent of neuronal proportion (Figure 39).
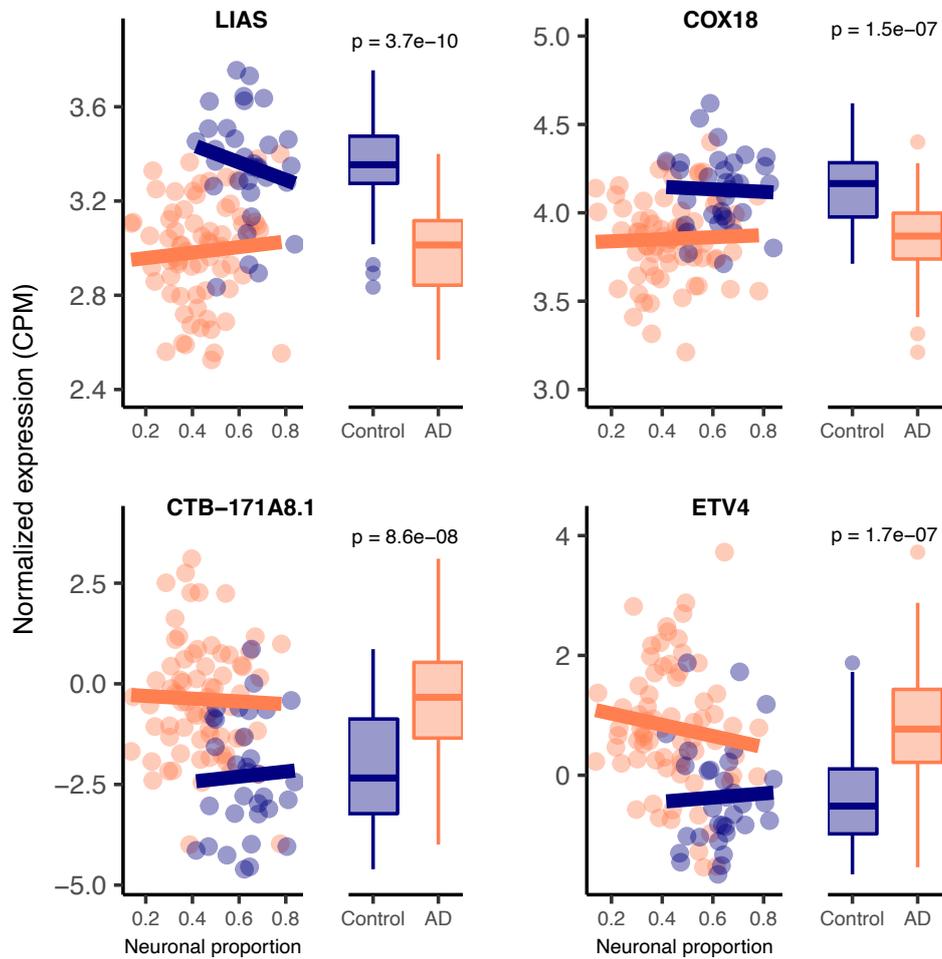
Figure 39 – Expression of selected gene candidates for AD-specific alterations

Expression of manually selected gene candidates for AD-specific alterations (labelled in orange in Figure 38) in Control and AD samples – scatterplots against neuronal proportion on the left, boxplots of distribution by condition on the right. Coloured solid lines in represent linear regressions. T-tests, for which p-values are indicated, were used to compare gene expression mean differences between Control and AD samples.

Moreover, genes that have previously been reported as playing a role in AD in the DisGeNet database, namely *CDK5* [442], *CDK5R1* [443], *FERMT2* [444] and *HSD17B10* [445], were actually found to be associated with neurodegeneration rather than with the disease component (Figure 40).
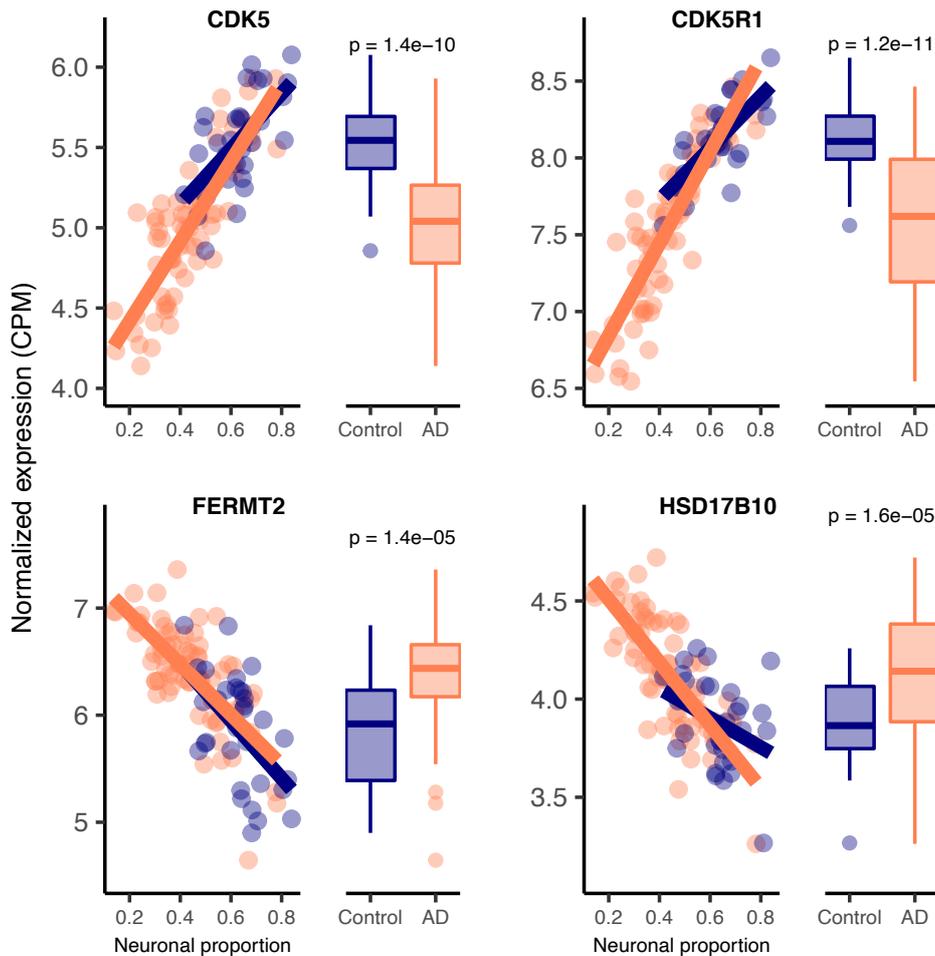
Figure 40 – Expression of selected DisgeNet genes
Expression of manually selected DisgeNet genes (labelled in light blue in Figure 38). Coloured solid lines in represent linear regressions. T-tests, for which p-values are indicated, were used to compare gene expression mean differences between Control and AD samples.

Additionally, with the *Interaction* effect we were also able to detect genes, such as *PNPLA5* and *PTPN20A* (Figure 41), whose expression was differentially altered with cellular composition in AD brains compared with non-AD samples. It is worth noting that AD genes specific of a cell type, as defined by Kelley *et al.* [434], are also more related with the neuronal composition effect ($p_{GSEA} = 0.0001$) than with the disease effect ($p_{GSEA} = 0.6$) (Figures 38A-B).
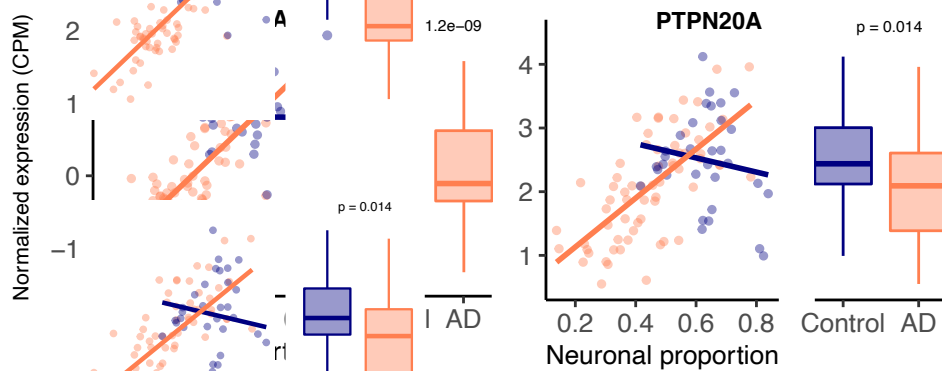
Figure 41 – Expression of selected genes with high AD-Neurodegeneration interaction effect

Expression of genes selected as examples of high Interaction effect in Control and AD samples – scatterplots against neuronal proportion on the left, boxplots of distribution by condition on the right. T-tests, for which p-values are indicated, were used to compare gene expression mean differences between Control and AD samples.

Moreove⋯ ⋯nes seem to be related with cell survival and in ⋯wn-regulated ones with oxidative phosphorylation and Parkinson's disease (Figure 42).
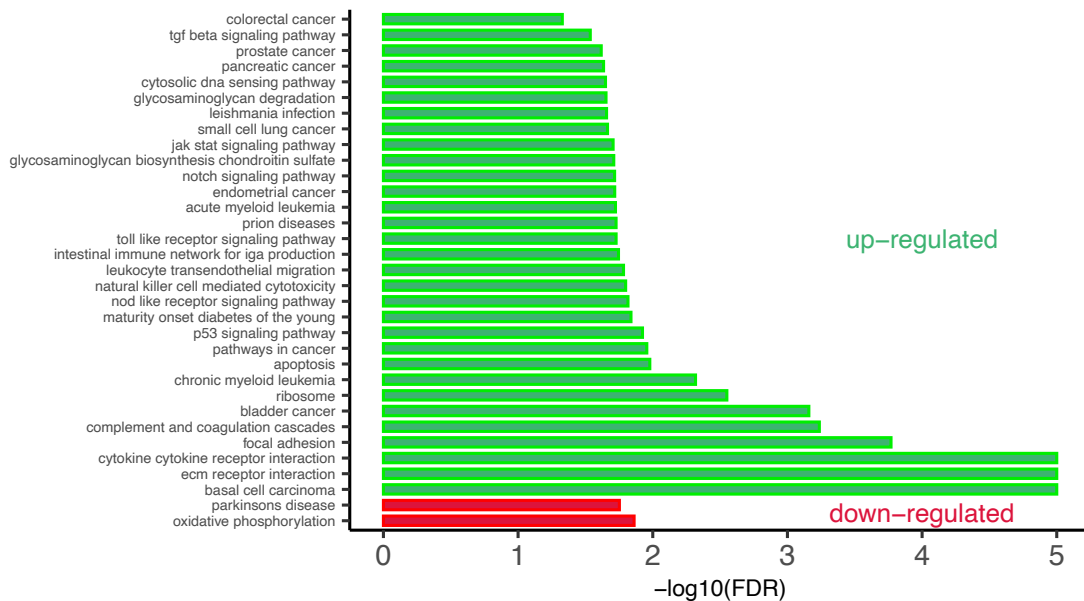
Figure 42 – KEGG pathways altered in AD

Significance of enrichment of KEGG pathways in genes up-regulated (green) and down-regulated (red) in MayoClinic AD samples compared to Controls.

In order to validate those results, we used

(lateral temporal lobe) [397], herein named N

match the larger MayoClinic dataset (tempo

Although the Nativio dataset did not pres

composition between AD and non-AD samp

significantly younger donors (p = 2.7e-10)

samples is significantly different (p = 0.033)

44).
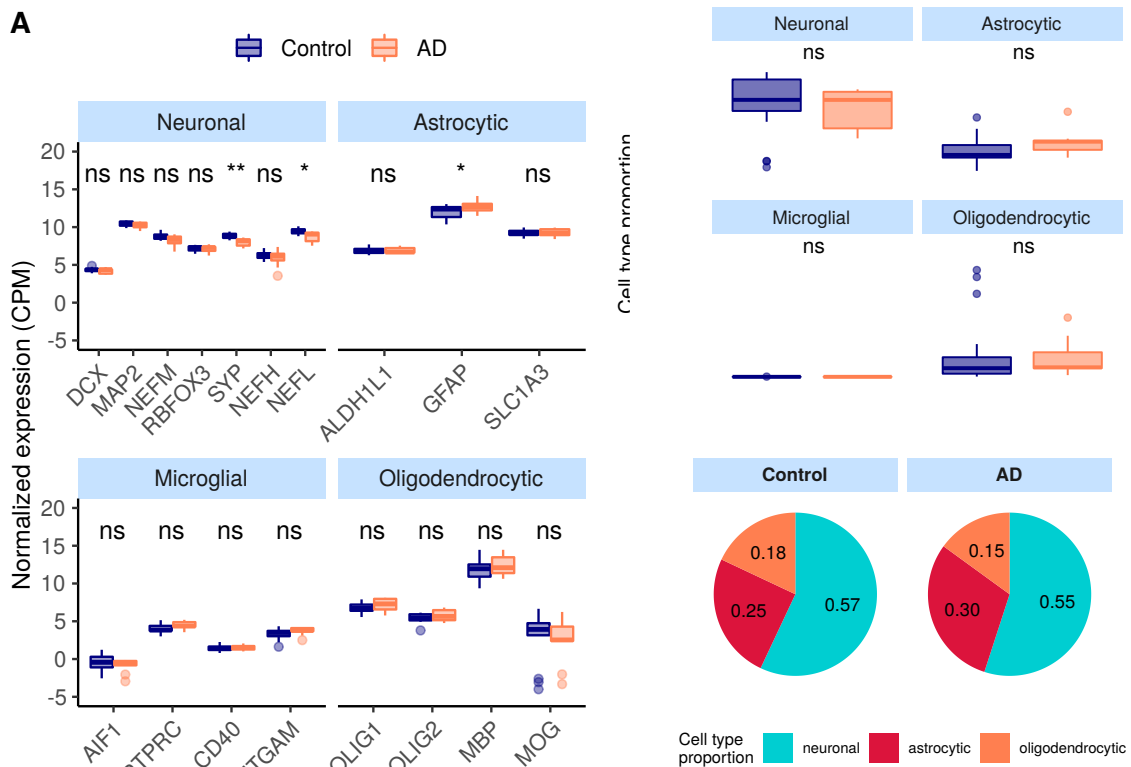
Figure 43 – Estimated cellular composition of Nativio brain samples
(A) Neuronal, astrocytic, microglial and oligodendrocytic known markers' expression in the
Nativio samples. T-tests were used to compare gene expression mean differences between
Control and AD samples. **(B)** Estimates of the composition of Nativio samples in each main
cell type based on the human cell type gene expression signature. Wilcoxon signed-rank
tests were used to compare differences in proportions between Control and AD samples.
Legend: ns: non-significant, ****: p <= 0.0001, ***: p <= 0.001, **: p <= 0.01, *: p <= 0.05.
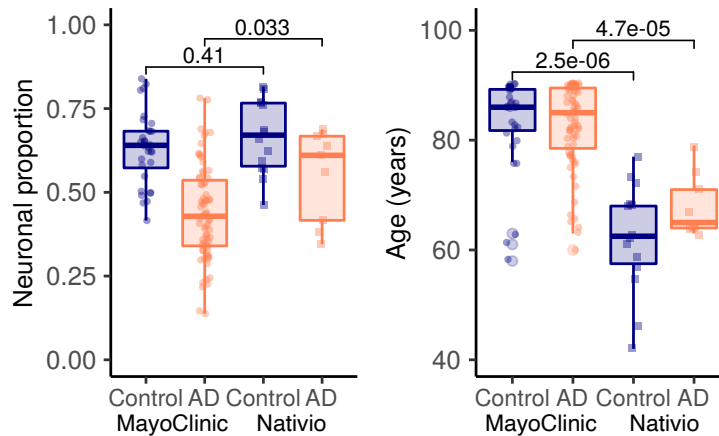
Figure 44 – Comparison of neuronal proportion and age between MayoClinic and Nativio samples

Boxplots of distributions of neuronal proportion (left) and age of donors (right) in Control and AD samples from the MayoClinic and Nativio datasets. Wilcoxon signed-rank tests were used to compare differences in neuronal proportion and age of samples in the same condition between datasets.

Moreover, we ~~...~~ sion changes between the Ma ~~...~~ bles S7-S9).
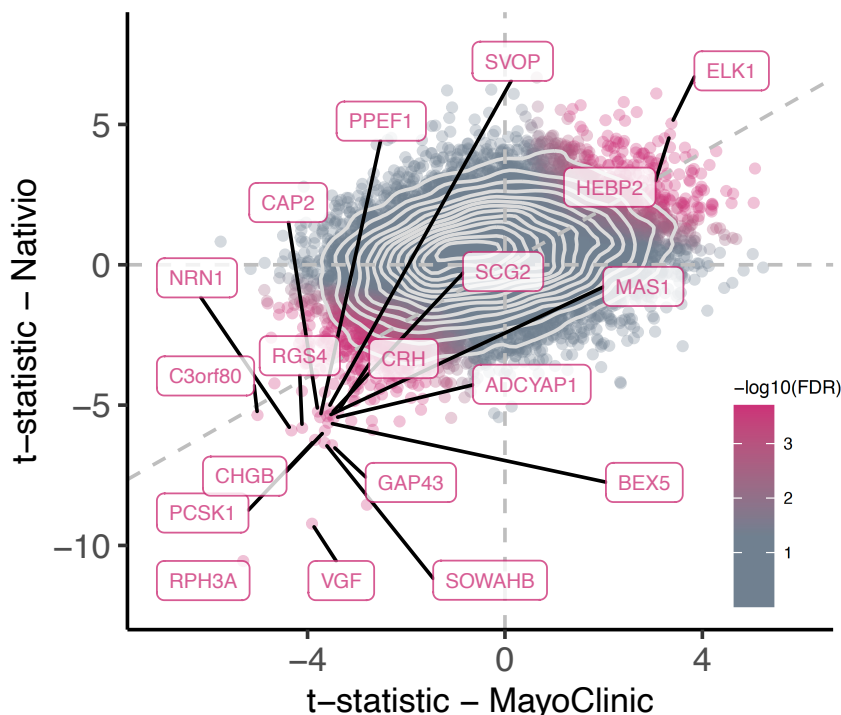
Figure 45 – Comparison of t-statistics of AD-associated differential gene expression between the MayoClinic and Nativio datasets

Scatter plot comparing the t-statistics of differential gene expression associated with the AD effect in MayoClinic and Nativio samples. Points (genes) are coloured according to the FDR of the random permutation test on the product of the t-statistics (v. Materials and Methods). Labelled genes are those significantly differentially expressed (FDR < 0.05) in both datasets and significant in that permutation test (FDR < 0.05). Light gray dashed zero and identity lines, light gray solid contour density lines.
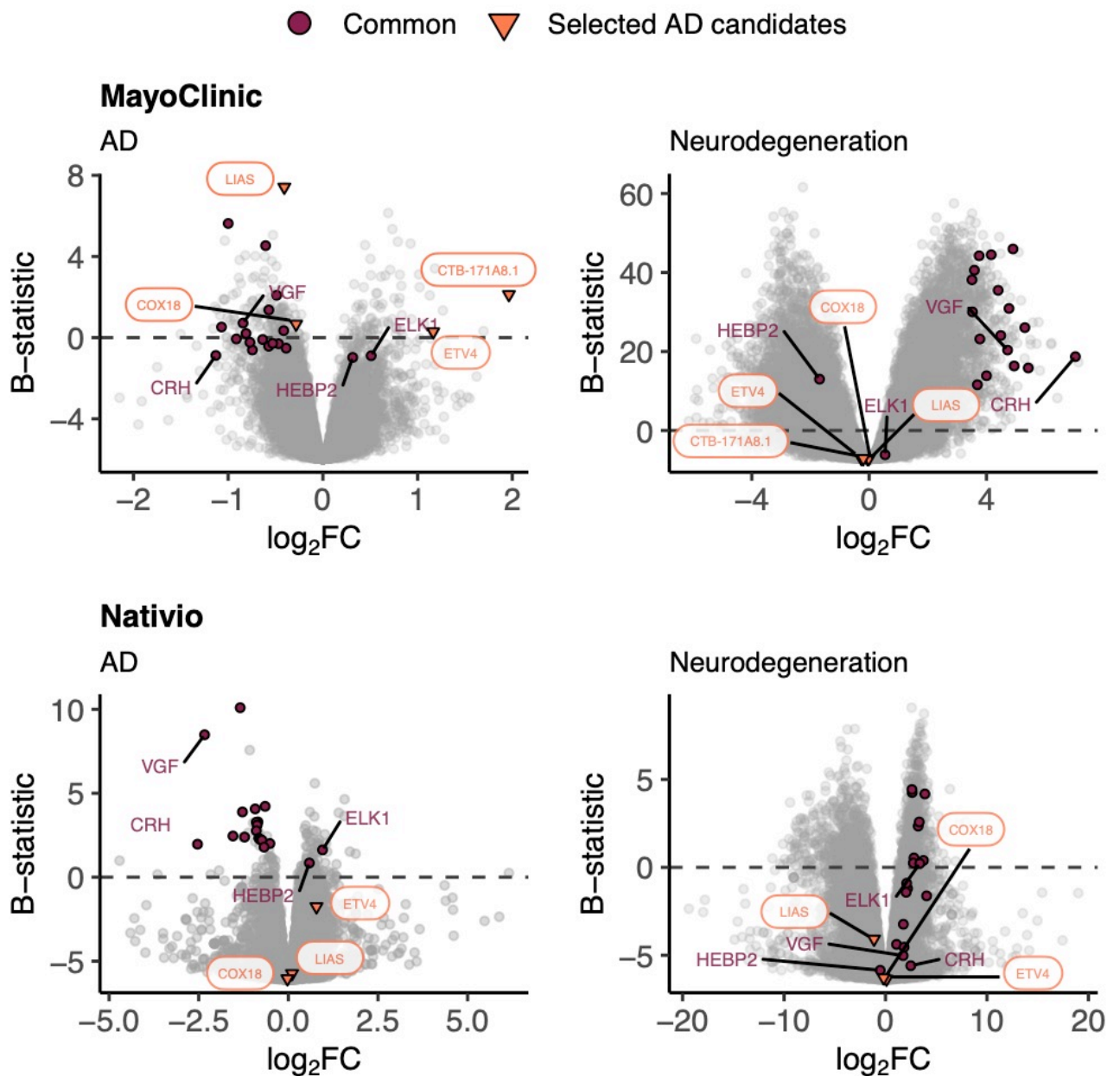
Figure 46 – Volcano plots of differential gene expression in MayoClinc and Nativio samples

Volcano plots, relating log2 fold-changes (log$_2$FC) and B-statistics, of differential gene expression associated with the of AD and Neurodegeneration effects in MayoClinic and Nativio samples. Genes highlighted in orange are those manually selected as candidates for AD-specific alterations already represented in Figure 39, those labelled in Figure 45 are here highlighted in purple ("Common"), and those here labelled in purple are presented in Figure 47.
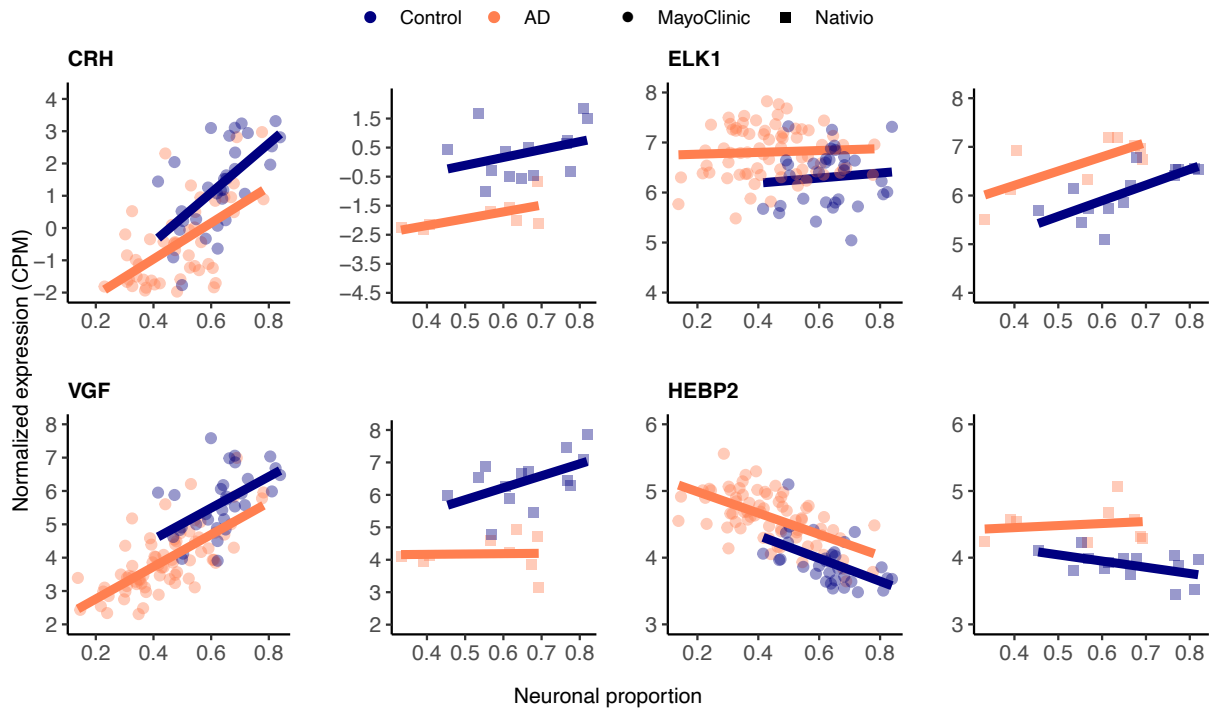
Figure 47 – AD-associated gene expression changes in common between the MayoClinic and Nativio datasets

Expression of manually selected "Common" genes in MayoClinic and Nativio samples. Coloured solid lines represent linear regressions.

5. PD alters cortical gene expre
neurodegeneration

We analysed the PD datasets following simil

transcriptomes. In the RNA-seq PD dataset (

MAP2) and two microglial (*CD40* and *I7*

alterations between PD and non-PD samples

significant differences in cellular composition a

48B) using both the human and the mouse si
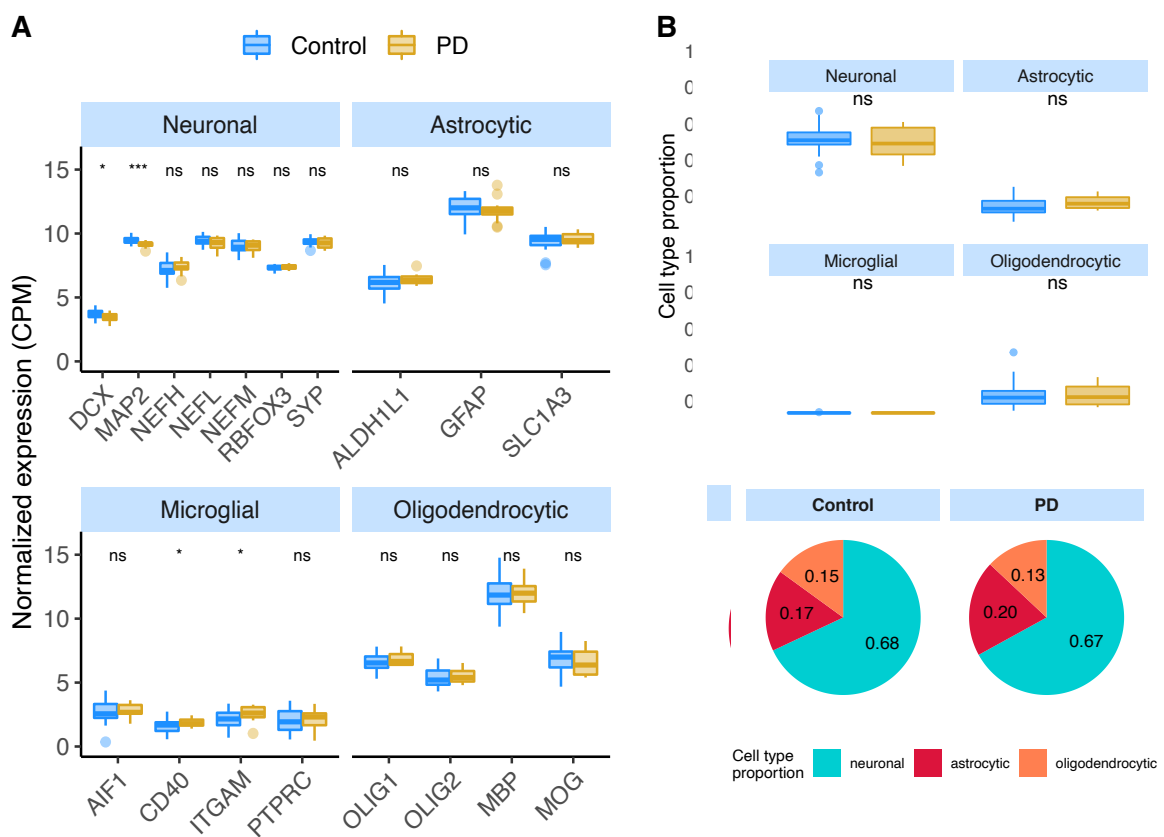
Figure 48 – Estimated cellular composition of Dumitriu brain samples
(A) Neuronal, astrocytic, microglial, and oligodendrocytic known markers' expression in the Dumitriu samples. T-tests were used to compare gene expression mean differences between diseased (PD) and non-diseased (Control) samples. **(B)** Estimates of the composition of Dumitriu samples in each main cell type based on the human cell type gene expression signature. Wilcoxon signed-rank tests were used to compare differences in proportions between diseased (PD) and non-diseased (Control) samples. Legend: ns: non-significant, ****: p <= 0.0001, ***: p <= 0.001, **: p <= 0.01, *: p <= 0.05
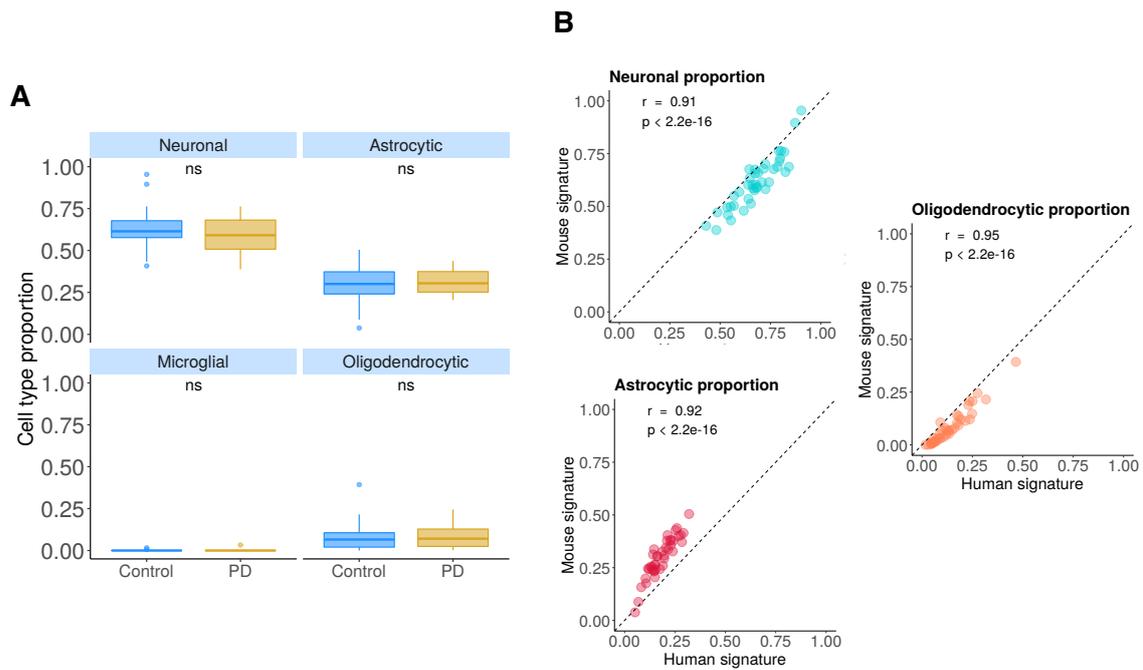
Figure 49 – Estimated cellular composition of Dumitriu brain samples using the mouse cell type gene expression signature

(A) Estimates of the composition of Dumitriu samples in each main cell type based on the mouse cell type gene expression signature. Wilcoxon signed-rank tests were used to compare differences in proportions between Control and PD samples. ns: non-significant, ****: p <= 0.0001. **(B)** Comparison between estimated proportions of different cell types in Dumitriu samples obtained from the human and mouse cell type signatures. Their Pearson's correlation coefficient (r) and respective p-value (p) are shown.
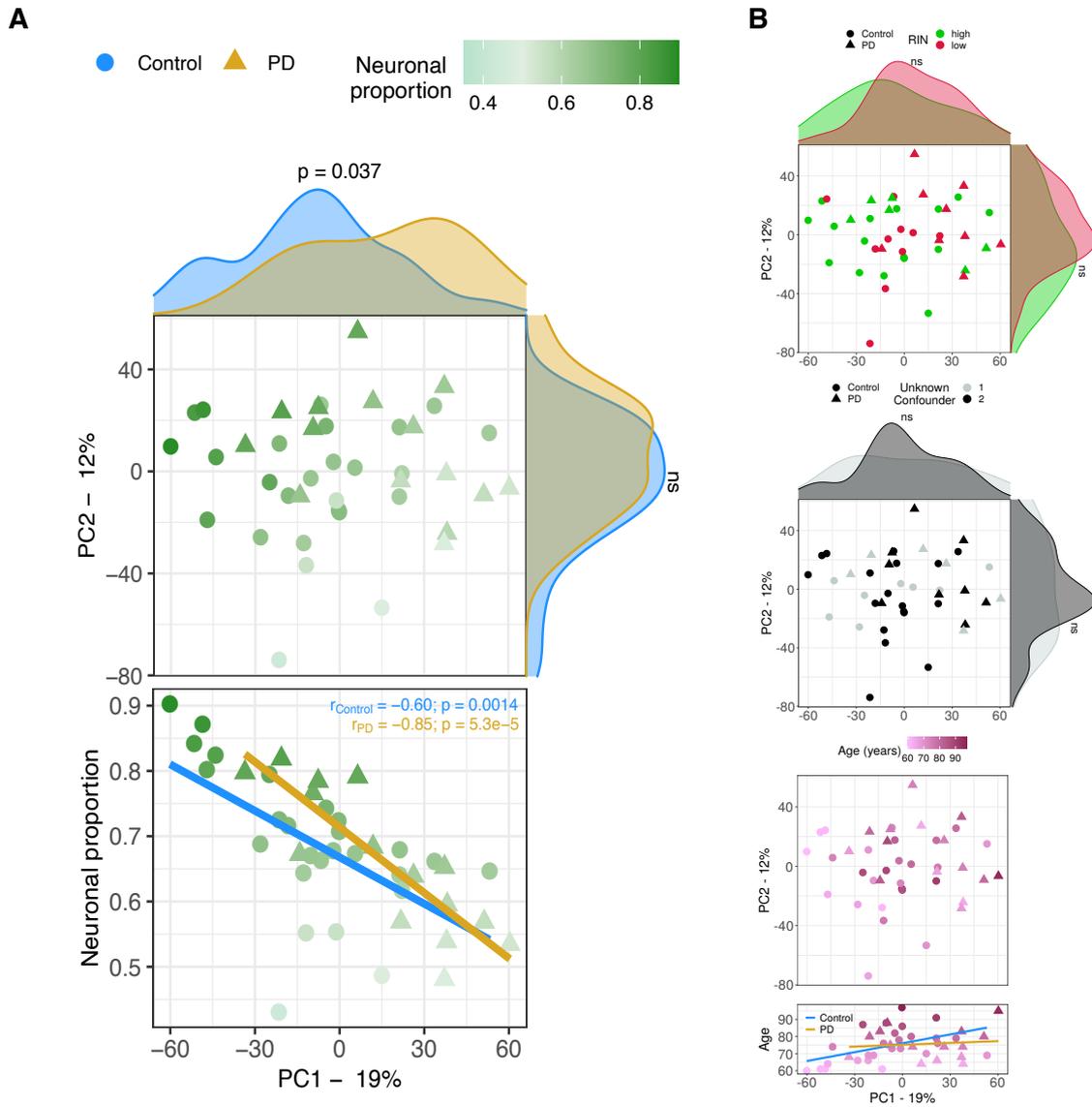
Figure 50 – PCA of the gene expression in Dumitriu samples
(A) Sample factorial map (upper plot) of components 1 (PC1) and 2 (PC2) of Principal Component Analysis (PCA) of the gene expression in Dumitriu samples, and their neuronal proportion related to PC1 loadings (lower plot). Indicated in the respective axes' labels are the percentages of data variance explained by PC1 and PC2. Kolmogorov-Smirnov tests were used to compare the distributions of PC1 and PC2 loadings between PD and Control samples, illustrated by the smoothed histograms along the respective axes of the PCA plot. In the lower plots, the coloured solid lines represent the linear regressions between neuronal proportions and PC1 loadings for PD and Control Samples. The respective Pearson's correlation coefficients (r) and associated significance (p) are also indicated. **(B)** Same as (A) but samples are coloured according to their RIN (top), Unknown confounder (middle) and Age (bottom). Indicated in the respective axes' labels are the percentages of data variance explained by PC1 and PC2. Kolmogorov-Smirnov tests were used to compare the distributions of PC1 and PC2 loadings between RIN groups (top) and Unknown confounder (middle), illustrated by the smoothed histograms along the respective axes of the PCA plots (ns: non-significant). In the lower right plot, the coloured solid lines represent the linear regressions between age and PC1 loadings for PD and Control Samples. Legend: ns: non-significant

A

	PC1	PC2	PC3	PC4	PC5
Oligodendrocytic proportion	0.001	6.8e-7	0.080	0.871	0.454
Astrocytic proportion	2.7e-5	0.469	0.019	0.022	0.003
Neuronal proportion	1.4e-6	0.001	0.640	0.382	0.412
Age	0.037	0.706	0.755	0.891	0.879
Confounder	0.519	0.625	0.607	0.810	0.979
RIN	0.241	0.553	0.890	0.553	0.761
Condition	0.037	0.328	0.909	0.596	0.086

B
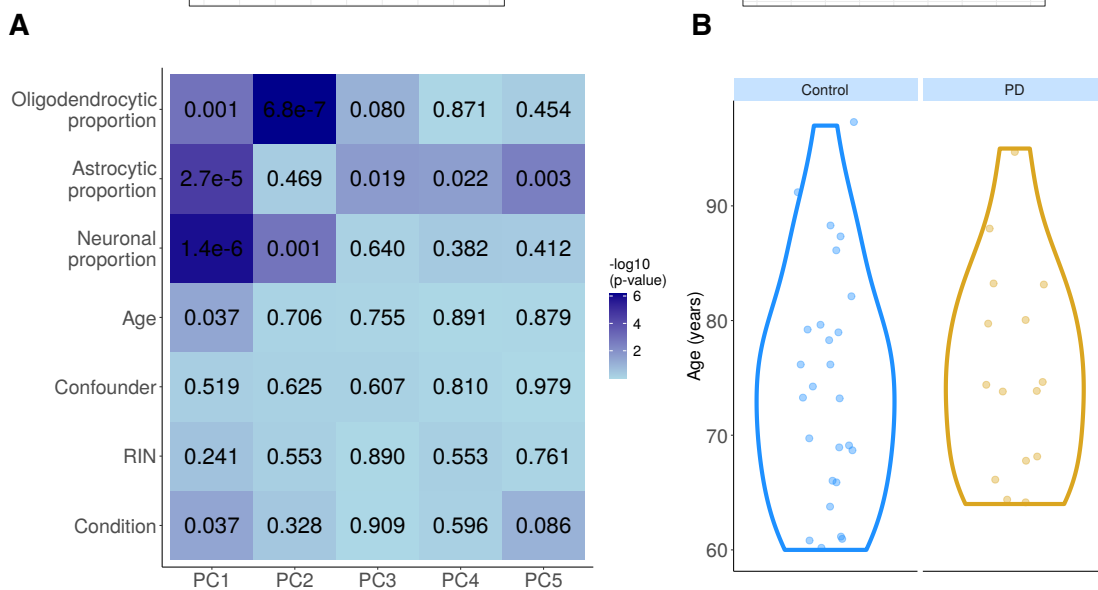
Figure 51 – Relationship between known effects on gene expression in Dumitriu samples
(A) Heatmap of significance, given by p-values, of the association between the loadings of each of the first 5 components of PCA and the seven annotated potentially explanatory sample variables. Spearman's correlation and Kolmogorov-Smirnov tests were used respectively for categorical (Condition, Confounder and RIN) and continuous (proportions of astrocytes, neurons and oligodendrocytes, and Age) variables. **(B)** Violin plots of distributions of age of samples, discriminated between disease status.

Next, gene expression was modelled for each gene as a function of the technical variables (RIN and unknown confounder), neuronal proportion (i.e. neurodegeneration), intrinsic PD and Age (Figure 52, Table S10). No PD-neurodegeneration interaction effect was considered because no significant differences in cell type proportions between PD and non-PD samples were detected (Figure 48B).

102
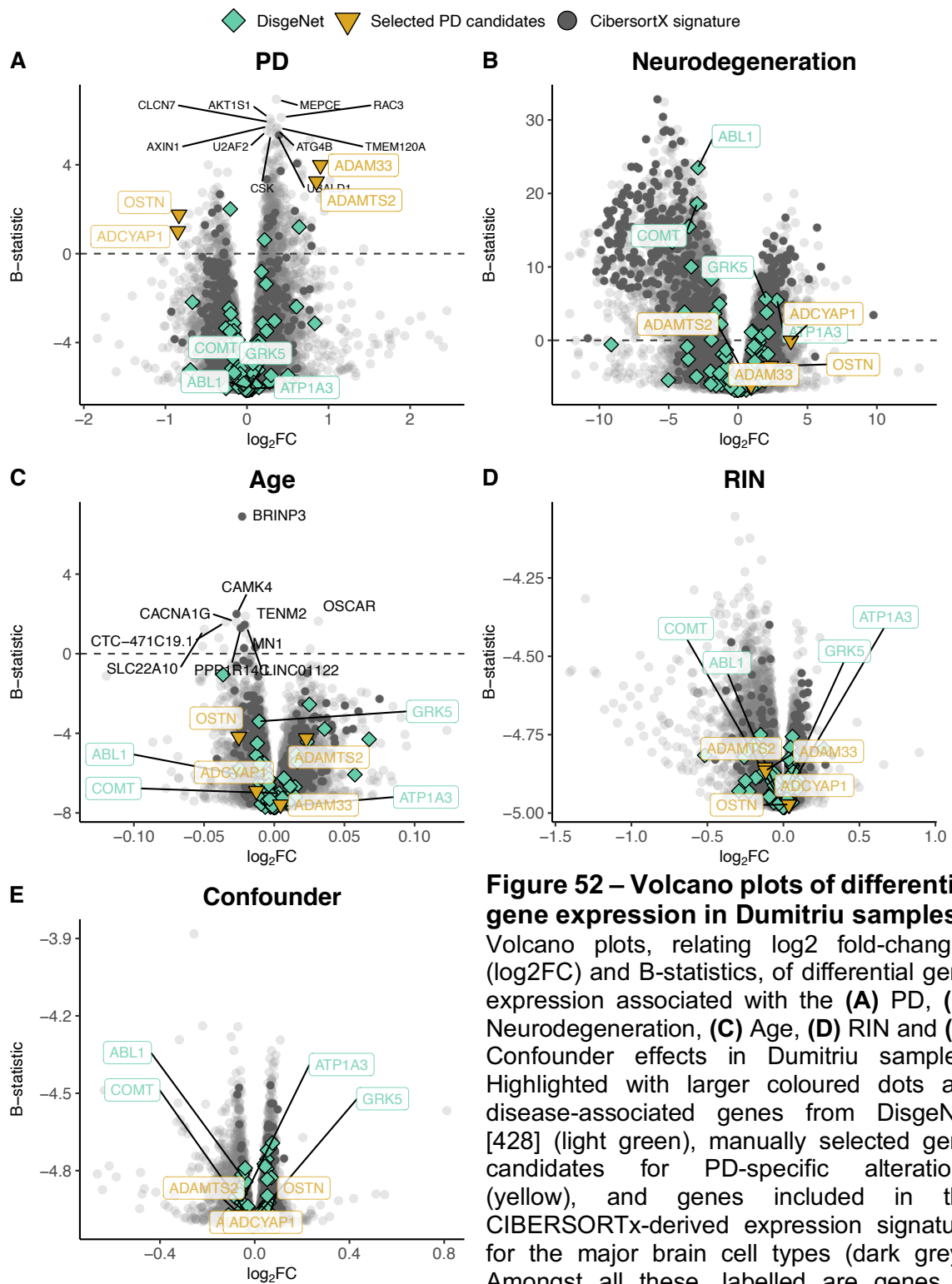
Figure 52 – Volcano plots of differential gene expression in Dumitriu samples

Volcano plots, relating log2 fold-changes (log2FC) and B-statistics, of differential gene expression associated with the **(A)** PD, **(B)** Neurodegeneration, **(C)** Age, **(D)** RIN and **(E)** Confounder effects in Dumitriu samples. Highlighted with larger coloured dots are disease-associated genes from DisgeNet [428] (light green), manually selected gene candidates for PD-specific alterations (yellow), and genes included in the CIBERSORTx-derived expression signature for the major brain cell types (dark grey). Amongst all these, labelled are genes of particular interest, with individual expression profiles plotted in Figure 50. The other labelled genes are the top 10 differentially expressed genes.

We were thereby able to discriminate genes with a strong disease effect (Figures 52A and 53A) from those essentially altered by neurodegeneration (Figures 52B and 53B). In fact, according to our analysis, genes reported as playing a role in PD (*ABL1* [446], *COMT* [447], *GRK5* [448] and *APT1A3* [449]) were found associated with neurodegeneration rather than the disease itself (Figure 53B).
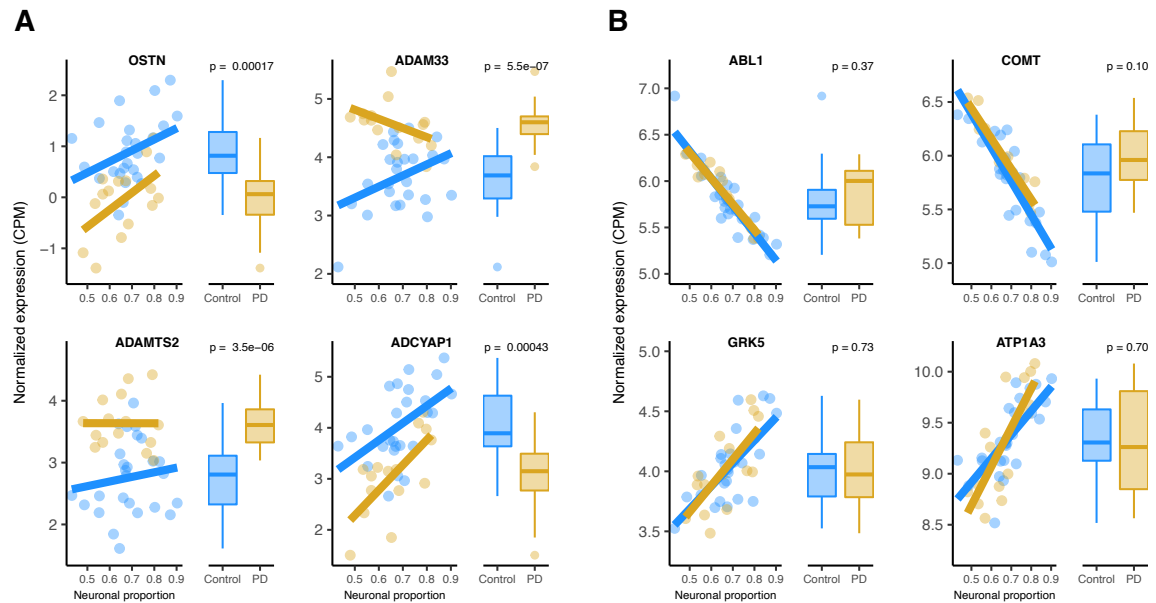
Figure 53 – Expression of selected gene candidates for PD-specific alterations and DisgeNet genes
(**A**) Expression of manually selected gene candidates for PD-specific alterations (labelled in yellow in (Figure 48) in Control and PD samples – scatterplots against neuronal proportion on the left, boxplots of distribution by condition on the right. (**B**) Same as (A) for selected DisgeNet genes (labelled in light green in Figure 48). Coloured solid lines in (A) and (B) represent linear regressions. T-tests, for which p-values are indicated, were used

Moreover, most genes specifically up-regulated in PD brains are annotated as being involved in oxidative phosphorylation and Parkinson's disease (Figure 54).
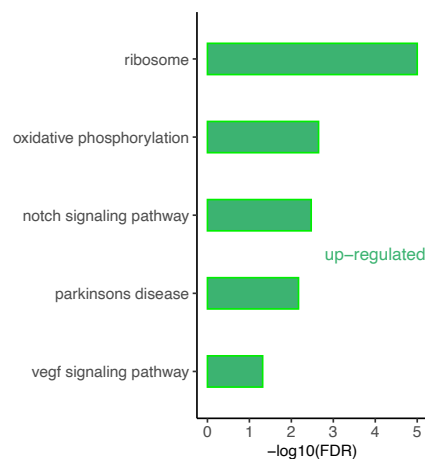
Figure 54 – KEGG pathways altered in PD
Significance of enrichment of KEGG pathways in genes up-regulated (green) in Dumitriu PD samples compared to Controls.

Although RNA-seq provides a more precise quantification of gene expression than microarrays [304], we could not find any other independent PD RNA-seq dataset matching, in terms of brain region, the Dumitriu study and therefore resorted to the Zhang microarray study. This independent dataset did not present any significant cellular composition alteration between PD and non-PD samples (Figure 55) either.
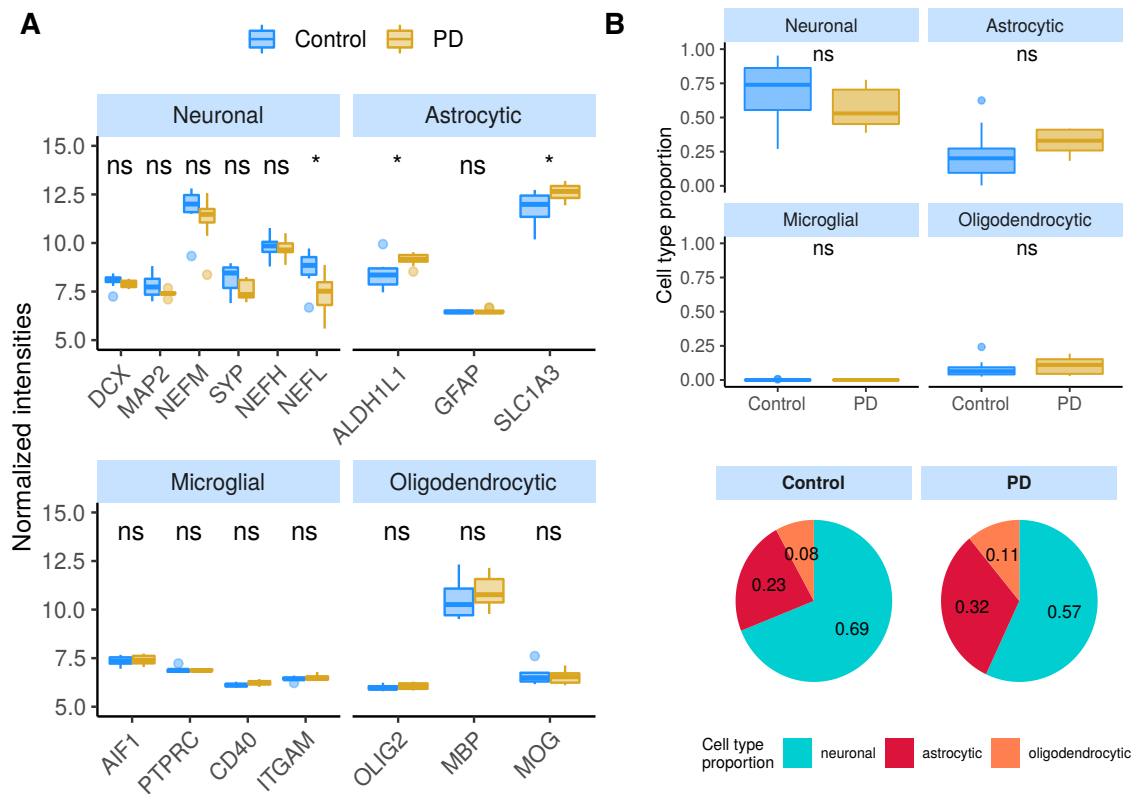
Figure 55 – Estimated cellular composition of Zhang brain samples
(A) Neuronal, astrocytic, microglial and oligodendrocytic known markers' expression in the Zhang samples. T-tests were used to compare gene expression mean differences between Control and PD samples. **(B)** Estimates of the composition of Zhang samples in each main cell type based on the human cell type gene expression signature. Wilcoxon signed-rank tests were used to compare differences in proportions between Control and PD samples.

Additionally, we found no significant differences in neuronal proportion estimates or age between samples from the Dumitriu and Zhang studies (Figure 56).
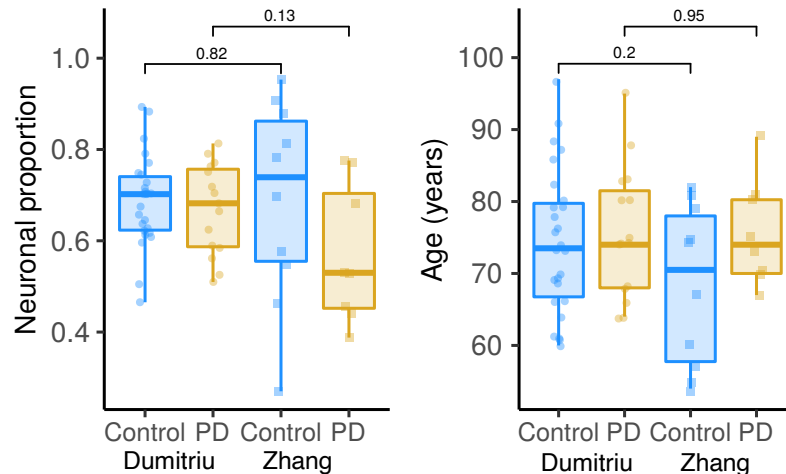
Figure 56 – Comparison of neuronal proportion and age between Dumitriu and Zhang samples

Boxplots of distributions of neuronal proportion (left) and age of donors (right) in Control and PD samples from the Dumitriu and Zhang datasets. Wilcoxon signed-rank tests were used to compare differences in neuronal proportion and age of samples in the same condition between datasets.

We find ge...   ...o analysed PD

datasets (F...   ...*ABCB6* (Figure
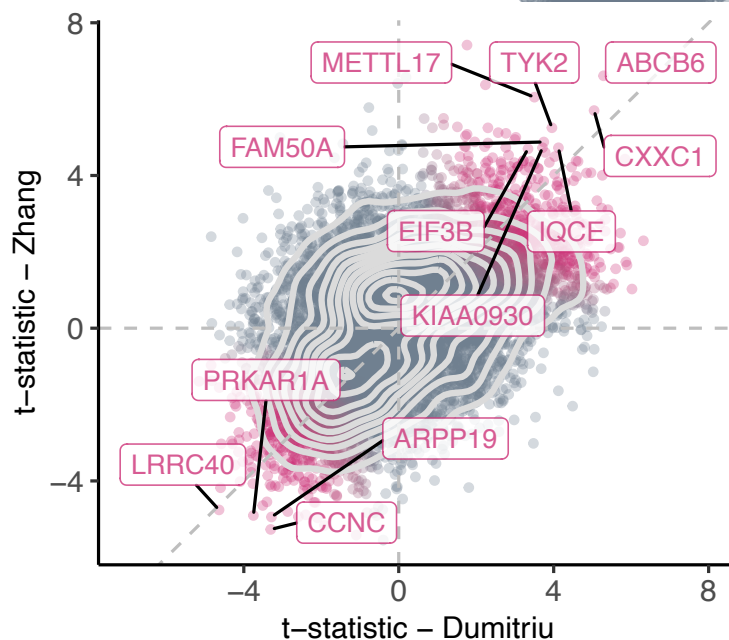
Figure 57 – Comparison of t-statistics of PD-associated differential gene expression between the Dumitriu and Zhang datasets

Scatter plot comparing the t-statistics of differential gene expression associated with the PD effect in Dumitriu and Zhang samples. Points (genes) are coloured according to the FDR of the random permutation test on the product of the t-statistics (v. Materials and Methods). Labelled genes are those significantly differentially expressed (FDR < 0.05 – Dumitriu and FDR < 0.11 – Zhang, v. Materials and Methods) in both datasets and significant in that permutation test (FDR < 0.05). Light gray dashed zero and identity lines, light gray solid contour density lines.

59). However, from the selected PD candidates as examples shown in Figure 53, only *ADAMTS2* and *ADCYAP1* were profiled in the Zhang dataset and did not recapitulate the changes observed in the Dumitriu dataset (Figure 58).

Figure 58 – Volcano plots of differential gene expression in Dumitriu and Zhang samples
Volcano plots, relating log2 fold-changes (log$_2$FC) and B-statistics, of differential gene expression associated with the of PD and Neurodegeneration effects in Dumitriu and Zhang samples. Genes highlighted in orange are those manually selected as candidates for PD-specific alterations already represented in Figure 53, those labelled in Figure 57 are here highlighted in purple ("Common"), and those labelled in purple are presented in Figure 59.

Figure 59 – PD-associated gene expression changes in common between the Dumitriu and Zhang datasets

Expression of manually selected "Common" genes in Dumitriu and Zhang samples. Coloured solid lines represent linear regressions.

AD- and PD-associated gene expression changes in human brains are very correlated (Figure 60A, Tables S14-S15), suggesting commonalities in the molecular mechanisms underlying both diseases.
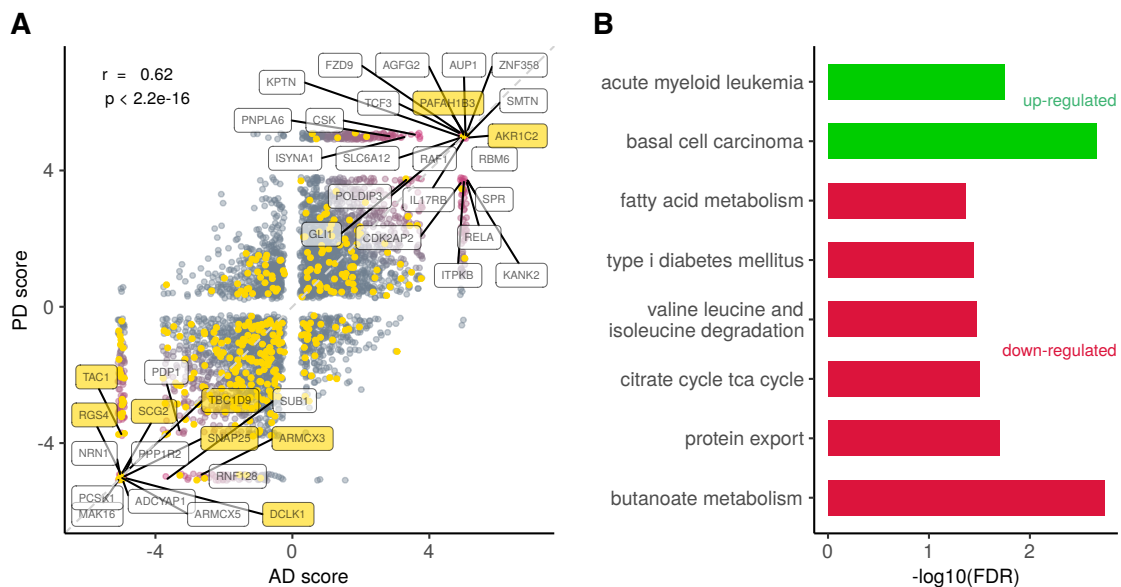
Figure 60 – Common AD- and PD-associated gene expression alterations
(A) Scatter plot comparing the combined scores of differential gene expression (v. Materials and Methods) associated with the AD and the PD effects. Labelled genes are those highly significant (FDR < 0.0005) in the random permutation test of the product of scores (v. Materials and Methods). The Pearson's correlation coefficient (r) between scores and associated significance (p) are also indicated. Neuronal gene markers included in the CIBERSORTx-derived cell-type expression signature depicted in yellow. Identity line in dashed gray. **(B)** Significance of enrichment of KEGG pathways in genes up-regulated (green) and down-regulated (red) in both AD and PD (v. Materials and Methods).

Although some neuronal markers are amongst the genes commonly altered by AD and PD, most of them are not, indicating effectivity in decoupling the neurodegeneration effect on gene expression (Figure 60A). Genes consistently up-regulated in both diseases are linked to Wnt signaling (basal cell carcinoma pathway) and NF-KB signaling (acute myeloid leukemia) (Figure 60B). Indeed, the genes driving the basal cell carcinoma pathway are *FZD9*, *FZD7*, *FZD2*, *DVL1* and *AXIN1*, all playing a role in the Wnt signaling pathway, which has already been linked to AD and PD [450]. The genes contributing the most to the acute myeloid leukemia pathway (*RAF1*, *RELA* and *IKBKB*) are related with NF-KB signaling, a

process already known to also play a role in AD and PD [451]. Genes consistently down-regulated in both diseases are linked essentially to cell metabolism (Figure 60B). Although the magnitude of disease-induced changes in gene expression is generally modest (as expected, as samples from the same type of tissue are being compared), reassuringly they are overall quite independent from the neuronal composition of the brain samples (Figure 61).
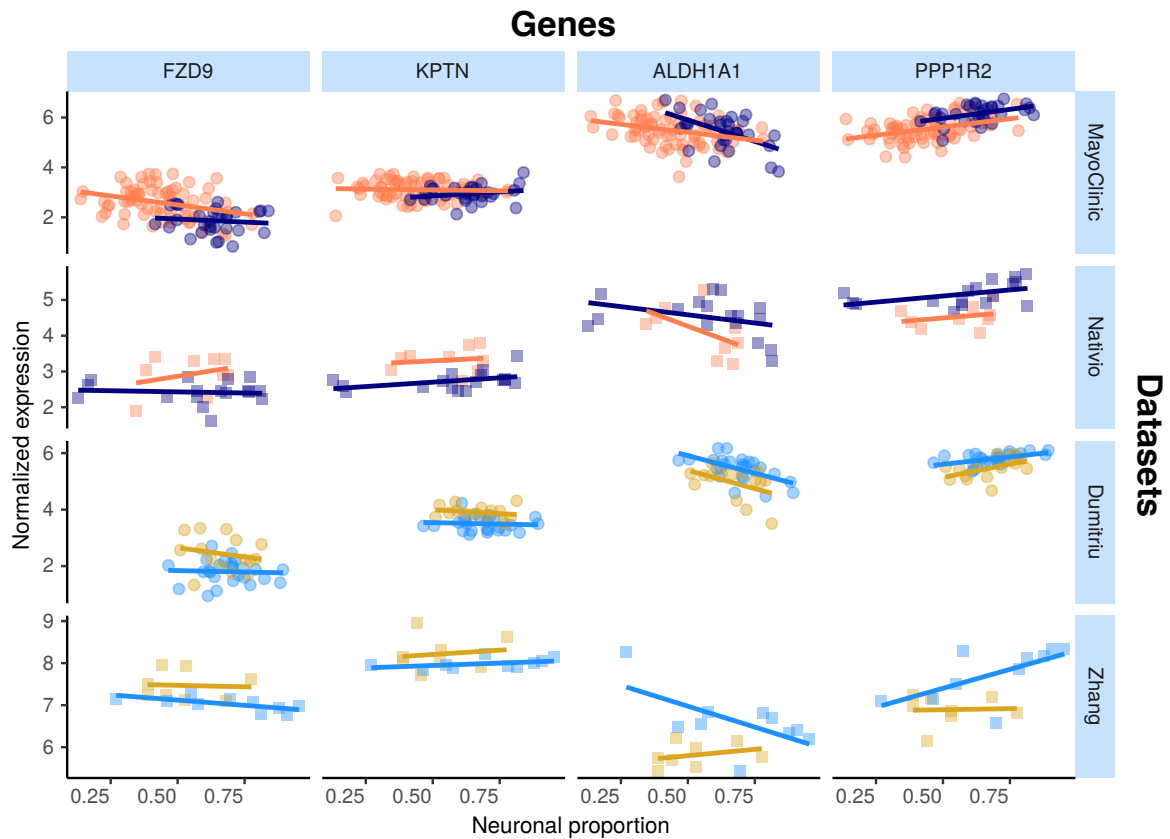
Figure 61 – Expression of selected genes commonly altered in AD and PD in samples from all analysed datasets against their neuronal proportion
Coloured solid lines represent linear regressions.

We used cTRAP [435] to identify drugs that, when delivered to human cell lines, cause similar (correlated) or opposite (anti-correlated) gene expression changes to those we observed as intrinsically associated to AD and PD (Figure 62).
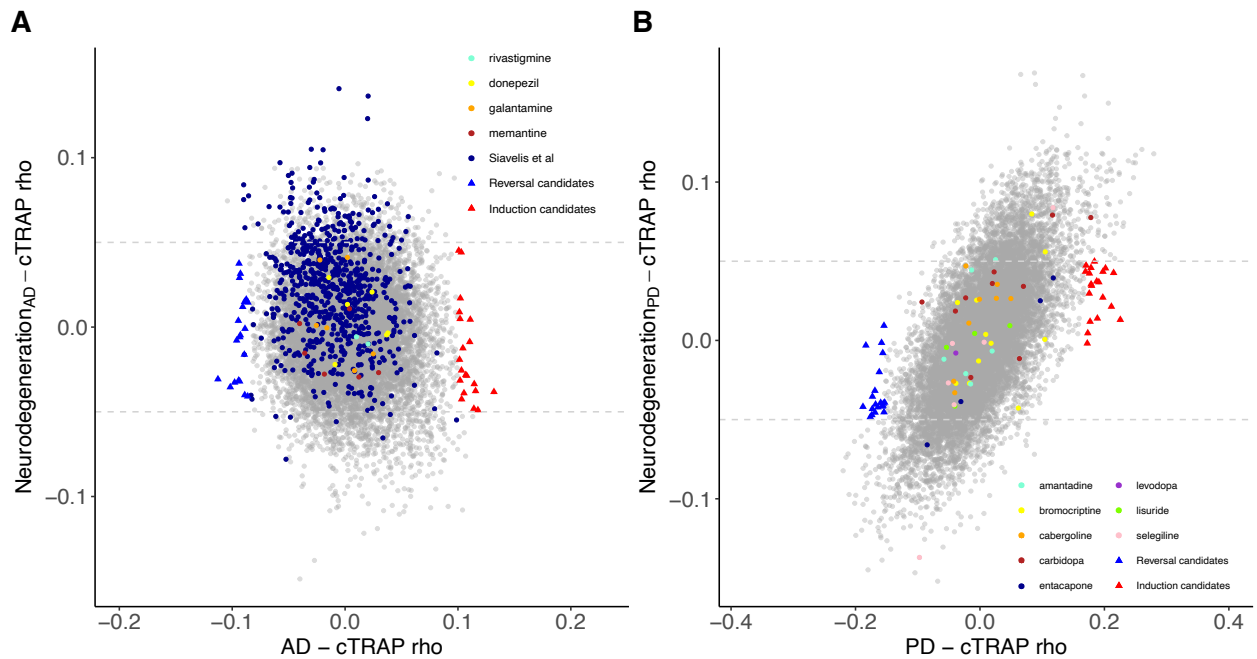
Figure 62 – Comparison of the cTRAP-derived cross-gene Spearman's correlation between AD/PD and the Neurodegeneration effects
(A) Scatter plot comparing, between the AD and the Neurodegeneration effects, the cTRAP-derived cross-gene Spearman's correlation coefficients (rho) of their differential expression combined scores with perturbation z-scores for cMap compounds. Highlighted with blue and red triangles are compounds selected as top candidates for respectively reversal and induction of AD-associated gene expression alterations (Figure 29A; v. Materials and Methods). Coloured circles highlight compounds in use for AD treatments, including those listed by [452]. **(B)** Scatter plot comparing, between the PD and the Neurodegeneration effects, the cTRAP-derived cross-gene Spearman's correlation coefficients (rho) of their differential expression combined scores with perturbation z-scores for cMap compounds. Highlighted with blue and red triangles are compounds selected as top candidates for respectively reversal and induction of PD-associated gene expression alterations (Figure 29B; v. Materials and Methods). Coloured circles highlight compounds in use for PD treatments.

Interestingly, gene expression perturbations induced by drugs known to be used in the clinic to treat AD [452] (donepezil, galantamine, memantine and rivastigmine) and PD [453] (amantadine, bromocriptine, cabergoline, carbidopa, entacapone, levodopa, lisuride and selegiline) were not amongst the most correlated with those by the respective target diseases (Figure 62), Tables S17-S18).
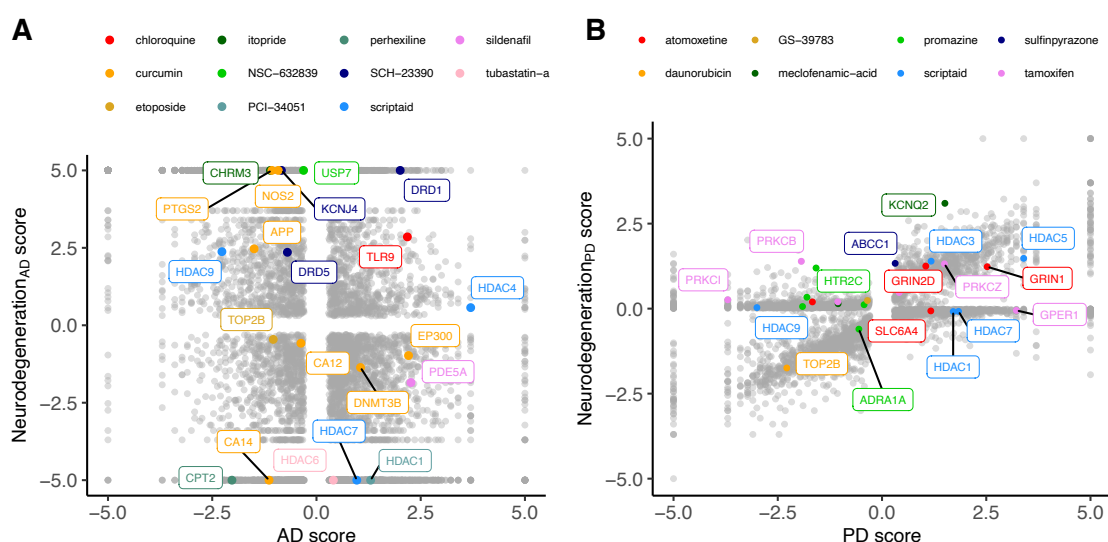
Figure 63 – Comparison of the combined scores of differential gene expression between the AD/ PD and the Neurodegeneration effects
(A) Scatter plot comparing the combined scores of differential gene expression between the AD and the Neurodegeneration effects. Highlighted genes are known targets of selected candidate compounds for reversal of AD-associated gene expression alterations (Figure 29A). **(B)** Scatter plot comparing the combined scores of differential gene expression between the PD and the Neurodegeneration effects. Highlighted genes are known targets of selected candidate compounds for reversal of PD-associated gene expression alterations (Figure 29B).

Siavelis et al. [452] had followed a similar approach, although they did not decouple the neurodegeneration effect, having identified 27 drugs linked to the AD phenotype (Figure 62A). Chloroquine and scriptaid seem promising drug candidates for AD since their known targets are indeed overexpressed in AD and vary very little with neurodegeneration (Figure 63A). Scriptaid also seems promising for PD therapeutics for similar reasons (Figure 63B).

Additionally, gene expression changes upon metaraminol administration showed up as being the most anti-correlated with those commonly induced by AD and PD (Figure 64), being metaraminol therefore a potential candidate drug to be tested for repurposing. Gene expression changes upon wortmannin administration are, in a

dose dependent manner, the most correlated with those commonly induced by AD and PD (Figure 64).
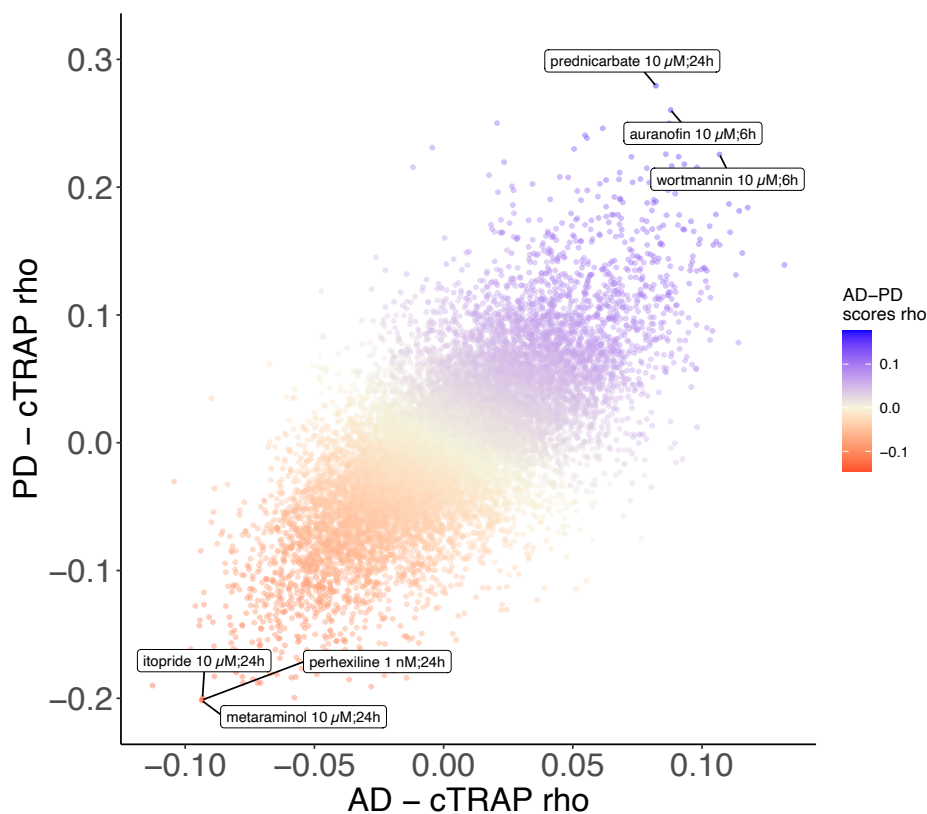
Figure 64 – Comparison of the cTRAP-derived cross-gene Spearman's correlation coefficients between the AD and the PD effects
Scatter plot comparing, between the AD and the PD effects, the cTRAP-derived cross-gene Spearman's correlation coefficients (rho) of their differential expression combined scores with perturbation z-scores for cMap compounds. Points (compounds) are coloured according to the cross-gene Spearman's correlation coefficients of their perturbation z-scores with the scores for common AD-PD differential expression (v. Materials and Methods). Labelled compounds are the 3 most correlated and the 3 most anti-correlated compounds.

V- Discussion

In this thesis, we investigated the impact of cellular composition on Alzheimer's and Parkinson's diseases' molecular effects in human brains.

1. Neural cellular markers' expression is altered in AD brains

AD and PD brains are characterized by a loss of neurons and an increase of astrocytic reactivity when compared to age-matched healthy brain samples [270,454–456]. Signatures of these changes will be confounded with disease-intrinsic molecular alterations, both systemic and cell type-specific, in any differential expression analysis between diseased and healthy brains. We confirmed this by looking at the expression of known neuronal, astrocytic, oligodendrocytic and microglial markers in AD and PD transcriptomic datasets. We indeed found neuronal and astrocytic markers significantly downregulated and upregulated, respectively, in MayoClinic AD samples compared to controls (Figure 34A). Although microglia were reported to be involved in AD [457] and PD [458], we only observed a significant increase in one (*CD40*) out of four microglial markers tested in AD (Figure 34A) and in two (*CD40* and *ITGAM*) in PD samples (Figure 48A). Since microglia represent a small subset of human brain cells (5% to 15% of human brain cells [459]), there were likely too few microglial cells in the profiled brain sections for their transcriptomic signal to be properly detected, as suggested by our digital cytometry estimates (Figures 34B and 48B). Still, the detection of a significant increase in *CD40* and *ITGAM* microglial markers in PD samples needs further investigation, as the highest concentration of microglia in the brain is located in the *substantia nigra* [277], the first region affected by the loss of dopaminergic neurons in PD [152]. This could then induce a more reactive response of microglia in PD cortices.

2. Neural cell type gene expression signatures can be used to accurately estimate the cellular composition of artificial brain tissue samples from their transcriptomes

Based on the evidence that cellular composition was altered in AD and PD brain samples, we computationally estimated therein the proportion of the main brain cell types: neurons, astrocytes, microglia and oligodendrocytes. We derived a gene expression signature (1962 genes – Table S2) from a publicly available single-cell RNA-seq dataset of human adult cortical samples [460] to distinguish those four cell types. To test the specificity of those signatures, we used CIBERSORTx [423] to estimate the composition of samples from an independent single-cell RNA-seq dataset [271] of human neurons, microglia, astrocytes and oligodendrocytes. Each of these cells was mostly assigned to its respective pre-annotated cell type (Figure 32A). Some oligodendrocyte samples showed a small presence of the other three cell types that might be related with the myelin of oligodendrocytes having some debris of astrocytes, microglia and neurons attached, given that oligodendrocytes closely interact with those cells [461]. With the further advances in scRNA-seq technologies and the accumulation of human brain single-cell datasets in healthy and diseased conditions [462], the major brain cell type signatures will be further improved and allow an increase the sensitivity of digital cytometry.

3. Cellular composition is significantly altered in AD brains

After validating the cell type signatures, we used them to estimate the proportion of neurons, astrocytes, microglia and oligodendrocytes in AD and PD brain samples from their bulk transcriptomes. In line with differences in expression in canonical markers illustrated in Figure 34A, the estimated neuronal proportion was significantly lower in AD compared with control brains (Figure 34B). Some samples reached up to 60-90% of neurons, much higher than estimates based on cell counting [459,463]. This is likely related with the neuronal RNA content being up to two fold as much as that of glial cells [464]. In this study we are therefore estimating the relative contribution by each cell type to the total amount of mRNA in the bulk samples and not their actual proportion of the total number of cells.

4. Neuronal loss-independent intrinsic disease effects on gene expression in the human brain can be linearly modelled

Linear models are a commonly used statistical approach to model gene expression as a function of relevant explanatory variables. Here, these were potential technical biases (RIN and an unknown confounder variable), age, sex (for AD datasets), estimated neuronal proportion (neurodegeneration), disease (categorical AD or PD) and, for the AD datasets, interaction between neurodegeneration and disease. Considering that AD and PD are age-related neurodegenerative disorders, it is expected that most of their associated gene expression changes in the brain are result from the loss of neurons and ageing, therefore the need to estimate their independent effects and decouple them from the intrinsic molecular effects of the diseases that we are interested in. Using those models, we identified genes whose expression was significantly affected by the intrinsic (systemic) disease effect (Figures 39 and 53A), as well as genes whose expression was mostly explained by the other effects (Figures 38 and 52).

However, we were not able to completely decouple the explanatory variables, as the associated moderated t statistics of differential expression were to some extent correlated with each other (Figure 65). The correlations between RIN and the intrinsic disease and neurodegeneration effects may be explained by potential agonal conditions, such as patients being in a coma or their brains undergoing hypoxia just before death, preceding the collection of *post-mortem* samples [465]. For AD, with the *Interaction* effect, we were able to detect genes whose expression varies differently upon neurodegeneration in AD samples (Figure 41). For example, the *PNPLA5* gene is involved in lipid metabolism [466] and is thought to play a role in the autophagy biogenesis [467]. Those processes have been implicated in AD [468,469] and a variant in *PNPLA5* was reported to be associated with the *APOE* genotype directly linked to AD [470]. Another example is *PTPN20A*, encoding a phosphatase with a dynamic subcellular distribution that targets sites of actin
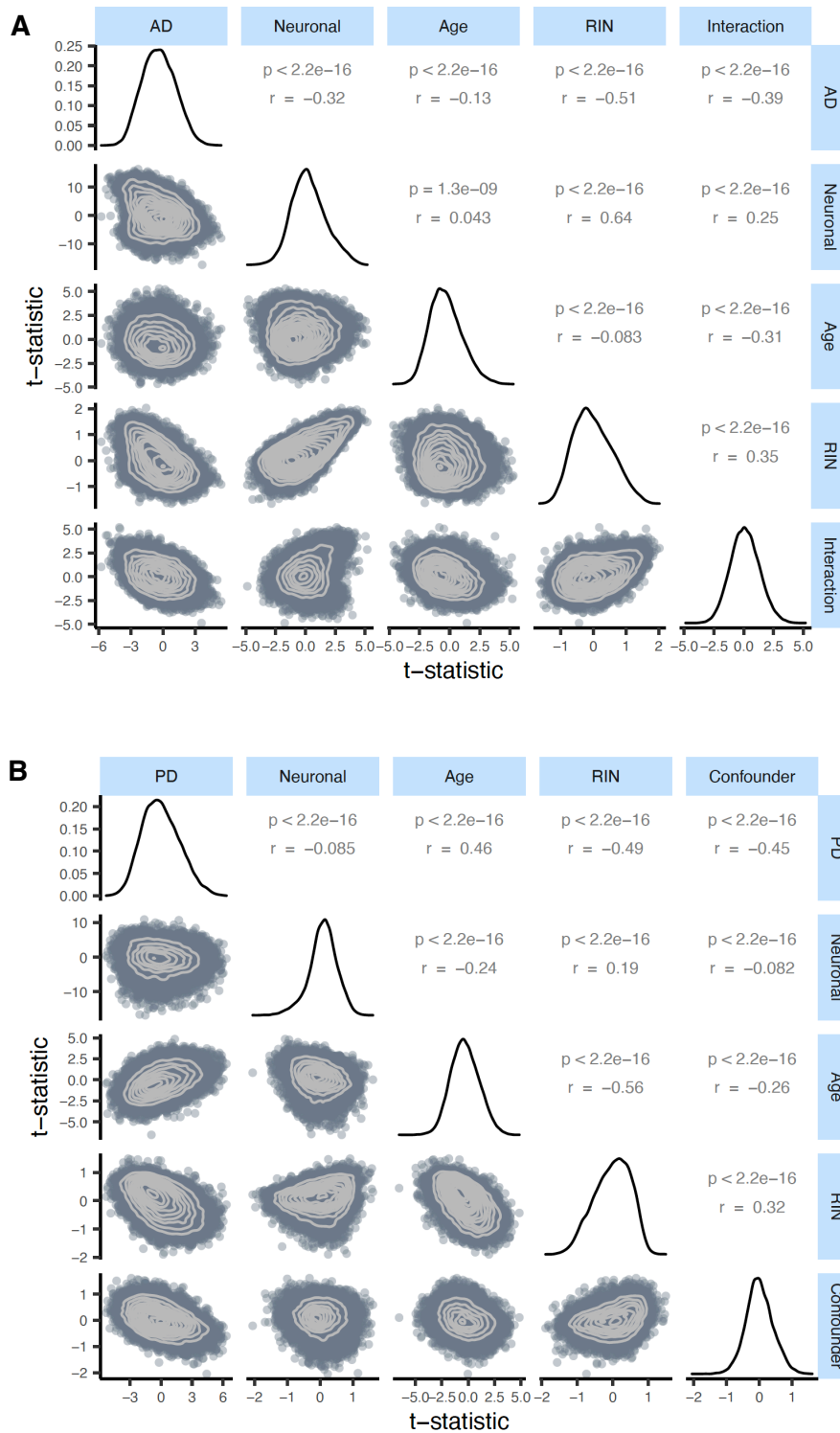
Figure 65 – Comparison of t-statistics of differential expression between modelled effects in AD and PD
Below the diagonal: scatter plots (with light gray solid contour density lines) comparing the t-statistics of differential gene expression between pairs of modelled effects for the MayoClinic **(A)** and Dumitriu **(B)** datasets. Diagonal: smoothed histograms of distributions of t-statistics of t-statistics of differential gene expression for the modelled effects. Above the diagonal: Pearson's correlation coefficients (r), and associated significance (p), of t-statistics of differential gene expression between pairs of modelled effects.

polymerization, a fundamental cellular process [471]. Although, to our knowledge, no reports have linked *PTPN20A* to AD, it might indicate that, concomitant with the loss of other neurons, AD neurons suffer more structural changes than non-AD neurons.

The importance of decoupling the intrinsic disease effect from others can be seen in Figures 40 and 53B. Looking at some of the genes already reported as potentially playing a role in AD (e.g. *CDK5* [442]) or PD (e.g. *COMT* [447]), we observed that alterations in their expression were mostly driven by neurodegeneration, i.e. by changes in cellular composition, but not so much by an intrinsic cell type-independent disease effect. This suggests that some genes previously reported as candidates for playing a role in AD or PD may be "false positives" for their association with the diseases' aetiology and, given their cell-type specificity, have been found dysregulated due to changes in cellular composition [434].

As shown in Figures 45 and 57, the results of differential expression analyses are significantly correlated between independent datasets. Although some genes initially selected as candidates for intrinsic disease markers, such as *ETV4* and *LIAS* for AD, were not found to behave consistently in both datasets, others previously described as playing a role in AD and PD, such as *RPH3A* [472] and *CXXC1* [473], were consistent. We identified genes such as *HEBP2* and *PRKAR1A* to be respectively AD and PD-specific (Figure 49 and Figure 59) and, to our knowledge, they had not been previously linked with the disorders. *HEBP2* is known to play a role in mitochondria and its inhibition has been shown to be important for HeLa cells survival upon oxidative stress [474]. Considering that *HEBP2* is upregulated in our AD samples, its overexpression may contribute to the sudden death of neuronal cells upon the AD-characteristic high oxidative stress environment [475]. Moreover, although *HEBP2* has not yet been linked to AD, its homologue *HEBP1* has been described as potentially playing a role in neurons' ability to sense cytotoxicity over the course of the disease [476]. When PRKAR1A, the cAMP-dependent protein kinase type I-alpha regulatory subunit, is not working properly, it causes an hyperactivation of PKA signalling and its loss of function has been shown to cause cell death and muscle impairment [477], two PD-related phenotypes.

5. AD and PD brains share common gene alterations

Being the two most common neurodegenerative disorders in the world, it has already been suggested that AD and PD could share a common mechanism of neurodegeneration [388,478]. For instance, *Greenfiel et al*. proposed that the common mechanism may be associated with the aberrant activation of a developmental process involving a non-classical, non-enzymatic action of acetylcholinesterase [479]. Our results suggest that the genes whose expression is commonly altered in AD and PD are essentially related with cell metabolism and NF-KB and Wnt signaling pathways (Figure 60B), which were already reported as playing a role in PD [450,451,480,481] . Oxidative phosphorylation and Parkinson's disease pathways were significantly altered in both diseases but enriched in genes downregulated in the MayoClinic AD samples (Figure 42) and upregulated in Dumitriu PD samples (Figure 54). The putative upregulation of the oxidative phosphorylation pathway in PD is mostly driven by NADH dehydrogenase genes such as *NDUFS8*, *NDUFS7* and *NDUFA11*, which take part in mitochondria's complex I, already reported to be impaired in PD [482]. Oxidative phosphorylation's apparent downregulation in AD is mostly driven by *COX* genes such as *COX11* and *COX15*. The most consistent defect in mitochondrial electron transport enzymes in AD is indeed a deficiency in COX [483], mitochondria complex IV [483]. Genes highlighted in Figure 60 should also be considered as candidate targets for functional manipulation in both AD- and PD-related studies, since they may unveil mechanisms that are disrupted in similar ways in both disorders.

6. *In silico* chemo-transcriptomic analyses could act as preliminary screens for drug repurposing in AD and PD

Drug discovery for human diseases is a slow and costly process [484], drug repurposing being therefore seen as a faster, safer and cheaper alternative [452]. Using *cTRAP* [435], we identified drugs, already in clinical trials or launched, that potentially induce gene expression changes that are significantly anti-correlated with those caused by AD and PD (Figures 62A-B). For AD, we identified compounds already linked with the disease. For instance, chloroquine, an antimalarial drug, was

shown to increase tau proteolysis [485] as well as to be neuroprotective upon brain injury by diminishing inflammation and neuronal autophagic death [486]. Tubastatin-a, an HDAC6 inhibitor, was used in AD mice leading to alleviated behavioral deficits, alterations on amyloid-beta load and reduced tau phosphorylation [487]. Sildenafil, usually used to treat erectile dysfunction, is currently being investigated in AD therapeutics [488]. Amisulpride and citalopram, two antipsychotic drugs, have been used in AD [489,490]. Curcumin has been implicated in AD therapeutics, apparently decreasing beta-amyloid plaques as well as slowing neurodegeneration and acting as an anti-inflammatory [491]. Doxycycline is a compound known to cross the blood-brain barrier and a very promising candidate since it reduced amyloid-beta oligomers and neuroinflammation in AD mouse models [492]. Etoposide needs to be further explored, given a study reporting it as an inducer of cellular senescence and mitochondrial dysfunction in cultured rat astrocytes [493] but knowing that rat cell lines may not recapitulate all the molecular cues of the human brain microenvironment. To our knowledge, no research has been reported on the use of interesting candidates panobinostat, dimenhydrinate and perhexiline in AD. Indeed, perhexiline is involved in the inhibition of mTOR pathway which is related with autophagy, a process known to be altered in AD [494], and panobinostat acts as an HDAC inhibitor, leading to the hypothesis that it may play a role similar to that of tubastatin-a. For PD, we also identified compounds previously linked to the disease. Atomoxetine, an inhibitor of the norepinephrine reuptake, has been studied in PD therapeutics since the noradrenergic system is involved in executive functions impaired in PD [495]. Meclofenamic acid, a non-steroid anti-inflammatory drug, has been shown to have an anti-fibrillogenic effect on alpha-synuclein fibrils *in vitro* [496]. Tamoxifen, an estrogen modulator, has also been related with PD treatment but is associated with controversial findings. Although tamoxifen demonstrated neuroprotective effects in some animal and *in vitro* studies [497,498], it has been shown in some cohorts of female breast cancer patients that its usage may increase PD risk [499,500]. However, given that our PD analyses were performed only in male samples, our results could suggest a sex-specific mode of action of tamoxifen in PD. Additionally, myricetin has neuroprotective effects in different PD *Drosophila* and rat models [501,502]. To our knowledge, other drugs such as genipin and praziquantel have not yet been related to PD and could be interesting to further explore for repurposing in that context. For instance, genipin is the main component

of a Chinese medicinal herb and was shown to have anti-inflammatory and neuroprotective effects that could be beneficial for neurogenerative diseases such as PD [503]. Praziquantel, an anthelmintic compound, could be a very interesting candidate since niclosamide, another anthelmintic drug, has been suggested to be beneficial in PD through the activation of the PINK1 pathway that is usually impaired in PD [504].

Metaraminol, an adrenergic agonist that also stimulates the release of norepinephrine and primarily used as a vasoconstrictor in the treatment of hypotension [505], induces the gene expression changes most anti-correlated with those by both AD and PD (Figure 64). To our knowledge, there is no association between metaraminol and AD and PD therapeutics. However, adrenergic agonists can decrease noradrenergic degeneration, a characteristic condition of AD patients [506]. As for PD, using adrenergic agonists along with levodopa treatment has been shown to lead to a diminishment in parkinsonian symptoms [507]. Perhexiline can act as an inhibitor of mTORC1, a protein kinase involved in autophagy, and is able to stimulate autophagy [508]. One common shared feature between AD and PD is indeed autophagy decrease [509], which might explain the anti-correlation between its transcriptomic impact and the expression profiles changes induced by AD and PD (Figure 64). Itopride, a dopamine D2 antagonist with acetylcholinesterase inhibitory actions [505], has already been studied as a potential drug for AD given its very similar structure to curcumin, shown to decrease the accumulation of Aß aggregates [510]. Moreover, it is also used for increasing gastrointestinal motility, a symptom that is prominent in PD patients, although it also seems to induce parkinsonism [511]. We also found scriptaid (Figure 63), a histone deacetylase (HDAC) inhibitor. HDAC enzymes have already been linked to neurodegenerative diseases and there are already several applications of HDAC inhibitors being tested in such context [512]. Interestingly, gene expression changes induced by wortmannin, auranofin and prednicarbate, were the most correlated with those by AD and PD. Indeed, wortmannin has been shown to increase Alzheimer-like tau phosphorylation *in vivo* [513,514] and to diminish the effect of an anti-apoptotic compound in an *in vitro* PD model [515]. Auranofin, a drug used as an antirheumatic agent, has indeed been linked with AD and PD, but not as an inducer of both disorders [516]. This result needs to be further explored as, for instance, auranofin

seems to act through glial cells but does not stop cytokines secretion from astrocytes [517,518]. Additionally, these findings result from work in cell lines [517] and mice [518], models that do not recapitulate all the molecular cues of the human brain microenvironment. To our knowledge, there is no association between prednicarbate, a corticosteroid drug with an anti-inflammatory action, and AD and PD therapeutics besides the recommendation of not being used together with memantine, one of the few FDA approved drugs for AD, since it inhibits its action [519]. These results show the potential of using *in silico* tools to find existing drugs that could be tested as candidates for the treatment of neurodegenerative diseases.

7. Conclusion

In summary, our results show the relevance of modelling and accounting for cell type composition when analysing molecular alterations associated with neurodegenerative disorders, thereby helping to identify candidate gene targets that are related with the disease itself rather than the consequent loss of neurons. They also illustrate the interest of performing *in silico* analysis of chemical perturbagens as preliminary screens for drug repurposing, helping to find new, more effective drug therapies that could mitigate, or even reverse, some of those neurodegenerative disorders' phenotypes.

VII – Future perspectives

To our knowledge, this is the first study that decouples the effects of cellular composition, ageing and sex from the intrinsic disease effect of AD and PD on gene expression in human brains. However, our study has limitations. We focused on the four major brain cell types but our approach is not sensitive enough to estimate the relative amount of mRNA contributed by microglia, therefore missing the transcriptomic signal of their physiology. Moreover, although we validated our results using independent public datasets, an additional local experimental validation is not feasible due to extreme difficulty in having access to human samples that would be suitable independent replicates of those used to generate the analysed datasets. Additionally, drugs currently used for AD and PD treatment were not among those our analysis deemed more likely able to revert the AD-/PD-specific gene expression changes. This likely reflects the differences between gene expression changes induced by drugs in cancer cell lines (i.e. those available in CMap [436], on which *cTRAP* [435] relies) and those the same drugs would induce in brain cells.

We expect the permanent development of single-cell technologies to help increase the resolution of our understanding of the nuances in each human brain cell type, as well as which molecular perturbations therein are critical to the onset and progression of neurodegenerative diseases such as AD and PD. In fact, there are already some studies using single-cell RNA-seq to characterize the cellular composition in normal brains [322,460,520], in neurogenesis and somatic reprogramming to neurons [521,522], as well as in AD brains [341,523]. Nevertheless, as single-cell data are still accumulating and there are several bulk transcriptomes available for brains affected by neurodegenerative disorders, approaches like ours could help in the meantime to unveil some of cellular and molecular complexity associated with neurodegeneration in humans.

VII – References

1. Batista-García-Ramó K, Fernández-Verdecia C. What We Know About the Brain Structure–Function Relationship. Behav Sci (Basel). 2018;8: 39. doi:10.3390/bs8040039

2. Hedman AM, van Haren NEM, Schnack HG, Kahn RS, Hulshoff Pol HE. Human brain changes across the life span: A review of 56 longitudinal magnetic resonance imaging studies. Hum Brain Mapp. 2012;33: 1987–2002. doi:10.1002/hbm.21334

3. Ghannam JY, Al Kharazi KA. Neuroanatomy, Cranial Meninges [Internet]. StatPearls. 2020. Available: http://www.ncbi.nlm.nih.gov/pubmed/30969704

4. McCullar KS, Rhodes PC, Underhill SA, Nagel JKS. Application of Bio-Inspired Design to Minimize Material Diversity. Volume 4: 21st Design for Manufacturing and the Life Cycle Conference; 10th International Conference on Micro- and Nanosystems. American Society of Mechanical Engineers; 2016. doi:10.1115/DETC2016-59684

5. Greenberg RW, Lane EL, Cinnamon J, Farmer P, Hyman RA. The cranial meninges: Anatomic considerations. Semin Ultrasound, CT MRI. 1994;15: 454–465. doi:10.1016/S0887-2171(05)80017-4

6. Adeeb N, Mortazavi MM, Deep A, Griessenauer CJ, Watanabe K, Shoja MM, et al. The pia mater: a comprehensive review of literature. Child's Nerv Syst. 2013;29: 1803–1810. doi:10.1007/s00381-013-2044-5

7. Kwee RM, Kwee TC. Virchow-Robin Spaces at MR Imaging. RadioGraphics. 2007;27: 1071–1086. doi:10.1148/rg.274065722

8. Seeley RR, Stephens TD, Tate P. Organização Funcional do Tecido Nervoso. Anatomia e Fisiologia - 6a edição. 2003. pp. 378–379.

9. Chedotal A, Richards LJ. Wiring the Brain: The Biology of Neuronal Guidance. Cold Spring Harb Perspect Biol. 2010;2: a001917–a001917. doi:10.1101/cshperspect.a001917

10. Bui T, M Das J. Neuroanatomy, Cerebral Hemisphere [Internet]. StatPearls. 2020. Available: http://www.ncbi.nlm.nih.gov/pubmed/31747196

11. Lanciego JL, Luquin N, Obeso JA. Functional Neuroanatomy of the Basal Ganglia. Cold Spring Harb Perspect Med. 2012;2: a009621–a009621.

doi:10.1101/cshperspect.a009621

12.   Kreutzer JS, DeLuca J, Caplan B, editors. Encyclopedia of Clinical Neuropsychology [Internet]. New York, NY: Springer New York; 2011. doi:10.1007/978-0-387-79948-3

13.   El-Baba RM, Schury MP. Neuroanatomy, Frontal Cortex [Internet]. StatPearls. 2020. Available: http://www.ncbi.nlm.nih.gov/pubmed/32119370

14.   Hathaway WR, Newton BW. Neuroanatomy, Prefrontal Cortex [Internet]. StatPearls. 2020. Available: http://www.ncbi.nlm.nih.gov/pubmed/29763094

15.   Rehman A, Al Khalili Y. Neuroanatomy, Occipital Lobe [Internet]. StatPearls. 2020. Available: http://www.ncbi.nlm.nih.gov/pubmed/31335040

16.   Javed K, Wroten M. Neuroanatomy, Wernicke Area [Internet]. StatPearls. 2020. Available: http://www.ncbi.nlm.nih.gov/pubmed/30422593

17.   McDonald AJ, Mott DD. Functional neuroanatomy of amygdalohippocampal interconnections and their role in learning and memory. J Neurosci Res. 2017;95: 797–820. doi:10.1002/jnr.23709

18.   von Bartheld CS, Bahney J, Herculano-Houzel S. The search for true numbers of neurons and glial cells in the human brain: A review of 150 years of cell counting. J Comp Neurol. 2016;524: 3865–3895. doi:10.1002/cne.24040

19.   Zeng H, Sanes JR. Neuronal cell-type classification: challenges, opportunities and the path forward. Nat Rev Neurosci. 2017;18: 530–546. doi:10.1038/nrn.2017.85

20.   Butt A, Verkhratsky A. Neuroglia: Realising their true potential. Brain Neurosci Adv. 2018;2: 239821281881749. doi:10.1177/2398212818817495

21.   Sofroniew M V., Vinters H V. Astrocytes: biology and pathology. Acta Neuropathol. 2010;119: 7–35. doi:10.1007/s00401-009-0619-8

22.   Colonna M, Butovsky O. Microglia Function in the Central Nervous System During Health and Neurodegeneration. Annu Rev Immunol. 2017;35: 441–468. doi:10.1146/annurev-immunol-051116-052358

23.   Prinz M, Jung S, Priller J. Microglia Biology: One Century of Evolving Concepts. Cell. 2019;179: 292–311. doi:10.1016/j.cell.2019.08.053

24.   Cai Z, Hussain MD, Yan L-J. Microglia, neuroinflammation, and beta-amyloid protein in Alzheimer's disease. Int J Neurosci. 2014;124: 307–321. doi:10.3109/00207454.2013.833510

25.   Qian L, Flood PM. Microglial cells and Parkinson's disease. Immunol Res. Humana Press Inc; 2008;41: 155–164. doi:10.1007/s12026-008-8018-0

26.   Simons M, Nave K-A. Oligodendrocytes: Myelination and Axonal Support. Cold Spring Harb Perspect Biol. 2016;8: a020479. doi:10.1101/cshperspect.a020479

27.   De Strooper B, Karran E. The Cellular Phase of Alzheimer's Disease. Cell. 2016;164: 603–615. doi:10.1016/j.cell.2015.12.056

28.   Crawford AH, Stockley JH, Tripathi RB, Richardson WD, Franklin RJM. Oligodendrocyte progenitors: Adult stem cells of the central nervous system? Exp Neurol. 2014;260: 50–55. doi:10.1016/j.expneurol.2014.04.027

29.   Zhang Y, Barres BA. Astrocyte heterogeneity: an underappreciated topic in neurobiology. Curr Opin Neurobiol. 2010;20: 588–594. doi:10.1016/j.conb.2010.06.005

30.   Lawson LJ, Perry VH, Dri P, Gordon S. Heterogeneity in the distribution and morphology of microglia in the normal adult mouse brain. Neuroscience. 1990;39: 151–170. doi:10.1016/0306-4522(90)90229-W

31.   Stogsdill JA, Eroglu C. The interplay between neurons and glia in synapse development and plasticity. Curr Opin Neurobiol. 2017;42: 1–8. doi:10.1016/j.conb.2016.09.016

32.   Gomes FCA, Spohr TCLS, Martinez R, Moura Neto V. Cross-talk between neurons and glia: highlights on soluble factors. Brazilian J Med Biol Res. Brazilian Journal of Medical and Biological Research; 2001;34: 611–620. doi:10.1590/S0100-879X2001000500008

33.   Abbott NJ, Rönnbäck L, Hansson E. Astrocyte–endothelial interactions at the blood–brain barrier. Nat Rev Neurosci. 2006;7: 41–53. doi:10.1038/nrn1824

34.   Carroll WM. The global burden of neurological disorders. Lancet Neurol. 2019;18: 418–419. doi:10.1016/S1474-4422(19)30029-8

35.   Feigin VL, Nichols E, Alam T, Bannick MS, Beghi E, Blake N, et al. Global, regional, and national burden of neurological disorders, 1990–2016: a systematic analysis for the Global Burden of Disease Study 2016. Lancet Neurol. 2019;18: 459–480. doi:10.1016/S1474-4422(18)30499-X

36.   Feigin VL, Abajobir AA, Abate KH, Abd-Allah F, Abdulle AM, Abera SF, et al. Global, regional, and national burden of neurological disorders during 1990–

2015: a systematic analysis for the Global Burden of Disease Study 2015. Lancet Neurol. 2017;16: 877–897. doi:10.1016/S1474-4422(17)30299-5

37.   Patterson C. World Alzheimer Report 2018. 2018;

38.   Lane CA, Hardy J, Schott JM. Alzheimer's disease. Eur J Neurol. 2018;25: 59–70. doi:10.1111/ene.13439

39.   Land KC, Lamb VL. Demography of Aging. International Encyclopedia of Public Health. Elsevier; 2017. pp. 226–232. doi:10.1016/B978-0-12-803678-5.00101-6

40.   Bekris LM, Yu CE, Bird TD, Tsuang DW. Genetics of Alzheimer disease. J Geriatr Psychiatry Neurol. 2010;23: 213–227. doi:10.1177/0891988710383571

41.   Mayeux R, Stern Y. Epidemiology of Alzheimer Disease. Cold Spring Harb Perspect Med. 2012;2: a006239–a006239. doi:10.1101/cshperspect.a006239

42.   World Alzheimer Report 2015 [Internet]. 2015. Available: http://www.alz.co.uk/research/WorldAlzheimerReport2015.pdf

43.   Mielke MM, Ferretti MT, Iulita MF, Hayden K, Khachaturian AS. Sex and gender in Alzheimer's disease – Does it matter? Alzheimer's Dement. 2018;14: 1101–1103. doi:10.1016/j.jalz.2018.08.003

44.   Bali J, Gheinani AH, Zurbriggen S, Rajendran L. Role of genes linked to sporadic Alzheimer's disease risk in the production of -amyloid peptides. Proc Natl Acad Sci. 2012;109: 15307–15311. doi:10.1073/pnas.1201632109

45.   Brickell KL, Steinbart EJ, Rumbaugh M, Payami H, Schellenberg GD, Van Deerlin V, et al. Early-Onset Alzheimer Disease in Families With Late-Onset Alzheimer Disease. Arch Neurol. 2006;63: 1307. doi:10.1001/archneur.63.9.1307

46.   Campion D, Dumanchin C, Hannequin D, Dubois B, Belliard S, Puel M, et al. Early-Onset Autosomal Dominant Alzheimer Disease: Prevalence, Genetic Heterogeneity, and Mutation Spectrum. Am J Hum Genet. 1999;65: 664–670. doi:10.1086/302553

47.   Masters CL, Bateman R, Blennow K, Rowe CC, Sperling RA, Cummings JL. Alzheimer's disease. Nat Rev Dis Prim. Macmillan Publishers Limited; 2015;1: 15056. doi:10.1038/nrdp.2015.56

48.   Jost BC, Grossberg GT. The Natural History of Alzheimer's Disease: A Brain

Bank Study. J Am Geriatr Soc. 1995;43: 1248–1255. doi:10.1111/j.1532-5415.1995.tb07401.x

49. Canevelli M, Piscopo P, Talarico G, Vanacore N, Blasimme A, Crestini A, et al. Familial Alzheimer's disease sustained by presenilin 2 mutations: Systematic review of literature and genotype–phenotype correlation. Neurosci Biobehav Rev. 2014;42: 170–179. doi:10.1016/j.neubiorev.2014.02.010

50. Lanoiselée H-M, Nicolas G, Wallon D, Rovelet-Lecrux A, Lacour M, Rousseau S, et al. APP, PSEN1, and PSEN2 mutations in early-onset Alzheimer disease: A genetic screening study of familial and sporadic cases. Miller BL, editor. PLOS Med. 2017;14: e1002270. doi:10.1371/journal.pmed.1002270

51. Corder E, Saunders A, Strittmatter W, Schmechel D, Gaskell P, Small G, et al. Gene dose of apolipoprotein E type 4 allele and the risk of Alzheimer's disease in late onset families. Science. 1993;261: 921–923. doi:10.1126/science.8346443

52. Strittmatter WJ, Weisgraber KH, Huang DY, Dong LM, Salvesen GS, Pericak-Vance M, et al. Binding of human apolipoprotein E to synthetic amyloid beta peptide: isoform-specific effects and implications for late-onset Alzheimer disease. Proc Natl Acad Sci. 1993;90: 8098–8102. doi:10.1073/pnas.90.17.8098

53. Guerreiro R, Wojtas A, Bras J, Carrasquillo M, Rogaeva E, Majounie E, et al. TREM2 Variants in Alzheimer's Disease. N Engl J Med. 2013;368: 117–127. doi:10.1056/NEJMoa1211851

54. Jonsson T, Stefansson H, Steinberg S, Jonsdottir I, Jonsson P V., Snaedal J, et al. Variant of TREM2 Associated with the Risk of Alzheimer's Disease. N Engl J Med. 2013;368: 107–116. doi:10.1056/NEJMoa1211103

55. Karch CM, Goate AM. Alzheimer's Disease Risk Genes and Mechanisms of Disease Pathogenesis. Biol Psychiatry. 2015;77: 43–51. doi:10.1016/j.biopsych.2014.05.006

56. Escott-Price V, Sims R, Bannister C, Harold D, Vronskaya M, Majounie E, et al. Common polygenic variation enhances risk prediction for Alzheimer's disease. Brain. 2015;138: 3673–3684. doi:10.1093/brain/awv268

57. Xu W, Tan L, Wang H-F, Jiang T, Tan M-S, Tan L, et al. Meta-analysis of

modifiable risk factors for Alzheimer's disease. J Neurol Neurosurg Psychiatry. 2015; jnnp-2015-310548. doi:10.1136/jnnp-2015-310548

58.   Perl DP. Neuropathology of Alzheimer's Disease. Mt Sinai J Med A J Transl Pers Med. 2010;77: 32–42. doi:10.1002/msj.20157

59.   DeTure MA, Dickson DW. The neuropathological diagnosis of Alzheimer's disease. Mol Neurodegener. 2019;14: 32. doi:10.1186/s13024-019-0333-5

60.   Dickerson BC, Bakkour A, Salat DH, Feczko E, Pacheco J, Greve DN, et al. The Cortical Signature of Alzheimer's Disease: Regionally Specific Cortical Thinning Relates to Symptom Severity in Very Mild to Mild AD Dementia and is Detectable in Asymptomatic Amyloid-Positive Individuals. Cereb Cortex. 2009;19: 497–510. doi:10.1093/cercor/bhn113

61.   Dickerson BC, Stoub TR, Shah RC, Sperling RA, Killiany RJ, Albert MS, et al. Alzheimer-signature MRI biomarker predicts AD dementia in cognitively normal adults. Neurology. 2011;76: 1395–1402. doi:10.1212/WNL.0b013e3182166e96

62.   Piguet O, Double KL, Kril JJ, Harasty J, Macdonald V, McRitchie DA, et al. White matter loss in healthy ageing: A postmortem analysis. Neurobiol Aging. 2009;30: 1288–1295. doi:10.1016/j.neurobiolaging.2007.10.015

63.   Montine TJ, Phelps CH, Beach TG, Bigio EH, Cairns NJ, Dickson DW, et al. National Institute on Aging–Alzheimer's Association guidelines for the neuropathologic assessment of Alzheimer's disease: a practical approach. Acta Neuropathol. 2012;123: 1–11. doi:10.1007/s00401-011-0910-3

64.   Serrano-Pozo A, Frosch MP, Masliah E, Hyman BT. Neuropathological Alterations in Alzheimer Disease. Cold Spring Harb Perspect Med. 2011;1: a006189–a006189. doi:10.1101/cshperspect.a006189

65.   Gouras GK, Olsson TT, Hansson O. β-amyloid Peptides and Amyloid Plaques in Alzheimer's Disease. Neurotherapeutics. 2015;12: 3–11. doi:10.1007/s13311-014-0313-y

66.   Potter R, Patterson BW, Elbert DL, Ovod V, Kasten T, Sigurdson W, et al. Increased in Vivo Amyloid- 42 Production, Exchange, and Loss in Presenilin Mutation Carriers. Sci Transl Med. 2013;5: 189ra77-189ra77. doi:10.1126/scitranslmed.3005615

67.   Gómez-Isla T, Growdon WB, McNamara MJ, Nochlin D, Bird TD, Arango JC, et al. The impact of different presenilin 1 andpresenilin 2 mutations on

amyloid deposition, neurofibrillary changes and neuronal loss in the familial Alzheimer's disease brain. Brain. 1999;122: 1709–1719. doi:10.1093/brain/122.9.1709

68. Thal DR, Rüb U, Orantes M, Braak H. Phases of Aβ-deposition in the human brain and its relevance for the development of AD. Neurology. 2002;58: 1791–1800. doi:10.1212/WNL.58.12.1791

69. Braak H, Braak E. Neuropathological stageing of Alzheimer-related changes. Acta Neuropathol. 1991;82: 239–259. doi:10.1007/BF00308809

70. Mendes S, Rodrigues EMT, Barbosa-Morais NL. Evaluating cortical transcriptomic differences between Alzheimer's Disease PSEN-1 mutated mouse models and human patients, and their implications in drug development. Universidade de Lisboa. 2020.

71. Ingelsson M, Fukumoto H, Newell KL, Growdon JH, Hedley-Whyte ET, Frosch MP, et al. Early A accumulation and progressive synaptic loss, gliosis, and tangle formation in AD brain. Neurology. 2004;62: 925–931. doi:10.1212/01.WNL.0000115115.98960.37

72. HYMAN BT, MARZLOFF K, ARRIAGADA P V. The Lack of Accumulation of Senile Plaques or Amyloid Burden in Alzheimer's Disease Suggests a Dynamic Balance Between Amyloid Deposition and Resolution. J Neuropathol Exp Neurol. 1993;52: 594–600. doi:10.1097/00005072-199311000-00006

73. Noguchi-Shinohara M, Komatsu J, Samuraki M, Matsunari I, Ikeda T, Sakai K, et al. Cerebral Amyloid Angiopathy-Related Microbleeds and Cerebrospinal Fluid Biomarkers in Alzheimer's Disease. Friedland R, editor. J Alzheimer's Dis. 2016;55: 905–913. doi:10.3233/JAD-160651

74. Overk CR, Masliah E. Pathogenesis of synaptic degeneration in Alzheimer's disease and Lewy body disease. Biochem Pharmacol. 2014;88: 508–516. doi:10.1016/j.bcp.2014.01.015

75. Forner S, Baglietto-Vargas D, Martini AC, Trujillo-Estrada L, LaFerla FM. Synaptic Impairment in Alzheimer's Disease: A Dysregulated Symphony. Trends Neurosci. 2017;40: 347–357. doi:10.1016/j.tins.2017.04.002

76. Terry RD, Masliah E, Salmon DP, Butters N, DeTeresa R, Hill R, et al. Physical basis of cognitive alterations in alzheimer's disease: Synapse loss is the major correlate of cognitive impairment. Ann Neurol. 1991;30: 572–

580. doi:10.1002/ana.410300410

77. Sanabria-Castro A, Alvarado-Echeverría I, Monge-Bonilla C. Molecular Pathogenesis of Alzheimer's Disease: An Update. Ann Neurosci. 2017;24: 46–54. doi:10.1159/000464422

78. Reinhard C, Hébert SS, De Strooper B. The amyloid-β precursor protein: integrating structure with biological function. EMBO J. 2005;24: 3996–4006. doi:10.1038/sj.emboj.7600860

79. Wang D-S, Dickson DW, Malter JS. Beta- Amyloid Degradation and Alzheimer's Disease. J Biomed Biotechnol. 2006;2006: 1–12. doi:10.1155/JBB/2006/58406

80. Hayden EY, Teplow DB. Amyloid β-protein oligomers and Alzheimer's disease. Alzheimers Res Ther. 2013;5: 60. doi:10.1186/alzrt226

81. Esparza TJ, Zhao H, Cirrito JR, Cairns NJ, Bateman RJ, Holtzman DM, et al. Amyloid-beta oligomerization in Alzheimer dementia versus high-pathology controls. Ann Neurol. 2013;73: 104–119. doi:10.1002/ana.23748

82. Terry A V., Buccafusco JJ. The Cholinergic Hypothesis of Age and Alzheimer's Disease-Related Cognitive Deficits: Recent Challenges and Their Implications for Novel Drug Development. J Pharmacol Exp Ther. 2003;306: 821–827. doi:10.1124/jpet.102.041616

83. Mesulam M. The Cholinergic Lesion of Alzheimer's Disease: Pivotal Factor or Side Show? Learn Mem. 2004;11: 43–49. doi:10.1101/lm.69204

84. Shen J, Wu J. Nicotinic Cholinergic Mechanisms in Alzheimer's Disease. 2015. pp. 275–292. doi:10.1016/bs.irn.2015.08.002

85. Ni R, Marutle A, Nordberg A. Modulation of α7 Nicotinic Acetylcholine Receptor and Fibrillar Amyloid-β Interactions in Alzheimer's Disease Brain. J Alzheimer's Dis. 2013;33: 841–851. doi:10.3233/JAD-2012-121447

86. Area-Gomez E, de Groof A, Bonilla E, Montesinos J, Tanji K, Boldogh I, et al. A key role for MAM in mediating mitochondrial dysfunction in Alzheimer disease. Cell Death Dis. 2018;9: 335. doi:10.1038/s41419-017-0215-0

87. Area-Gomez E, Schon EA. On the Pathogenesis of Alzheimer's Disease: The MAM Hypothesis. FASEB J. 2017;31: 864–867. doi:10.1096/fj.201601309

88. Schon EA, Area-Gomez E. Mitochondria-associated ER membranes in Alzheimer disease. Mol Cell Neurosci. 2013;55: 26–36.

doi:10.1016/j.mcn.2012.07.011

89. Przedborski S, Vila M, Jackson-Lewis V. Series Introduction: Neurodegeneration: What is it and where are we? J Clin Invest. 2003;111: 3–10. doi:10.1172/JCI200317522

90. Clarke PH. Developmental cell death: morphological diversity and multiple mechanisms. Anat Embryol (Berl). 1990;181. doi:10.1007/BF00174615

91. Wicklund L, Leão RN, Strömberg A-M, Mousavi M, Hovatta O, Nordberg A, et al. β-Amyloid 1-42 Oligomers Impair Function of Human Embryonic Stem Cell-Derived Forebrain Cholinergic Neurons. Combs C, editor. PLoS One. 2010;5: e15600. doi:10.1371/journal.pone.0015600

92. Xu X, Lei Y, Luo J, Wang J, Zhang S, Yang X-J, et al. Prevention of β-amyloid induced toxicity in human iPS cell-derived neurons by inhibition of Cyclin-dependent kinases and associated cell cycle events. Stem Cell Res. 2013;10: 213–227. doi:10.1016/j.scr.2012.11.005

93. Vazin T, Ball KA, Lu H, Park H, Ataeijannati Y, Head-Gordon T, et al. Efficient derivation of cortical glutamatergic neurons from human pluripotent stem cells: A model system to study neurotoxicity in Alzheimer's disease. Neurobiol Dis. 2014;62: 62–72. doi:10.1016/j.nbd.2013.09.005

94. Nieweg K, Andreyeva A, van Stegen B, Tanriöver G, Gottmann K. Alzheimer's disease-related amyloid-β induces synaptotoxicity in human iPS cell-derived neurons. Cell Death Dis. 2015;6: e1709–e1709. doi:10.1038/cddis.2015.72

95. Hong W, Wang Z, Liu W, O'Malley TT, Jin M, Willem M, et al. Diffusible, highly bioactive oligomers represent a critical minority of soluble Aβ in Alzheimer's disease brain. Acta Neuropathol. 2018;136: 19–40. doi:10.1007/s00401-018-1846-7

96. Berry BJ, Smith AST, Long CJ, Martin CC, Hickman JJ. Physiological Aβ Concentrations Produce a More Biomimetic Representation of the Alzheimer's Disease Phenotype in iPSC Derived Human Neurons. ACS Chem Neurosci. 2018;9: 1693–1701. doi:10.1021/acschemneuro.8b00067

97. Muratore CR, Rice HC, Srikanth P, Callahan DG, Shin T, Benjamin LNP, et al. The familial Alzheimer's disease APPV717I mutation alters APP processing and Tau expression in iPSC-derived neurons. Hum Mol Genet. 2014;23: 3523–3536. doi:10.1093/hmg/ddu064

98. Penney J, Ralvenius WT, Tsai L-H. Modeling Alzheimer's disease with iPSC-derived brain cells. Mol Psychiatry. 2019; doi:10.1038/s41380-019-0468-3

99. Lin Y-T, Seo J, Gao F, Feldman HM, Wen H-L, Penney J, et al. APOE4 Causes Widespread Molecular and Cellular Alterations Associated with Alzheimer's Disease Phenotypes in Human iPSC-Derived Brain Cell Types. Neuron. 2018;98: 1141-1154.e7. doi:10.1016/j.neuron.2018.05.008

100. Wadhwani AR, Affaneh A, Van Gulden S, Kessler JA. Neuronal apolipoprotein E4 increases cell death and phosphorylated tau release in alzheimer disease. Ann Neurol. 2019;85: 726–739. doi:10.1002/ana.25455

101. Muratore CR, Zhou C, Liao M, Fernandez MA, Taylor WM, Lagomarsino VN, et al. Cell-type Dependent Alzheimer's Disease Phenotypes: Probing the Biology of Selective Neuronal Vulnerability. Stem Cell Reports. 2017;9: 1868–1884. doi:10.1016/j.stemcr.2017.10.015

102. Liao M-C, Muratore CR, Gierahn TM, Sullivan SE, Srikanth P, De Jager PL, et al. Single-Cell Detection of Secreted Aβ and sAPPα from Human IPSC-Derived Neurons and Astrocytes. J Neurosci. 2016;36: 1730–1746. doi:10.1523/JNEUROSCI.2735-15.2016

103. Frost GR, Li Y-M. The role of astrocytes in amyloid production and Alzheimer's disease. Open Biol. 2017;7: 170228. doi:10.1098/rsob.170228

104. Rodríguez JJ, Olabarria M, Chvatal A, Verkhratsky A. Astroglia in dementia and Alzheimer's disease. Cell Death Differ. 2009;16: 378–385. doi:10.1038/cdd.2008.172

105. Nagele RG, D'Andrea MR, Lee H, Venkataraman V, Wang H-Y. Astrocytes accumulate Aβ42 and give rise to astrocytic amyloid plaques in Alzheimer disease brains. Brain Res. 2003;971: 197–209. doi:10.1016/S0006-8993(03)02361-8

106. Rodríguez-Arellano JJ, Parpura V, Zorec R, Verkhratsky A. Astrocytes in physiological aging and Alzheimer's disease. Neuroscience. 2016;323: 170–182. doi:10.1016/j.neuroscience.2015.01.007

107. Rasmussen MK, Mestre H, Nedergaard M. The glymphatic pathway in neurological disorders. Lancet Neurol. 2018;17: 1016–1024. doi:10.1016/S1474-4422(18)30318-1

108. Nagele RG, Wegiel J, Venkataraman V, Imaki H, Wang K-C, Wegiel J.

Contribution of glial cells to the development of amyloid plaques in Alzheimer's disease. Neurobiol Aging. 2004;25: 663–674. doi:10.1016/j.neurobiolaging.2004.01.007

109. Carter SF, Scholl M, Almkvist O, Wall A, Engler H, Langstrom B, et al. Evidence for Astrocytosis in Prodromal Alzheimer Disease Provided by 11C-Deuterium-L-Deprenyl: A Multitracer PET Paradigm Combining 11C-Pittsburgh Compound B and 18F-FDG. J Nucl Med. 2012;53: 37–46. doi:10.2967/jnumed.110.087031

110. Kraft AW, Hu X, Yoon H, Yan P, Xiao Q, Wang Y, et al. Attenuating astrocyte activation accelerates plaque pathogenesis in APP/PS1 mice. FASEB J. 2013;27: 187–198. doi:10.1096/fj.12-208660

111. Kamphuis W, Kooijman L, Orre M, Stassen O, Pekny M, Hol EM. GFAP and vimentin deficiency alters gene expression in astrocytes and microglia in wild-type mice and changes the transcriptional response of reactive glia in mouse model for Alzheimer's disease. Glia. 2015;63: 1036–1056. doi:10.1002/glia.22800

112. Olabarria M, Noristani HN, Verkhratsky A, Rodríguez JJ. Concomitant astroglial atrophy and astrogliosis in a triple transgenic animal model of Alzheimer's disease. Glia. 2010; NA-NA. doi:10.1002/glia.20967

113. Perlmutter LS, Scott SA, Barrón E, Chui HC. MHC class II-positive microglia in human brain: Association with alzheimer lesions. J Neurosci Res. 1992;33: 549–558. doi:10.1002/jnr.490330407

114. Rozemuller JM, Der^Valk P van, Eikelenboom P. Activated microglia and cerebral amyloid deposits in alzheimer's disease. Res Immunol. 1992;143: 646–649. doi:10.1016/0923-2494(92)80050-U

115. Wolf SA, Boddeke HWGM, Kettenmann H. Microglia in Physiology and Disease. Annu Rev Physiol. 2017;79: 619–643. doi:10.1146/annurev-physiol-022516-034406

116. Hansen D V., Hanson JE, Sheng M. Microglia in Alzheimer's disease. J Cell Biol. 2018;217: 459–472. doi:10.1083/jcb.201709069

117. Ulrich JD, Ulland TK, Colonna M, Holtzman DM. Elucidating the Role of TREM2 in Alzheimer's Disease. Neuron. 2017;94: 237–248. doi:10.1016/j.neuron.2017.02.042

118. Yeh FL, Hansen D V., Sheng M. TREM2, Microglia, and Neurodegenerative

Diseases. Trends Mol Med. 2017;23: 512–533. doi:10.1016/j.molmed.2017.03.008

119. Mazaheri F, Snaidero N, Kleinberger G, Madore C, Daria A, Werner G, et al. TREM2 deficiency impairs chemotaxis and microglial responses to neuronal injury. EMBO Rep. 2017;18: 1186–1198. doi:10.15252/embr.201743922

120. Zheng H, Jia L, Liu C-C, Rong Z, Zhong L, Yang L, et al. TREM2 Promotes Microglial Survival by Activating Wnt/β-Catenin Pathway. J Neurosci. 2017;37: 1772–1784. doi:10.1523/JNEUROSCI.2459-16.2017

121. Kleinberger G, Yamanishi Y, Suarez-Calvet M, Czirr E, Lohmann E, Cuyvers E, et al. TREM2 mutations implicated in neurodegeneration impair cell surface transport and phagocytosis. Sci Transl Med. 2014;6: 243ra86-243ra86. doi:10.1126/scitranslmed.3009093

122. Goedert M, Spillantini MG, Del Tredici K, Braak H. 100 years of Lewy pathology. Nat Rev Neurol. Nature Publishing Group; 2013;9: 13–24. doi:10.1038/nrneurol.2012.242

123. Yeh FL, Wang Y, Tom I, Gonzalez LC, Sheng M. TREM2 Binds to Apolipoproteins, Including APOE and CLU/APOJ, and Thereby Facilitates Uptake of Amyloid-Beta by Microglia. Neuron. 2016;91: 328–340. doi:10.1016/j.neuron.2016.06.015

124. Wang Y, Ulland TK, Ulrich JD, Song W, Tzaferis JA, Hole JT, et al. TREM2-mediated early microglial response limits diffusion and toxicity of amyloid plaques. J Exp Med. 2016;213: 667–675. doi:10.1084/jem.20151948

125. Braak H, Braak E. Development of Alzheimer-related neurofibrillary changes in the neocortex inversely recapitulates cortical myelogenesis. Acta Neuropathol. 1996;92: 197–201.

126. Butt AM, De La Rocha IC, Rivera A. Oligodendroglial Cells in Alzheimer's Disease. 2019. pp. 325–333. doi:10.1007/978-981-13-9913-8_12

127. Lee S, Viqar F, Zimmerman ME, Narkhede A, Tosto G, Benzinger TLS, et al. White matter hyperintensities are a core feature of Alzheimer's disease: Evidence from the dominantly inherited Alzheimer network. Ann Neurol. 2016;79: 929–939. doi:10.1002/ana.24647

128. Bartzokis G. Alzheimer's disease as homeostatic responses to age-related myelin breakdown. Neurobiol Aging. 2011;32: 1341–1371. doi:10.1016/j.neurobiolaging.2009.08.007

129. Tse K-H, Herrup K. DNA damage in the oligodendrocyte lineage and its role in brain aging. Mech Ageing Dev. 2017;161: 37–50. doi:10.1016/j.mad.2016.05.006

130. Nasrabady SE, Rizvi B, Goldman JE, Brickman AM. White matter changes in Alzheimer's disease: a focus on myelin and oligodendrocytes. Acta Neuropathol Commun. 2018;6: 22. doi:10.1186/s40478-018-0515-3

131. Cai Z, Xiao M. Oligodendrocytes and Alzheimer's disease. Int J Neurosci. 2016;126: 97–104. doi:10.3109/00207454.2015.1025778

132. Hane FT, Robinson M, Lee BY, Bai O, Leonenko Z, Albert MS. Recent Progress in Alzheimer's Disease Research, Part 3: Diagnosis and Treatment. J Alzheimer's Dis. 2017;57: 645–665. doi:10.3233/JAD-160907

133. Mucke L. Alzheimer's disease. Nature. 2009;461: 895–897. doi:10.1038/461895a

134. Reitz C. Genetic diagnosis and prognosis of Alzheimer's disease: challenges and opportunities. Expert Rev Mol Diagn. 2015;15: 339–348. doi:10.1586/14737159.2015.1002469

135. Hort J, O'Brien JT, Gainotti G, Pirttila T, Popescu BO, Rektorova I, et al. EFNS guidelines for the diagnosis and management of Alzheimer's disease. Eur J Neurol. 2010;17: 1236–1248. doi:10.1111/j.1468-1331.2010.03040.x

136. Frisoni GB, Fox NC, Jack CR, Scheltens P, Thompson PM. The clinical use of structural MRI in Alzheimer disease. Nat Rev Neurol. 2010;6: 67–77. doi:10.1038/nrneurol.2009.215

137. Clark CM. Use of Florbetapir-PET for Imaging β-Amyloid Pathology. JAMA. 2011;305: 275. doi:10.1001/jama.2010.2008

138. Ikonomovic MD, Buckley CJ, Heurling K, Sherwin P, Jones PA, Zanette M, et al. Post-mortem histopathology underlying β-amyloid PET imaging following flutemetamol F 18 injection. Acta Neuropathol Commun. 2016;4: 130. doi:10.1186/s40478-016-0399-z

139. Sabri O, Sabbagh MN, Seibyl J, Barthel H, Akatsu H, Ouchi Y, et al. Florbetaben PET imaging to detect amyloid beta plaques in Alzheimer's disease: Phase 3 study. Alzheimer's Dement. 2015;11: 964–974. doi:10.1016/j.jalz.2015.02.004

140. Olsson B, Lautner R, Andreasson U, Öhrfelt A, Portelius E, Bjerke M, et al. CSF and blood biomarkers for the diagnosis of Alzheimer's disease: a

systematic review and meta-analysis. Lancet Neurol. 2016;15: 673–684.
doi:10.1016/S1474-4422(16)00070-3

141. Davatzikos C, Bhatt P, Shaw LM, Batmanghelich KN, Trojanowski JQ.
Prediction of MCI to AD conversion, via MRI, CSF biomarkers, and pattern
classification. Neurobiol Aging. 2011;32: 2322.e19-2322.e27.
doi:10.1016/j.neurobiolaging.2010.05.023

142. Albert MS, DeKosky ST, Dickson D, Dubois B, Feldman HH, Fox NC, et al.
The diagnosis of mild cognitive impairment due to Alzheimer's disease:
Recommendations from the National Institute on Aging-Alzheimer's
Association workgroups on diagnostic guidelines for Alzheimer's disease.
Alzheimer's Dement. 2011;7: 270–279. doi:10.1016/j.jalz.2011.03.008

143. H. Ferreira-Vieira T, M. Guimaraes I, R. Silva F, M. Ribeiro F. Alzheimer's
disease: Targeting the Cholinergic System. Curr Neuropharmacol. 2016;14:
101–115. doi:10.2174/1570159X13666150716165726

144. Epperly T, Dunay MA, Boice JL. Alzheimer Disease: Pharmacologic and
Nonpharmacologic Therapies for Cognitive and Functional Symptoms. Am
Fam Physician. 2017;95: 771–778. Available:
http://www.ncbi.nlm.nih.gov/pubmed/28671413

145. Wang R, Reddy PH. Role of Glutamate and NMDA Receptors in Alzheimer's
Disease. J Alzheimer's Dis. 2017;57: 1041–1048. doi:10.3233/JAD-160763

146. Casey DA. Pharmacotherapy of neuropsychiatric symptoms of dementia. P
T. 2015;40: 284–7. Available:
http://www.ncbi.nlm.nih.gov/pubmed/25859124

147. Gasser T. Mendelian forms of Parkinson's disease. Biochim Biophys Acta.
Elsevier B.V.; 2009;1792: 587–96. doi:10.1016/j.bbadis.2008.12.007

148. Dorsey ER, Elbaz A, Nichols E, Abd-Allah F, Abdelalim A, Adsuar JC, et al.
Global, regional, and national burden of Parkinson's disease, 1990–2016: a
systematic analysis for the Global Burden of Disease Study 2016. Lancet
Neurol. 2018;17: 939–953. doi:10.1016/S1474-4422(18)30295-3

149. Dorsey ER, Constantinescu R, Thompson JP, Biglan KM, Holloway RG,
Kieburtz K, et al. Projected number of people with Parkinson disease in the
most populous nations, 2005 through 2030. Neurology. 2007;68: 384–386.
doi:10.1212/01.wnl.0000247740.47667.03

150. Lees AJ, Hardy J, Revesz T. Parkinson's disease. Lancet. Elsevier Ltd;

2009;373: 2055–66. doi:10.1016/S0140-6736(09)60492-X

151. Cerri S, Mus L, Blandini F. Parkinson's Disease in Women and Men: What's the Difference? J Parkinsons Dis. 2019;9: 501–515. doi:10.3233/JPD-191683

152. Badger JL, Cordero-Llana O, Hartfield EM, Wade-Martins R. Parkinson's disease in a dish - Using stem cells as a molecular tool. Neuropharmacology. 2014;76 Pt A: 88–96. doi:10.1016/j.neuropharm.2013.08.035

153. Kouli A, Torsney KM, Kuan W-L. Parkinson's Disease: Etiology, Neuropathology, and Pathogenesis. Parkinson's Disease: Pathogenesis and Clinical Aspects. 2018. doi:http://dx.doi.org/10.15586/codonpublications .parkinsonsdisease.2018.ch1

154. Emamzadeh FN, Surguchov A. Parkinson's Disease: Biomarkers, Treatment, and Risk Factors. Front Neurosci. 2018;12. doi:10.3389/fnins.2018.00612

155. Sveinbjornsdottir S. The clinical symptoms of Parkinson's disease. J Neurochem. 2016;139: 318–324. doi:10.1111/jnc.13691

156. Wierzejska R. Can coffee consumption lower the risk of Alzheimer's disease and Parkinson's disease? A literature review. Arch Med Sci. 2017;3: 507–514. doi:10.5114/aoms.2016.63599

157. Breckenridge CB, Berry C, Chang ET, Sielken RL, Mandel JS. Association between Parkinson's Disease and Cigarette Smoking, Rural Living, Well-Water Consumption, Farming and Pesticide Use: Systematic Review and Meta-Analysis. Guedes RNC, editor. PLoS One. 2016;11: e0151841. doi:10.1371/journal.pone.0151841

158. Ascherio A, Zhang SM, Hernán MA, Kawachi I, Colditz GA, Speizer FE, et al. Prospective study of caffeine consumption and risk of Parkinson's disease in men and women. Ann Neurol. 2001;50: 56–63. doi:10.1002/ana.1052

159. Simon DK, Tanner CM, Brundin P. Parkinson Disease Epidemiology, Pathology, Genetics, and Pathophysiology. Clin Geriatr Med. 2020;36: 1–12. doi:10.1016/j.cger.2019.08.002

160. Langston J, Ballard P, Tetrud J, Irwin I. Chronic Parkinsonism in humans due to a product of meperidine-analog synthesis. Science. 1983;219: 979–

980. doi:10.1126/science.6823561

161. Tanner CM, Kamel F, Ross GW, Hoppin JA, Goldman SM, Korell M, et al. Rotenone, Paraquat, and Parkinson's Disease. Environ Health Perspect. 2011;119: 866–872. doi:10.1289/ehp.1002839

162. Betarbet R, Sherer TB, MacKenzie G, Garcia-Osuna M, Panov A V., Greenamyre JT. Chronic systemic pesticide exposure reproduces features of Parkinson's disease. Nat Neurosci. 2000;3: 1301–1306. doi:10.1038/81834

163. Gasser T. Usefulness of Genetic Testing in PD and PD Trials: A Balanced Review. J Parkinsons Dis. 2015;5: 209–215. doi:10.3233/JPD-140507

164. Billingsley KJ, Bandres-Ciga S, Saez-Atienzar S, Singleton AB. Genetic risk factors in Parkinson's disease. Cell Tissue Res. 2018;373: 9–20. doi:10.1007/s00441-018-2817-y

165. Deng H, Wang P, Jankovic J. The genetics of Parkinson disease. Ageing Res Rev. 2018;42: 72–85. doi:10.1016/j.arr.2017.12.007

166. Konno T, Ross OA, Puschmann A, Dickson DW, Wszolek ZK. Autosomal dominant Parkinson's disease caused by SNCA duplications. Parkinsonism Relat Disord. 2016;22: S1–S6. doi:10.1016/j.parkreldis.2015.09.007

167. Healy DG, Falchi M, O'Sullivan SS, Bonifati V, Durr A, Bressman S, et al. Phenotype, genotype, and worldwide genetic penetrance of LRRK2-associated Parkinson's disease: a case-control study. Lancet Neurol. 2008;7: 583–590. doi:10.1016/S1474-4422(08)70117-0

168. Martin I, Kim JW, Dawson VL, Dawson TM. LRRK2 pathobiology in Parkinson's disease. J Neurochem. 2014;131: 554–565. doi:10.1111/jnc.12949

169. Skipper L, Wilkes K, Toft M, Baker M, Lincoln S, Hulihan M, et al. Linkage Disequilibrium and Association of MAPT H1 in Parkinson Disease. Am J Hum Genet. 2004;75: 669–677. doi:10.1086/424492

170. Williams ET, Chen X, Moore DJ. VPS35, the Retromer Complex and Parkinson's Disease. J Parkinsons Dis. 2017;7: 219–233. doi:10.3233/JPD-161020

171. Vilariño-Güell C, Wider C, Ross OA, Dachsel JC, Kachergus JM, Lincoln SJ, et al. VPS35 Mutations in Parkinson Disease. Am J Hum Genet. 2011;89: 162–167. doi:10.1016/j.ajhg.2011.06.001

172. Deng H, Gao K, Jankovic J. The VPS35 gene and Parkinson's disease. Mov Disord. 2013;28: 569–575. doi:10.1002/mds.25430

173. Halperin A, Elstein D, Zimran A. Increased incidence of Parkinson disease among relatives of patients with Gaucher disease. Blood Cells, Mol Dis. 2006;36: 426–428. doi:10.1016/j.bcmd.2006.02.004

174. Neudorfer O, Giladi N, Elstein D, Abrahamov A, Turezkite T, Aghai E, et al. Occurrence of Parkinson's syndrome in type 1 Gaucher disease. QJM. 1996;89: 691–694. doi:10.1093/qjmed/89.9.691

175. Lwin A. Glucocerebrosidase mutations in subjects with parkinsonism. Mol Genet Metab. 2004;81: 70–73. doi:10.1016/j.ymgme.2003.11.004

176. Payne K, Walls B, Wojcieszek J. Approach to Assessment of Parkinson Disease with Emphasis on Genetic Testing. Med Clin North Am. 2019;103: 1055–1075. doi:10.1016/j.mcna.2019.08.003

177. Sidransky E, Nalls MA, Aasly JO, Aharon-Peretz J, Annesi G, Barbosa ER, et al. Multicenter Analysis of Glucocerebrosidase Mutations in Parkinson's Disease. N Engl J Med. 2009;361: 1651–1661. doi:10.1056/NEJMoa0901281

178. Anheim M, Elbaz A, Lesage S, Durr A, Condroyer C, Viallet F, et al. Penetrance of Parkinson disease in glucocerebrosidase gene mutation carriers. Neurology. 2012;78: 417–420. doi:10.1212/WNL.0b013e318245f476

179. Kalia L V, Lang AE. Parkinson's disease. Lancet. 2015;386: 896–912. doi:10.1016/S0140-6736(14)61393-3

180. Schulte C, Gasser T. Genetic basis of Parkinson's disease: inheritance, penetrance, and expression. Appl Clin Genet. 2011; 67. doi:10.2147/TACG.S11639

181. Truban D, Hou X, Caulfield TR, Fiesel FC, Springer W. PINK1, Parkin, and Mitochondrial Quality Control: What can we Learn about Parkinson's Disease Pathobiology? J Parkinsons Dis. 2017;7: 13–29. doi:10.3233/JPD-160989

182. Singleton AB, Farrer MJ, Bonifati V. The genetics of Parkinson's disease: Progress and therapeutic implications. Mov Disord. 2013;28: 14–23. doi:10.1002/mds.25249

183. Ramirez A, Heimbach A, Gründemann J, Stiller B, Hampshire D, Cid LP, et

al. Hereditary parkinsonism with dementia is caused by mutations in ATP13A2, encoding a lysosomal type 5 P-type ATPase. Nat Genet. 2006;38: 1184–1191. doi:10.1038/ng1884

184. Heiko B, Ghebremedhin E, Rüb U, Bratzke H, Del Tredici K. Stages in the development of Parkinson's disease-related pathology. Cell Tissue Res. 2004;318: 121–134. doi:10.1007/s00441-004-0956-9

185. Dickson DW. Parkinson's Disease and Parkinsonism: Neuropathology. Cold Spring Harb Perspect Med. 2012;2: a009258–a009258. doi:10.1101/cshperspect.a009258

186. Lashuel HA, Overk CR, Oueslati A, Masliah E. The many faces of α-synuclein: from structure and toxicity to therapeutic target. Nat Rev Neurosci. 2013;14: 38–48. doi:10.1038/nrn3406

187. Xu L, Pu J. Alpha-Synuclein in Parkinson's Disease: From Pathogenetic Dysfunction to Potential Clinical Application. Parkinsons Dis. 2016;2016: 1–10. doi:10.1155/2016/1720621

188. Stefanis L. a-Synuclein in Parkinson's Disease. Cold Spring Harb Perspect Med. 2012;2: a009399–a009399. doi:10.1101/cshperspect.a009399

189. Barrett PJ, Timothy Greenamyre J. Post-translational modification of α-synuclein in Parkinson's disease. Brain Res. 2015;1628: 247–253. doi:10.1016/j.brainres.2015.06.002

190. Cox D, Carver JA, Ecroyd H. Preventing α-synuclein aggregation: The role of the small heat-shock molecular chaperone proteins. Biochim Biophys Acta - Mol Basis Dis. 2014;1842: 1830–1843. doi:10.1016/j.bbadis.2014.06.024

191. Lücking CB, Brice* A. Alpha-synuclein and Parkinson's disease. Cell Mol Life Sci. 2000;57: 1894–1908. doi:10.1007/PL00000671

192. Compta Y, Parkkinen L, O'Sullivan SS, Vandrovcova J, Holton JL, Collins C, et al. Lewy- and Alzheimer-type pathologies in Parkinson's disease dementia: which is more important? Brain. 2011;134: 1493–1505. doi:10.1093/brain/awr031

193. Irwin DJ, Lee VM-Y, Trojanowski JQ. Parkinson's disease dementia: convergence of α-synuclein, tau and amyloid-β pathologies. Nat Rev Neurosci. 2013;14: 626–636. doi:10.1038/nrn3549

194. Braak H, Tredici K Del, Rüb U, de Vos RA., Jansen Steur EN., Braak E.

Staging of brain pathology related to sporadic Parkinson's disease. Neurobiol Aging. 2003;24: 197–211. doi:10.1016/S0197-4580(02)00065-9

195. Recasens A, Dehay B. Alpha-synuclein spreading in Parkinson's disease. Front Neuroanat. 2014;8. doi:10.3389/fnana.2014.00159

196. Kordower JH, Chu Y, Hauser RA, Freeman TB, Olanow CW. Lewy body–like pathology in long-term embryonic nigral transplants in Parkinson's disease. Nat Med. 2008;14: 504–506. doi:10.1038/nm1747

197. Li J-Y, Englund E, Holton JL, Soulet D, Hagell P, Lees AJ, et al. Lewy bodies in grafted neurons in subjects with Parkinson's disease suggest host-to-graft disease propagation. Nat Med. 2008;14: 501–503. doi:10.1038/nm1746

198. Masuda-Suzukake M, Nonaka T, Hosokawa M, Oikawa T, Arai T, Akiyama H, et al. Prion-like spreading of pathological α-synuclein in brain. Brain. 2013;136: 1128–1138. doi:10.1093/brain/awt037

199. Mendez I, Viñuela A, Astradsson A, Mukhida K, Hallett P, Robertson H, et al. Dopamine neurons implanted into people with Parkinson's disease survive without pathology for 14 years. Nat Med. 2008;14: 507–509. doi:10.1038/nm1752

200. Zhang G, Xia Y, Wan F, Ma K, Guo X, Kou L, et al. New Perspectives on Roles of Alpha-Synuclein in Parkinson's Disease. Front Aging Neurosci. 2018;10. doi:10.3389/fnagi.2018.00370

201. Borghi R, Marchese R, Negro A, Marinelli L, Forloni G, Zaccheo D, et al. Full length α-synuclein is present in cerebrospinal fluid from Parkinson's disease and normal subjects. Neurosci Lett. 2000;287: 65–67. doi:10.1016/S0304-3940(00)01153-8

202. EL-AGNAF OMA, SALEM SA, PALEOLOGOU KE, COOPER LJ, FULLWOOD NJ, GIBSON MJ, et al. α-Synuclein implicated in Parkinson's disease is present in extracellular biological fluids, including human plasma. FASEB J. 2003;17: 1945–1947. doi:10.1096/fj.03-0098fje

203. Emmanouilidou E, Melachroinou K, Roumeliotis T, Garbis SD, Ntzouni M, Margaritis LH, et al. Cell-Produced -Synuclein Is Secreted in a Calcium-Dependent Manner by Exosomes and Impacts Neuronal Survival. J Neurosci. 2010;30: 6838–6851. doi:10.1523/JNEUROSCI.5699-09.2010

204. Lee H-J, Bae E-J, Lee S-J. Extracellular α-synuclein—a novel and crucial

factor in Lewy body diseases. Nat Rev Neurol. 2014;10: 92–98. doi:10.1038/nrneurol.2013.275

205. Shrivastava AN, Redeker V, Fritz N, Pieri L, Almeida LG, Spolidoro M, et al. α-synuclein assemblies sequester neuronal α3-Na + /K + - ATP ase and impair Na + gradient. EMBO J. 2015;34: 2408–2423. doi:10.15252/embj.201591397

206. Mao X, Ou MT, Karuppagounder SS, Kam T-I, Yin X, Xiong Y, et al. Pathological -synuclein transmission initiated by binding lymphocyte-activation gene 3. Science. 2016;353: aah3374–aah3374. doi:10.1126/science.aah3374

207. Shi M, Liu C, Cook TJ, Bullock KM, Zhao Y, Ginghina C, et al. Plasma exosomal α-synuclein is likely CNS-derived and increased in Parkinson's disease. Acta Neuropathol. 2014;128: 639–650. doi:10.1007/s00401-014-1314-y

208. Karpowicz RJ, Trojanowski JQ, Lee VM-Y. Transmission of α-synuclein seeds in neurodegenerative disease: recent developments. Lab Investig. 2019;99: 971–981. doi:10.1038/s41374-019-0195-z

209. Stuendl A, Kunadt M, Kruse N, Bartels C, Moebius W, Danzer KM, et al. Induction of α-synuclein aggregate formation by CSF exosomes from patients with Parkinson's disease and dementia with Lewy bodies. Brain. 2016;139: 481–494. doi:10.1093/brain/awv346

210. Klingelhoefer L, Reichmann H. Pathogenesis of Parkinson disease—the gut–brain axis and environmental factors. Nat Rev Neurol. 2015;11: 625–636. doi:10.1038/nrneurol.2015.197

211. Santos SF, de Oliveira HL, Yamada ES, Neves BC, Pereira A. The Gut and Parkinson's Disease—A Bidirectional Pathway. Front Neurol. 2019;10. doi:10.3389/fneur.2019.00574

212. Dutta SK, Verma S, Jain V, Surapaneni BK, Vinayek R, Phillips L, et al. Parkinson's Disease: The Emerging Role of Gut Dysbiosis, Antibiotics, Probiotics, and Fecal Microbiota Transplantation. J Neurogastroenterol Motil. 2019;25: 363–376. doi:10.5056/jnm19044

213. Forsyth CB, Shannon KM, Kordower JH, Voigt RM, Shaikh M, Jaglin JA, et al. Increased Intestinal Permeability Correlates with Sigmoid Mucosa alpha-Synuclein Staining and Endotoxin Exposure Markers in Early Parkinson's

Disease. Oreja-Guevara C, editor. PLoS One. 2011;6: e28032. doi:10.1371/journal.pone.0028032

214. Xilouri M, Brekk OR, Stefanis L. Alpha-synuclein and Protein Degradation Systems: a Reciprocal Relationship. Mol Neurobiol. 2013;47: 537–551. doi:10.1007/s12035-012-8341-2

215. Ravanan P, Srikumar IF, Talwar P. Autophagy: The spotlight for cellular stress responses. Life Sci. 2017;188: 53–67. doi:10.1016/j.lfs.2017.08.029

216. Nedelsky NB, Todd PK, Taylor JP. Autophagy and the ubiquitin-proteasome system: collaborators in neuroprotection. Biochim Biophys Acta. Elsevier B.V.; 2008;1782: 691–9. doi:10.1016/j.bbadis.2008.10.002

217. Bordone M, Araujo I, Lewis PA. Characterisation of PRKRA and WDR45 gene function, involved in Parkinson's disease. Universidade do Algarve. 2014.

218. Anglade P, Vyas S, Javoy-Agid F, Herrero MT, Michel PP, Marquez J, et al. Apoptosis and autophagy in nigral neurons of patients with Parkinson's disease. Histol Histopathol. 1997;12: 25–31. Available: http://www.ncbi.nlm.nih.gov/pubmed/9046040

219. Ebrahimi-Fakhari D, Wahlster L, McLean PJ. Protein degradation pathways in Parkinson's disease: curse or blessing. Acta Neuropathol. 2012;124: 153–172. doi:10.1007/s00401-012-1004-6

220. Moors TE, Hoozemans JJM, Ingrassia A, Beccari T, Parnetti L, Chartier-Harlin M-C, et al. Therapeutic potential of autophagy-enhancing agents in Parkinson's disease. Mol Neurodegener. 2017;12: 11. doi:10.1186/s13024-017-0154-3

221. Xilouri M, Brekk OR, Stefanis L. Autophagy and Alpha-Synuclein: Relevance to Parkinson's Disease and Related Synucleopathies. Mov Disord. 2016;31: 178–192. doi:10.1002/mds.26477

222. Hershko A, Ciechanover A. The ubiquitin system. Annu Rev Biochem. 1998;67: 425–479. doi:10.1146/annurev.biochem.67.1.425

223. Lim K-L, Tan JM. Role of the ubiquitin proteasome system in Parkinson's disease. BMC Biochem. 2007;8: S13. doi:10.1186/1471-2091-8-S1-S13

224. Braun BC, Glickman M, Kraft R, Dahlmann B, Kloetzel P-M, Finley D, et al. The base of the proteasome regulatory particle exhibits chaperone-like activity. Nat Cell Biol. 1999;1: 221–226. doi:10.1038/12043

225. McNaught KS., Jenner P. Proteasomal function is impaired in substantia nigra in Parkinson's disease. Neurosci Lett. 2001;297: 191–194. doi:10.1016/S0304-3940(00)01701-8

226. Ullrich C, Mlekusch R, Kuschnig A, Marksteiner J, Humpel C. Ubiquitin Enzymes, Ubiquitin and Proteasome Activity in Blood Mononuclear Cells of MCI, Alzheimer and Parkinson Patients. Curr Alzheimer Res. 2010;7: 549–555. doi:10.2174/156720510792231766

227. St. P. McNaught K, Belizaire R, Isacson O, Jenner P, Olanow CW. Altered Proteasomal Function in Sporadic Parkinson's Disease. Exp Neurol. 2003;179: 38–46. doi:10.1006/exnr.2002.8050

228. Zhang Y, Gao J, Chung KKK, Huang H, Dawson VL, Dawson TM. Parkin functions as an E2-dependent ubiquitin- protein ligase and promotes the degradation of the synaptic vesicle-associated protein, CDCrel-1. Proc Natl Acad Sci. 2000;97: 13354–13359. doi:10.1073/pnas.240347797

229. Leroy E, Boyer R, Auburger G, Leube B, Ulm G, Mezey E, et al. The ubiquitin pathway in Parkinson's disease. Nature. 1998;395: 451–452. doi:10.1038/26652

230. Zeng B-Y, Bukhatwa S, Hikima A, Rose S, Jenner P. Reproducible nigral cell loss after systemic proteasomal inhibitor administration to rats. Ann Neurol. 2006;60: 248–252. doi:10.1002/ana.20932

231. Bedford L, Hay D, Devoy A, Paine S, Powe DG, Seth R, et al. Depletion of 26S Proteasomes in Mouse Brain Neurons Causes Neurodegeneration and Lewy-Like Inclusions Resembling Human Pale Bodies. J Neurosci. 2008;28: 8189–8198. doi:10.1523/JNEUROSCI.2218-08.2008

232. Franco-Iborra S, Vila M, Perier C. The Parkinson Disease Mitochondrial Hypothesis. Neurosci. 2016;22: 266–277. doi:10.1177/1073858415574600

233. Chen C, Turnbull DM, Reeve AK. Mitochondrial Dysfunction in Parkinson's Disease—Cause or Consequence? Biology (Basel). 2019;8: 38. doi:10.3390/biology8020038

234. Mullin S, Schapira A. α-Synuclein and Mitochondrial Dysfunction in Parkinson's Disease. Mol Neurobiol. 2013;47: 587–597. doi:10.1007/s12035-013-8394-x

235. Ryan BJ, Hoek S, Fon EA, Wade-Martins R. Mitochondrial dysfunction and mitophagy in Parkinson's: from familial to sporadic disease. Trends Biochem

Sci. 2015;40: 200–210. doi:10.1016/j.tibs.2015.02.003

236. Guardia-Laguarta C, Area-Gomez E, Rub C, Liu Y, Magrane J, Becker D, et al. a-Synuclein Is Localized to Mitochondria-Associated ER Membranes. J Neurosci. 2014;34: 249–259. doi:10.1523/JNEUROSCI.2507-13.2014

237. Canet-Avilés RM, Wilson MA, Miller DW, Ahmad R, McLendon C, Bandyopadhyay S, et al. The Parkinson's disease protein DJ-1 is neuroprotective due to cysteine-sulfinic acid-driven mitochondrial localization. Proc Natl Acad Sci. 2004;101: 9103–9108. doi:10.1073/pnas.0402959101

238. Wang X, Yan MH, Fujioka H, Liu J, Wilson-Delfosse A, Chen SG, et al. LRRK2 regulates mitochondrial dynamics and function through direct interaction with DLP1. Hum Mol Genet. 2012;21: 1931–1944. doi:10.1093/hmg/dds003

239. Stafa K, Tsika E, Moser R, Musso A, Glauser L, Jones A, et al. Functional interaction of Parkinson's disease-associated LRRK2 with members of the dynamin GTPase superfamily. Hum Mol Genet. 2014;23: 2055–2077. doi:10.1093/hmg/ddt600

240. Nguyen HN, Byers B, Cord B, Shcheglovitov A, Byrne J, Gujar P, et al. LRRK2 Mutant iPSC-Derived DA Neurons Demonstrate Increased Susceptibility to Oxidative Stress. Cell Stem Cell. 2011;8: 267–280. doi:10.1016/j.stem.2011.01.013

241. Reinhardt P, Schmid B, Burbulla LF, Schöndorf DC, Wagner L, Glatza M, et al. Genetic Correction of a LRRK2 Mutation in Human iPSCs Links Parkinsonian Neurodegeneration to ERK-Dependent Changes in Gene Expression. Cell Stem Cell. 2013;12: 354–367. doi:10.1016/j.stem.2013.01.008

242. De Virgilio A, Greco A, Fabbrini G, Inghilleri M, Rizzo MI, Gallo A, et al. Parkinson's disease: Autoimmunity and neuroinflammation. Autoimmun Rev. 2016;15: 1005–1011. doi:10.1016/j.autrev.2016.07.022

243. Davidson A, Diamond B. Autoimmune Diseases. Mackay IR, Rosen FS, editors. N Engl J Med. 2001;345: 340–350. doi:10.1056/NEJM200108023450506

244. Allen Reish HE, Standaert DG. Role of α-Synuclein in Inducing Innate and Adaptive Immunity in Parkinson Disease. J Parkinsons Dis. 2015;5: 1–19.

doi:10.3233/JPD-140491

245. Fiszer U, Mix E, Fredrikson S, Kostulas V, Olsson T, Link H. γδ+ T cells are increased in patients with Parkinson's disease. J Neurol Sci. 1994;121: 39–45. doi:10.1016/0022-510X(94)90154-6

246. Benkler M, Agmon-Levy N, Shoenfeld Y. Parkinson's disease, autoimmunity, and olfaction. Int J Neurosci. 2009;119: 2133–2143. doi:10.3109/00207450903178786

247. Carvey PM, McRae A, Lint TF, Ptak LR, Lo ES, Goetz CG, et al. The potential use of a dopamine neuron antibody and a striatal-derived neurotrophic factor as diagnostic markers in Parkinson's disease. Neurology. 1991;41: 53–58. doi:10.1212/WNL.41.5_Suppl_2.53

248. Orr CF, Rowe DB, Mizuno Y, Mori H, Halliday GM. A possible role for humoral immunity in the pathogenesis of Parkinson's disease. Brain. 2005;128: 2665–2674. doi:10.1093/brain/awh625

249. Chen S, Le WD, Xie WJ, Alexianu ME, Engelhardt JI, Siklós L, et al. Experimental Destruction of Substantia Nigra Initiated by Parkinson Disease Immunoglobulins. Arch Neurol. 1998;55: 1075. doi:10.1001/archneur.55.8.1075

250. Garretti F, Agalliu D, Lindestam Arlehamn CS, Sette A, Sulzer D. Autoimmunity in Parkinson's Disease: The Role of α-Synuclein-Specific T Cells. Front Immunol. 2019;10. doi:10.3389/fimmu.2019.00303

251. Sulzer D, Alcalay RN, Garretti F, Cote L, Kanter E, Agin-Liebes J, et al. T cells from patients with Parkinson's disease recognize α-synuclein peptides. Nature. 2017;546: 656–661. doi:10.1038/nature22815

252. Saiki M, Baker A, Williams-Gray CH, Foltynie T, Goodman RS, Taylor CJ, et al. Association of the human leucocyte antigen region with susceptibility to Parkinson's disease. J Neurol Neurosurg Psychiatry. 2010;81: 890–891. doi:10.1136/jnnp.2008.162883

253. Gao X, Chen H, Schwarzschild MA, Ascherio A. Use of ibuprofen and risk of Parkinson disease. Neurology. 2011;76: 863–869. doi:10.1212/WNL.0b013e31820f2d79

254. Yasuda T, Nakata Y, Mochizuki H. α-Synuclein and Neuronal Cell Death. Mol Neurobiol. 2013;47: 466–483. doi:10.1007/s12035-012-8327-0

255. Barzilai A, Melamed E. Molecular mechanisms of selective dopaminergic

neuronal death in Parkinson's disease. Trends Mol Med. 2003;9: 126–132. doi:10.1016/S1471-4914(03)00020-0

256. Zecca L, Zucca FA, Costi P, Tampellini D, Gatti A, Gerlach M, et al. The neuromelanin of human substantia nigra: structure, synthesis and molecular behaviour. 2003. pp. 145–155. doi:10.1007/978-3-7091-0643-3_8

257. Zucca FA, Vanna R, Cupaioli FA, Bellei C, De Palma A, Di Silvestre D, et al. Neuromelanin organelles are specialized autolysosomes that accumulate undegraded proteins and lipids in aging human brain and are likely involved in Parkinson's disease. npj Park Dis. 2018;4: 17. doi:10.1038/s41531-018-0050-8

258. Carballo-Carbajal I, Laguna A, Romero-Giménez J, Cuadros T, Bové J, Martinez-Vicente M, et al. Brain tyrosinase overexpression implicates age-dependent neuromelanin production in Parkinson's disease pathogenesis. Nat Commun. 2019;10: 973. doi:10.1038/s41467-019-08858-y

259. Dias V, Junn E, Mouradian MM. The Role of Oxidative Stress in Parkinson's Disease. J Parkinsons Dis. 2013;3: 461–491. doi:10.3233/JPD-130230

260. Subramaniam S. Selective Neuronal Death in Neurodegenerative Diseases: The Ongoing Mystery. Yale J Biol Med. 2019;92: 695–705. Available: http://www.ncbi.nlm.nih.gov/pubmed/31866784

261. Giguère N, Burke Nanni S, Trudeau L-E. On Cell Loss and Selective Vulnerability of Neuronal Populations in Parkinson's Disease. Front Neurol. 2018;9. doi:10.3389/fneur.2018.00455

262. Greffard S, Verny M, Bonnet A-M, Seilhean D, Hauw J-J, Duyckaerts C. A stable proportion of Lewy body bearing neurons in the substantia nigra suggests a model in which the Lewy body causes neuronal death. Neurobiol Aging. 2010;31: 99–103. doi:10.1016/j.neurobiolaging.2008.03.015

263. Junn E, Mouradian MM. Human α-Synuclein over-expression increases intracellular reactive oxygen species levels and susceptibility to dopamine. Neurosci Lett. 2002;320: 146–150. doi:10.1016/S0304-3940(02)00016-2

264. Saha AR, Ninkina NN, Hanger DP, Anderton BH, Davies AM, Buchman VL. Induction of neuronal death by α-synuclein. Eur J Neurosci. 2000;12: 3073–3077. doi:10.1046/j.1460-9568.2000.00210.x

265. Galvin JE. Interaction of alpha-synuclein and dopamine metabolites in the pathogenesis of Parkinson's disease: a case for the selective vulnerability of

the substantia nigra. Acta Neuropathol. 2006;112: 115–126. doi:10.1007/s00401-006-0096-2

266. Xu S, Chan P. Interaction between Neuromelanin and Alpha-Synuclein in Parkinson's Disease. Biomolecules. 2015;5: 1122–1142. doi:10.3390/biom5021122

267. Perez RG, Waymire JC, Lin E, Liu JJ, Guo F, Zigmond MJ. A role for alpha-synuclein in the regulation of dopamine biosynthesis. J Neurosci. 2002;22: 3090–9. doi:20026307

268. Cabezas R, Avila M, Gonzalez J, El-Bachá RS, Báez E, García-Segura LM, et al. Astrocytic modulation of blood brain barrier: perspectives on Parkinson's disease. Front Cell Neurosci. Frontiers Media SA; 2014;8: 211. doi:10.3389/fncel.2014.00211

269. Scharr DG, Sieber B-A, Dreyfus CF, Black IB. Regional and Cell-Specific Expression of GDNF in Rat Brain. Exp Neurol. 1993;124: 368–371. doi:10.1006/exnr.1993.1207

270. Booth HDE, Hirst WD, Wade-Martins R. The Role of Astrocyte Dysfunction in Parkinson's Disease Pathogenesis. Trends Neurosci. 2017;40: 358–370. doi:10.1016/j.tins.2017.04.001

271. Zhang Y, Sloan SA, Clarke LE, Grant GA, Gephart MGH, Barres Correspondence BA, et al. Purification and Characterization of Progenitor and Mature Human Astrocytes Reveals Transcriptional and Functional Differences with Mouse. Neuron. 2016;89: 37–53. doi:10.1016/j.neuron.2015.11.013

272. Mullett SJ, Hinkle DA. DJ-1 knock-down in astrocytes impairs astrocyte-mediated neuroprotection against rotenone. Neurobiol Dis. 2009;33: 28–36. doi:10.1016/j.nbd.2008.09.013

273. Larsen NJ, Ambrosi G, Mullett SJ, Berman SB, Hinkle DA. DJ-1 knock-down impairs astrocyte mitochondrial function. Neuroscience. 2011;196: 251–264. doi:10.1016/j.neuroscience.2011.08.016

274. Jäkel S, Dimou L. Glial Cells and Their Function in the Adult Brain: A Journey through the History of Their Ablation. Front Cell Neurosci. Frontiers Media SA; 2017;11: 24. doi:10.3389/fncel.2017.00024

275. Sofroniew M V. Astrocyte barriers to neurotoxic inflammation. Nat Rev Neurosci. 2015;16: 249–263. doi:10.1038/nrn3898

276. Cabezas R, Fidel M, Torrente D, Santos El-Bach R, Morales L, Gonzalez J, et al. Astrocytes Role in Parkinson: A Double-Edged Sword. Neurodegenerative Diseases. InTech; 2013. doi:10.5772/54305

277. Block ML, Zecca L, Hong J-S. Microglia-mediated neurotoxicity: uncovering the molecular mechanisms. Nat Rev Neurosci. 2007;8: 57–69. doi:10.1038/nrn2038

278. Le W, Wu J, Tang Y. Protective Microglia and Their Regulation in Parkinson's Disease. Front Mol Neurosci. Frontiers Media SA; 2016;9: 89. doi:10.3389/fnmol.2016.00089

279. Kanaan NM, Kordower JH, Collier TJ. Age and region-specific responses of microglia, but not astrocytes, suggest a role in selective vulnerability of dopamine neurons after 1-methyl-4-phenyl-1,2,3,6-tetrahydropyridine exposure in monkeys. Glia. NIH Public Access; 2008;56: 1199–214. doi:10.1002/glia.20690

280. Hamza TH, Zabetian CP, Tenesa A, Laederach A, Montimurro J, Yearout D, et al. Common genetic variation in the HLA region is associated with late-onset sporadic Parkinson's disease. Nat Genet. 2010;42: 781–785. doi:10.1038/ng.642

281. Gerhard A, Pavese N, Hotton G, Turkheimer F, Es M, Hammers A, et al. In vivo imaging of microglial activation with [11C](R)-PK11195 PET in idiopathic Parkinson's disease. Neurobiol Dis. 2006;21: 404–412. doi:10.1016/j.nbd.2005.08.002

282. Bartels AL, Willemsen ATM, Doorduin J, de Vries EFJ, Dierckx RA, Leenders KL. [11C]-PK11195 PET: Quantification of neuroinflammation and a monitor of anti-inflammatory treatment in Parkinson's disease? Parkinsonism Relat Disord. 2010;16: 57–59. doi:10.1016/j.parkreldis.2009.05.005

283. Doorn KJ, Moors T, Drukarch B, van de Berg WD, Lucassen PJ, van Dam A-M. Microglial phenotypes and toll-like receptor 2 in the substantia nigra and hippocampus of incidental Lewy body disease cases and Parkinson's disease patients. Acta Neuropathol Commun. 2014;2: 90. doi:10.1186/s40478-014-0090-1

284. Ho MS. Microglia in Parkinson's Disease. 2019. pp. 335–353. doi:10.1007/978-981-13-9913-8_13

285. Djelloul M, Holmqvist S, Boza-Serrano A, Azevedo C, Yeung MS, Goldwurm S, et al. Alpha-Synuclein Expression in the Oligodendrocyte Lineage: an In Vitro and In Vivo Study Using Rodent and Human Models. Stem Cell Reports. 2015;5: 174–184. doi:10.1016/j.stemcr.2015.07.002

286. Ettle B, Reiprich S, Deusser J, Schlachetzki JCM, Xiang W, Prots I, et al. Intracellular alpha-synuclein affects early maturation of primary oligodendrocyte progenitor cells. Mol Cell Neurosci. 2014;62: 68–78. doi:10.1016/j.mcn.2014.06.012

287. Grigoletto J, Pukaß K, Gamliel A, Davidi D, Katz-Brull R, Richter-Landsberg C, et al. Higher levels of myelin phospholipids in brains of neuronal α-Synuclein transgenic mice precede myelin loss. Acta Neuropathol Commun. 2017;5: 37. doi:10.1186/s40478-017-0439-3

288. Zhan W, Kang GA, Glass GA, Zhang Y, Shirley C, Millin R, et al. Regional alterations of brain microstructure in Parkinson's disease using diffusion tensor imaging. Mov Disord. 2012;27: 90–97. doi:10.1002/mds.23917

289. Auning E, Kjærvik VK, Selnes P, Aarsland D, Haram A, Bjørnerud A, et al. White matter integrity and cognition in Parkinson's disease: a cross-sectional study. BMJ Open. 2014;4: e003976. doi:10.1136/bmjopen-2013-003976

290. Gallagher C, Bell B, Bendlin B, Palotti M, Okonkwo O, Sodhi A, et al. White Matter Microstructural Integrity and Executive Function in Parkinson's Disease. J Int Neuropsychol Soc. 2013;19: 349–354. doi:10.1017/S1355617712001373

291. Gattellaro G, Minati L, Grisoli M, Mariani C, Carella F, Osio M, et al. White Matter Involvement in Idiopathic Parkinson Disease: A Diffusion Tensor Imaging Study. Am J Neuroradiol. 2009;30: 1222–1226. doi:10.3174/ajnr.A1556

292. Dean DC, Sojkova J, Hurley S, Kecskemeti S, Okonkwo O, Bendlin BB, et al. Alterations of Myelin Content in Parkinson's Disease: A Cross-Sectional Neuroimaging Study. PLoS One. 2016;11: e0163774. doi:10.1371/journal.pone.0163774

293. Marsili L, Rizzo G, Colosimo C. Diagnostic Criteria for Parkinson's Disease: From James Parkinson to the Concept of Prodromal Disease. Front Neurol. 2018;9. doi:10.3389/fneur.2018.00156

294. Caproni S, Colosimo C. Diagnosis and Differential Diagnosis of Parkinson Disease. Clin Geriatr Med. 2020;36: 13–24. doi:10.1016/j.cger.2019.09.014

295. Berardelli A, Wenning GK, Antonini A, Berg D, Bloem BR, Bonifati V, et al. EFNS/MDS-ES recommendations for the diagnosis of Parkinson's disease. Eur J Neurol. 2013;20: 16–34. doi:10.1111/ene.12022

296. Balestrino R, Schapira AHV. Parkinson disease. Eur J Neurol. 2020;27: 27–42. doi:10.1111/ene.14108

297. Connolly BS, Lang AE. Pharmacological Treatment of Parkinson Disease. JAMA. 2014;311: 1670. doi:10.1001/jama.2014.3654

298. Fox SH, Katzenschlager R, Lim S-Y, Ravina B, Seppi K, Coelho M, et al. The Movement Disorder Society Evidence-Based Medicine Review Update: Treatments for the motor symptoms of Parkinson's disease. Mov Disord. 2011;26: S2–S41. doi:10.1002/mds.23829

299. Yarnall A, Rochester L, Burn DJ. The interplay of cholinergic function, attention, and falls in Parkinson's disease. Mov Disord. 2011;26: 2496–2503. doi:10.1002/mds.23932

300. Malek N. Deep Brain Stimulation in Parkinson's Disease. Neurol India. 2019;67: 968. doi:10.4103/0028-3886.266268

301. Chiken S, Nambu A. Mechanism of Deep Brain Stimulation. Neurosci. 2016;22: 313–322. doi:10.1177/1073858415581986

302. Chen T, Mirzadeh Z, Lambert M, Gonzalez O, Moran A, Shetter AG, et al. Cost of Deep Brain Stimulation Infection Resulting in Explantation. Stereotact Funct Neurosurg. 2017;95: 117–124. doi:10.1159/000457964

303. Lowe R, Shirley N, Bleackley M, Dolan S, Shafee T. Transcriptomics technologies. PLOS Comput Biol. 2017;13: e1005457. doi:10.1371/journal.pcbi.1005457

304. Wang Z, Gerstein M, Snyder M. RNA-Seq: a revolutionary tool for transcriptomics. Nat Rev Genet. 2009;10: 57–63. doi:10.1038/nrg2484

305. Zhao W, He X, Hoadley KA, Parker JS, Hayes D, Perou CM. Comparison of RNA-Seq by poly (A) capture, ribosomal RNA depletion, and DNA microarray for expression profiling. BMC Genomics. 2014;15: 419. doi:10.1186/1471-2164-15-419

306. Patel H, Dobson RJB, Newhouse SJ. A Meta-Analysis of Alzheimer's Disease Brain Transcriptomic Data. J Alzheimer's Dis. 2019;68: 1635–1656.

doi:10.3233/JAD-181085

307. Twine NA, Janitz K, Wilkins MR, Janitz M. Whole Transcriptome Sequencing Reveals Gene Expression and Splicing Differences in Brain Regions Affected by Alzheimer's Disease. Preiss T, editor. PLoS One. 2011;6: e16266. doi:10.1371/journal.pone.0016266

308. Mills JD, Nalpathamkalam T, Jacobs HIL, Janitz C, Merico D, Hu P, et al. RNA-Seq analysis of the parietal cortex in Alzheimer's disease reveals alternatively spliced isoforms related to lipid metabolism. Neurosci Lett. 2013;536: 90–95. doi:10.1016/j.neulet.2012.12.042

309. Magistri M, Velmeshev D, Makhmutova M, Faghihi MA. Transcriptomics Profiling of Alzheimer's Disease Reveal Neurovascular Defects, Altered Amyloid-β Homeostasis, and Deregulated Expression of Long Noncoding RNAs. J Alzheimer's Dis. 2015;48: 647–665. doi:10.3233/JAD-150398

310. Annese A, Manzari C, Lionetti C, Picardi E, Horner DS, Chiara M, et al. Whole transcriptome profiling of Late-Onset Alzheimer's Disease patients provides insights into the molecular changes involved in the disease. Sci Rep. 2018;8: 4282. doi:10.1038/s41598-018-22701-2

311. Wan Y-W, Al-Ouran R, Mangleburg CG, Perumal TM, Lee T V., Allison K, et al. Meta-Analysis of the Alzheimer's Disease Human Brain Transcriptome and Functional Dissection in Mouse Models. Cell Rep. 2020;32: 107908. doi:10.1016/j.celrep.2020.107908

312. Kelly J, Moyeed R, Carroll C, Albani D, Li X. Gene expression meta-analysis of Parkinson's disease and its relationship with Alzheimer's disease. Mol Brain. 2019;12: 16. doi:10.1186/s13041-019-0436-5

313. Riley BE, Gardai SJ, Emig-Agius D, Bessarabova M, Ivliev AE, Schüle B, et al. Systems-Based Analyses of Brain Regions Functionally Impacted in Parkinson's Disease Reveals Underlying Causal Mechanisms. Cookson MR, editor. PLoS One. 2014;9: e102909. doi:10.1371/journal.pone.0102909

314. Dumitriu A, Golji J, Labadorf AT, Gao B, Beach TG, Myers RH, et al. Integrative analyses of proteomics and RNA transcriptomics implicate mitochondrial processes, protein folding pathways and GWAS loci in Parkinson disease. BMC Med Genomics. BioMed Central; 2016;9: 5. doi:10.1186/s12920-016-0164-y

315. Benoit SM, Xu H, Schmid S, Alexandrova R, Kaur G, Thiruvahindrapuram B,

et al. Expanding the search for genetic biomarkers of Parkinson's disease into the living brain. Neurobiol Dis. 2020;140: 104872. doi:10.1016/j.nbd.2020.104872

316. Verheijen J, Sleegers K. Understanding Alzheimer Disease at the Interface between Genetics and Transcriptomics. Trends Genet. 2018;34: 434–447. doi:10.1016/j.tig.2018.02.007

317. Svensson V, Vento-Tormo R, Teichmann SA. Exponential scaling of single-cell RNA-seq in the past decade. Nat Protoc. 2018;13: 599–604. doi:10.1038/nprot.2017.149

318. Mu Q, Chen Y, Wang J. Deciphering Brain Complexity Using Single-cell Sequencing. Genomics Proteomics Bioinformatics. 2019;17: 344–366. doi:10.1016/j.gpb.2018.07.007

319. Patel AP, Tirosh I, Trombetta JJ, Shalek AK, Gillespie SM, Wakimoto H, et al. Single-cell RNA-seq highlights intratumoral heterogeneity in primary glioblastoma. Science. 2014;344: 1396–1401. doi:10.1126/science.1254257

320. Darmanis S, Sloan SA, Zhang Y, Enge M, Caneda C, Shuer LM, et al. A survey of human brain transcriptome diversity at the single cell level. Proc Natl Acad Sci. 2015;112: 7285–7290. doi:10.1073/pnas.1507125112

321. Pollen AA, Nowakowski TJ, Chen J, Retallack H, Sandoval-Espinosa C, Nicholas CR, et al. Molecular Identity of Human Outer Radial Glia during Cortical Development. Cell. 2015;163: 55–67. doi:10.1016/j.cell.2015.09.004

322. Lake BB, Ai R, Kaeser GE, Salathia NS, Yung YC, Liu R, et al. Neuronal subtypes and diversity revealed by single-nucleus RNA sequencing of the human brain. Science. 2016;352: 1586–1590. doi:10.1126/science.aaf1204

323. Bakken TE, Hodge RD, Miller JA, Yao Z, Nguyen TN, Aevermann B, et al. Single-nucleus and single-cell transcriptomes compared in matched cortical cell types. Soriano E, editor. PLoS One. 2018;13: e0209648. doi:10.1371/journal.pone.0209648

324. Habib N, Avraham-Davidi I, Basu A, Burks T, Shekhar K, Hofree M, et al. Massively parallel single-nucleus RNA-seq with DroNc-seq. Nat Methods. 2017;14: 955–958. doi:10.1038/nmeth.4407

325. Lake BB, Chen S, Sos BC, Fan J, Kaeser GE, Yung YC, et al. Integrative single-cell analysis of transcriptional and epigenetic states in the human adult brain. Nat Biotechnol. 2018;36: 70–80. doi:10.1038/nbt.4038

326. Nowakowski TJ, Bhaduri A, Pollen AA, Alvarado B, Mostajo-Radji MA, Di Lullo E, et al. Spatiotemporal gene expression trajectories reveal developmental hierarchies of the human cortex. Science. 2017;358: 1318–1323. doi:10.1126/science.aap8809

327. Fan X, Dong J, Zhong S, Wei Y, Wu Q, Yan L, et al. Spatial transcriptomic survey of human embryonic cerebral cortex by single-cell RNA-seq analysis. Cell Res. 2018;28: 730–745. doi:10.1038/s41422-018-0053-3

328. Zhong S, Zhang S, Fan X, Wu Q, Yan L, Dong J, et al. A single-cell RNA-seq survey of the developmental landscape of the human prefrontal cortex. Nature. 2018;555: 524–528. doi:10.1038/nature25980

329. Spaethling JM, Na Y-J, Lee J, Ulyanova A V., Baltuch GH, Bell TJ, et al. Primary Cell Culture of Live Neurosurgically Resected Aged Adult Human Brain Cells and Single Cell Transcriptomics. Cell Rep. 2017;18: 791–803. doi:10.1016/j.celrep.2016.12.066

330. Yuan J, Sims PA. An Automated Microwell Platform for Large-Scale Single Cell RNA-Seq. Sci Rep. 2016;6: 33883. doi:10.1038/srep33883

331. Müller S, Liu SJ, Di Lullo E, Malatesta M, Pollen AA, Nowakowski TJ, et al. Single-cell sequencing maps gene expression to mutational phylogenies in PDGF - and EGF -driven gliomas. Mol Syst Biol. 2016;12: 889. doi:10.15252/msb.20166969

332. Lee J-K, Wang J, Sa JK, Ladewig E, Lee H-O, Lee I-H, et al. Spatiotemporal genomic architecture informs precision oncology in glioblastoma. Nat Genet. 2017;49: 594–599. doi:10.1038/ng.3806

333. Wang Q, Hu B, Hu X, Kim H, Squatrito M, Scarpace L, et al. Tumor Evolution of Glioma-Intrinsic Gene Expression Subtypes Associates with Immunological Changes in the Microenvironment. Cancer Cell. 2017;32: 42-56.e6. doi:10.1016/j.ccell.2017.06.003

334. Darmanis S, Sloan SA, Croote D, Mignardi M, Chernikova S, Samghababi P, et al. Single-Cell RNA-Seq Analysis of Infiltrating Neoplastic Cells at the Migrating Front of Human Glioblastoma. Cell Rep. 2017;21: 1399–1410. doi:10.1016/j.celrep.2017.10.030

335. Tirosh I, Venteicher AS, Hebert C, Escalante LE, Patel AP, Yizhak K, et al. Single-cell RNA-seq supports a developmental hierarchy in human oligodendroglioma. Nature. 2016;539: 309–313. doi:10.1038/nature20123

336. Venteicher AS, Tirosh I, Hebert C, Yizhak K, Neftel C, Filbin MG, et al. Decoupling genetics, lineages, and microenvironment in IDH-mutant gliomas by single-cell RNA-seq. Science. 2017;355: eaai8478. doi:10.1126/science.aai8478

337. Hovestadt V, Smith KS, Bihannic L, Filbin MG, Shaw ML, Baumgartner A, et al. Resolving medulloblastoma cellular architecture by single-cell genomics. Nature. 2019;572: 74–79. doi:10.1038/s41586-019-1434-6

338. Velmeshev D, Schirmer L, Jung D, Haeussler M, Perez Y, Mayer S, et al. Single-cell genomics identifies cell type–specific molecular changes in autism. Science. 2019;364: 685–689. doi:10.1126/science.aav8130

339. Lang C, Campbell KR, Ryan BJ, Carling P, Attar M, Vowles J, et al. Single-Cell Sequencing of iPSC-Dopamine Neurons Reconstructs Disease Progression and Identifies HDAC4 as a Regulator of Parkinson Cell Phenotypes. Cell Stem Cell. 2019;24: 93-106.e6. doi:10.1016/j.stem.2018.10.023

340. Schirmer L, Velmeshev D, Holmqvist S, Kaufmann M, Werneburg S, Jung D, et al. Neuronal vulnerability and multilineage diversity in multiple sclerosis. Nature. 2019;573: 75–82. doi:10.1038/s41586-019-1404-z

341. Mathys H, Davila-Velderrain J, Peng Z, Gao F, Mohammadi S, Young JZ, et al. Single-cell transcriptomic analysis of Alzheimer's disease. Nature. 2019;570: 332–337. doi:10.1038/s41586-019-1195-2

342. Zhou Y, Song WM, Andhey PS, Swain A, Levy T, Miller KR, et al. Human and mouse single-nucleus transcriptomics reveal TREM2-dependent and TREM2-independent cellular responses in Alzheimer's disease. Nat Med. 2020;26: 131–142. doi:10.1038/s41591-019-0695-9

343. Schena M, Shalon D, Davis RW, Brown PO. Quantitative Monitoring of Gene Expression Patterns with a Complementary DNA Microarray. Science. 1995;270: 467–470. doi:10.1126/science.270.5235.467

344. Christie JD. Microarrays. Crit Care Med. 2005;33: S449–S452. doi:10.1097/01.CCM.0000186078.26361.96

345. Sealfon SC, Chu TT. RNA and DNA Microarrays. 2011. pp. 3–34. doi:10.1007/978-1-59745-551-0_1

346. Barbulovic-Nad I, Lucente M, Sun Y, Zhang M, Wheeler AR, Bussmann M. Bio-Microarray Fabrication Techniques—A Review. Crit Rev Biotechnol.

2006;26: 237–259. doi:10.1080/07388550600978358

347. Sánchez A, de Villa MCR. A Tutorial Review of Microarray Data Analysis. 2008.

348. Ozsolak F, Milos PM. RNA sequencing: advances, challenges and opportunities. Nat Rev Genet. 2011;12: 87–98. doi:10.1038/nrg2934

349. Levin JZ, Yassour M, Adiconis X, Nusbaum C, Thompson DA, Friedman N, et al. Comprehensive comparative analysis of strand-specific RNA sequencing methods. Nat Methods. 2010;7: 709–715. doi:10.1038/nmeth.1491

350. Xu X, Zhang Y, Williams J, Antoniou E, McCombie WR, Wu S, et al. Parallel comparison of Illumina RNA-Seq and Affymetrix microarray platforms on transcriptomic profiles generated from 5-aza-deoxy-cytidine treated HT-29 colon cancer cells and simulated datasets. BMC Bioinformatics. BioMed Central Ltd; 2013;14 Suppl 9: S1. doi:10.1186/1471-2105-14-S9-S1

351. Zhao S, Fung-Leung W-P, Bittner A, Ngo K, Liu X. Comparison of RNA-Seq and Microarray in Transcriptome Profiling of Activated T Cells. Zhang S-D, editor. PLoS One. 2014;9: e78644. doi:10.1371/journal.pone.0078644

352. Mortazavi A, Williams BA, McCue K, Schaeffer L, Wold B. Mapping and quantifying mammalian transcriptomes by RNA-Seq. Nat Methods. 2008;5: 621–628. doi:10.1038/nmeth.1226

353. Wang C, Gong B, Bushel PR, Thierry-Mieg J, Thierry-Mieg D, Xu J, et al. The concordance between RNA-seq and microarray data depends on chemical treatment and transcript abundance. Nat Biotechnol. 2014;advance on. doi:10.1038/nbt.3001

354. Tang F, Barbacioru C, Wang Y, Nordman E, Lee C, Xu N, et al. mRNA-Seq whole-transcriptome analysis of a single cell. Nat Methods. 2009;6: 377–382. doi:10.1038/nmeth.1315

355. Kolodziejczyk AA, Kim JK, Svensson V, Marioni JC, Teichmann SA. The Technology and Biology of Single-Cell RNA Sequencing. Mol Cell. 2015;58: 610–620. doi:10.1016/j.molcel.2015.04.005

356. Keays KM, Owens GP, Ritchie AM, Gilden DH, Burgoon MP. Laser capture microdissection and single-cell RT-PCR without RNA purification. J Immunol Methods. 2005;302: 90–98. doi:10.1016/j.jim.2005.04.018

357. Frumkin D, Wasserstrom A, Itzkovitz S, Harmelin A, Rechavi G, Shapiro E.

Amplification of multiple genomic loci from single cells isolated by laser micro-dissection of tissues. BMC Biotechnol. 2008;8: 17. doi:10.1186/1472-6750-8-17

358. Hwang B, Lee JH, Bang D. Single-cell RNA sequencing technologies and bioinformatics pipelines. Exp Mol Med. 2018;50: 96. doi:10.1038/s12276-018-0071-8

359. Mazutis L, Gilbert J, Ung WL, Weitz DA, Griffiths AD, Heyman JA. Single-cell analysis and sorting using droplet-based microfluidics. Nat Protoc. 2013;8: 870–891. doi:10.1038/nprot.2013.046

360. HUG H, SCHULER R. Measurement of the Number of Molecules of a Single mRNA Species in a Complex mRNA Preparation. J Theor Biol. 2003;221: 615–624. doi:10.1006/jtbi.2003.3211

361. Fu GK, Hu J, Wang P-H, Fodor SPA. Counting individual DNA molecules by the stochastic attachment of diverse labels. Proc Natl Acad Sci. 2011;108: 9026–9031. doi:10.1073/pnas.1017621108

362. Stegle O, Teichmann SA, Marioni JC. Computational and analytical challenges in single-cell transcriptomics. Nat Rev Genet. 2015;16: 133–145. doi:10.1038/nrg3833

363. Qiu P. Embracing the dropouts in single-cell RNA-seq analysis. Nat Commun. 2020;11: 1169. doi:10.1038/s41467-020-14976-9

364. Sekula M, Gaskins J, Datta S. Detection of differentially expressed genes in discrete single-cell RNA sequencing data using a hurdle model with correlated random effects. Biometrics. 2019;75: 1051–1062. doi:10.1111/biom.13074

365. AlJanahi AA, Danielsen M, Dunbar CE. An Introduction to the Analysis of Single-Cell RNA-Sequencing Data. Mol Ther - Methods Clin Dev. 2018;10: 189–196. doi:10.1016/j.omtm.2018.07.003

366. Avila Cobos F, Vandesompele J, Mestdagh P, De Preter K. Computational deconvolution of transcriptomics data from mixed cell populations. Bioinformatics. 2018;34: 1969–1979. doi:10.1093/bioinformatics/bty019

367. Quon G, Haider S, Deshwar AG, Cui A, Boutros PC, Morris Q. Computational purification of individual tumor gene expression profiles leads to significant improvements in prognostic prediction. Genome Med. 2013;5: 29. doi:10.1186/gm433

368. Li B, Severson E, Pignon J-C, Zhao H, Li T, Novak J, et al. Comprehensive analyses of tumor immunity: implications for cancer immunotherapy. Genome Biol. 2016;17: 174. doi:10.1186/s13059-016-1028-7

369. Angelova M, Charoentong P, Hackl H, Fischer ML, Snajder R, Krogsdam AM, et al. Characterization of the immunophenotypes and antigenomes of colorectal cancers reveals distinct tumor escape mechanisms and novel targets for immunotherapy. Genome Biol. 2015;16: 64. doi:10.1186/s13059-015-0620-6

370. Ahn J, Yuan Y, Parmigiani G, Suraokar MB, Diao L, Wistuba II, et al. DeMix: deconvolution for mixed cancer transcriptomes using raw measured data. Bioinformatics. 2013;29: 1865–1871. doi:10.1093/bioinformatics/btt301

371. Abbas AR, Wolslegel K, Seshasayee D, Modrusan Z, Clark HF. Deconvolution of Blood Microarray Data Identifies Cellular Activation Patterns in Systemic Lupus Erythematosus. Tan P, editor. PLoS One. 2009;4: e6098. doi:10.1371/journal.pone.0006098

372. Zhong Y, Wan Y-W, Pang K, Chow LM, Liu Z. Digital sorting of complex tissues for cell type-specific gene expression profiles. BMC Bioinformatics. 2013;14: 89. doi:10.1186/1471-2105-14-89

373. Shen-Orr SS, Tibshirani R, Khatri P, Bodian DL, Staedtler F, Perry NM, et al. Cell type–specific gene expression differences in complex tissues. Nat Methods. 2010;7: 287–289. doi:10.1038/nmeth.1439

374. Liebner DA, Huang K, Parvin JD. MMAD: microarray microdissection with analysis of differences is a computational tool for deconvoluting cell type-specific contributions from tissue samples. Bioinformatics. 2014;30: 682–689. doi:10.1093/bioinformatics/btt566

375. Gong T, Hartmann N, Kohane IS, Brinkmann V, Staedtler F, Letzkus M, et al. Optimal Deconvolution of Transcriptional Profiling Data Using Quadratic Programming with Application to Complex Clinical Blood Samples. Rattray M, editor. PLoS One. 2011;6: e27156. doi:10.1371/journal.pone.0027156

376. Aran D, Hu Z, Butte AJ. xCell: digitally portraying the tissue cellular heterogeneity landscape. Genome Biol. 2017;18: 220. doi:10.1186/s13059-017-1349-1

377. Newman AM, Liu CL, Green MR, Gentles AJ, Feng W, Xu Y, et al. Robust enumeration of cell subsets from tissue expression profiles. Nat Methods.

2015;12: 453–457. doi:10.1038/nmeth.3337

378. Qiao W, Quon G, Csaszar E, Yu M, Morris Q, Zandstra PW. PERT: A Method for Expression Deconvolution of Human Blood Samples from Varied Microenvironmental and Developmental Conditions. Bonneau R, editor. PLoS Comput Biol. 2012;8: e1002838. doi:10.1371/journal.pcbi.1002838

379. Kuhn A, Thu D, Waldvogel HJ, Faull RLM, Luthi-Carter R. Population-specific expression analysis (PSEA) reveals molecular changes in diseased brain. Nat Methods. 2011;8: 945–947. doi:10.1038/nmeth.1710

380. Wang X, Park J, Susztak K, Zhang NR, Li M. Bulk tissue cell type deconvolution with multi-subject single-cell expression reference. Nat Commun. 2019;10: 380. doi:10.1038/s41467-018-08023-x

381. Kang K, Meng Q, Shats I, Umbach DM, Li M, Li Y, et al. CDSeq: A novel complete deconvolution method for dissecting heterogeneous samples using gene expression data. Przytycka TM, editor. PLOS Comput Biol. 2019;15: e1007510. doi:10.1371/journal.pcbi.1007510

382. Shen-Orr SS, Gaujoux R. Computational deconvolution: extracting cell type-specific information from heterogeneous samples. Curr Opin Immunol. 2013;25: 571–578. doi:10.1016/j.coi.2013.09.015

383. Frishberg A, Peshes-Yaloz N, Cohn O, Rosentul D, Steuerman Y, Valadarsky L, et al. Cell composition analysis of bulk genomics using single-cell data. Nat Methods. 2019;16: 327–332. doi:10.1038/s41592-019-0355-5

384. Steen CB, Liu CL, Alizadeh AA, Newman AM. Profiling Cell Type Abundance and Expression in Bulk Tissues with CIBERSORTx. 2020. pp. 135–157. doi:10.1007/978-1-0716-0301-7_7

385. Steen CB, Liu CL, Alizadeh AA, Newman AM. Stem Cell Transcriptional Networks [Internet]. Kidder BL, editor. Stem Cell Transcriptional Networks. New York, NY: Springer US; 2020. doi:10.1007/978-1-0716-0301-7

386. Bortolomeazzi M, Keddar MR, Ciccarelli FD, Benedetti L. Identification of non-cancer cells from cancer transcriptomic data. Biochim Biophys Acta - Gene Regul Mech. 2019; 194445. doi:10.1016/j.bbagrm.2019.194445

387. Li Z, Farias FHG, Dube U, Del-Aguila JL, Mihindukulasuriya KA, Fernandez MV, et al. The TMEM106B FTLD-protective variant, rs1990621, is also associated with increased neuronal proportion. Acta Neuropathol. 2020;139: 45–61. doi:10.1007/s00401-019-02066-0

388. Xie A, Gao J, Xu L, Meng D. Shared mechanisms of neurodegeneration in alzheimer's disease and parkinson's disease. Biomed Res Int. Hindawi Publishing Corporation; 2014;2014. doi:10.1155/2014/648740

389. Zarow C, Lyness SA, Mortimer JA, Chui HC. Neuronal Loss Is Greater in the Locus Coeruleus Than Nucleus Basalis and Substantia Nigra in Alzheimer and Parkinson Diseases. Arch Neurol. 2003;60: 337. doi:10.1001/archneur.60.3.337

390. Niccoli T, Partridge L. Ageing as a risk factor for disease. Curr Biol. Elsevier Ltd; 2012;22: R741–R752. doi:10.1016/j.cub.2012.07.024

391. Goedert M. Alzheimer's and Parkinson's diseases: The prion concept in relation to assembled Aβ, tau, and α-synuclein. Science. 2015;349. doi:10.1126/science.1255555

392. WHO | Ageing and health. In: World Health Organization. World Health Organization; 2015 p. Fact sheet N°404.

393. Srinivasan K, Friedman BA, Larson JL, Lauffer BE, Goldstein LD, Appling LL, et al. Untangling the brain's neuroinflammatory and neurodegenerative transcriptional responses. Nat Commun. 2016;7. doi:10.1038/ncomms11295

394. Zeisel A, Munoz-Manchado AB, Codeluppi S, Lonnerberg P, La Manno G, Jureus A, et al. Cell types in the mouse cortex and hippocampus revealed by single-cell RNA-seq. Science. 2015;347: 1138–1142. doi:10.1126/science.aaa1934

395. Allen M, Carrasquillo MM, Funk C, Heavner BD, Zou F, Younkin CS, et al. Human Whole Genome Genotype and Transcriptome Data for Alzheimer's and Other Neurodegenerative Diseases. Sci Data. 2016;3: 1–10. doi:https://doi.org/10.1038/sdata.2016.89

396. Ferrer I, Martinez A, Boluda S, Parchi P, Barrachina M. Brain banks: benefits, limitations and cautions concerning the use of post-mortem brain tissue for molecular studies. Cell Tissue Bank. 2008;9: 181–194. doi:10.1007/s10561-008-9077-0

397. Nativio R, Donahue G, Berson A, Lan Y, Amlie-Wolf A, Tuzer F, et al. Dysregulation of the epigenetic landscape of normal aging in Alzheimer's disease. Nat Neurosci. 2018;21. doi:10.1038/s41593-018-0101-9

398. Nussbaum R, Christopher E. Alzheimer's and Parkinson's Disease. N Engl J Med. 2003;348: 1356–64. doi:10.1056/NEJM2003ra020003

399. Zhang Y, James M, Middleton F a., Davis RL. Transcriptional analysis of multiple brain regions in Parkinson's disease supports the involvement of specific protein processing, energy metabolism, and signaling pathways, and suggests novel disease mechanisms. Am J Med Genet - Neuropsychiatr Genet. 2005;137 B: 5–16. doi:10.1002/ajmg.b.30195

400. Stratowa C. xps: Processing and Analysis of Affymetrix Oligonucleotide Arrays including Exon Arrays, Whole Genome Arrays and Plate Arrays. 2019.

401. R: A language and environment for statistical computing. R Foundation for Statistical Computing. 2018;

402. Gentleman RC, Gentleman RC, Carey VJ, Carey VJ, Bates DM, Bates DM, et al. Bioconductor: open software development for computational biology and bioinformatics. Genome Biol. 2004;5. doi:10.1186/gb-2004-5-10-r80

403. Kalpić D, Hlupić N, Lovrić M. Student's t-Tests. International Encyclopedia of Statistical Science. Berlin, Heidelberg: Springer Berlin Heidelberg; 2011. pp. 1559–1563. doi:10.1007/978-3-642-04898-2_641

404. Rey D, Neuhäuser M. Wilcoxon-Signed-Rank Test. International Encyclopedia of Statistical Science. Berlin, Heidelberg: Springer Berlin Heidelberg; 2011. pp. 1658–1659. doi:10.1007/978-3-642-04898-2_616

405. Lopes RHC. Kolmogorov-Smirnov Test. International Encyclopedia of Statistical Science. Berlin, Heidelberg: Springer Berlin Heidelberg; 2011. pp. 718–720. doi:10.1007/978-3-642-04898-2_326

406. Gu Z, Eils R, Schlesner M. Complex heatmaps reveal patterns and correlations in multidimensional genomic data. Bioinformatics. 2016;32: 2847–2849. doi:10.1093/bioinformatics/btw313

407. Ringnér M. What is principal component analysis? Nat Biotechnol. 2008;26: 303–304. doi:10.1038/nbt0308-303

408. Lê S, Josse J, Husson F. FactoMineR: An R package for multivariate analysis. J Stat Softw. 2008;25: 1–18. doi:10.18637/jss.v025.i01

409. Frankish A, Diekhans M, Ferreira A-M, Johnson R, Jungreis I, Loveland J, et al. GENCODE reference annotation for the human and mouse genomes. Nucleic Acids Res. 2019;47: D766–D773. doi:10.1093/nar/gky955

410. Bray NL, Pimentel H, Melsted P, Pachter L. Near-optimal probabilistic RNA-seq quantification. Nat Biotechnol. 2016;34: 525–527. doi:10.1038/nbt.3519

411. Lun ATL, McCarthy DJ, Marioni JC. A step-by-step workflow for low-level analysis of single-cell RNA-seq data. F1000Research. 2016;5: 2122. doi:10.12688/f1000research.9501.1

412. van der Maaten L, Hinton G. Visualizing Data using t-SNE. J Mach Learn Res. 2008;9: 2579–2605.

413. Qiu X, Mao Q, Tang Y, Wang L, Chawla R, Pliner HA, et al. Reversed graph embedding resolves complex single-cell trajectories. Nat Methods. 2017;14: 979–982. doi:10.1038/nmeth.4402

414. Trapnell C, Cacchiarelli D, Grimsby J, Pokharel P, Li S, Morse M, et al. The dynamics and regulators of cell fate decisions are revealed by pseudotemporal ordering of single cells. Nat Biotechnol. 2014;32: 381–386. doi:10.1038/nbt.2859

415. Qiu X, Hill A, Packer J, Lin D, Ma Y-A, Trapnell C. Single-cell mRNA quantification and differential analysis with Census. Nat Methods. 2017;14: 309–315. doi:10.1038/nmeth.4150

416. Tibshirani R, Hastie T, Narasimhan B, Chu G. Diagnosis of multiple cancer types by shrunken centroids of gene expression. Proc Natl Acad Sci. 2002;99: 6567–6572. doi:10.1073/pnas.082099299

417. L. Lun AT, Bach K, Marioni JC. Pooling across cells to normalize single-cell RNA sequencing data with many zero counts. Genome Biol. 2016;17: 75. doi:10.1186/s13059-016-0947-7

418. Ritchie ME, Phipson B, Wu D, Hu Y, Law CW, Shi W, et al. limma powers differential expression analyses for RNA-sequencing and microarray studies. Nucleic Acids Res. 2015;43: 1–13. doi:10.1093/nar/gkv007

419. Gautier L, Cope L, Bolstad BM, Irizarry R a. Affy - Analysis of Affymetrix GeneChip data at the probe level. Bioinformatics. 2004;20: 307–315. doi:10.1093/bioinformatics/btg405

420. Leek JT, Johnson WE, Parker HS, Jaffe AE, Storey JD. The sva package for removing batch effects and other unwanted variation in high-throughput experiments. Bioinformatics. 2012;28: 882–883. doi:10.1093/bioinformatics/bts034

421. Draghici S. Statistics and Data Analysis for Microarrays Using R and Bioconductir. Second. 2012.

422. Chen Y, Lun ATL, Smyth GK. From reads to genes to pathways: differential

expression analysis of RNA-Seq experiments using Rsubread and the edgeR quasi-likelihood pipeline. F1000Research. 2016;5. doi:10.12688/f1000research.8987.2

423. Newman AM, Steen CB, Liu CL, Gentles AJ, Chaudhuri AA, Scherer F, et al. Determining cell type abundance and expression from bulk tissues with digital cytometry. Nat Biotechnol. 2019;37: 773–782. doi:10.1038/s41587-019-0114-2

424. Picelli S, Björklund ÅK, Faridani OR, Sagasser S, Winberg G, Sandberg R. Smart-seq2 for sensitive full-length transcriptome profiling in single cells. Nat Methods. 2013;10: 1096–1098. doi:10.1038/nmeth.2639

425. Dai Z, Sheridan JM, Gearing LJ, Moore DL, Su S, Dickins R a, et al. shRNA-seq data analysis with edgeR. F1000Research. 2014;3: 95. doi:10.12688/f1000research.4204

426. Smyth GK. Linear Models and Empirical Bayes Methods for Assessing Differential Expression in Microarray Experiments. Stat Appl Genet Mol Biol. 2004;3: 1–25. doi:10.2202/1544-6115.1027

427. Afshartous D, Preston RA. Key Results of Interaction Models with Centering. J Stat Educ. 2011;19. doi:10.1080/10691898.2011.11889620

428. R Development Core Team R. R: A Language and Environment for Statistical Computing. In: 2008 [Internet]. Available: www.R-project.org

429. Piñero J, Ramírez-Anguita JM, Saüch-Pitarch J, Ronzano F, Centeno E, Sanz F, et al. The DisGeNET knowledge platform for disease genomics: 2019 update. Nucleic Acids Res. 2019; doi:10.1093/nar/gkz1021

430. Kanehisa M, Sato Y, Kawashima M, Furumichi M, Tanabe M. KEGG as a reference resource for gene and protein annotation. Nucleic Acids Res. 2016;44: D457–D462. doi:10.1093/nar/gkv1070

431. Väremo L, Nielsen J, Nookaew I. Enriching the gene set analysis of genome-wide data by incorporating directionality of gene expression and combining statistical hypotheses and methods. Nucleic Acids Res. 2013;41: 4378–4391. doi:10.1093/nar/gkt111

432. Subramanian A, Tamayo P, Mootha VK, Mukherjee S, Ebert BL, Gillette M a, et al. Gene set enrichment analysis: a knowledge-based approach for interpreting genome-wide expression profiles. Proc Natl Acad Sci U S A. 2005;102: 15545–15550. doi:10.1073/pnas.0506580102

433. Mootha VK, Lindgren CM, Eriksson K-F, Subramanian A, Sihag S, Lehar J, et al. PGC-1alpha-responsive genes involved in oxidative phosphorylation are coordinately downregulated in human diabetes. Nat Genet. 2003;34: 267–273. doi:10.1038/ng1180

434. Kelley KW, Nakao-Inoue H, Molofsky A V., Oldham MC. Variation among intact tissue samples reveals the core transcriptional features of human CNS cell classes. Nat Neurosci. 2018;21: 1171–1184. doi:10.1038/s41593-018-0216-z

435. de Almeida B, Saraiva-Agostinho N, Barbosa-Morais NL. cTRAP: Identification of candidate causal perturbations from differential gene expression data. Bioconductor. 2019;

436. Subramanian A, Narayan R, Corsello SM, Peck DD, Natoli TE, Lu X, et al. A Next Generation Connectivity Map: L1000 Platform and the First 1,000,000 Profiles. Cell. Cell Press; 2017;171: 1437-1452.e17. doi:10.1016/j.cell.2017.10.049

437. Tanapat P. Neuronal Cell Markers. Mater Methods. 2013;3. doi:10.13070/mm.en.3.196

438. Preston AN, Cervasio DA, Laughlin ST. Visualizing the brain's astrocytes. 2019. pp. 129–151. doi:10.1016/bs.mie.2019.02.006

439. Ponomarev ED, Shriver LP, Dittel BN. CD40 Expression by Microglial Cells Is Required for Their Completion of a Two-Step Activation Process during Central Nervous System Autoimmune Inflammation. J Immunol. 2006;176: 1402–1410. doi:10.4049/jimmunol.176.3.1402

440. Ligon KL, Alberta JA, Kho AT, Weiss J, Kwaan MR, Nutt CL, et al. The Oligodendroglial Lineage Marker OLIG2 Is Universally Expressed in Diffuse Gliomas. J Neuropathol Exp Neurol. 2004;63: 499–509. doi:10.1093/jnen/63.5.499

441. Hodge RD, Bakken TE, Miller JA, Smith KA, Barkan ER, Graybuck LT, et al. Conserved cell types with divergent features in human versus mouse cortex. Nature. 2019;573: 61–68. doi:10.1038/s41586-019-1506-7

442. Liu S-LL, Wang C, Jiang T, Tan L, Xing A, Yu J-TT. The Role of Cdk5 in Alzheimer's Disease. Mol Neurobiol. Molecular Neurobiology; 2016;53: 4328–4342. doi:10.1007/s12035-015-9369-x

443. Moncini S, Lunghi M, Valmadre A, Grasso M, Del Vescovo V, Riva P, et al.

The miR-15/107 Family of microRNA Genes Regulates CDK5R1/p35 with Implications for Alzheimer's Disease Pathogenesis. Mol Neurobiol. 2017;54: 4329–4342. doi:10.1007/s12035-016-0002-4

444. Shulman JM, Imboywa S, Giagtzoglou N, Powers MP, Hu Y, Devenport D, et al. Functional screening in Drosophila identifies Alzheimer's disease susceptibility genes and implicates Tau-mediated mechanisms. Hum Mol Genet. 2014;23: 870–877. doi:10.1093/hmg/ddt478

445. Marques A, Fernandes P, Ramos M. ABAD: A Potential Therapeutic Target for Abeta-Induced Mitochondrial Dysfunction in Alzheimers Disease. Mini-Reviews Med Chem. 2009;9: 1002–1008. doi:10.2174/138955709788681627

446. Mahul-Mellier A-L, Fauvet B, Gysbers A, Dikiy I, Oueslati A, Georgeon S, et al. c-Abl phosphorylates α-synuclein and regulates its degradation: implication for α-synuclein clearance and contribution to the pathogenesis of Parkinson's disease. Hum Mol Genet. 2014;23: 2858–2879. doi:10.1093/hmg/ddt674

447. Jiménez-Jiménez FJ, Alonso-Navarro H, García-Martín E, Agúndez JAG. COMT gene and risk for Parkinson's disease. Pharmacogenet Genomics. 2014;24: 331–339. doi:10.1097/FPC.0000000000000056

448. Liu P, Wang X, Gao N, Zhu H, Dai X, Xu Y, et al. G protein-coupled receptor kinase 5, overexpressed in the α-synuclein up-regulation model of Parkinson's disease, regulates bcl-2 expression. Brain Res. 2010;1307: 134–141. doi:10.1016/j.brainres.2009.10.036

449. Haq IU, Snively BM, Sweadner KJ, Suerken CK, Cook JF, Ozelius LJ, et al. Revising rapid-onset dystonia–parkinsonism: Broadening indications for ATP1A3 testing. Mov Disord. 2019;34: 1528–1536. doi:10.1002/mds.27801

450. Harvey K, Marchetti B. Regulating Wnt signaling: a strategy to prevent neurodegeneration and induce regeneration. J Mol Cell Biol. 2014;6: 1–2. doi:10.1093/jmcb/mju002

451. Mattson MP, Meffert MK. Roles for NF-κB in nerve cell survival, plasticity, and disease. Cell Death Differ. 2006;13: 852–860. doi:10.1038/sj.cdd.4401837

452. Siavelis JC, Bourdakou MM, Athanasiadis EI, Spyrou GM, Nikita KS. Bioinformatics methods in drug repurposing for Alzheimer's disease. Brief

Bioinform. 2016;17: 322–335. doi:10.1093/bib/bbv048

453. Zahoor I, Shafi A, Haq E. Pharmacological Treatment of Parkinson's Disease [Internet]. Parkinson's Disease: Pathogenesis and Clinical Aspects. 2018. Available: http://www.ncbi.nlm.nih.gov/pubmed/30702845

454. MacDonald V, Halliday GM. Selective loss of pyramidal neurons in the pre-supplementary motor cortex in Parkinson's disease. Mov Disord. 2002;17: 1166–1173. doi:10.1002/mds.10258

455. Gomez-Isla T, Hollister R, West H, Mui S, Growdon JH, Petersen RC, et al. Neurond Loss Correlates with but Exceeds Neurofibrillary Tangles in Alzheimer 's Disease. Ann Neurol. 1997;41: 17–24. doi:https://doi.org/10.1002/ana.410410106

456. Verkhratsky A, Olabarria M, Noristani HN, Yeh C, Rodriguez JJ. Astrocytes in Alzheimer ' s Disease. 2010;7: 399–412.

457. Solito E, Sastre M. Microglia function in Alzheimer's disease. Front Pharmacol. 2012;3 FEB: 1–10. doi:10.3389/fphar.2012.00014

458. Le W, Wu J, Tang Y. Protective Microglia and Their Regulation in Parkinson's Disease. Front Mol Neurosci. 2016;9: 1–13. doi:10.3389/fnmol.2016.00089

459. Pelvig DP, Pakkenberg H, Stark AK, Pakkenberg B. Neocortical glial cell numbers in human brains. Neurobiol Aging. 2008;29: 1754–1762. doi:10.1016/j.neurobiolaging.2007.04.013

460. Darmanis S, Sloan SA, Zhang Y, Enge M, Caneda C, Shuer LM, et al. A survey of human brain transcriptome diversity at the single cell level. Proc Natl Acad Sci. 2015;112: 7285–7290. doi:10.1073/pnas.1507125112

461. Domingues HS, Portugal CC, Socodato R, Relvas JB. Oligodendrocyte, Astrocyte, and Microglia Crosstalk in Myelin Development, Damage, and Repair. Front Cell Dev Biol. 2016;4. doi:10.3389/fcell.2016.00071

462. Mathys H, Davila-Velderrain J, Peng Z, Gao F, Mohammadi S, Young JZ, et al. Single-cell transcriptomic analysis of Alzheimer's disease. Nature. 2019;571: E1–E1. doi:10.1038/s41586-019-1329-6

463. Herculano-Houzel S. The human brain in numbers: a linearly scaled-up primate brain. Front Hum Neurosci. Frontiers Media SA; 2009;3: 31. doi:10.3389/neuro.09.031.2009

464. Filipchenko RE, Pevzner LZ, Slonim AD. RNA content in the neurons and

glia of the hypothalamic nuclei after intermittent cooling. Neurosience Behav Physiol. 1976;223: 69–71.

465. Tomita H, Vawter MP, Walsh DM, Evans SJ, Choudary P V, Li J, et al. Effect of agonal and postmortem factors on gene expression profile: quality control in microarray analyses of postmortem human brain. Biol Psychiatry. 2004;55: 346–352. doi:10.1016/j.biopsych.2003.10.013

466. Kim K-Y, Jang H-J, Yang YR, Park K-I, Seo J, Shin I-W, et al. SREBP-2/PNPLA8 axis improves non-alcoholic fatty liver disease through activation of autophagy. Sci Rep. 2016;6: 35732. doi:10.1038/srep35732

467. Dupont N, Chauhan S, Arko-Mensah J, Castillo EF, Masedunskas A, Weigert R, et al. Neutral Lipid Stores and Lipase PNPLA5 Contribute to Autophagosome Biogenesis. Curr Biol. 2014;24: 609–620. doi:10.1016/j.cub.2014.02.008

468. Zarrouk A, Debbabi M, Bezine M, Karym EM, Badreddine A, Rouaud O, et al. Lipid Biomarkers in Alzheimer's Disease. Curr Alzheimer Res. 2018;15: 303–312. doi:10.2174/1567205014666170505101426

469. Li Q, Liu Y, Sun M. Autophagy and Alzheimer's Disease. Cell Mol Neurobiol. 2017;37: 377–388. doi:10.1007/s10571-016-0386-8

470. Cruchaga C, Kauwe JSK, Nowotny P, Bales K, Pickering EH, Mayo K, et al. Cerebrospinal fluid APOE levels: an endophenotype for genetic studies for Alzheimer's disease. Hum Mol Genet. 2012;21: 4558–4571. doi:10.1093/hmg/dds296

471. Fodero-Tavoletti MT, Hardy MP, Cornell B, Katsis F, Sadek CM, Mitchell CA, et al. Protein tyrosine phosphatase hPTPN20a is targeted to sites of actin polymerization. Biochem J. 2005;389: 343–354. doi:10.1042/BJ20041932

472. Tan MGK, Lee C, Lee JH, Francis PT, Williams RJ, Ramírez MJ, et al. Decreased rabphilin 3A immunoreactivity in Alzheimer's disease is associated with Aβ burden. Neurochem Int. 2014;64: 29–36. doi:10.1016/j.neuint.2013.10.013

473. Diao H, Li X, Hu S. The identification of dysfunctional crosstalk of pathways in Parkinson disease. Gene. 2013;515: 159–162. doi:10.1016/j.gene.2012.11.003

474. Szigeti A, Hocsak E, Rapolti E, Racz B, Boronkai A, Pozsgai E, et al. Facilitation of Mitochondrial Outer and Inner Membrane Permeabilization

and Cell Death in Oxidative Stress by a Novel Bcl-2 Homology 3 Domain Protein. J Biol Chem. 2010;285: 2140–2151. doi:10.1074/jbc.M109.015222

475. Tönnies E, Trushina E. Oxidative Stress, Synaptic Dysfunction, and Alzheimer's Disease. J Alzheimer's Dis. 2017;57: 1105–1121. doi:10.3233/JAD-161088

476. Yagensky O, Kohansal-Nodehi M, Gunaseelan S, Rabe T, Zafar S, Zerr I, et al. Increased expression of heme-binding protein 1 early in Alzheimer's disease is linked to neurotoxicity. Elife. 2019;8. doi:10.7554/eLife.47498

477. Gangoda L, Doerflinger M, Srivastava R, Narayan N, Edgington LE, Orian J, et al. Loss of Prkar1a leads to Bcl-2 family protein induction and cachexia in mice. Cell Death Differ. 2014;21: 1815–1824. doi:10.1038/cdd.2014.98

478. Calne DB, Eisen A, McGeer E, Spencer P. ALZHEIMER'S DISEASE, PARKINSON'S DISEASE,AND MOTONEURONE DISEASE: ABIOTROPIC INTERACTION BETWEEN AGEING AND ENVIRONMENT? Lancet. 1986;22: 1067–1070.

479. Greenfield S, Vaux D. Parkinson's disease, Alzheimer's disease and motor neurone disease: identifying a common mechanism. Neuroscience. 2002;113: 485–492. doi:10.1016/S0306-4522(02)00194-X

480. Cai H, Cong W, Ji S, Rothman S, Maudsley S, Martin B. Metabolic Dysfunction in Alzheimers Disease and Related Neurodegenerative Disorders. Curr Alzheimer Res. 2012;9: 5–17. doi:10.2174/156720512799015064

481. Seo J, Park M. Molecular crosstalk between cancer and neurodegenerative diseases. Cell Mol Life Sci. 2019; doi:10.1007/s00018-019-03428-3

482. Keeney PM. Parkinson's Disease Brain Mitochondrial Complex I Has Oxidatively Damaged Subunits and Is Functionally Impaired and Misassembled. J Neurosci. 2006;26: 5256–5264. doi:10.1523/JNEUROSCI.0984-06.2006

483. Kish SJ, Bergeron C, Rajput A, Dozic S, Mastrogiacomo F, Chang L-J, et al. Brain Cytochrome Oxidase in Alzheimer's Disease. J Neurochem. 1992;59: 776–779. doi:10.1111/j.1471-4159.1992.tb09439.x

484. Insa R. Drug Repositioning: Bringing New Life to Shelved Assets and Existing Drugs . Edited by Michael J. Barratt and Donald E. Frail. ChemMedChem. 2013;8: 336–337. doi:10.1002/cmdc.201200552

485. Zhang J, Peng C, Shi H, Wang S, Wang Q, Wang J. Inhibition of Autophagy Causes Tau Proteolysis by Activating Calpain in Rat Brain. J Alzheimer's Dis. 2009;16: 39–47. doi:10.3233/JAD-2009-0908

486. CUI C-M, GAO J-L, CUI Y, SUN L-Q, WANG Y-C, WANG K-J, et al. Chloroquine exerts neuroprotection following traumatic brain injury via suppression of inflammation and neuronal autophagic death. Mol Med Rep. 2015;12: 2323–2328. doi:10.3892/mmr.2015.3611

487. Zhang L, Liu C, Wu J, Tao J, Sui X, Yao Z, et al. Tubastatin A/ACY-1215 Improves Cognition in Alzheimer's Disease Transgenic Mice. J Alzheimer's Dis. 2014;41: 1193–1205. doi:10.3233/JAD-140066

488. Sanders O. Sildenafil for the Treatment of Alzheimer's Disease: A Systematic Review. J Alzheimer's Dis Reports. 2020;4: 91–106. doi:10.3233/ADR-200166

489. Porsteinsson AP, Drye LT, Pollock BG, Devanand DP, Frangakis C, Ismail Z, et al. Effect of Citalopram on Agitation in Alzheimer Disease. JAMA. 2014;311: 682. doi:10.1001/jama.2014.93

490. Mauri M, Mancioli A, Rebecchi V, Corbetta S, Colombo C, Bono G. Amisulpride in the treatment of behavioural disturbances among patients with moderate to severe Alzheimer's disease. Acta Neurol Scand. 2006;114: 97–101. doi:10.1111/j.1600-0404.2006.00660.x

491. Chen M, Du Z-Y, Zheng X, Li D-L, Zhou R-P, Zhang K. Use of curcumin in diagnosis, prevention, and treatment of Alzheimer's disease. Neural Regen Res. 2018;13: 742. doi:10.4103/1673-5374.230303

492. Balducci C, Forloni G. Doxycycline for Alzheimer's Disease: Fighting β-Amyloid Oligomers and Neuroinflammation. Front Pharmacol. 2019;10. doi:10.3389/fphar.2019.00738

493. Bang M, Kim DG, Gonzales EL, Kwon KJ, Shin CY. Etoposide Induces Mitochondrial Dysfunction and Cellular Senescence in Primary Cultured Rat Astrocytes. Biomol Ther (Seoul). 2019;27: 530–539. doi:10.4062/biomolther.2019.151

494. Jaeger PA, Wyss-Coray T. Beclin 1 Complex in Autophagy and Alzheimer Disease. Arch Neurol. 2010;67. doi:10.1001/archneurol.2010.258

495. Warner CB, Ottman AA, Brown JN. The Role of Atomoxetine for Parkinson Disease–Related Executive Dysfunction. J Clin Psychopharmacol. 2018;38:

627–631. doi:10.1097/JCP.0000000000000963

496. Hirohata M, Ono K, Morinaga A, Yamada M. Non-steroidal anti-inflammatory drugs have potent anti-fibrillogenic and fibril-destabilizing effects for α-synuclein fibrils in vitro. Neuropharmacology. 2008;54: 620–627. doi:10.1016/j.neuropharm.2007.11.010

497. Mosquera L, Colón JM, Santiago JM, Torrado AI, Meléndez M, Segarra AC, et al. Tamoxifen and estradiol improved locomotor function and increased spared tissue in rats after spinal cord injury: Their antioxidant effect and role of estrogen receptor alpha. Brain Res. 2014;1561: 11–22. doi:10.1016/j.brainres.2014.03.002

498. Lee E-SY, Yin Z, Milatovic D, Jiang H, Aschner M. Estrogen and Tamoxifen Protect against Mn-Induced Toxicity in Rat Cortical Primary Cultures of Neurons and Astrocytes. Toxicol Sci. 2009;110: 156–167. doi:10.1093/toxsci/kfp081

499. Latourelle JC, Dybdahl M, Destefano AL, Myers RH, Lash TL. Risk of Parkinson's disease after tamoxifen treatment. BMC Neurol. 2010;10: 23. doi:10.1186/1471-2377-10-23

500. Hong C-T, Chan L, Hu C-J, Lin C-M, Hsu C-Y, Lin M-C. Tamoxifen and the Risk of Parkinson's Disease in Female Patients with Breast Cancer in Asian People: A Nationwide Population-Based Study. J Breast Cancer. 2017;20: 356. doi:10.4048/jbc.2017.20.4.356

501. Huang B, Liu J, Ma D, Chen G, Wang W, Fu S. Myricetin prevents dopaminergic neurons from undergoing neuroinflammation-mediated degeneration in a lipopolysaccharide-induced Parkinson's disease model. J Funct Foods. 2018;45: 452–461. doi:10.1016/j.jff.2018.04.018

502. Dhanraj V, Karuppaiah J, Balakrishnan R, Elangovan N. Myricetin attenuates neurodegeneration and cognitive impairment in Parkinsonism. Front Biosci (Elite Ed). 2018;10: 481–494. Available: http://www.ncbi.nlm.nih.gov/pubmed/29772521

503. Li Y, Li L, Hölscher C. Therapeutic Potential of Genipin in Central Neurodegenerative Diseases. CNS Drugs. 2016;30: 889–897. doi:10.1007/s40263-016-0369-9

504. Barini E, Miccoli A, Tinarelli F, Mulholland K, Kadri H, Khanim F, et al. The Anthelmintic Drug Niclosamide and Its Analogues Activate the Parkinson's

Disease Associated Protein Kinase PINK1. ChemBioChem. 2018;19: 425–429. doi:10.1002/cbic.201700500

505. National Center for Biotechnology Information. PubChem Database. Metaraminol, CID=5906 [Internet]. Available: https://pubchem.ncbi.nlm.nih.gov/compound/Metaraminol

506. Gannon M, Che P, Chen Y, Jiao K, Roberson ED, Wang Q. Noradrenergic dysfunction in Alzheimer's disease. Front Neurosci. 2015;9. doi:10.3389/fnins.2015.00220

507. Alexander GM, Schwartzman RJ, Nukes TA, Grothusen JR, Hooker MD. 2-Adrenergic agonist as adjunct therapy to levodopa in Parkinson's disease. Neurology. 1994;44: 1511–1511. doi:10.1212/WNL.44.8.1511

508. Balgi AD, Fonseca BD, Donohue E, Tsang TCF, Lajoie P, Proud CG, et al. Screen for Chemical Modulators of Autophagy Reveals Novel Therapeutic Inhibitors of mTORC1 Signaling. Cao Y, editor. PLoS One. 2009;4: e7124. doi:10.1371/journal.pone.0007124

509. Fujikake N, Shin M, Shimizu S. Association Between Autophagy and Neurodegenerative Diseases. Front Neurosci. 2018;12. doi:10.3389/fnins.2018.00255

510. Ngo ST, Fang S-T, Huang S-H, Chou C-L, Huy PDQ, Li MS, et al. Anti-arrhythmic Medication Propafenone a Potential Drug for Alzheimer's Disease Inhibiting Aggregation of Aβ: In Silico and in Vitro Studies. J Chem Inf Model. 2016;56: 1344–1356. doi:10.1021/acs.jcim.6b00029

511. Shin H-W, Chung SJ. Drug-Induced Parkinsonism. J Clin Neurol. 2012;8: 15. doi:10.3988/jcn.2012.8.1.15

512. Gupta R, Ambasta RK, Kumar P. Pharmacological intervention of histone deacetylase enzymes in the neurodegenerative disorders. Life Sci. 2020;243: 117278. doi:10.1016/j.lfs.2020.117278

513. Liu S-J, Wang J-Z. Alzheimer-like tau phosphorylation induced by wortmannin in vivo and its attenuation by melatonin. Acta Pharmacol Sin. 2002;23: 183–7. Available: http://www.ncbi.nlm.nih.gov/pubmed/11866882

514. XU G-G, DENG Y-Q, LIU S-J, LI H-L, WANG J-Z. Prolonged Alzheimer-like Tau Hyperphosphorylation Induced by Simultaneous Inhibition of Phosphoinositol-3 Kinase and Protein Kinase C in N2a cells. Acta Biochim Biophys Sin (Shanghai). 2005;37: 349–354. doi:10.1111/j.1745-

7270.2005.00050.x

515. Limboonreung T, Tuchinda P, Chongthammakun S. Chrysoeriol mediates mitochondrial protection via PI3K/Akt pathway in MPP+ treated SH-SY5Y cells. Neurosci Lett. 2020;714: 134545. doi:10.1016/j.neulet.2019.134545

516. Roder C, Thomson MJ. Auranofin: Repurposing an Old Drug for a Golden New Age. Drugs R D. 2015;15: 13–20. doi:10.1007/s40268-015-0083-y

517. Madeira JM, Bajwa E, Stuart MJ, Hashioka S, Klegeris A. Gold drug auranofin could reduce neuroinflammation by inhibiting microglia cytotoxic secretions and primed respiratory burst. J Neuroimmunol. 2014;276: 71–79. doi:10.1016/j.jneuroim.2014.08.615

518. Madeira JM, Renschler CJ, Mueller B, Hashioka S, Gibson DL, Klegeris A. Novel protective properties of auranofin: Inhibition of human astrocyte cytotoxic secretions and direct neuroprotection. Life Sci. 2013;92: 1072–1080. doi:10.1016/j.lfs.2013.04.005

519. Wishart DS, Feunang YD, Guo AC, Lo EJ, Marcu A, Grant JR, et al. DrugBank 5.0: a major update to the DrugBank database for 2018. Nucleic Acids Res. 2018;46: D1074–D1082. doi:10.1093/nar/gkx1037

520. Hagenauer MH, Schulmann A, Li JZ, Vawter MP, Walsh DM, Thompson RC, et al. Inference of cell type composition from human brain transcriptomic datasets illuminates the effects of age, manner of death, dissection, and psychiatric diagnosis. 2017.

521. Treutlein B, Lee QY, Camp JG, Mall M, Koh W, Shariati SAM, et al. Dissecting direct reprogramming from fibroblast to neuron using single-cell RNA-seq. Nature. 2016;534: 391–395. doi:10.1038/nature18323

522. Shin J, Berg DA, Zhu Y, Shin JY, Song J, Bonaguidi MA, et al. Single-Cell RNA-Seq with Waterfall Reveals Molecular Cascades underlying Adult Neurogenesis. Cell Stem Cell. 2015;17: 360–372. doi:10.1016/j.stem.2015.07.013

523. Grubman A, Chew G, Ouyang JF, Sun G, Choo XY, McLean C, et al. A single-cell atlas of entorhinal cortex from individuals with Alzheimer's disease reveals cell-type-specific gene expression regulation. Nat Neurosci. 2019;22: 2087–2097. doi:10.1038/s41593-019-0539-4

All the supplementary tables can be found at
https://imm.medicina.ulisboa.pt/group/distrans/MarieBordone_PhD2020_SuppTabl
es.zip

Table S1 – CIBERSORTx estimates of the cellular composition of brain samples from all datasets.

- **Sample ID** is the sample's identifier.
- **Condition** is the sample's disease status (i.e., AD/PD or Control).
- **Neuronal proportion** is the proportion of neurons in the sample estimated by CIBERSORTx.
- **Astrocytic proportion** is the proportion of astrocytes in the sample estimated by CIBERSORTx.
- **Microglial proportion** is the proportion of microglia in the sample estimated by CIBERSORTx.
- **Oligodendrocytic proportion** is the proportion of oligodendrocytes in the sample estimated by CIBERSORTx.
- **Correlation** is the highest Pearson's correlation coefficient between gene expression profiles of artificial mixture samples, generated by CIBERSORTx using a comprehensive range of imputed cell fractions, the cell-type expression signature and the sample's gene expression profile. The estimated sample's cellular composition is indeed that of the most correlated artificial mixture sample.
- **RMSE** is the Root Mean Squared Error of the CIBERSORTx-modelled gene expression profile (i.e., that from the most correlated imputed artificial mixture) when compared to the actual (empirical) sample's gene expression.

Note: the p-values of the aforementioned correlation tests are not shown because they are all virtually zero.

Table S2 – Human brain cell types gene expression signature.

Relative expression, in arbitrary units (with 1 being the minimum), in the main human brain cell types of the genes selected by CIBERSORTx as able to discriminate between them.

Table S3 – Mouse brain cell types gene expression signature.

Relative expression, in arbitrary units (with 1 being the minimum), in the main murine brain cell types of the genes selected by CIBERSORTx as able to discriminate between them.

Table S4 – Artificial mixture samples.

Cell-type proportions of the 300 artificial mixture samples generated through chimeric libraries of 35 million reads, with numbers of randomly sampled read from the cell-type-specific pools also shown.

Table S5 – Modes of Action of cMap compounds.

Table S6 – Differential Gene Expression – MayoClinic dataset.

For each linearly modelled effect (i.e. each tab):

- **logFC** is the gene's $\log_2$(fold-change) in expression associated with the effect.
- **AveExpr** is the gene's average expression (in $\log_2$(CPM)) over all samples.
- **t** is the moderated t-statistic of differential gene expression.
- **P.Value** is the p-value associated with the t-statistic.
- **adj.P.Val** is the p-value associated with the t-statistic corrected for multiple testing by the Benjamini-Hochberg FDR procedure.
- **B** is B-statistic, i.e. the empirical Bayesian log-odds that the gene is differentially expressed.

Table S7 – Differential Gene Expression – Nativio dataset.

For each linearly modelled effect (i.e. each tab):

- **logFC** is the gene's $\log_2$(fold-change) in expression associated with the effect.
- **AveExpr** is the gene's average expression (in $\log_2$(CPM)) over all samples.
- **t** is the moderated t-statistic of differential gene expression.
- **P.Value** is the p-value associated with the t-statistic.
- **adj.P.Val** is the p-value associated with the t-statistic corrected for multiple testing by the Benjamini-Hochberg FDR procedure.

- **B** is B-statistic, i.e. the empirical Bayesian log-odds that the gene is differentially expressed.

Table S8 – Combined AD effect's scores from t-statistics of differential expression of common genes in the MayoClinic and Nativio datasets.

Table S9 – Combined Neurodegeneration effect's scores from t-statistics of differential expression of common genes in the MayoClinic and Nativio datasets.

Table S10 – Differential Gene Expression – Dumitriu dataset.
For each linearly modelled effect (i.e. each tab):
- **logFC** is the gene's $\log_2$(fold-change) in expression associated with the effect.
- **AveExpr** is the gene's average expression (in $\log_2$(CPM)) over all samples.
- **t** is the moderated t-statistic of differential gene expression.
- **P.Value** is the p-value associated with the t-statistic.
- **adj.P.Val** is the p-value associated with the t-statistic corrected for multiple testing by the Benjamini-Hochberg FDR procedure.
- **B** is B-statistic, i.e. the empirical Bayesian log-odds that the gene is differentially expressed.

Table S11 – Differential Gene Expression – Zhang dataset.
For each linearly modelled effect (i.e. each tab):
- **logFC** is the gene's $\log_2$(fold-change) in expression associated with the effect.
- **AveExpr** is the gene's average expression (in $\log_2$(CPM)) over all samples.
- **t** is the moderated t-statistic of differential gene expression.
- **P.Value** is the p-value associated with the t-statistic.
- **adj.P.Val** is the p-value associated with the t-statistic corrected for multiple testing by the Benjamini-Hochberg FDR procedure.
- **B** is B-statistic, i.e. the empirical Bayesian log-odds that the gene is differentially expressed.

Table S12 – Combined PD effect's scores from t-statistics of differential expression of common genes in the Dumitriu and Zhang datasets.

Table S13 – Combined Neurodegeneration effect's scores from t-statistics of differential expression of common genes in the Dumitriu and Zhang datasets.

Table S14 – Joint AD&PD Disease effect's scores from the combined AD and PD effects' scores.

Table S15 – Joint AD&PD Neurodegeneration effect's scores from the combined Neurodegeneration effects' scores from the AD and PD datasets.

Table S16 – cTRAP results: cMap compound perturbations and AD-associated gene expression changes.
- **cMAP perturbation** is the identifier of the chemical perturbation that incorporates information on the compound, cell line, time of exposure and dosage.
- **Compound** is the common name of the drug used.
- **Spearman's rho AD** is the correlation between the compound's perturbation z-scores and the AD differential expression combined scores.
- **Spearman's rho Neurodegeneration** is the correlation between the compound's perturbation z-scores and the Neurodegeneration differential expression combined scores.
- **Mode of Action** lists the compound's known modes of action.
- **Targets** are the known compound's gene targets.
- **Disease area** stands for the medical field in which the compound is already being administrated.
- **Phase** indicates the stage of clinical trials the drugs is in.

Table S17 – cTRAP results: cMap compound perturbations and PD-associated gene expression changes**.**
- **cMAP perturbation** is the identifier of the chemical perturbation that incorporates information on the compound, cell line, time of exposure and dosage.

- **Compound** is the common name of the drug used.
- **Spearman's rho PD** is the correlation between the compound's perturbation z-scores and the PD differential expression combined scores.
- **Spearman's rho Neurodegeneration** is the correlation between the compound's perturbation z-scores and the Neurodegeneration differential expression combined scores.
- **Mode of Action** lists the compound's known modes of action.
- **Targets** are the known compound's gene targets.
- **Disease area** stands for the medical field in which the compound is already being administrated.
- **Phase** indicates the stage of clinical trials the drugs is in.

Table S18 – cTRAP results: cMap compound perturbations and common AD- and PD- associated gene expression changes.
- **cMAP perturbation** is the identifier of the chemical perturbation that incorporates information on the compound, cell line, time of exposure and dosage.
- **Compound** is the common name of the drug used.
- **Spearman's rho AD&PD** is the correlation between the compound's perturbation z-scores and the AD-PD differential expression combined scores.
- **Spearman's rho Neurodegeneration** is the correlation between the compound's perturbation z-scores and the Neurodegeneration differential expression combined scores.
- **Mode of Action** lists the compound's known modes of action.
- **Targets** are the known compound's gene targets.
- **Disease area** stands for the medical field in which the compound is already being administrated.
- **Phase** indicates the stage of clinical trials the drugs is in.